SAND2020-4700PE

HERMES III - 2018

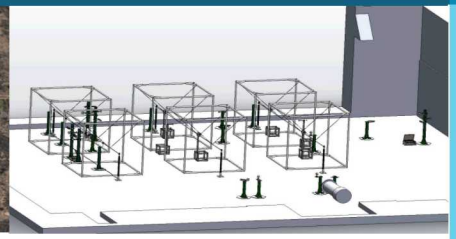

PRESENTED BY

Eric Berry; Donald P. McLemore

Presentation Contents

Presentation Contents

Executive Summary

There are 10 separate sections to this presentation, each focusing on one aspect of the overall analysis

I. Field and Test Article Analysis Overview

- This section lists the general objectives of the test and the specific special analyses that will address these overall objectives
- A group of shots, representative examples of the pulser states and shielding degradations of the test articles, was selected to carefully analyze and characterize,

II. The Final Corrections to the Data

- The data were corrected using techniques used in the previous tests
- However, an anomalous late-time "tail" existed on most of the electric and magnetic field corrected data
- Two possible explanations are offered for this behavior
  - A grounding problem between the pre-pulse and the post-pulse regions
  - The "tails" are caused by the current density of the electrons and ions created by the pulser

III. Corrected and Late-Time Adjusted Fields

- Listed by shot and platform

IV. Geometry and Response of Courtyard Field Sensors

- To test whether the source behaved as a point or distributed source, the log of the field amplitude was plotted against the log of the separation distance from the source
  - If the slope of the plots were consistently nearly "-2", this would suggest a point-source behavior
  - The slopes of these plots were in the range of -0.51 to -2.34, indicating a more distributed source region

V. Field Repeatability on the basis of Single Shot Response

- How well can other field responses for a given shot be predicted from a single shot response?
  - Could the distribution of fields within the Courtyard test space be predicted by knowing the field at a fixed location, say the Ex electric field on Platform 4?
  - There turns out to be significant variations between actual distributions and predicted distributions

Executive Summary (concluded)

VI. Environmental Interference

- The instrumentation transportainer caused electromagnetic scattering which can be seen in the 10-20 MHz frequency range more prominently on electric fields measured on Platform 2 and less noticeable on Platform 3

VII. Shielding Effectiveness

- Shielding effectiveness curves were constructed as frequency-domain ratios of an internal field or surface current density, measured inside a test article compared to the corresponding outside field or surface current density for the article
  - This offers a characterization of the shielding provided by the test article
  - Because this ratio can often be dividing very low field frequency-domain amplitudes to very large ones and have these ratios change substantially from frequency-to-frequency, the ratio is measured in decibels (dB) and smoothed to more easily see trends in the shielding
  - Four shots were chosen to demonstrate shielding effectiveness changes with shielding degradations (shot 670 for complete shielding and shots 675, 690 and 705 for various degradations)
  - One can easily see the overall shielding decrease (shielding effectiveness increase) with more severe degradations in the test article shielding

VIII. Courtyard Fields

- Corrected and late-time adjusted electric and magnetic fields are given for all fields for the chosen set of shots

IX. Test Article Fields and Surface Current Densities

- Corrected Internal test article fields and external and internal surface current densities are shown for the chosen set of shots

X. Signal Processing Advances

- Signal processing correction processes for correcting the data are described.

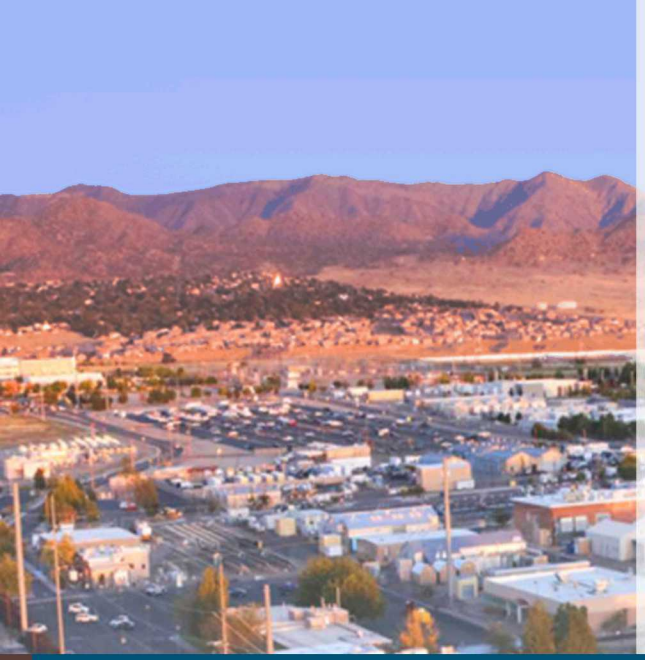

Test Shot Log

Test Shot Log (1 of 3)

Shot#	Date	Configuration	Doors	Peak Dose (kRad)	Total Dose (kRad)	Average Dose (kRad)	Dose Rate (Rad/sec)	Notes
10660	4/27/2018	Series 1 Config	Half	36	473.12	16.31	5.83E+11	Door width is roughly 14 5/8". DAS was fielded on REF stand
10661	4/27/2018	Series 1 Config	Half	41.6	561.07	19.35	6.67E+11	AWE PP 50 V. DAS was fielded on REF stand
10662	4/27/2018	Series 1 Config	Half	43.1	529.06	18.24	6.29E+11	AWE PP 50 V. DAS was fielded on REF stand.
10663	4/27/2018	Series 1 Config	Half	45.2	525.62	18.12	6.25E+11	AWE PP 50 V. DAS was fielded on REF stand.
10664	4/27/2018	Series 1 Config	Half	36	473.86	16.34	5.63E+11	AWE PP 50 V. DAS was fielded on REF stand.
10665	4/30/2018	Series 1 Config / CS/Cone/Body Rotated	Open	41	509.03	17.55	5.81E+11	AWE PP 50 V. AWE swapped pie pans.
10666	4/30/2018	Series 1 Config / CS/Cone/Body Rotated	Open	51.2	506.83	17.48	6.03E+11	AWE PP 50 V. HV box did not break down.
10667	4/30/2018	Series 1 Config / CS/Cone/Body Rotated	Open	52.1	555.76	19.16	6.49E+11	AWE PP 50 V.
10668	4/30/2018	Series 1 Config / CS/Cone/Body Rotated	Open	61.8	516.42	17.81	6.09E+11	AWE PP 50 V. Copper tape was used to completely cover REF-PP2V2. A piece of gaff tape was used to insulate the plate from the copper Faraday cage.
10669	5/1/2018	Series 1 Config / CS/Cone/Body Rotated	Open	41	482.14	16.63	5.94E+11	AWE PP 50 V.
10670	5/1/2018	Series 1 Config / CS/Cone/Body Rotated	Open	30.9	451.13	15.56	5.72E+11	AWE PP 50 V.
10671	5/1/2018	Series 1 Config / CS/Cone/Body Rotated	Open	35.1	450.25	15.53	5.28E+11	AWE PP 50 V. Opened slit 6 on the CS.
10672	5/1/2018	Series 1 Config / CS/Cone/Body Rotated	Open	38.6	495.83	17.1	5.86E+11	AWE PP 50 V. Opened slit 6 on the CS. Changed aperture on AWE frustrum (open slot).
10673	5/1/2018	Series 1 Config / CS/Cone/Body Rotated	Open	14.6	241.09	8.31	2.66E+11	AWE PP 50 V. Opened slit 6 on the CS. Changed aperture on AWE frustrum (open slot).
10674	5/1/2018	Series 1 Config / CS/Cone/Body Rotated	Open	47.8	527.85	18.2	6.15E+11	AWE PP 50 V. Opened slit 6 on the CS. Changed aperture on AWE frustrum (open slot). Removed Forward nose section of CN.
10675	5/1/2018	Series 1 Config / CS/Cone/Body Rotated	Open	43.6	512.67	17.68	6.14E+11	AWE PP 50 V. Opened slit 6 on the CS. Changed aperture on AWE frustrum (open slot). Removed Forward nose section of CN. Fielded DAS on stairs to MITL with PIN diodes installed within (Front - PIN2-Pb , Gap 1 - PIN1-Bare, Gap 2 - PIN1-Pb , Gap 3 - PIN2-Pb).
10676	5/2/2018	Series 1 Config / CS/Cone/Body Rotated	Open	41.5	552.93	19.07	6.76E+11	AWE PP 50 V. SNL PP fielded prior to shot. SNL PP unbiased. Opened slit 6 on the CS. Changed aperture on AWE frustrum (open slot). Removed Forward nose section of CN. Fielded DAS on stairs to MITL with PIN diodes installed within (Front - PIN2-Pb , Gap 1 - PIN1-Bare, Gap 2 - PIN1-Pb , Gap 3 - PIN2-Pb).
10677	5/2/2018	Series 1 Config / CS/Cone/Body Rotated	Open	36.4	520.4	17.94	6.32E+11	AWE PP 50 V. SNL PP unbiased. Opened slit 6 on the CS. Changed aperture on AWE frustrum (open slot). Removed Forward nose section of CN. Fielded DAS on stairs to MITL with PIN diodes installed within (Front - PIN2-Pb , Gap 1 - PIN1-Bare, Gap 2- PIN1-Pb , Gap 3 - PIN2-Pb). P2-AWEPP was shielded similar to REF-AWEPP prior to the shot. MITL fully mapped.
10678	5/2/2018	Series 1 Config / CS/Cone/Body Rotated	Open	37	480.15	16.56	6.42E+11	AWE PP 50 V. SNL PP unbiased. Opened slit 6 on the CS. Changed aperture on AWE frustrum (open slot). Removed Forward nose section of CN. Fielded Mini-DAS near converter. P1-AWEPP and P3-AWEPP were shielded similar to REF-PP2V2 prior to the shot. Bias T we removed from P3-SNLPP to troubleshoot signal. MITL fully mapped.
10679	5/2/2018	Series 1 Config / CS/Cone/Body Rotated	Open	49.4	499.56	17.23	6.63E+11	AWE PP 50 V. SNL PP 50 V. Opened slit 6 and 1 on the CS. Changed aperture on AWE frustrum (open slot). Removed Forward nose section and Aft copper tape cover from CN. Fielded Mini DAS near converter. Added H3 Bias T to P3-SNLPP after determining that PSPL5532A was malfunctioning. MITL fully mapped.
10680	5/2/2018	Series 1 Config / CS/Cone/Body Rotated	Open	43.1	462.51	15.95	6.04E+11	AWE PP 50 V. SNL PP 50 V. Opened slit 6 and 1 on the CS. Changed aperture on AWE frustrum (open slot) and rolled aperature away from source. Removed Forward nose section and Aft copper tape cover from CN. Fielded Mini DAS near converter.

Test Shot Log (2 of 3)

Shot#	Date	Configuration	Doors	Peak Dose (kRad)	Total Dose (kRad)	Average Dose (kRad)	Dose Rate (Rad/sec)	Notes
10681	5/2/2018	Series 1 Config / CS/Cone/Body Rotated	Open	42	444.32	15.32	5.67E+11	AWE PP 50 V. SNL PP 50 V. Opened slit 6 and 1 on the CS. Changed aperture on AWE frustrum (open slot) and rolled aperature away from source. Removed Forward nose section and Aft copper tape cover from CN. Fielded Mini DAS near converter.
10682	5/3/2018	Series 1 Config /Cone Rotated/CS and Body parallel to beam	Open	53.2	490.47	16.91	1.04E+13	AWE PP 50 V. SNL PP 100 V. Opened slit 6 and 1 on the CS. Changed aperture on AWE frustrum (open slot) and rolled aperature away from source. Removed Forward
10683	5/3/2018	Series 1 Config /Cone Rotated/CS and Body parallel to beam	Open	61	554.71	19.13	6.83E+11	AWE PP 50 V. SNL PP 100 V. Opened slit 6 and 1 on the CS. Changed aperture on AWE frustrum (open slot) and rolled aperature away from source. Removed Forward nose section and Aft copper tape cover from CN). Fielded Mini DAS near converter. Recognized that CN-WS and CN-WO were unshorted and uncapped. Signal lines were moved to position and terminated appropriately. SNL pie pan signal cable coils were moved outside of HERMES shield door and exposed lines were covered with humpback lead.
10684	5/3/2018	Series 1 Config /Cone Rotated/CS and Body parallel to beam	Open	56	526.64	18.16	6.53E+11	AWE PP 50 V. SNL PP 100 V. Opened slit 6 and 1 on the CS. Changed aperture on AWE frustrum (open slot) and rolled aperture away from source. Removed Forward nose section and Aft copper tape cover from CN. Fielded Mini DAS near converter. Cleaned connections on REF-SNLPP, signal is in the noise.
10685	5/3/2018	Series 1 Config /Cone/CS/Body parallel to beam	Open	34.1	403.97	13.93	4.49E+11	AWE PP 30 V. SNL PP 100 V. Opened slit 6 and 1 on the CS. Changed aperture on AWE frustrum (open slot) and aperture rolled awayfrom beam. Removed Forward nose section and Aft copper tape cover from CN. Fielded Mini DAS near converter.
10686	5/3/2018	Series 1 Config /Cone/CS/Body parallel to beam	Open	26.27	367.69	12.68	4.28E+11	AWE PP 30 V. SNL PP 100 V. Opened slit 6 and 1 on the CS. Changed aperture on AWE frustrum (open slot) and aperture rolled away from beam. Removed Forward nose section and Aft copper tape cover from CN. Fielded Mini DAS near converter.
10687	5/4/2018	Series 1 Config /Cone/CS/Body parallel to beam	Open	38.39	476.8	16.44	5.52E+11	AWE PP 100 V. SNL PP 100 V. Opened slit 6 and 1 on the CS. Changed aperture on AWE frustrum (open slot) and aperture rolled awayfrom beam. Removed Forward nose section and Aft copper tape cover from CN. Fielded Mini DAS near converter.
10688	5/4/2018	Series 1 Config /Cone/CS/Body parallel to beam	Open	40.99	480.08	16.55	5.79E+11	AWE PP 100 V. SNL PP 100 V. Opened slit 6 on the CS. Changed aperture on AWE frustrum (open slot) and aperture rolled away from beam. Removed Forward nose section from CN. Fielded Mini DAS near converter with copper towards converter.
10689	5/4/2018	Series 1 Config /Cone/CS/Body parallel to beam	Open	42.87	493.47	17.02	6.75E+11	AWE PP 12 V. SNL PP 100 V. Opened slit 6 on the CS. Changed aperture on AWE frustrum (open slot) and aperture toward beam. Removed Forward nose section from CN. Fielded Mini DAS near converter with copper towards converter. The bias T on REF-SNLPP was found to be damaged.
10690	5/4/2018	Series 1 Config /Cone/CS/Body parallel to beam	Open	51.03	531.23	18.32	6.94E+11	AWE PP 12 V. SNL PP 100 V. Opened slit 6 on the CS. Changed aperture on AWE frustrum (open slot) and aperture toward beam. Removed Forward nose section from CN. Fielded Mini DAS near converter with copper towards converter. Swapped bias T on REF-SNLPP with one from PIN2-BARE and replaced the bias T on PIN2-BARE with H3 bias T. (P3-SNLPP bias T was replaced instead of REF-SNLPP, this was corrected post shot).
10691	5/4/2018	Series 1 Config /Cone/CS/Body parallel to beam	Open	48.3	513.84	17.72	6.92E+11	GaAs bias -5 V. AWE PP 12 V. SNL PP 100 V. Opened slit 6 on the CS. Changed aperture on AWE frustrum (open slot) and aperture toward beam. Removed Forward nose section from CN. Fielded Mini DAS near converter with copper towards converter. GaAs diode was fielded near converter. Accidentally overwrote Shot 45 header file
10692	5/7/2018	Series 2 Config	Open	68.14	572.26	19.73	6.77E+11	GaAs bias -5 V. AWE PP 0 V. SNL PP 100 V. Opened slit 6 on the CS. Changed aperture on AWE frustrum (open slot) and aperture toward beam. Rotated test articles. Moved HV box to P4, CS to P3, and Body to P1. Accidentally overwrote Shot 45 header file. DC-NI, DC-NIB, and DC-NIZ were not connected. P2-SCD was noticed to be lower and narrower than previous shots. No noticeable cable damage was found, problem may be internal to SCD.
10693	5/7/2018	Series 2 Config	Open	57.11	506.42	17.46	6.02E+11	GaAs bias -5 V. AWE PP 0 V. SNL PP 100 V. Opened slit 6 on the CS. Changed aperture on AWE frustrum (open slot) and aperture toward beam.
10694	5/7/2018	Series 2 Config	Open	66.55	537.72	18.54	7.13E+11	AWE PP 50 V. SNL PP 100 V. Opened slit 6 on the CS. Changed aperture on AWE frustrum (open slot) and aperture toward beam. Mini DAS placed on stand between P2 and REF
10695	5/7/2018	Series 2 Config	Open	51.03	459.64	15.85	5.78E+11	AWE PP 50 V. SNL PP 100 V. Changed aperture on AWE frustrum (open slot) and aperture toward beam. Mini DAS placed on stand between P2 and REF. Covered all slits on CS.
10696	5/7/2018	Series 2 Config	Open					AWE PP 50 V. SNL PP 100 V. Changed aperture on AWE frustrum (open slot) and aperture toward beam. Mini DAS placed on stand between P2 and REF. Removed nose from CN body. Copper was placed in front of mini DAS.
10697	5/8/2018	Series 2 Config	Open					AWE PP 50 V. SNL PP 100 V. Bare PINs placed at stand between P2 and REF. Removed nose from CN body. Cone oriented nose down with aperture toward source. Reoriented all AWE pie pans (large pie pans at P2 and P3, small pie pans at P1 and P4, and medium pie pans at REF).

Test Shot Log (3 of 3)

Shot#	Date	Configuration	Doors	Peak Dose (kRad)	Total Dose (kRad)	Average Dose (kRad)	Dose Rate (Rad/sec)	Notes
10698	5/8/2018	Series 2 Config	Open					AWE PP 50 V. SNL PP 0 V. DAS with PINs (Front - PIN1_Bare, Gap 1 - PIN2-Bare, Gap 2 - PIN1-Pb, Gap 3 - PIN2-Pb) placed at stand between P2 and REF. Removed nose from CN body. Cone oriented nose down with aperture toward source. Opened both slit 1 and 6 on CS.
10699	5/8/2018	Series 2 Config	Open					AWE PP 50 V. SNL PP 0 V. DAS with PINs (Front - PIN1_Bare, Gap 4 - PIN2-Bare, Gap 5 - PIN1-Pb, Back - PIN2-Pb) placed at stand between P2 and REF. Removed nose from CN body. Cone oriented nose down with aperture toward source. Opened both slit 1 and 6 on CS.
10700	5/8/2018	Series 2 Config	Open					fielding TLDs on Step Wedge (Tim Webb). Inserted image plate into Compton spectrometer to measure accumulated dose.
10701	5/8/2018	Series 2 Config	Open					AWE PP 50 V. SNL PP 0 V. DAS with PINs (Front - PIN1_Bare, Gap 4 - PIN2-Bare, Gap 5 - PIN1-Pb, Back - PIN2-Pb) placed at stand between P2 and REF. Lead sheet was placed under DAS to explore scattering. Removed nose and opened aft port on CN body. Cone oriented nose down with aperture away from centerline. Opened both slit 1 and 6 on CS.
10702	5/8/2018	Series 2 Config	Open					AWE PP 50 V. SNL PP 0 V. DAS with PINs (Front - PIN1_Bare, Gap 4 - PIN2-Bare, Gap 5 - PIN1-Pb, Back - PIN2-Pb) placed at stand between P2 and REF. Lead sheet was placed under DAS to explore scattering. Removed nose and opened aft port on CN body. Cone oriented nose down with aperture away from centerline. Opened both slit 1 and 6 on CS.
10703	5/9/2018	Series 2 Config	Open	46.9				AWE PP 50 V. SNL PP 100 V. DAS PINs placed at stand between P2 and REF. Rotated CN and cylinder to be perpendicular to beam. Placed cone vertical with nose up. Removed nose and opened aft port on CN body. Cone oriented nose up with aperture toward centerline. Opened both slit 1 and 6 on CS.
10704	5/9/2018	Series 2 Config	Open	31.2				AWE PP 50 V. SNL PP 100 V. DAS with PINs (Front - PIN1_Bare, Gap 4 - PIN2-Bare, Gap 5 - PIN1-Pb, Back - PIN2-Pb) placed at stand between P2 and REF. Rotated CN and cylinder to be perpendicular to beam. Placed cone vertical with nose up. Removed nose and opened aft port on CN body. Cone oriented nose up with aperture toward centerline. Opened both slit 1 and 6 on CS.
10705	5/9/2018	Series 2 Config	Open	29.5				AWE PP 50 V. SNL PP 100 V. DAS with PINs (Front - PIN1_Bare, Gap 4 - PIN2-Bare, Gap 5 - PIN1-Pb, Back - PIN2-Pb) placed at stand between P2 and REF. Lead was placed beneath DAS to look for scattering. Rotated CN and cylinder to be perpendicular to beam. Placed cone vertical with nose up. Removed nose and opened aft port on CN body. Cone oriented nose up with aperture toward centerline. Opened both slit 1 and 6 on CS. Rotated AWE pie pans 90 degrees. Added a power T to P2-BX and routed to an integrator on scope 40/3.
10706	5/9/2018	Series 2 Config	Open					Lead was placed beneath DAS and on the sides of the DAS to look for scattering. Rotated CN and cylinder to be perpendicular to beam. Placed cone vertical with nose up. Installed nose and closed aft port on CN body. Cone oriented nose up with closed aperture toward centerline. Close all slits on CS.
10707	5/9/2018	Series 2 Config	Open					AWE PP 50 V. SNL PP 100 V. DAS with PINs (Front - PIN1_Bare, Gap 4 - PIN2-Bare, Gap 5 - PIN1-Pb, Back - PIN2-Pb) placed at stand between P2 and REF. Lead was placed beneath, on the sides, and behind the DAS to look for scattering. Rotated CN and cylinder to be perpendicular to beam. Placed cone vertical with nose up. Installed nose and closed aft port on CN body. Cone oriented nose up with closed aperture toward centerline. Closed all slits on CS.
10708	5/9/2018	Series 2 Config	Open					Lead was placed beneath, on the sides, and behind the DAS to look for scattering. Rotated CN and cylinder to be perpendicular to beam. Placed cone vertical with nose up. Installed nose and closed aft port on CN body. Cone oriented nose up with closed aperture toward centerline. Closed all slits on CS. Notified by facility personnel that a water line had become disconnected into the Marx tank. Facility and test personnel agreed to take one more shot and then begin oil draining and disassembly.
10709	5/10/2018	Series 2 Config	Half					AWE PP 50 V. SNL PP 100 V. DAS with PINs (Front - PIN1_Bare, Gap 4 - PIN2-Bare, Gap 5 - PIN1-Pb, Back - PIN2-Pb) placed at stand between P2 and REF. Lead was placed beneath, on the sides, and behind the DAS to look for scattering. Rotated CN and cylinder to be perpendicular to beam. Placed cone vertical with nose up. Installed nose and closed aft port on CN body. Cone oriented nose up with closed aperture toward centerline. Closed all slits on CS. Shot appeared to be very low. Facility personnel mentioned that a switch may be damaged.
10710	5/10/2018	Series 2 Config	Half					AWE PP 50 V. SNL PP 100 V. DAS with PINs (all exposed for comparison) placed at stand between P2 and REF. Lead was placed beneath, on the sides, and behind the DAS to look for scattering. Rotated W62 and cylinder to be perpendicular to beam. Placed cone vertical with nose up. Installed nose and closed aft port on CN body. Cone oriented nose up with closed aperture toward centerline. Closed all slits on CS. Prior to this shot a liquid resistor was found to be blown and was replaced. After several aborted Marx checks a Marx was pulled with a bad capacitor and replaced with a Marx on the stand.
10711	5/10/2018	Series 2 Config	Half					AWE PP 50 V. SNL PP 100 V. DAS with PINs (Front - PIN1_Bare, Gap 4 - PIN2-Bare, Gap 5 - PIN1-Pb, Back - PIN2-Pb) placed at stand between P2 and REF. Lead was placed beneath, on the sides, and behind the DAS to look for scattering. Rotated CN and cylinder to be perpendicular to beam. Placed cone vertical with nose up. Installed nose and closed aft port on CN body. Cone oriented nose up with closed aperture toward centerline. Closed all slits on CS.

2-D Layout of Courtyard

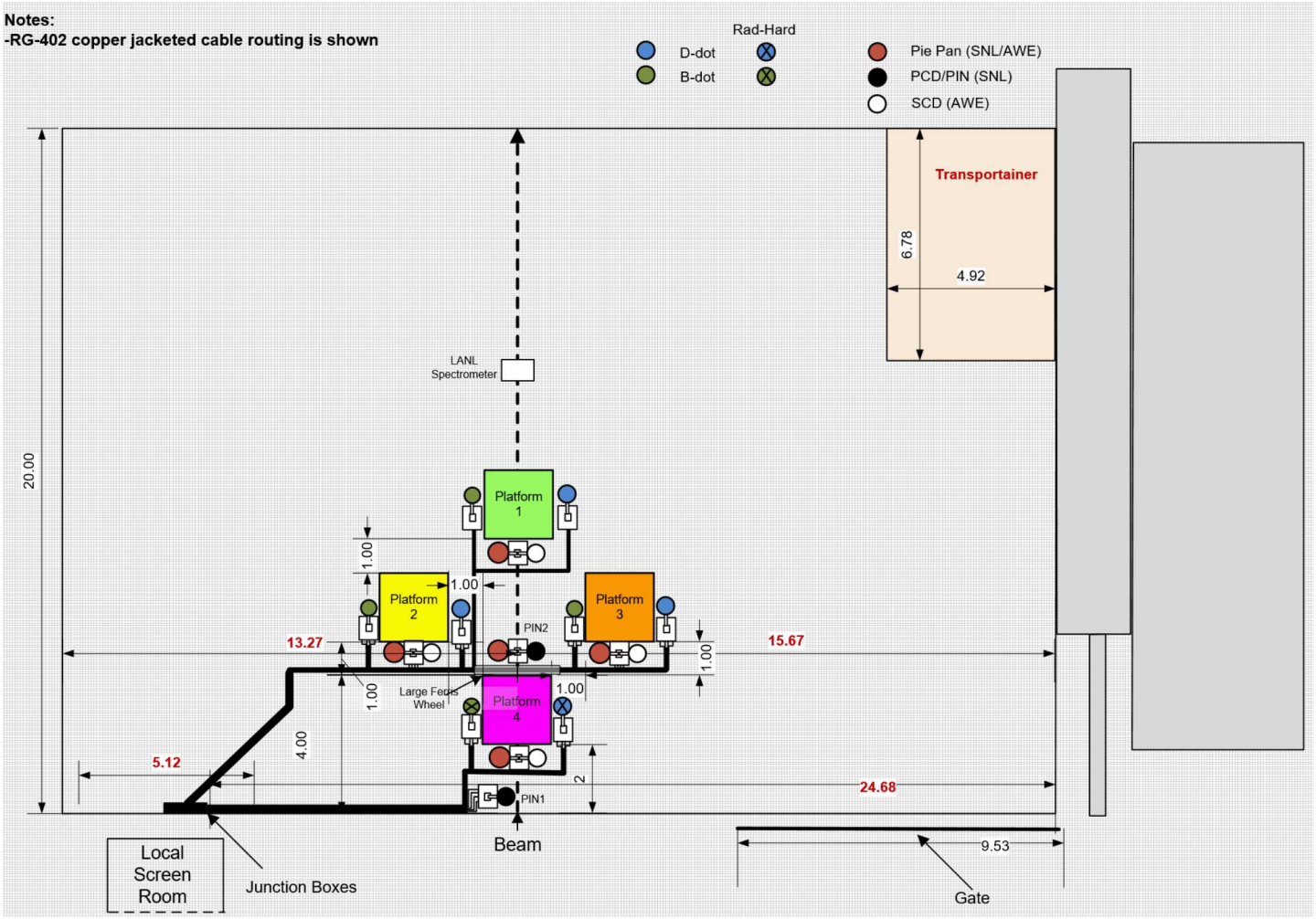

3-D Layout of Courtyard

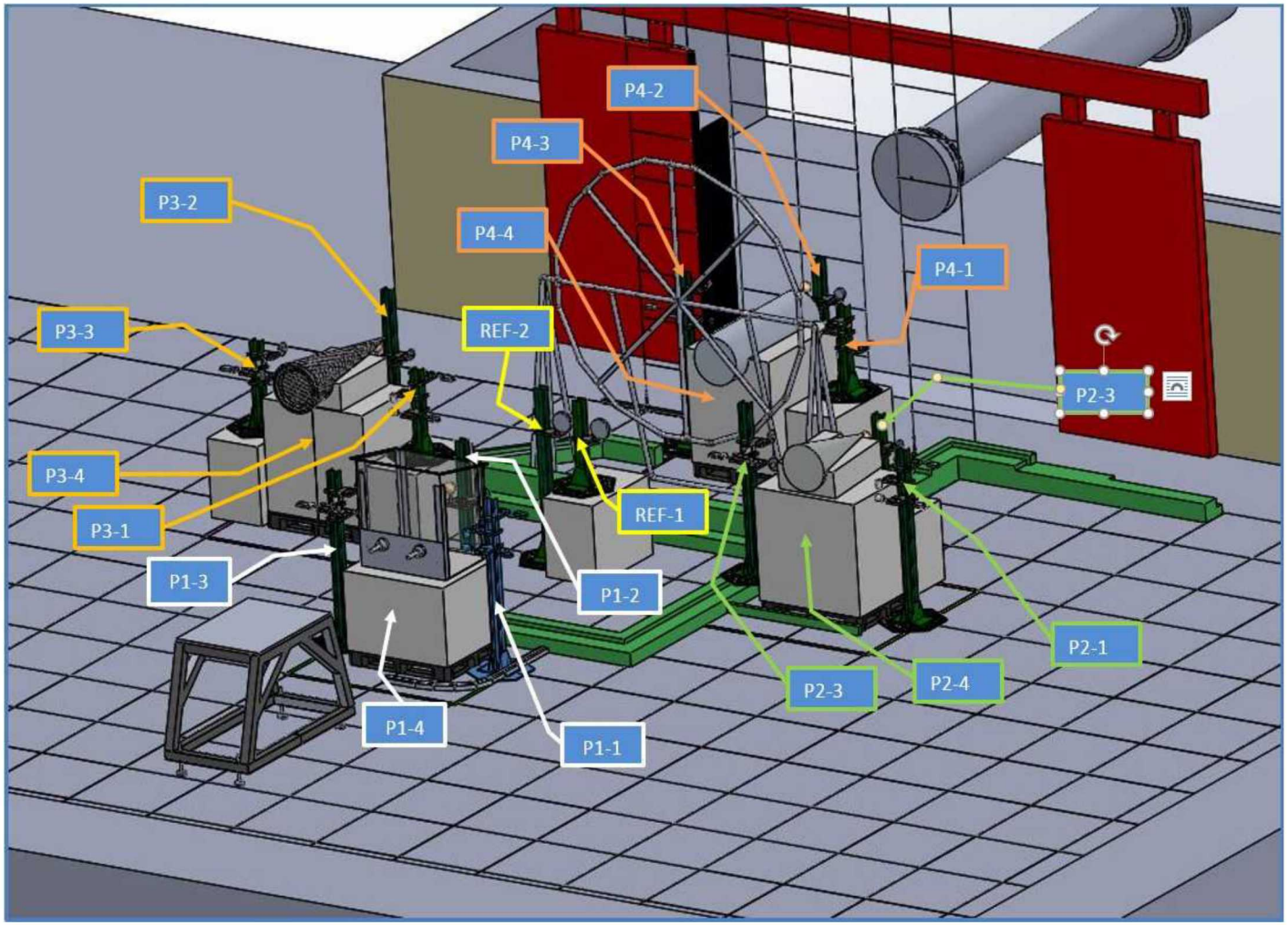

CN Test Points (Conical Body)

Conical Test Point Name	Location	Measured on Shots
CN-EA	Inside - Axial E -Field	10664, 10670, 10675, 10690 and 10705
CN-ER	Inside - Radial E-Field	10664, 10670, 10675, 10690 and 10705
CN-JA	Outside - Axial J	10664, 10670, 10675, 10690 and 10705
CN-JR	Outside - Radial J	10664, 10670, 10675, 10690 and 10705
CN-WO	Outside - Witness - Open	10675, 10690 and 10705
CN-WS	Outside - Witness - Short	10675, 10690 and 10705
CN-SPARE	Witness - Spare	

CS (Cylindrical Body) Test Points

Cylinder Test Point Name	Location	Measured on Shots
CSI_EA	Inside - Axial E -Field	10664, 10670, 10675, 10690 and 10705
CSI-ER	Inside - Radial E-Field	10664, 10670, 10675, 10690 and 10705
CSI-JA	Inside - Axial J	10664, 10670, 10675, 10690 and 10705
CSI-JR	Inside - Radial J	10664, 10670, 10675, 10690 and 10705
CSO-JA	Outside - Axial J	10664, 10670, 10675, 10690 and 10705

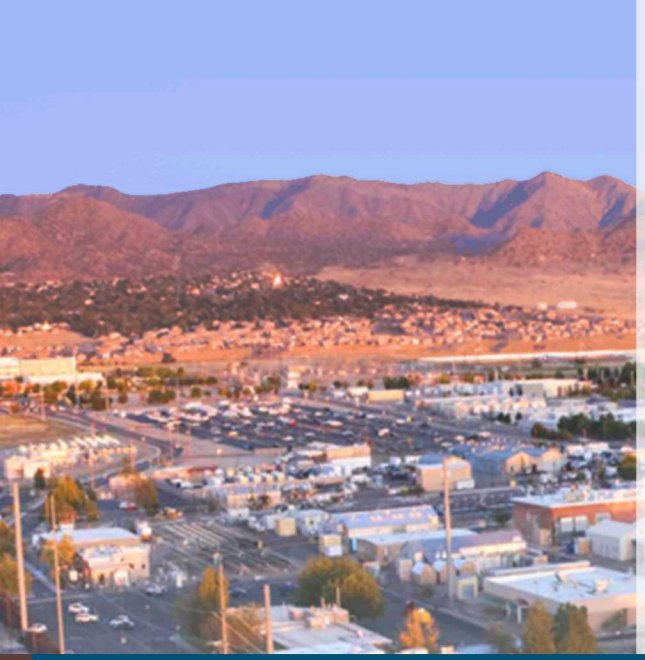

I. Field and Test Article Analysis Overview

Field and Test Article Analysis

The major goals for the HERMES 2018 test were threefold

- Characterize the field environments of the HERMES simulator
- Characterize and quantify the shielding of the test articles tested in the HERMES III environment
- Identify experimental/signal conditioning improvements for next tests

A set of simulator shots were selected that span the experiment variability ranges (see table on following page)

- Use these data to characterize and quantify (1) field environments and (2)shielding effectiveness on test articles

Field and Test Article Analysis, cont.

Shot #	Field/Radiation Variations/Peak Dose (kRad)/Tot Dose (kRad)/Dose Rate (Rad/sec)	Test Object Shielding Variations
10664	Source doors half open/36/474/5.6E+11	Series 1 Config.
10670	Source doors fully open/31/451/5.7E+11	Series 1 Config.; CS/ Cone Body rotated
10675	Source doors fully open/44/513/6.1E+11	Opened slit 6 on the CS. Changed aperture on AWE frustrum (open slot). Removed Forward nose section of CN.
10690	Source doors fully open/44/513/6.1E+11	Series 1 Config.; CS/ Cone Body parallel to beam Opened slit 6 on the CS. Changed aperture on AWE frustrum (open slot) and aperture facing beam. Removed Forward nose section from CN.
10705	Source doors fully open/30/NA/NA	Rotated CN and cylinder to be perpendicular to beam. Placed cone vertical with nose up. Removed nose and opened aft port on CN body. Cone oriented nose up with aperture toward centerline. Opened both slit 1 and 6 on CS.

Field and Test Article Analysis, cont.

Compare the time-domain electric and magnetic fields on each platform

- look at E and H fields (derived from D-Dot and B-Dot sensors) to illustrate field uniformity and consistency (late-time anomaly removed – more on this later)
- Look at amplitude variability within a shot (e.g. dependence on distance from source)
- Look at shot-to-shot variation adjustment techniques to evaluate field consistency

Compare the shielding effectiveness

- Look at shot-normalized shielding effectiveness for given known shielding degradations
- Compare shielding effectiveness for various source shots

Field and Test Article Analysis, concl.

Compare the Time Domain (TD) Electric and Magnetic Fields by Shot

- Plots of field variations on platforms are displayed for each shot, showing the corrected field data as a function of platform (location) to illustrate field distribution
- Fields measured under full source illumination (shots 10670, 10675, 10690 and 10705) are corrected for instrumentation losses/gains and comparisons of field components the platforms for selected shots

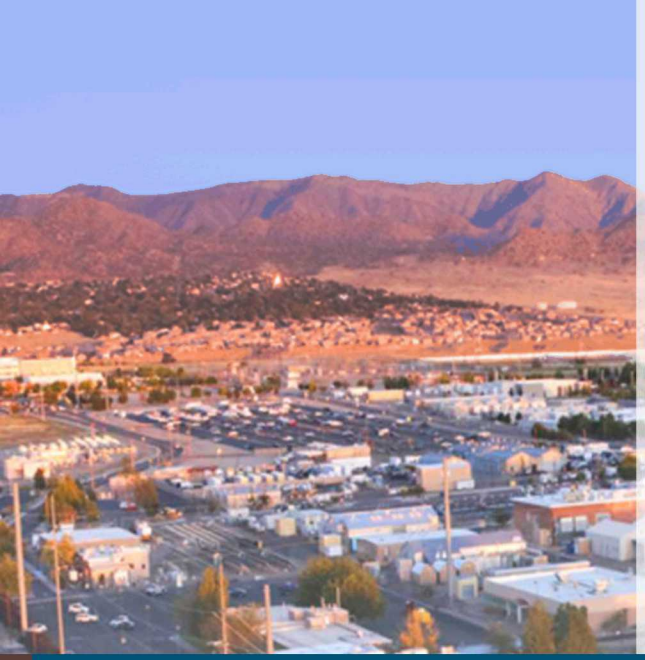

II. The Final Corrections to the Data

The Anomalous Late-Time Behavior

Taking the fields on platform 4 for shot 10670 (shown in the next slide), one can see the example of the anomalous late-time behavior

These fields have been corrected for line losses and voltage-to-incident electric fields (in units of V/M); note the late-time, trace tails that exist on many of the fields

- These non-zero, asymptotic, growing fields with high frequencies are not the typical electric or magnetic fields one would expect.

The first explanation offered for these anomalies was a shifting ground reference between the pre-pulse of the HERMES machine.

- If one looks at the raw data the zero voltage levels shifts between the pre-pulse and post-pulse time regions, so that a certain non-zero dc voltage would remain throughout the pulse
- Since the sensors are derivative sensors (ACD for electric fields and MGL for magnetic fields), these offsets, albeit small, contribute a constant times the long time for the integration. In other words, these offsets would cause late-time asymptotic growing amplitudes.

Raw Data

dt = 2 E-10 seconds
N = 7750 points
To = .0496 microseconds ≈ 50 ns
Tf = 1.5996 microseconds

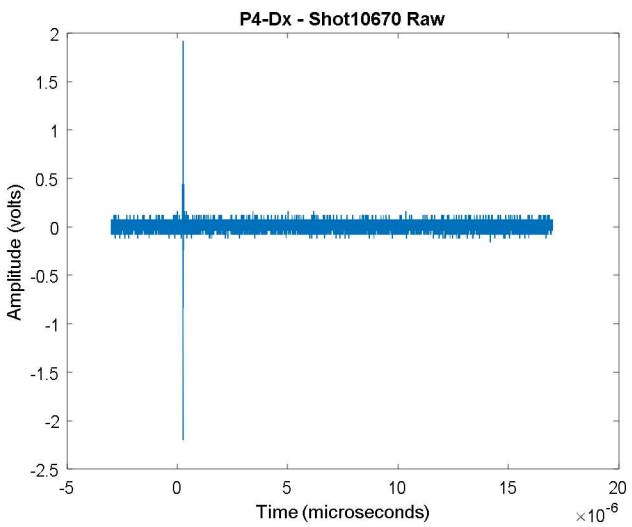

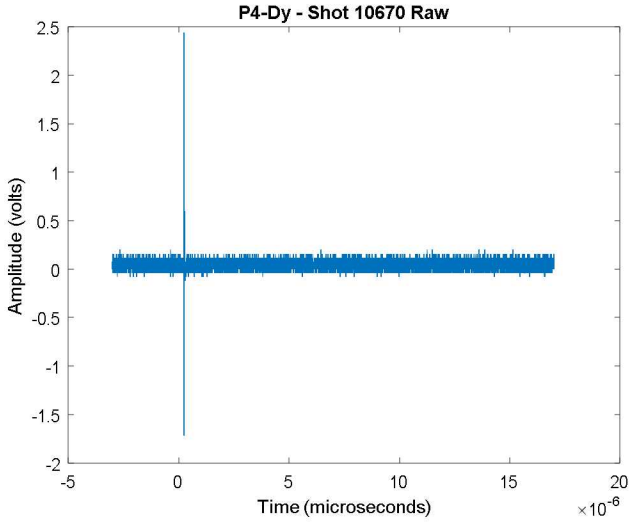

Corrected Efield and H-Field Examples from Shot 10670, Platform 4

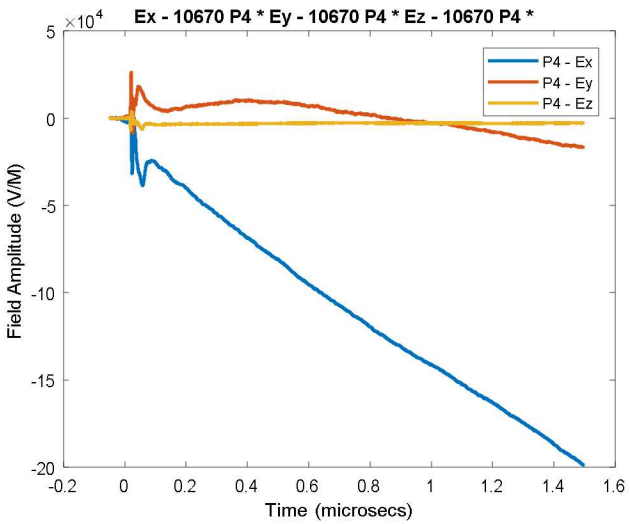

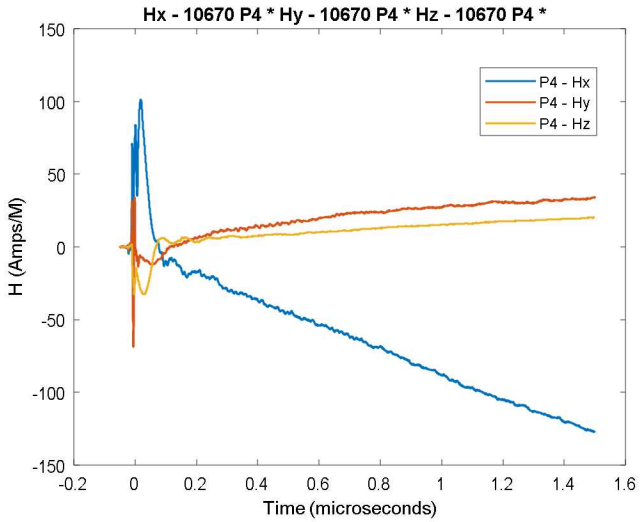

The First "Fix"

Under the assumptions of the dc-offset, the late time behavior of the measurements would be dominated by this integrated offset value, while the actual fields would have settled to zero in a relatively short time.

- Thus a polynomial "fit" of the entire waveform would be principally influenced by the late-time integration with little perturbation from the early time behavior
- A best-fit, third-degree polynomial was constructed for the entire waveform and subtracted from the original waveform, leaving the early-time field waveforms.
  - Results of this operation are shown on the next slide

Much more realistic "Tail-less" waveforms were obtained from this process

Corrected E-field and H-Field Examples from Shot 10670, Platform 4, With Growing, Asymptotic Late-Time Amplitudes Subtracted

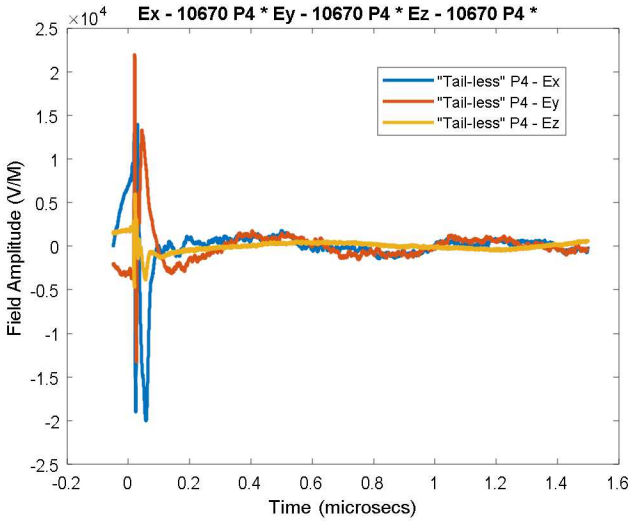

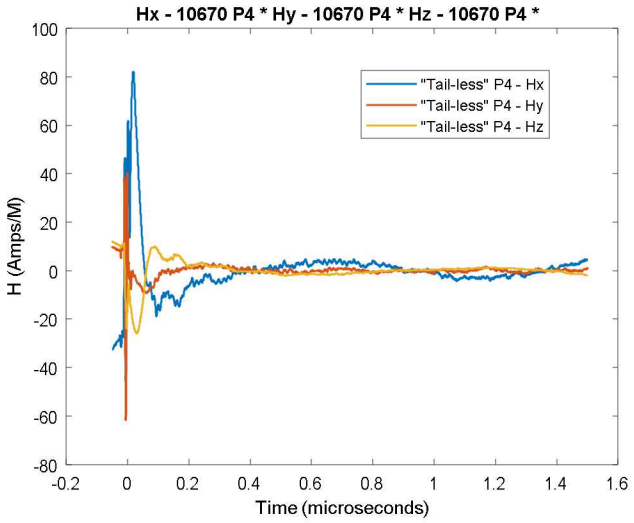

Example of "Extraction" Process, Ex – P4, shot 10670

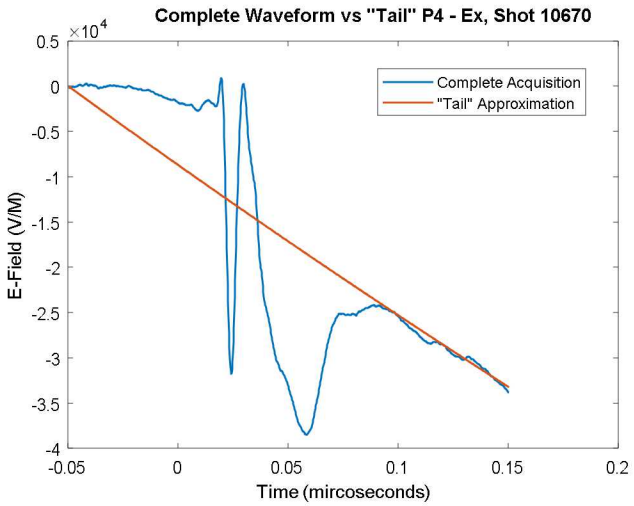

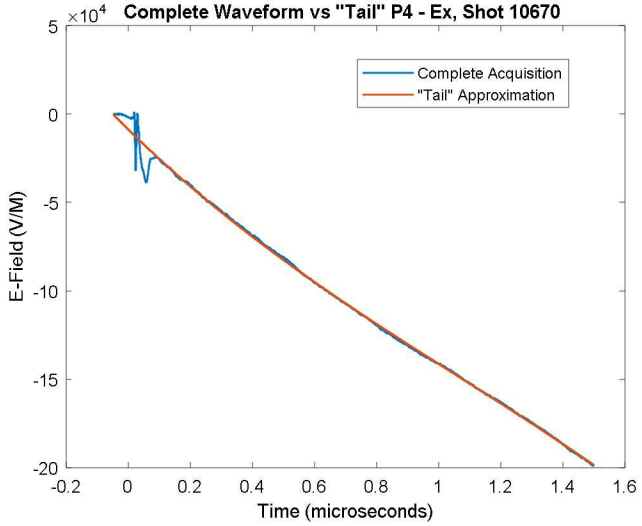

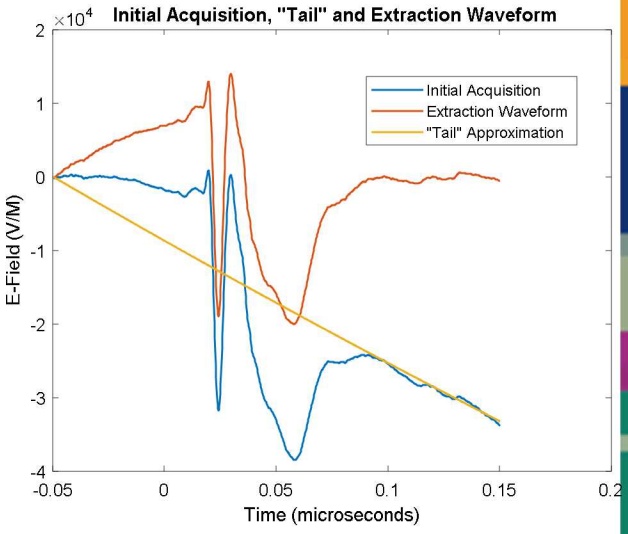

But Wait! Where is the Current Density?

We know that there is a current density in the experiment, verified by other sensors

- Why is it not showing up on our ASD measurements?

This explanation of an offset DC voltage gives us reasonable-looking field waveforms, but is there really a grounding issue with the acquisition measurements?

Could it be that the "Tail" is really a manifestation of the measured current density and not a voltage-offset error?

- The current density would have a step-function manifestation
- The current density random generation process would create a very large noise background (which we see in the data)

Theoretical Correction of D-dot Voltage under the Assumption of No Current Density (All signal conditioners previously accounted) Part I

From Maxwell's equations,

$$\nabla \times H = J + \dot{D} = \mathrm{J} + \frac{\partial D}{\partial t}$$

Multiplying by the infinitesimal area of a surface through which the current flows, dA, and integrating

$$\iint \nabla \times H \cdot dA = \iint \left(\mathrm{J} + \frac{\partial D}{\partial t}\right)\mathrm{dA}$$

But assuming no current density in the area of integration,

$$\iint \nabla \times H \cdot dA = \iint \left(\frac{\partial D}{\partial t}\right) \cdot \mathrm{dA}$$

And using Stokes theorem

$\iint \nabla \times H \cdot dA = \oint H \cdot dl$=I, the current through the loop bounding the area, A.

Thus, assuming J = 0,

$\iint \left(\frac{\partial D}{\partial t}\right)$dA = $\varepsilon_0 \left(\frac{\partial E}{\partial t}\right)$ A→ $\left(\frac{\partial E}{\partial t}\right)=\frac{I}{\varepsilon_0 A}$ and multiplying ε_0 & dividing by the sensor impedance, Z_s, and integrating

$$\left(\frac{\partial E}{\partial t}\right)=IZ_s/(\varepsilon_0 AZ_s)=\frac{v_s}{\varepsilon_0 AZ_s} \rightarrow E = \int_{-\infty}^{\infty} \frac{v_s}{\varepsilon_0 AZ_s}\mathrm{dt}$$

Theoretical Correction of D-dot Voltage under the Assumption of Current Density Present (All signal conditioners previously accounted) Part II

From Maxwell's equations,

$$\nabla \times H = J + \dot{D} = \mathrm{J} + \frac{\partial D}{\partial t}$$

Multiplying by the infinitesimal area of a surface through which the current flows, dA, and integrating

$$\iint \nabla \times H \cdot dA = \iint \left(\mathrm{J} + \frac{\partial D}{\partial t}\right) \cdot \mathrm{dA}$$

But assuming current density exists in the area of integration,

$$\iint \nabla \times H \cdot dA = \iint J \cdot dA + \iint \left(\frac{\partial D}{\partial t}\right) \cdot \mathrm{dA}$$

And using Stokes theorem

$\iint \nabla \times H \cdot dA = \oint H \cdot dl$=I, the current through the loop bounding the area.

But the current density, J, is the current density caused by the electrons released from the target, or J_c. Further, dividing both equation sides by ε_oA, we obtain

$$\iint J_c \cdot \mathrm{dA} + \iint \left(\frac{\partial D}{\partial t}\right) \cdot \mathrm{dA} = J_c\, A + \varepsilon_0 \left(\frac{\partial E}{\partial t}\right) A \rightarrow \frac{J_c}{\varepsilon_0} + \left(\frac{\partial E}{\partial t}\right) = \frac{I}{\varepsilon_0 A}$$

Theoretical Correction of D-dot Voltage under the Assumption of Current Density Present (All signal conditioners previously accounted) Part III

Multiplying and dividing by the sensor impedance yields

$$\frac{J_c\ Z_s}{\varepsilon_0} + \left(\frac{\partial E}{\partial t}\right) Z_s = \frac{IZ_s}{\varepsilon_0 A} = \frac{V_s}{\varepsilon_0 A} \rightarrow \frac{J_c}{\varepsilon_0} + \left(\frac{\partial E}{\partial t}\right) = \frac{V_s}{\varepsilon_0 A Z_s}$$

And

$$\left(\frac{\partial E}{\partial t}\right) = \frac{V_s}{\varepsilon_0 A Z_s} - \frac{J_c}{\varepsilon_0}$$

And

$$E = \int_{-\infty}^{\infty} \frac{v_s}{\varepsilon_0 A Z_s} dt - \int_{-\infty}^{\infty} \frac{J_c}{\varepsilon_0} dt \quad \text{(Equation 1)}$$

Theoretical Correction of D-dot Voltage under the Assumption of Current Density Present (All signal conditioners previously accounted) Part IV

Equation 1 actually describes the process we have been using to find the "free-field" or "no current density" equivalent in the electron and ionic environment

- We identify the "Tail" of the sensor measured field (this is the - $\int_{-\infty}^{\infty} \frac{J_c}{\varepsilon_0} dt$ term)
- Equation 1 states that we must find this term and subtract it from the original measurement to find the "free-field" component of the measurement
- This also implies that we can find the current density term by the "Tail" component of the measurement
- $E_{Tail} = \int_{-\infty}^{\infty} \frac{J_c}{\varepsilon_0} dt$ or $J_c = \varepsilon_0 \frac{\partial}{\partial t} E_{Tail}$

Current Density from ACD E-Field Measurement

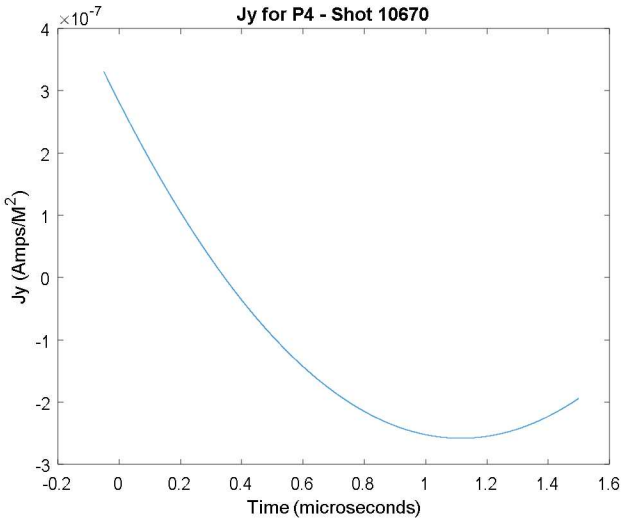

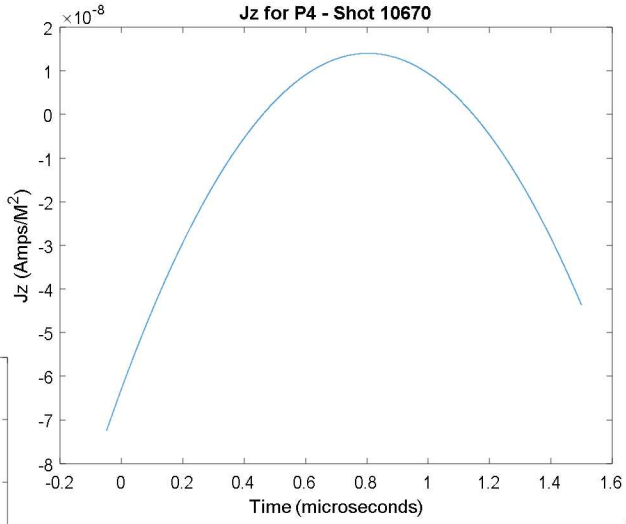

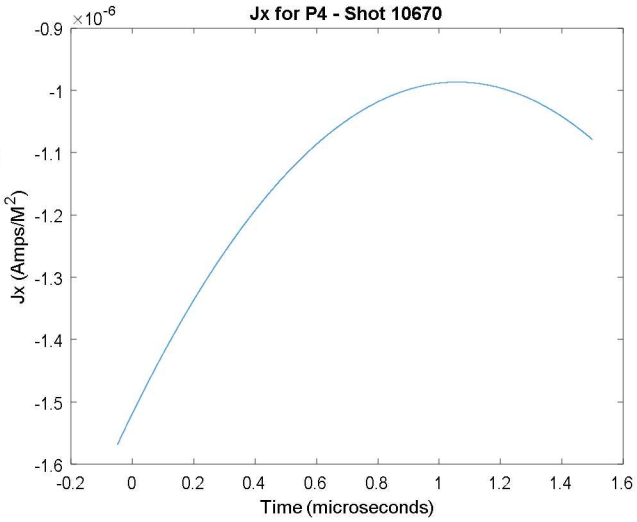

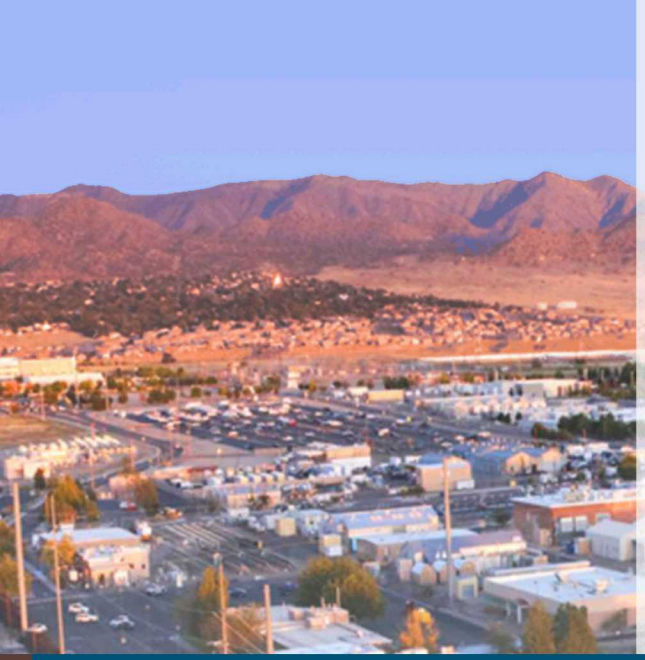

III. Corrected and Late-Time Adjusted Electric and Magnetic Fields

Shot 10664 –E-Fields

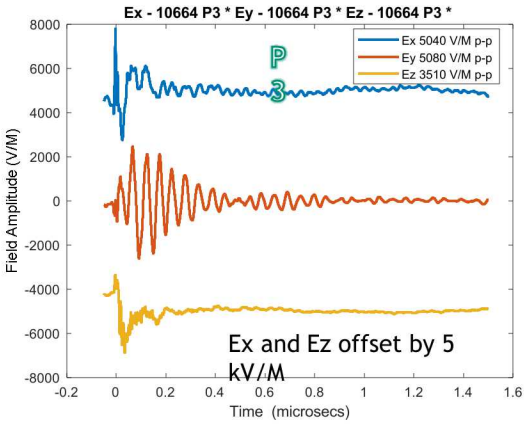

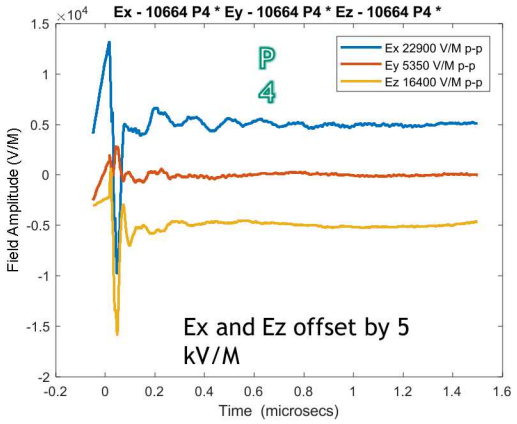

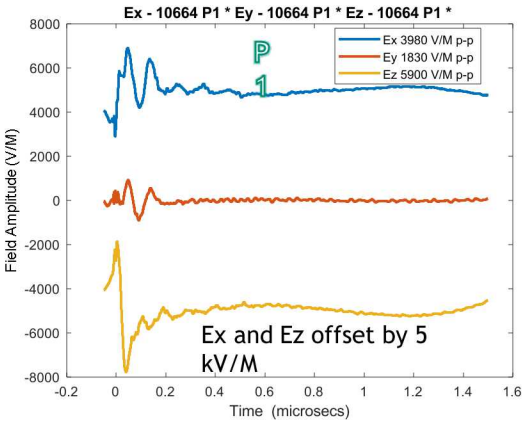

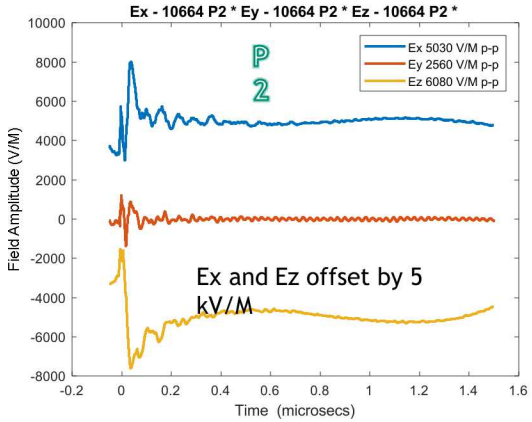

Shot 10664 –H-Fields

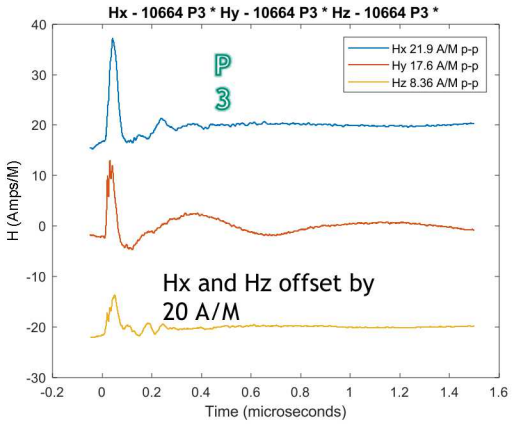

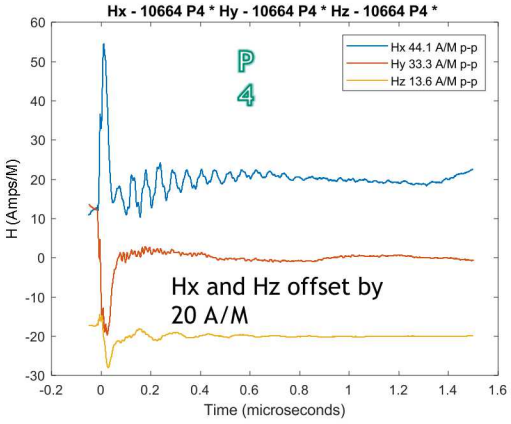

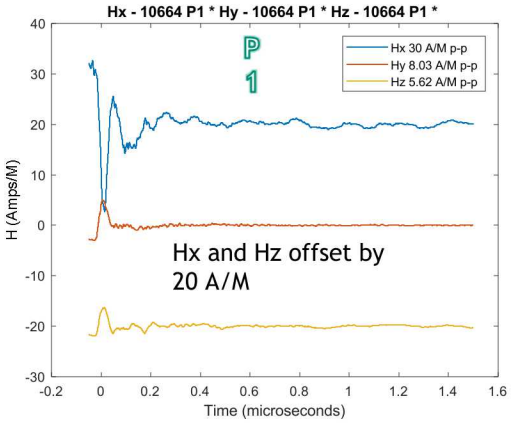

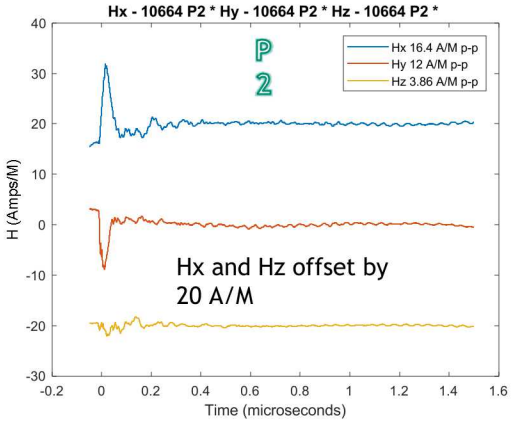

Shot 10670 – E-Fields

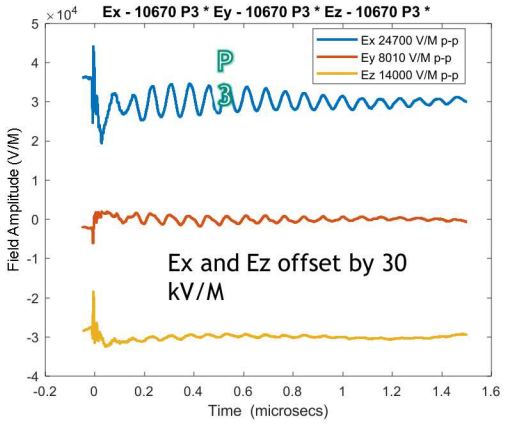

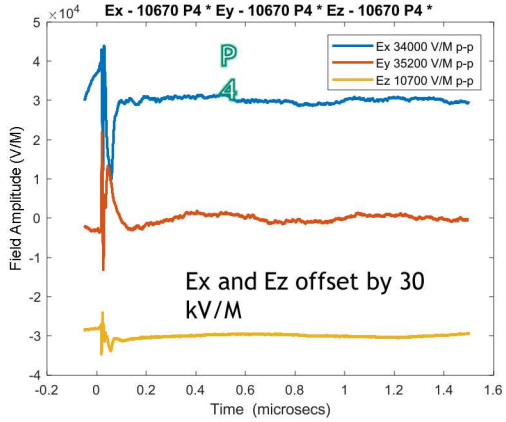

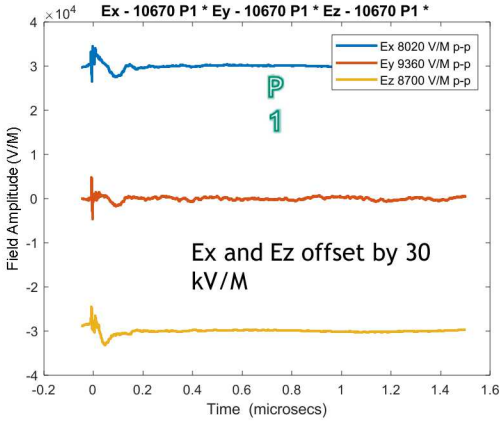

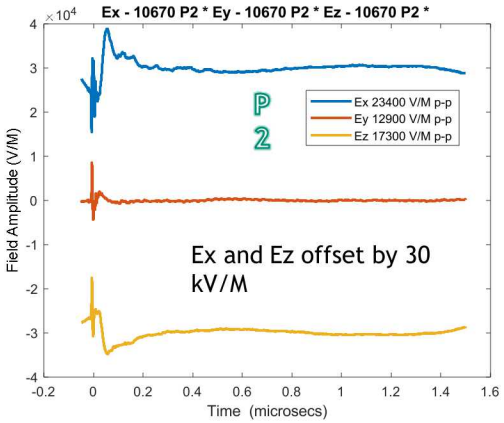

Shot 10670 – H-Fields

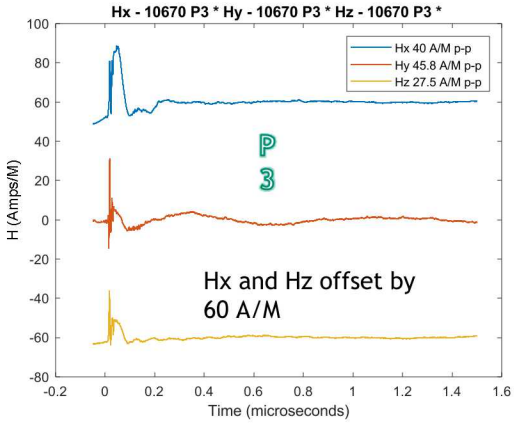

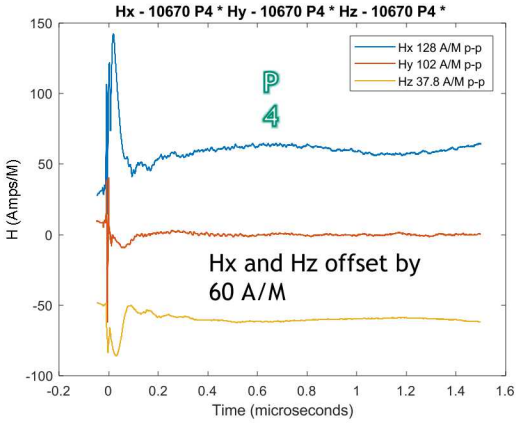

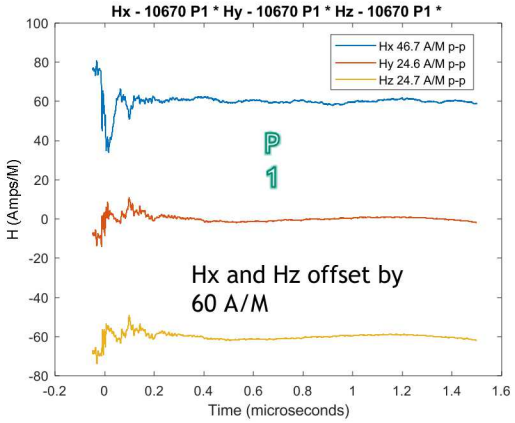

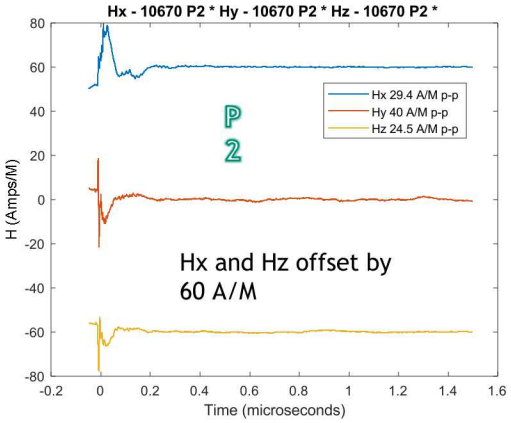

Shot 10675 – E-Fields

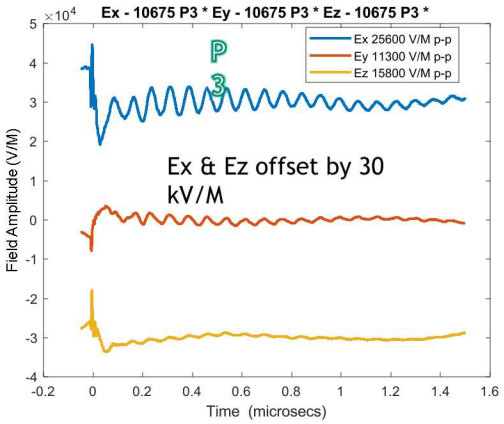

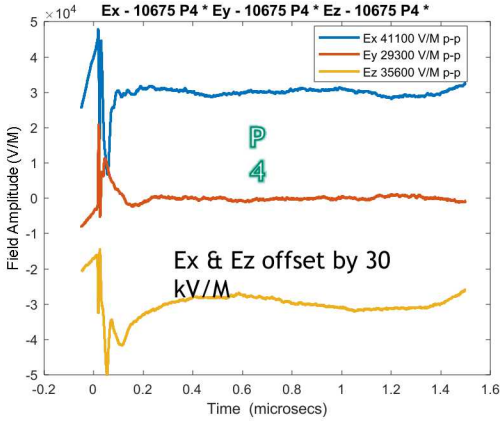

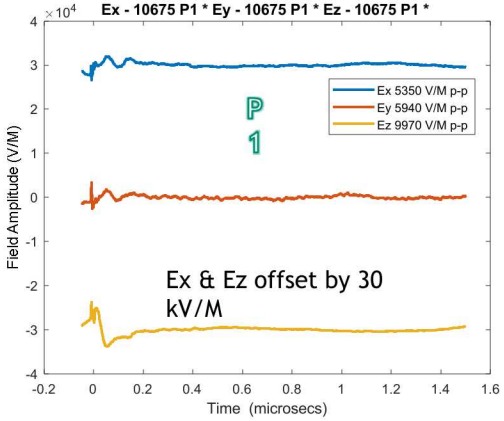

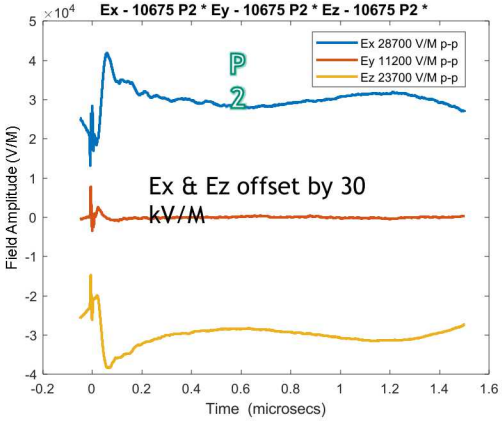

Shot 10675 – H-Fields

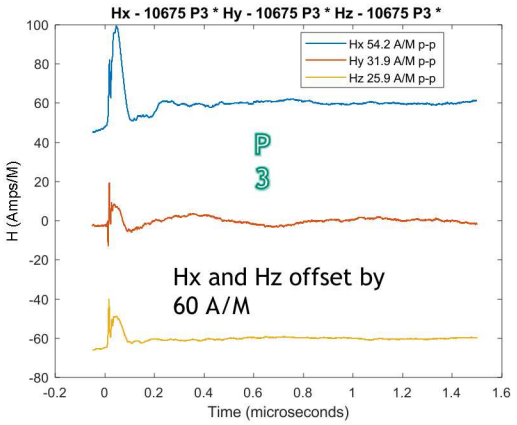

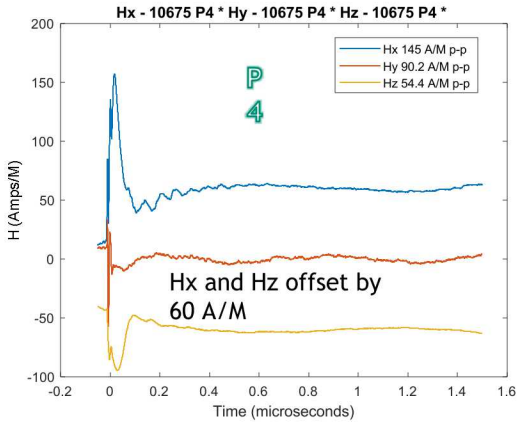

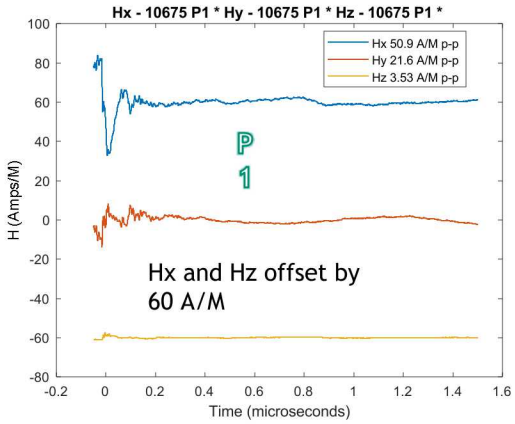

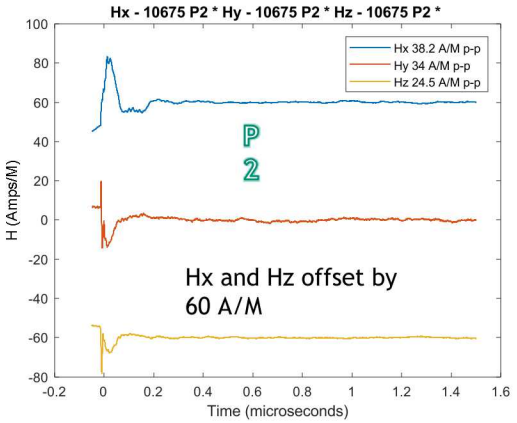

Shot 10690 – E-Fields

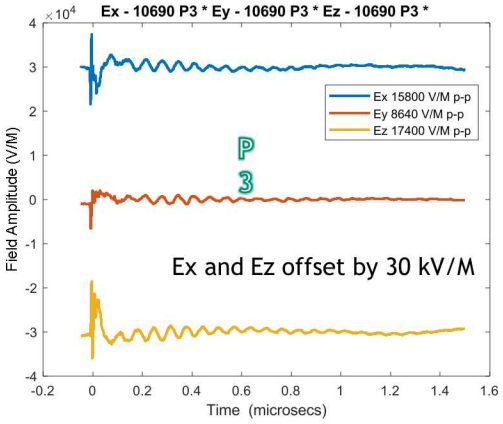

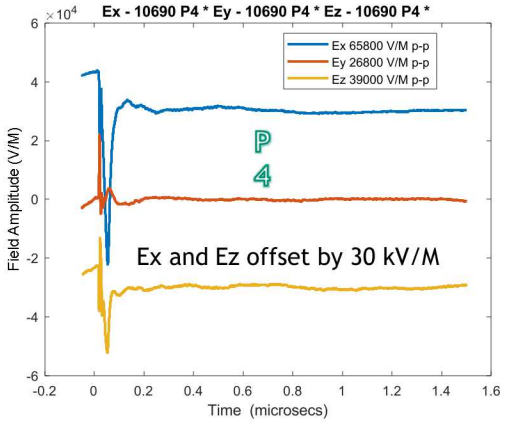

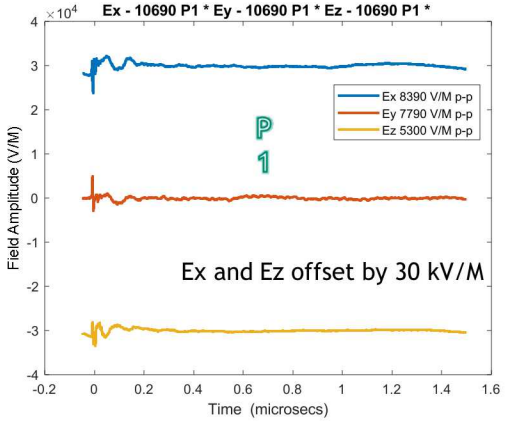

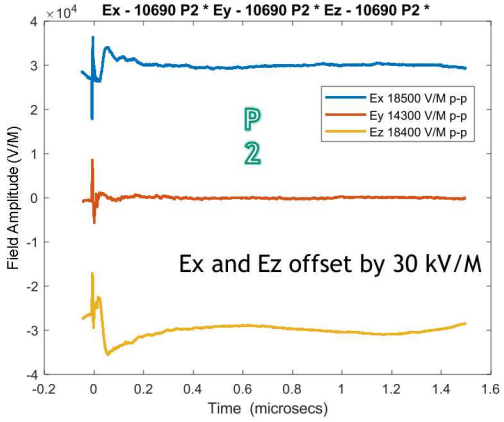

Shot 10690 – H-Fields

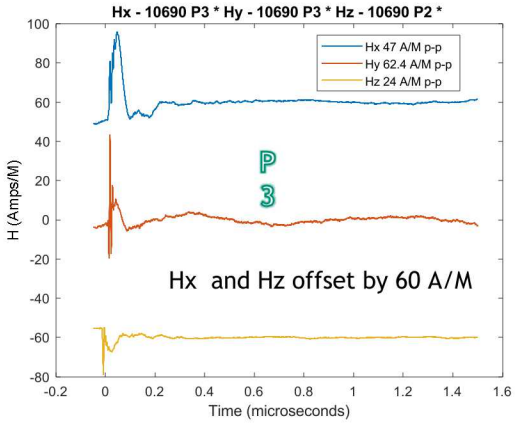

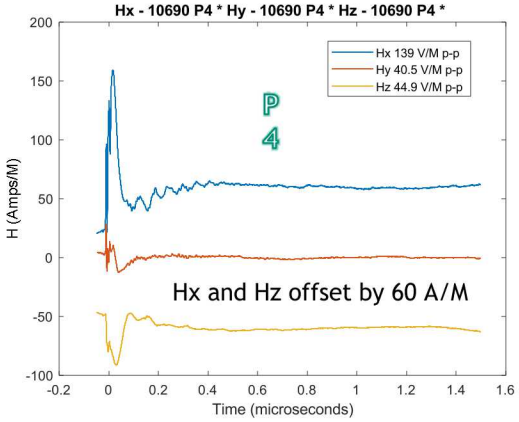

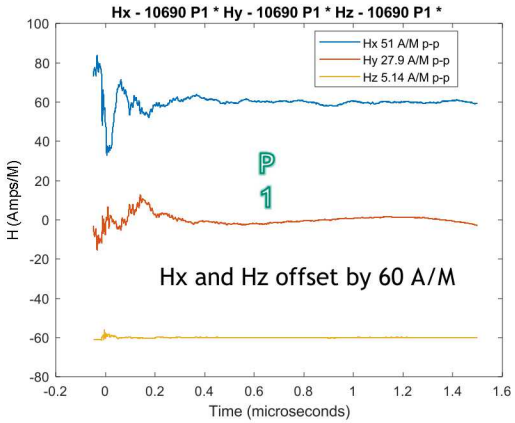

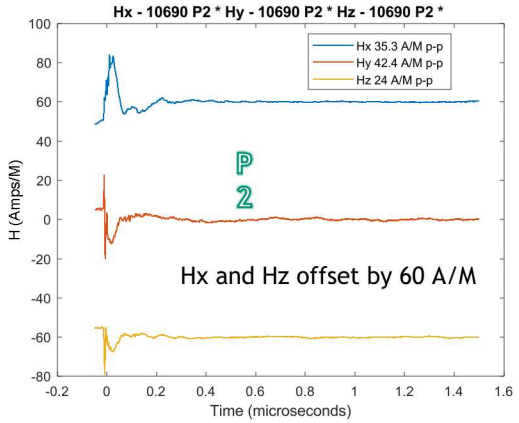

Shot 10705 – E-Fields

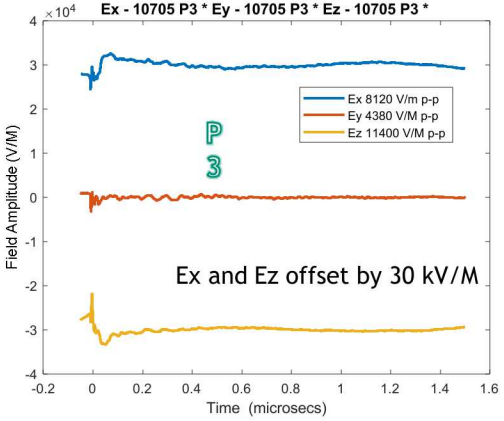

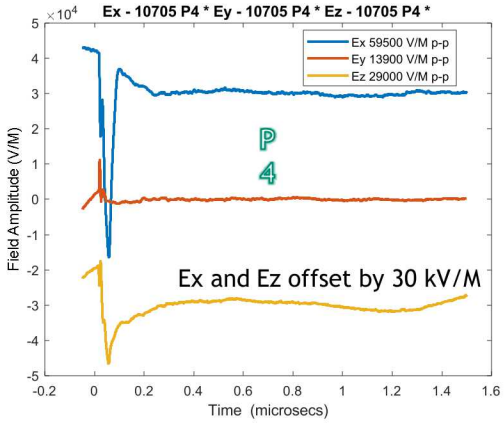

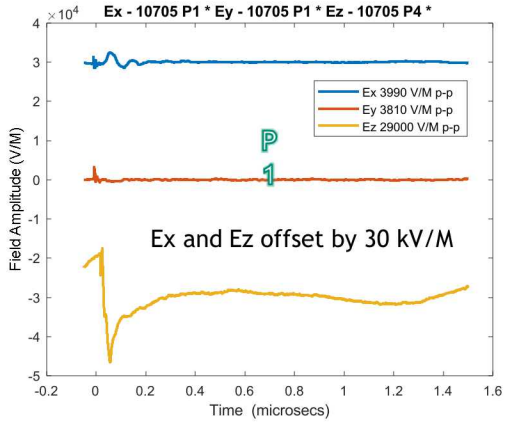

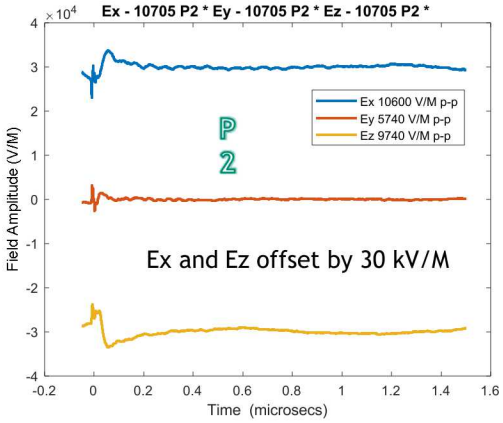

Shot 10705 – H-Fields

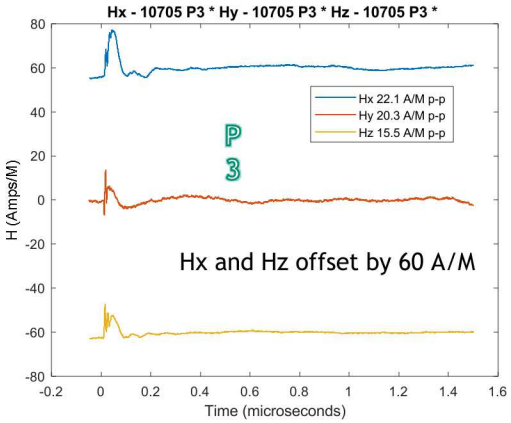

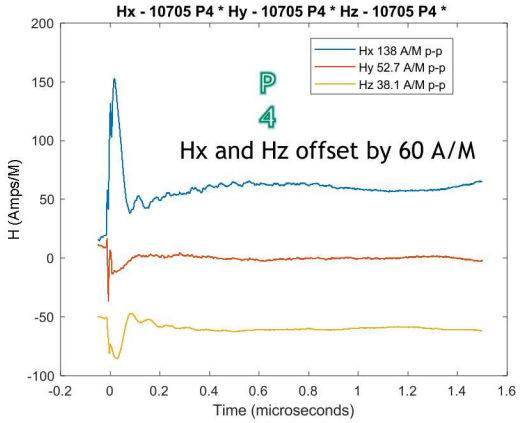

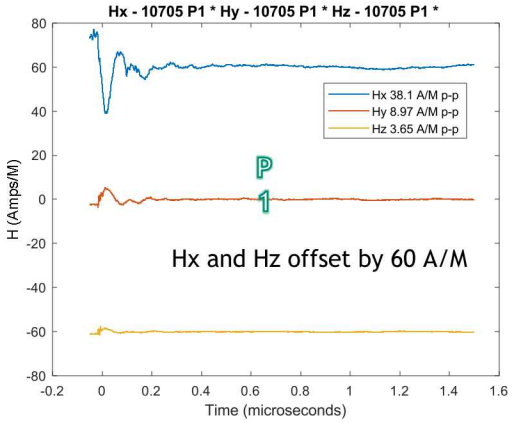

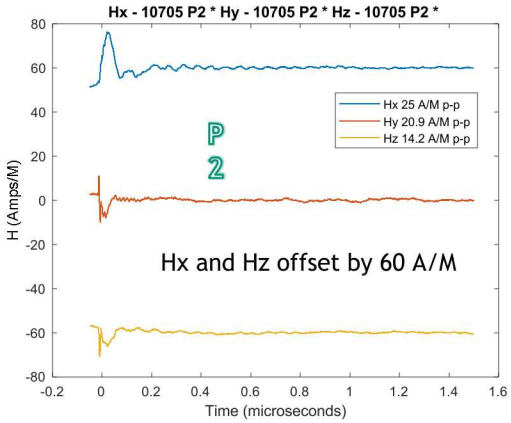

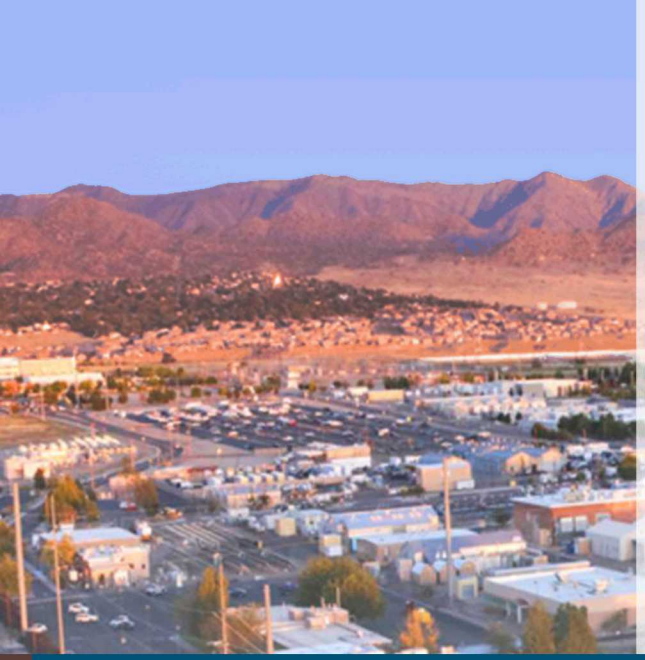

IV. Geometry and Response of Courtyard Sensors

Geometry & Response of Courtyard Sensors

- To determine if the source acted as a point source or a distributed source, the logarithm of the distance from the source head-plate to the field measurement was plotted against the logarithm of the amplitude of the field measurement

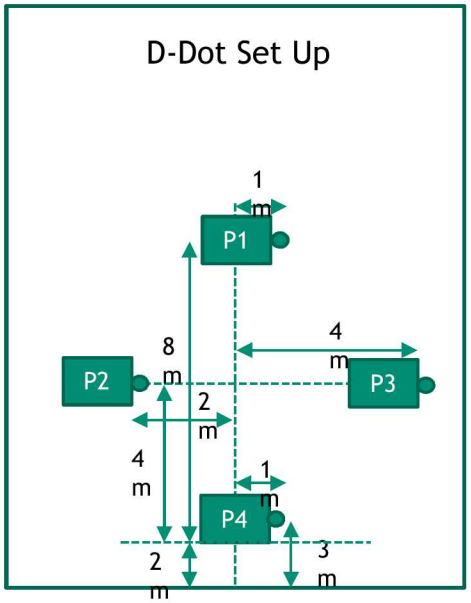

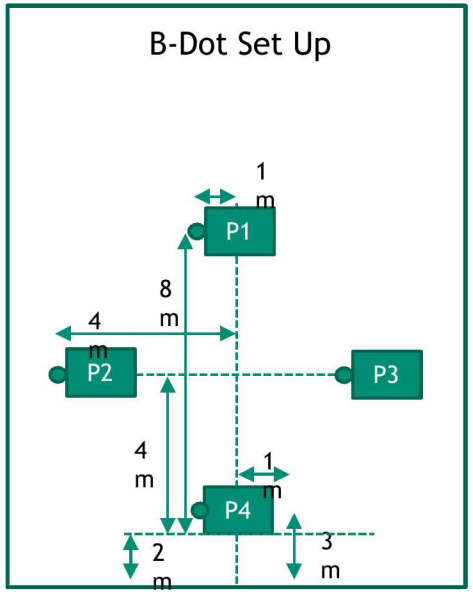

Sensor	Coord ln()	10664 ln()	10670 ln()	10675 ln()	10690 ln()	10705 ln()
P1 -Ex	2.31	8.29	8.99	8.58	9.03	8.29
P1-Hx	2.31	3.40	3.84	3.93	3.93	3.64
P2-Ex	1.84	8.52	10.06	10.26	9.83	9.27
P2-Hx	1.98	2.80	3.38	3.64	3.56	3.22
P3-Ex	1.98	8.53	10.11	10.15	9.67	9.00
P3-Hx	1.84	3.09	3.69	3.99	3.85	3.10
P4-Ex	1.15	10.04	10.43	10.62	11.09	10.99
P4-Hx	1.15	3.79	4.85	4.98	4.93	4.93

Inverse Square Law Distance Loss – Electric Fields

- If the source behaved as a point source the slope of the best fit straight line for these variables, would be -2. This is not true for the electric fields

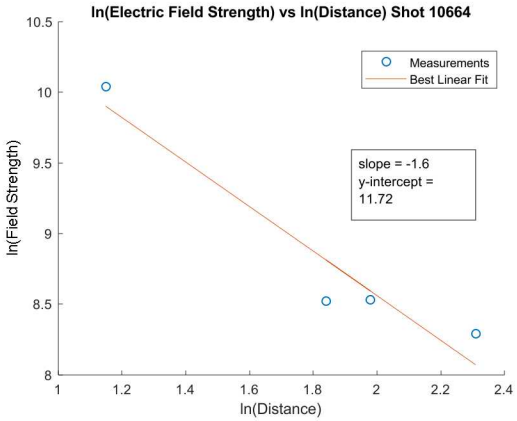

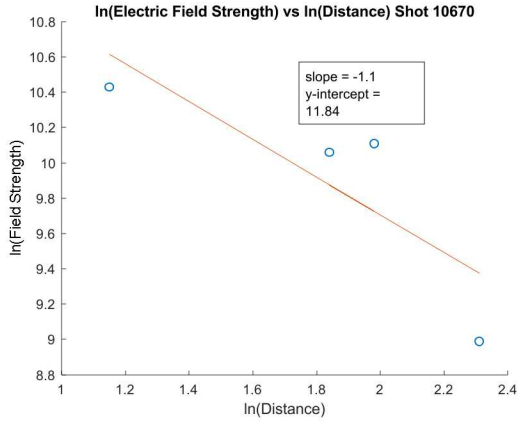

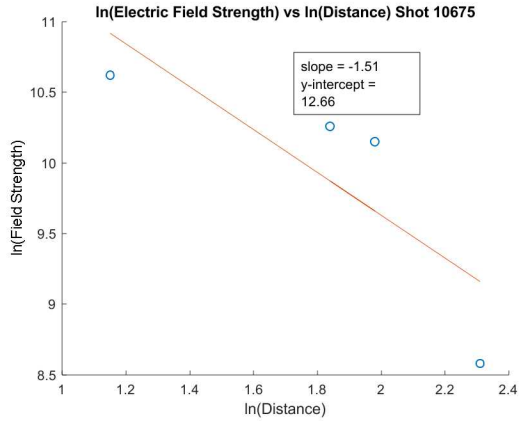

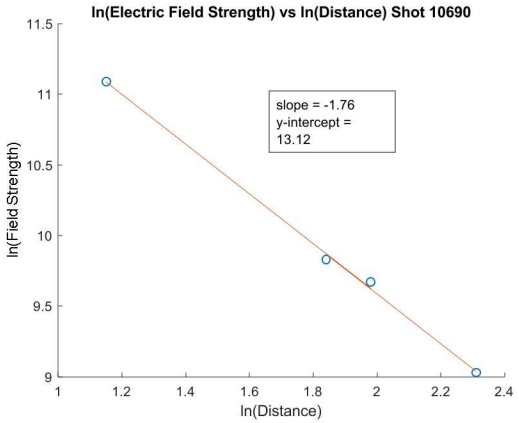

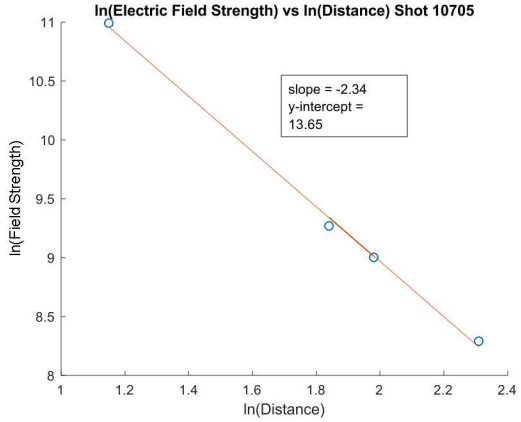

Inverse Square Law Distance Loss – Magnetic Fields

- If the source behaved as a point source the slope of the best fit straight line for these variables, would be -2. This is not true for the magnetic fields

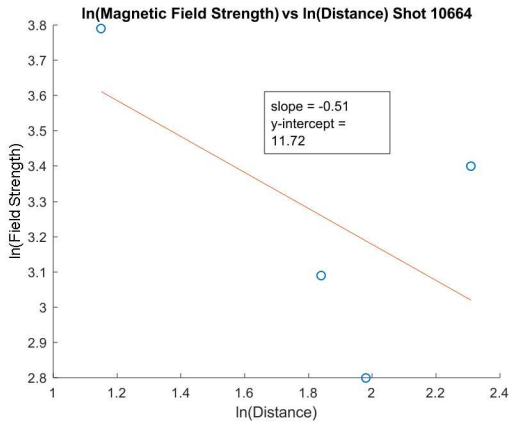

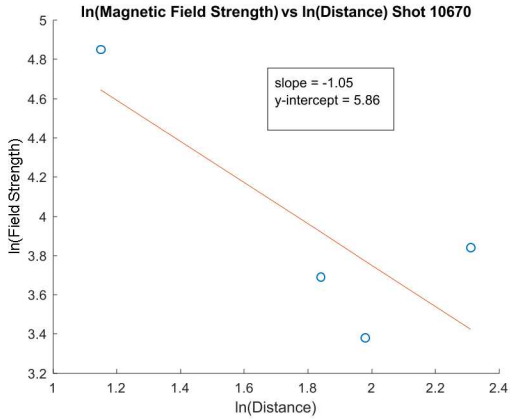

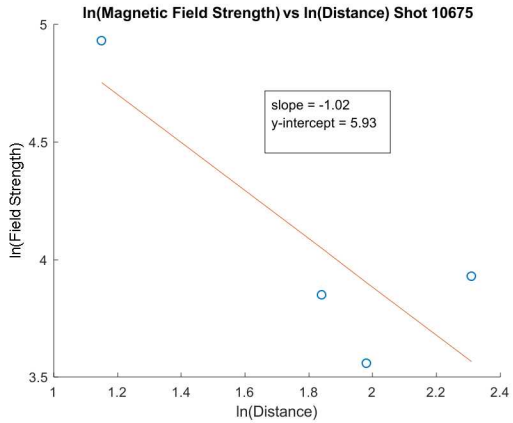

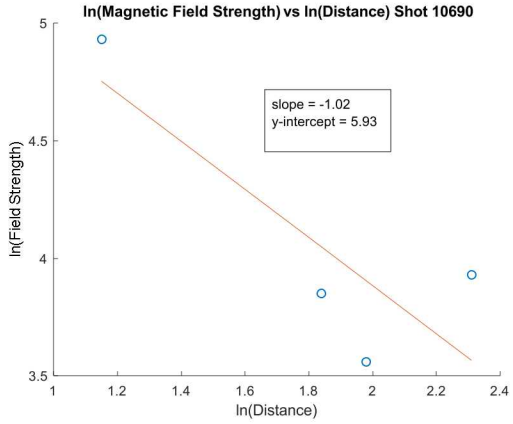

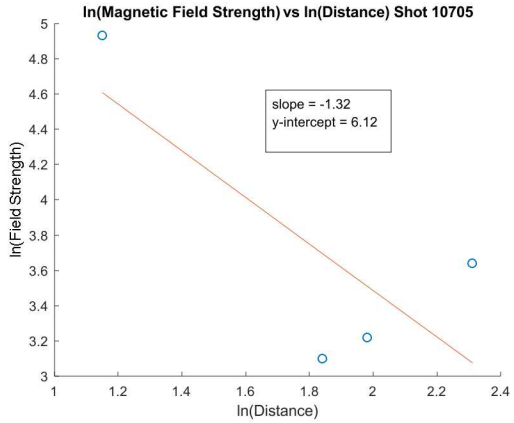

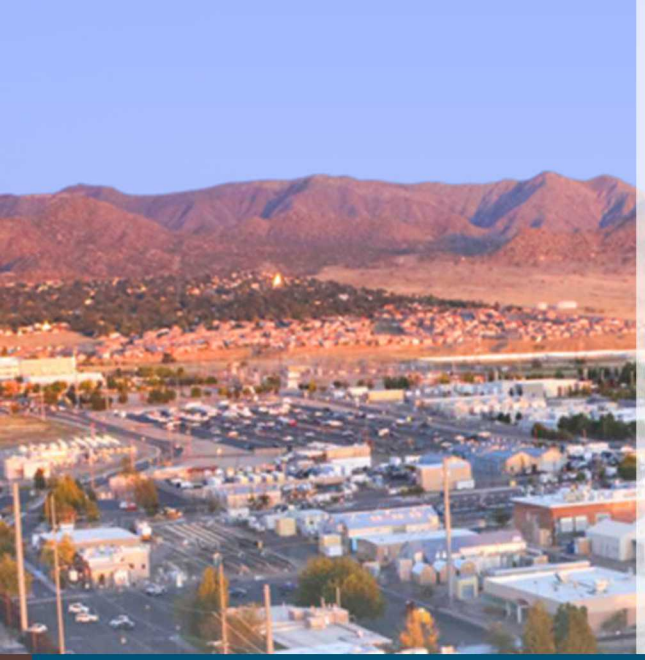

V. Field Predictability on Basis of Single Shot Response

Field Repeatability – Using Shot-to-Shot (S2S) Normalization

Certainly, the HERMES III is a Magnetic Insulated Line Oscillator (MILO) or Magnetically Insulated Transmission Line (MITL) and, as such, is certainly variable from shot-to-shot

- However, if one knew a single measurement on one platform for a given shot, does that define the other measurements that would be taken at other locations in the test volume?
- This, in a sense, would define the repeatability of the laboratory system
- This information could also be leverage in future tests to produce quick-look guidance with a goal of identifying questionable data early after the shot

Specifically, can the April 2018 data be such a potential "guide" for experimenters?

Shot Distribution Predictions

The first decision, is to identify a "reference" location; one that would likely be predictive for field amplitude and temporal characteristics throughout the laboratory volume.

- A likely candidate for this purpose would be the electric field location on Platform 4
  - It measures the field near the beam output of HERMES
  - Ex is the strongest field at this location
  - Thus the reference will be chosen at Ex-P4 (see slide 9)

A predictive field extrapolation will then be formed by a ratio of the frequency domain response of the Ex field on the other platforms to that on P4 and the reciprocal of this value becomes the predictive function for future fields, once the Ex-P4 response is measured

Shot Distribution Predictions, Part II

To test the potential utility of such a prediction process, we take the measured E-field data for shot 10690 (690), and try to predict these measurements using the data acquired during shots 10670 and 10675.

In equation form, the prediction function for shot 10670 is

$$PF_{670}^{690}(f)=\frac{\left|\tilde{E}_x^{P4,690}(f)\right|}{\left|\tilde{E}_x^{P4,670}(f)\right|}$$, and for shot 10675 is

$$PF_{675}^{690}(f)=\frac{\left|\tilde{E}_x^{P4,690}(f)\right|}{\left|\tilde{E}_x^{P4,675}(f)\right|},$$

Where

$\tilde{E}_x^{P4,690}(f)=\int_{-\infty}^{\infty} E_t^{P4,690}(t)e^{-i\omega t}\mathrm{dt}$; $\tilde{E}_x^{P4,670}(f)=\int_{-\infty}^{\infty} E_t^{P4,670}(t)e^{-i\omega t}\mathrm{dt}$

$\tilde{E}_x^{P4,675}(f)=\int_{-\infty}^{\infty} E_t^{P4,675}(t)e^{-i\omega t}\mathrm{dt}$

$\omega = 2\pi f; i = \sqrt{(-1)};$

Shot Distribution Predictions, Part III

Showing the process by example, the predicted Ey-field response on platform 3, $E_{y,pre}^{P3,690}$, for shot 690, using the measured data from shot 10670, would be

$$E_{y,pre}^{P3,690}(t) = \frac{1}{2\pi}\int_{-\infty}^{\infty} PF_{670}^{690}(f)\tilde{E}_{y,meas}^{P3,670}(f)e^{i\omega t}\,df$$

where

$\tilde{E}_{y,pre}^{P3,690}(f)$ = the predicted response for the E_y field for shot 690 on platform 3,

$\tilde{E}_{y,meas}^{P3,670}(f)$ = the measured response for the E_y field for shot 670 on platform 3, and

$PF_{670}^{690}(f)$ = the prediction function described in the previous slide.

The next few slides show the prediction functions used and the predictions compared to the actual measurements for shot 690.

Prediction Functions

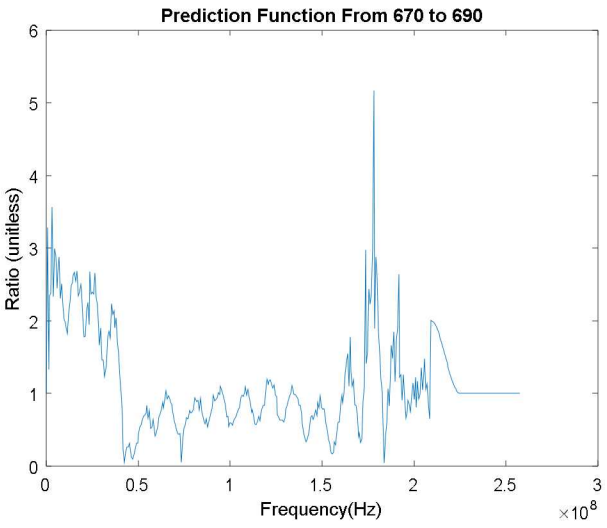

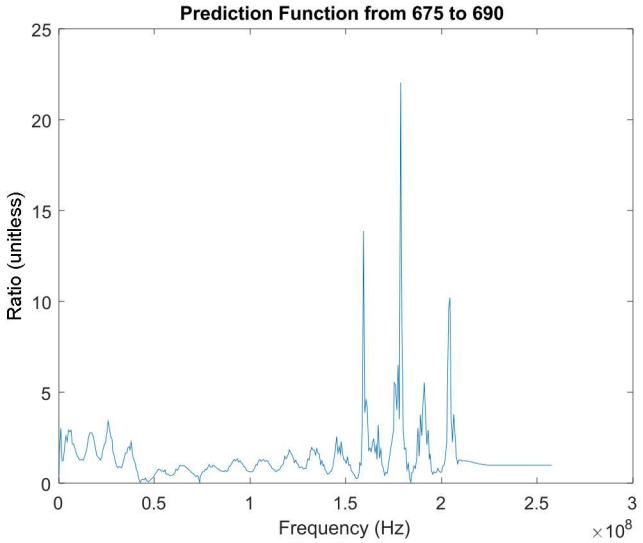

10670 Predictions vs 10690 Measurements

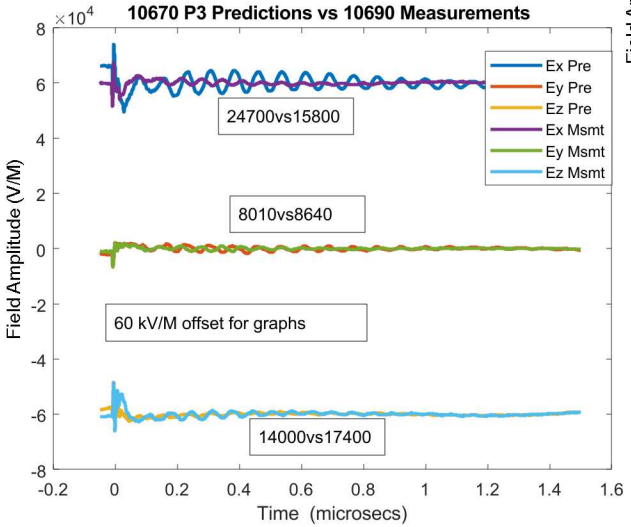

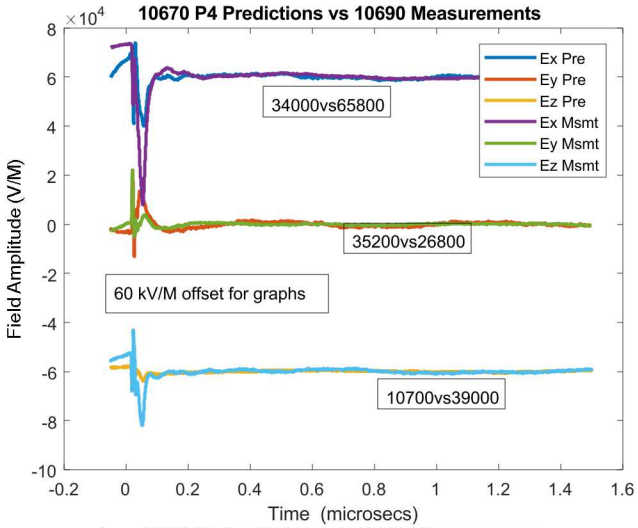

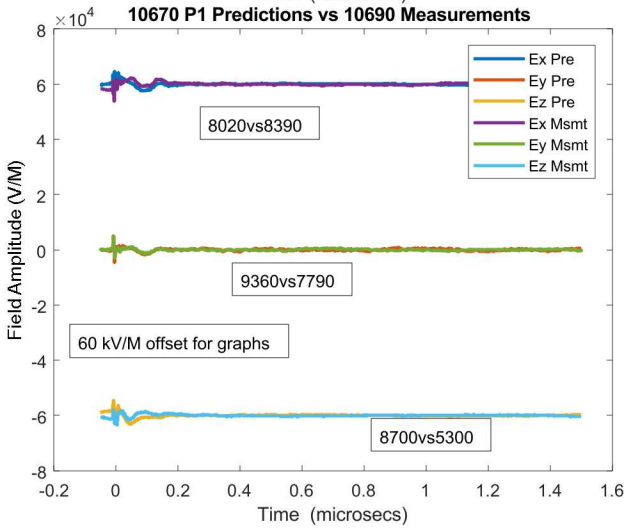

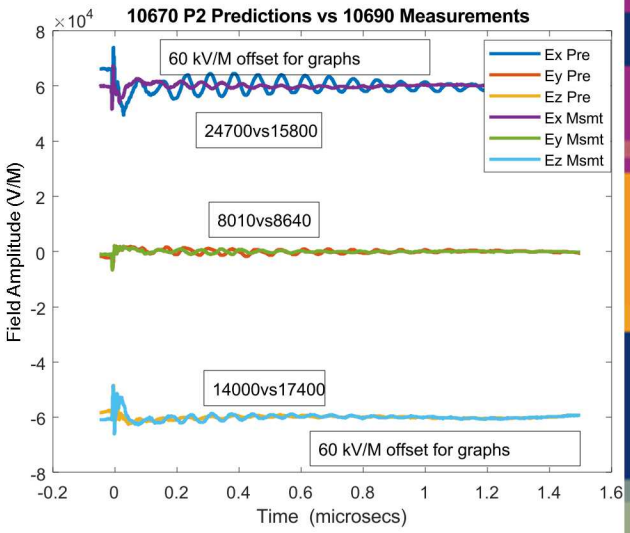

- The predictions for the larger amplitudes are less accurate

10675 Predictions vs 10690 Measurements

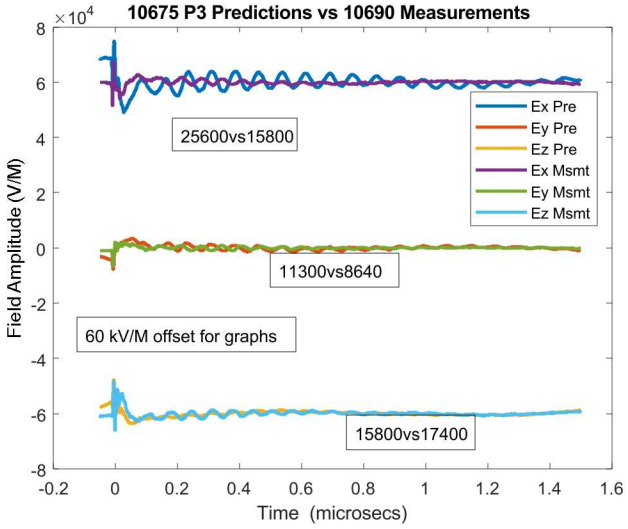

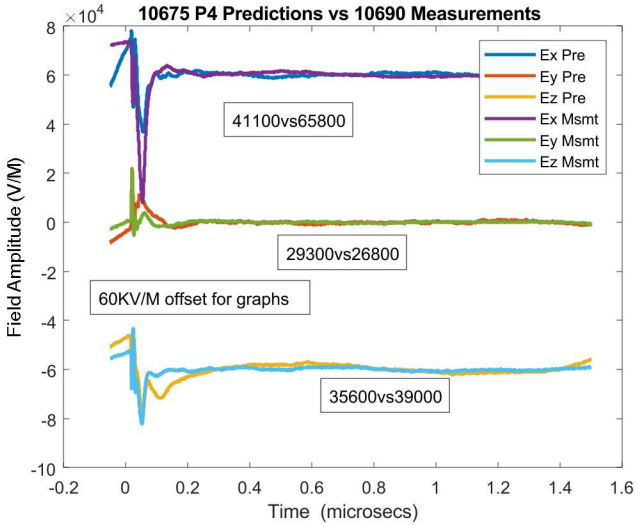

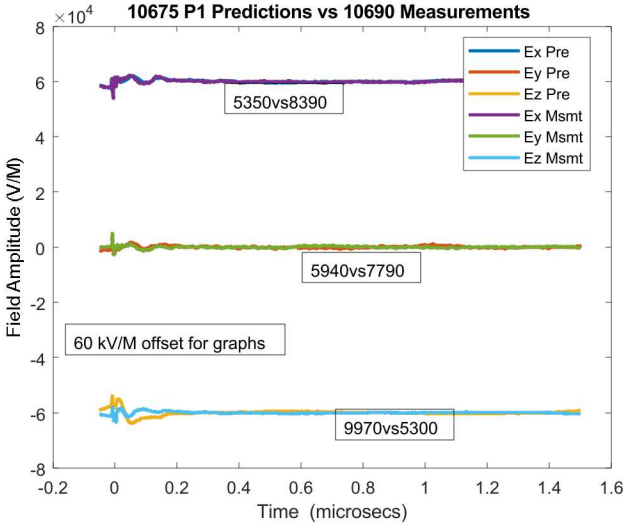

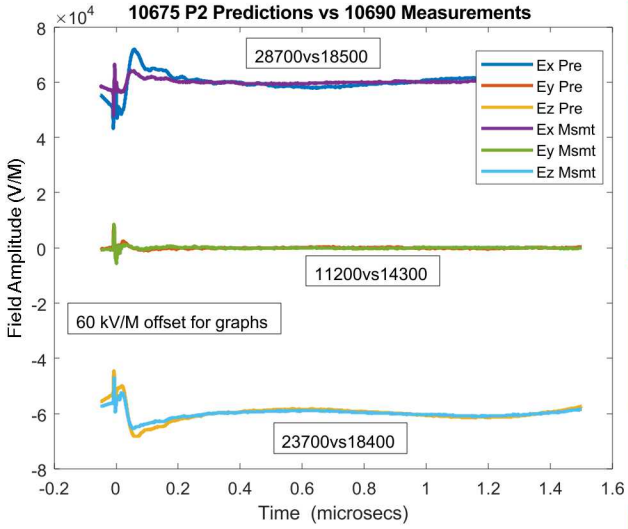

- The predictions for the larger amplitudes are less accurate

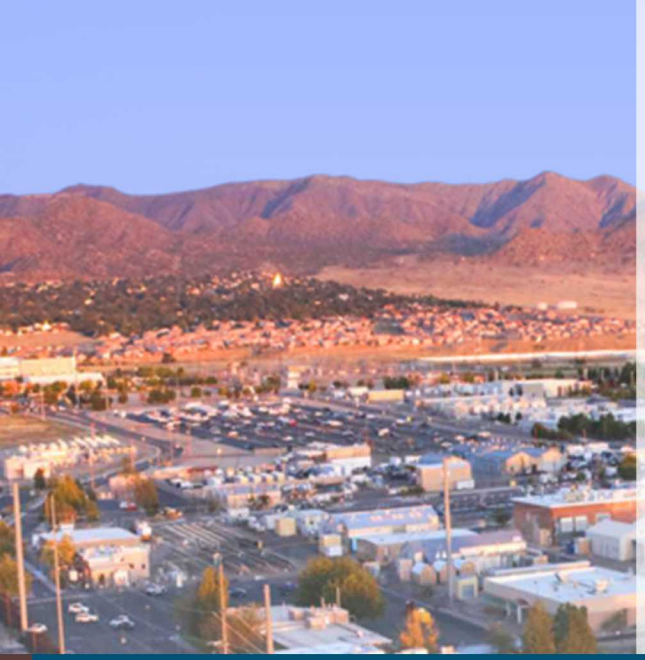

VI. Environmental Interference

Environmental Interference

The transportainer shown on the next page is located roughly 15 – 20 meters from Platform 3

The interference between reflections from the metal shelter and platform 3 will set up resonant responses in the 10 – 20+ MHz frequency ranges

These resonant responses are clearly seen in the frequency domain Fourier transforms of the time domain electric and magnetic fields measured on Platform 3 and to a lesser degree for those fields measured on Platform 2 (see curves that follow)

The Transportainer is 15-20 Meters from Sensors on Platform 3

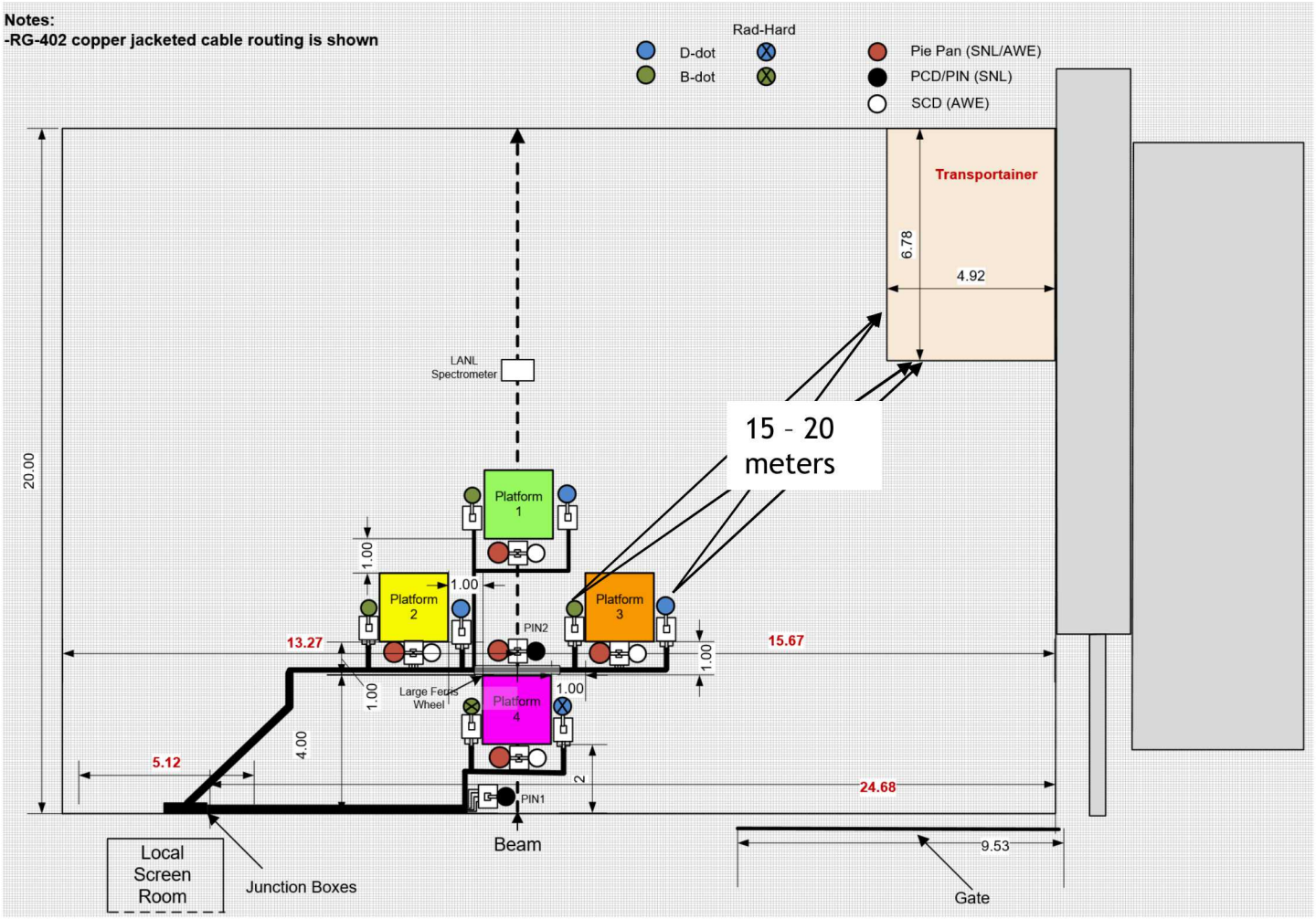

E-Field Frequency Response on Platforms 2-3

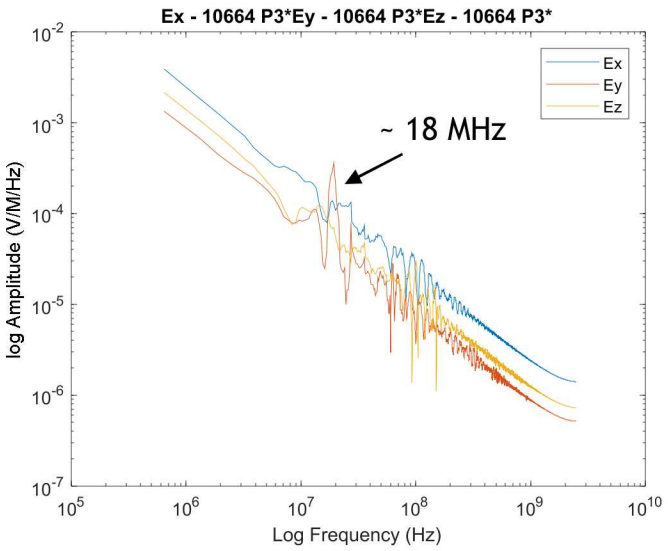

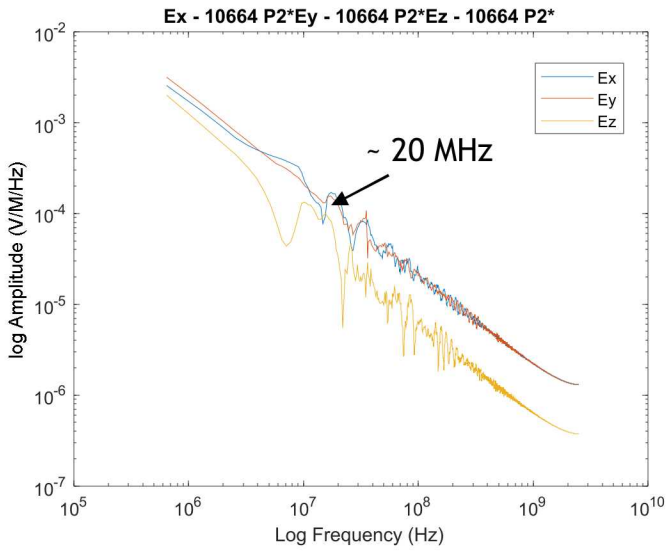

H-Field Frequency Response on Platforms 2-3

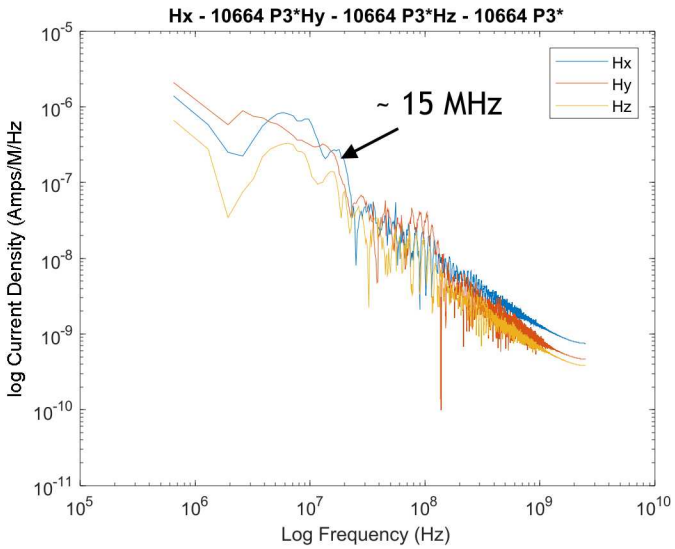

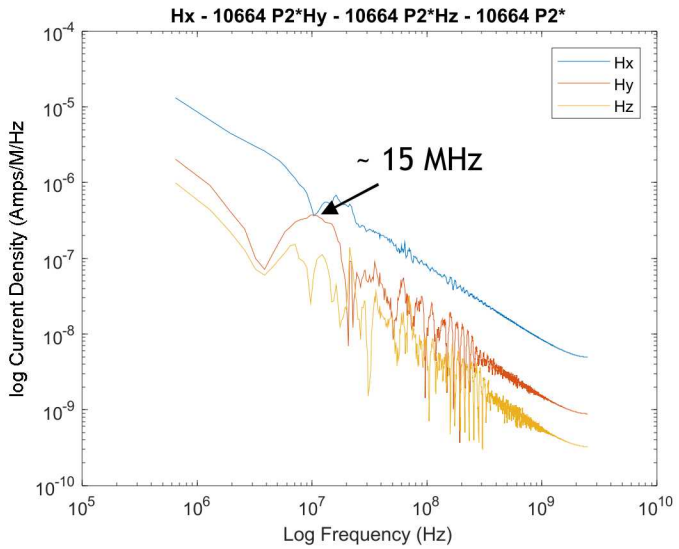

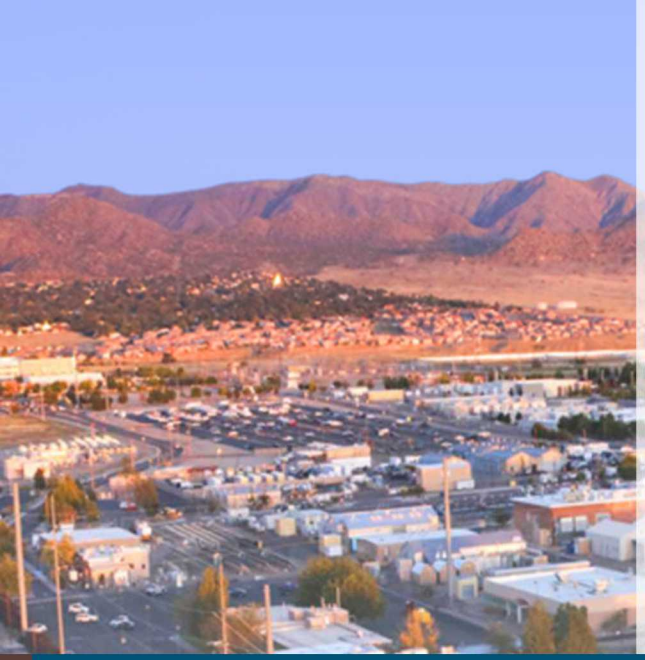

VII. Shielding Effectiveness

Shielding Effectiveness Measures

Shot Number	Orientation	Shielding Degradations	Shielding Effectiveness Ratios
10670	CS, Cone rotated but || to beam, CN parallel to beam	None	CN-ER/P3Ez; CN-EA/P3Ex or P3Ey CSI-EA/P4ExorP4Ey; CSI-ER/P4Ez CSI-JA/CSO-JA; CSI-JR/CSO-JA AF-EA/P2Ex or Ey; AF-ER/Ez
10675	CS, Cone rotated but || to beam, CN parallel to beam	Opened slit 6 on CS; Open slot Aperture on Cone ; Removed forward nose section from CN	CN-ER/P3Ez; CN-EA/P3EX or P3Ey CSI-EA/P4ExorP4Ey; CSI-ER/P4Ez CSI-JA/CSO-JA; CSI-JR/CSO-JA AF-EA/P2Ex or Ey; AF-ER/Ez
10690	CS and CN parallel to beam; Cone open slot pointed to beam,	Opened slit 6 on the CS. Changed aperture on AF (AWE frustrum-open slot) and moved aperture facing beam. Removed Forward nose section from CN.	CN-ER/P3Ez; CN-EA/P3EX or P3Ey CSI-EA/P4ExorP4Ey; CSI-ER/P4Ez CSI-JA/CSO-JA; CSI-JR/CSO-JA AF-EA/P2Ex or Ey; AF-ER/Ez
10705	CN, cylinder and Cone rotated to be perpendicular to beam, cone placed vertical with nose up	Opened slit 1 and 6 on CS; Open slot Aperture on Cone, aperture facing centerline ; Removed forward nose section and aft port from CN	CN-ER/P3Ez; CN-EA/P3EX or P3Ey CSI-EA/P4Ez; CSI-ER/P4ExorP4Ey CSI-JA/CSO-JA; CSI-JR/CSO-JA AF-EA/P2Ez ; AF-ER/Ex or Ey

Shielding Effectiveness (SE)

The first comparisons will be done on shot 670
- All intentional apertures closed

Two electric field SEs were calculated using internal CN fields and externally measured electric fields
- CN-ER against P3-Ez
- CN-EA against P3-Ex

Two electric field and two surface current SEs were calculated on the Cylinder, CS, using associated inside and outside electric fields and surface currents
- CSI-EA against P4-Ex and CSI-ER against P4-Ez
- CSI-JA against CSO-JA and CSI-JR against CSO-JA

Two electric field SEs were calculated with internal AF fields and associated external fields
- AF-EA against P2-Ex and AF-ER against P2-Ez

These measurements will be repeated for Shots 10675, 10690 and 10705, where intentional shielding degradations are introduced

Shot 10670 (CN) Shielding Effectiveness Measurements

All intentional apertures closed

Two generic types of SE measured with the E-fields on CN
- CN-ER against P3-Ez and CN-EA against P3-Ex

Note that the P3-Ex fields drive the internal fields stronger (i.e. the Ey field has a larger SE values).

Note also that the averaging process yields small SE values

Note that the SE decreases with increasing frequency up to ~ 500 MHz, and then becomes a function of the aperture coupling to the inside of the body

Also note that the body resonances of 1E8, 2E8, 3E8, 4E8 and 5E8 Hz are apparent in the SE measures; also note the interference from the data van reflections are also discernable

From here on, the large window gaussian averaging will be used

CN(670) Internal Fields Against External Drivers

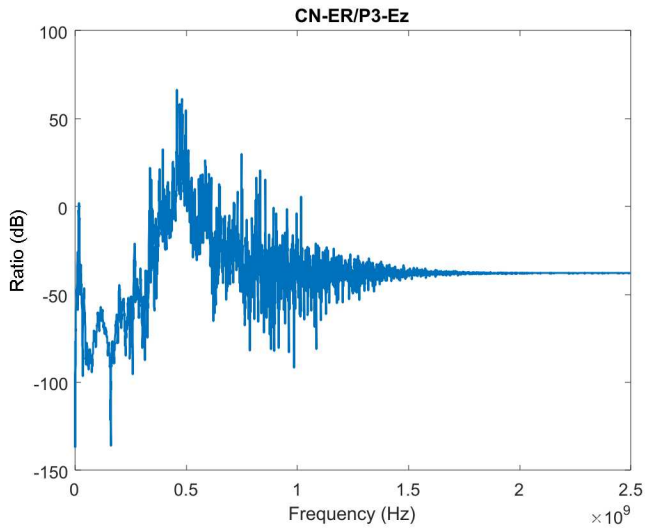

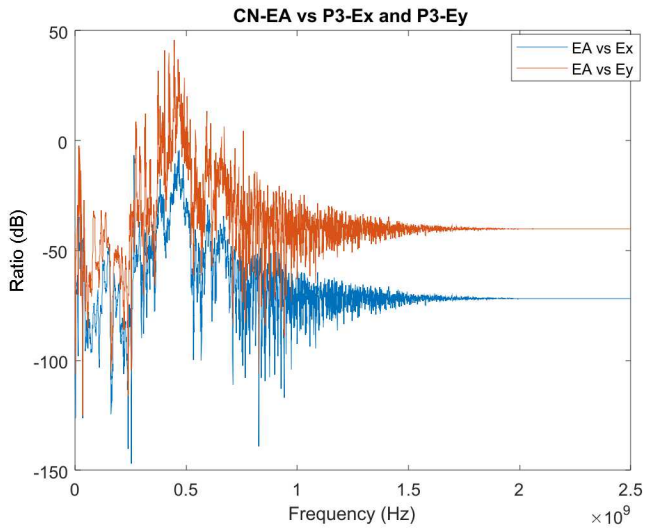

Reducing Noise CN(670)

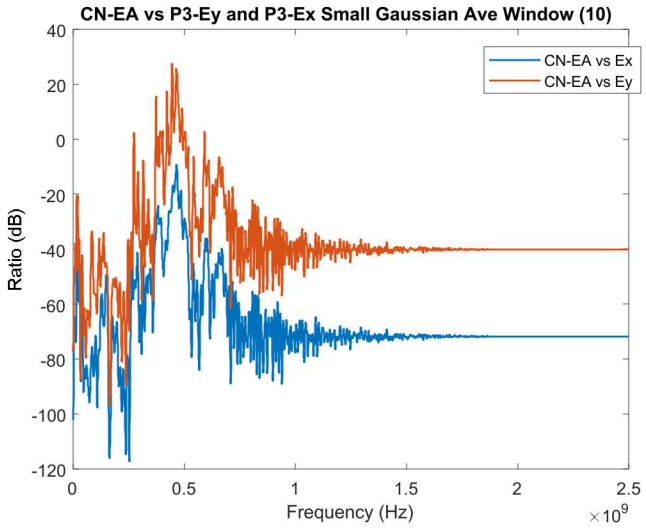

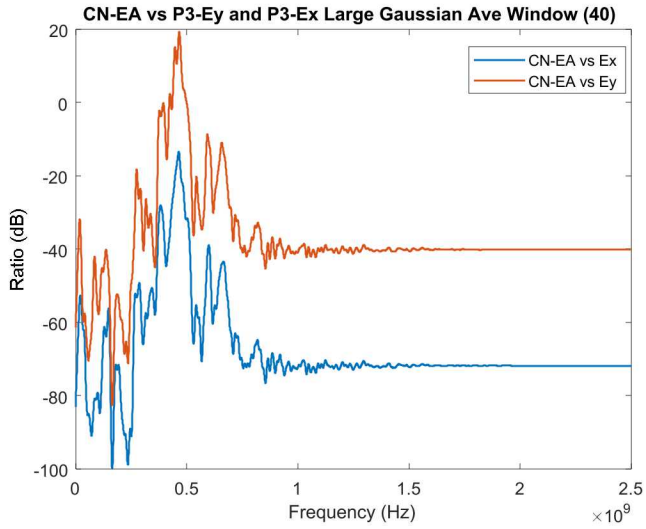

CN Internal Fields Against External Drivers & Reducing Noise (670)

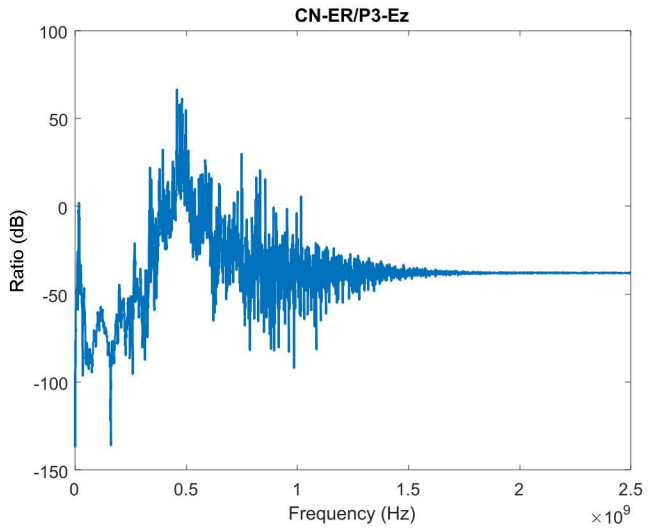

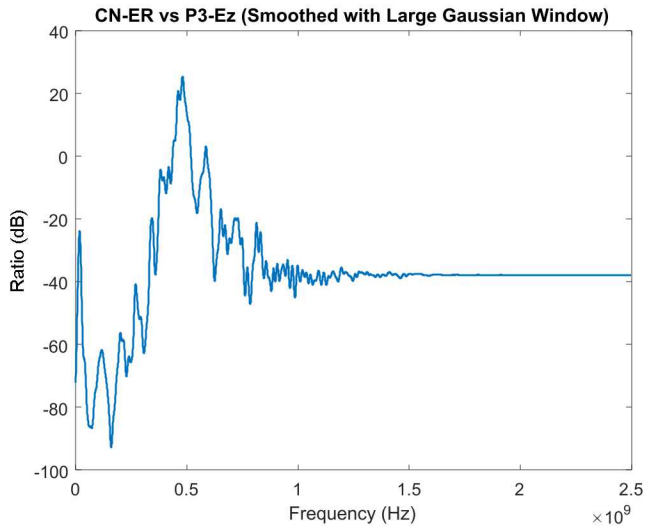

E-Field SE for CN (670)

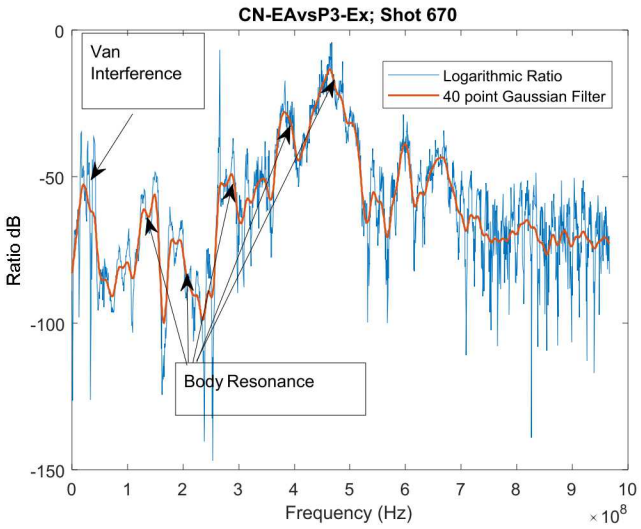

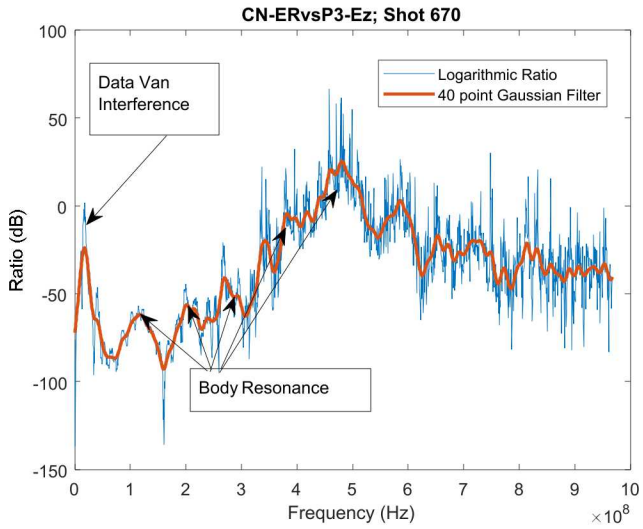

Shot 10670 (CS) Shielding Effectiveness Measurements

All intentional apertures closed

Four generic types of SE calculations using fields and surface currents on CS were generated

- CSI-EA against P4-Ex and CSI-ER against P4-Ez
- CSI-JA against CSO-JA and CSI-JR against CSO-JA

Note that some odd body resonances are apparent in the SE measures; also note that the circumferential resonance is visible, especially in the surface current SE measurements

E-Field SE for CS (670)

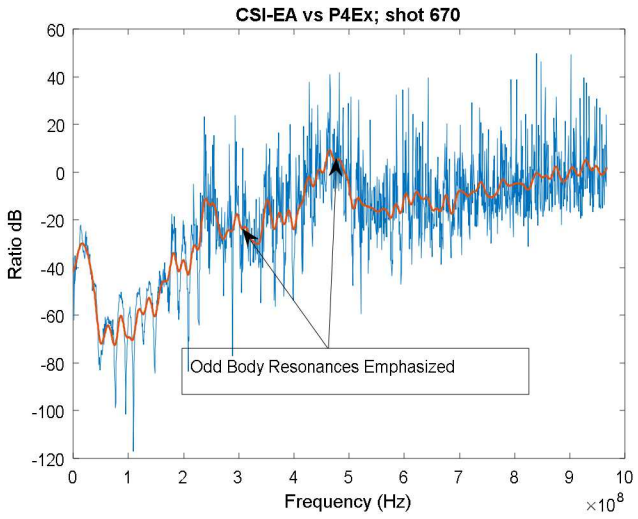

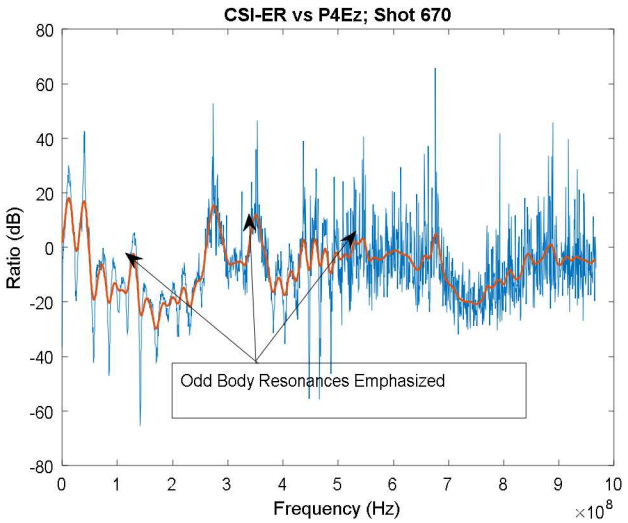

Current Density SE for CS (670)

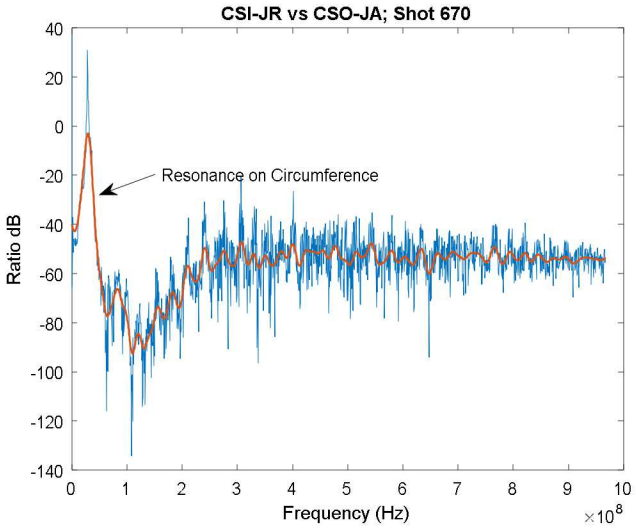

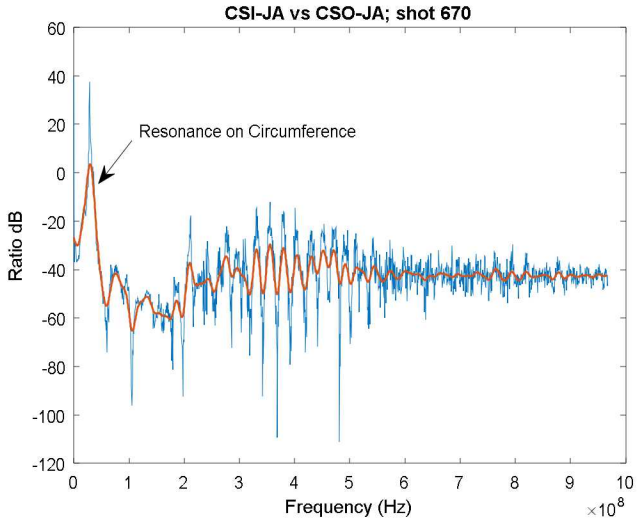

Shot 10670 (AF) Shielding Effectiveness Measurements

All intentional apertures closed

Two generic types of SE measured with the E-fields on AF

- AF-EA against P2-Ex
- AF-ER against P2-Ez

E-field SE AF (670)

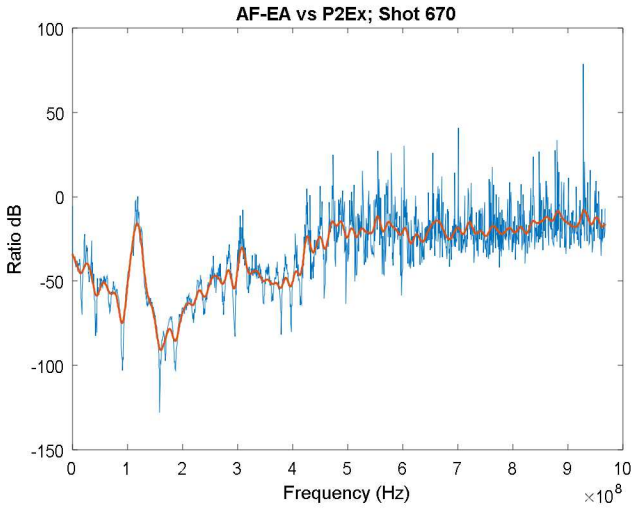

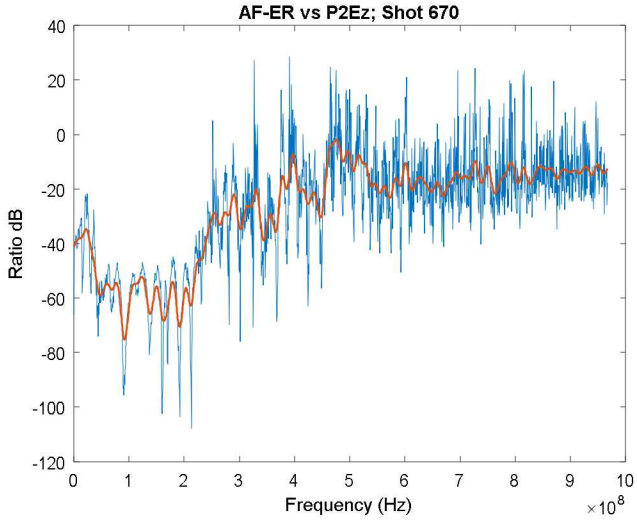

Shot 10675, 10670 Shielding Effectiveness Measurements

Intentional Degradations for this shot
- Removed forward nose section from CN
- Opened slit 6 on CS;
- Open slot Aperture on AF ;

Two electric field SEs were calculated using internal CN fields and externally measured electric fields
- CN ER against P3-Ez
- CN EA against P3-Ex

Two electric field and two surface current SEs were calculated on the Cylinder, CS, using associated inside and outside electric fields and surface currents
- CSI-EA against P4-Ex and CSI-ER against P4-Ez
- CSI-JA against CSO-JA and CSI-JR against CSO-JA

Two electric field SEs were calculated with internal AF fields and associated external fields
- AF-EA against P2-Ex and AF-ER against P2-Ez

E-Field SE for CN (675, 670)

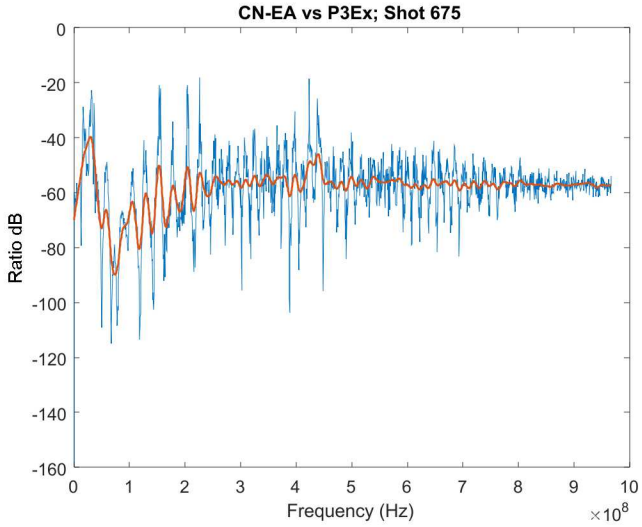

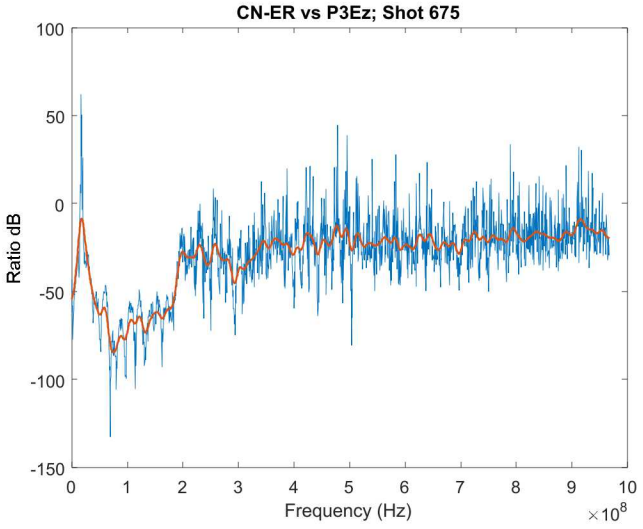

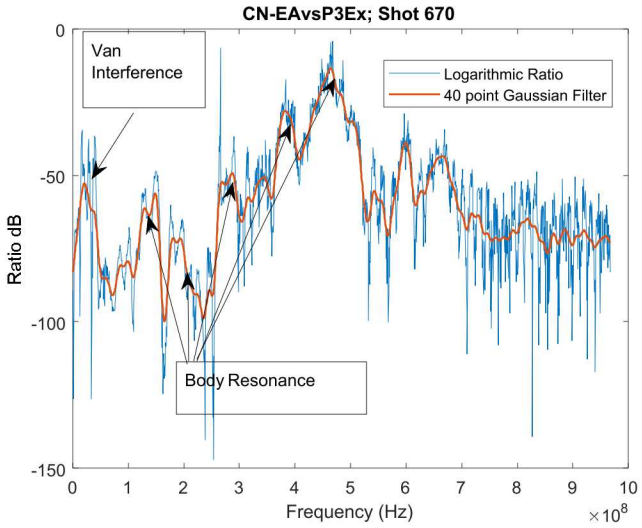

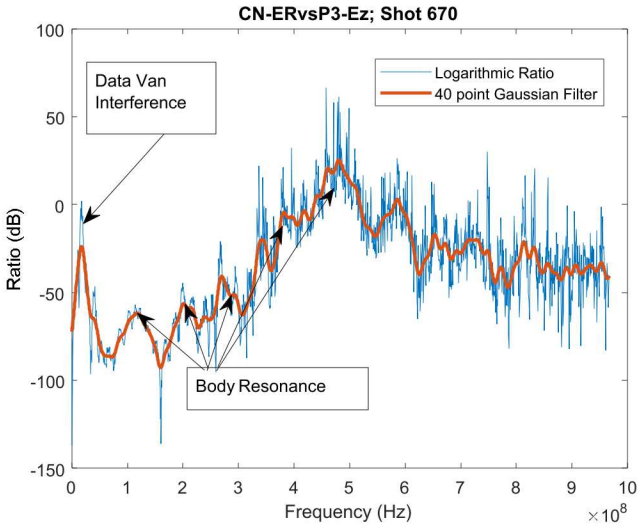

E-Field SE for CS (675, 670)

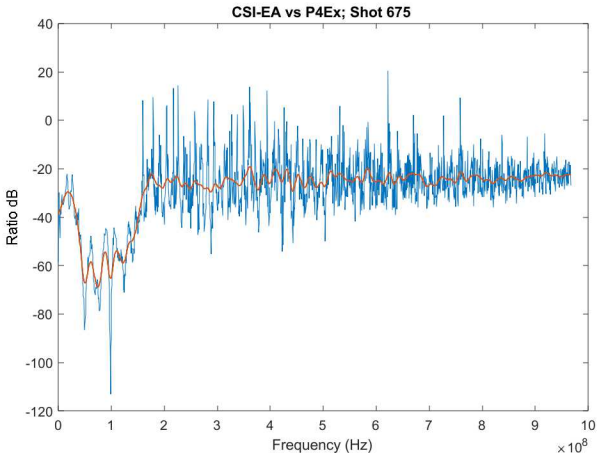

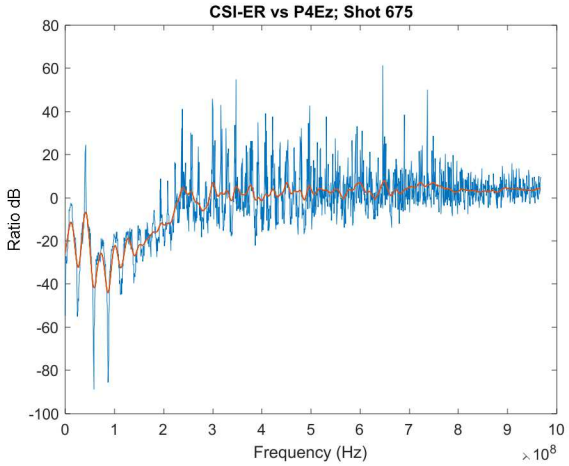

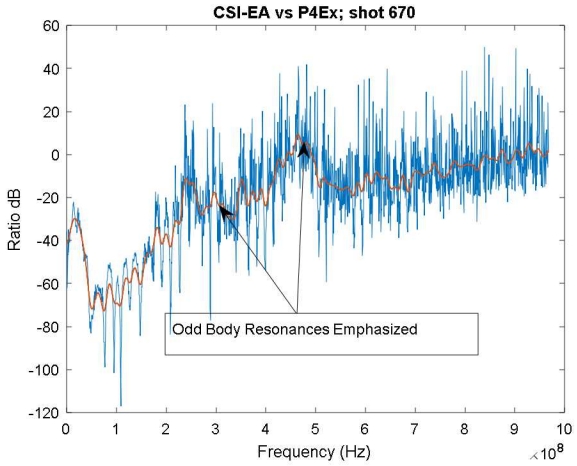

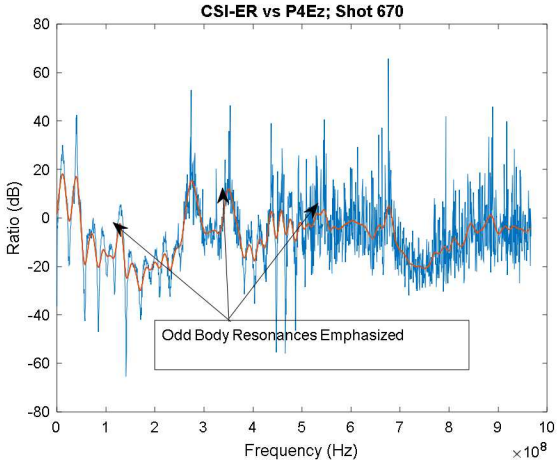

Current Density SE for CS (675, 670)

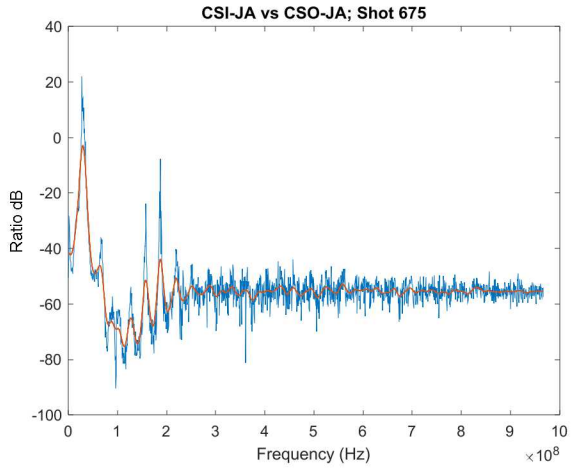

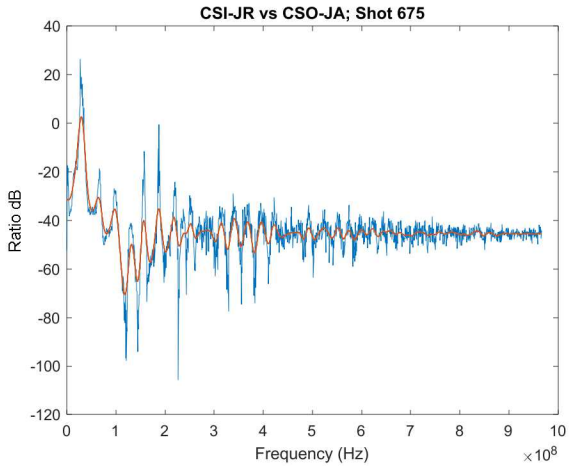

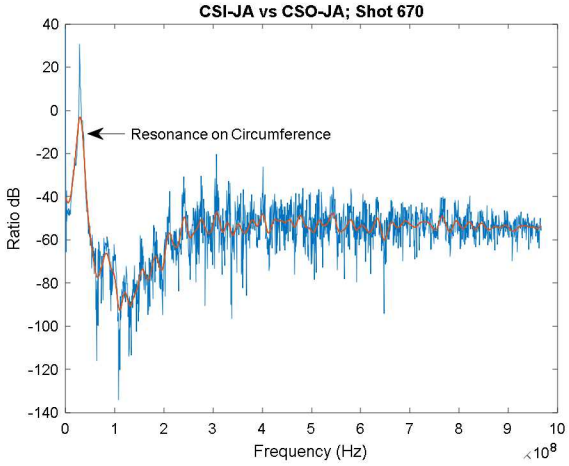

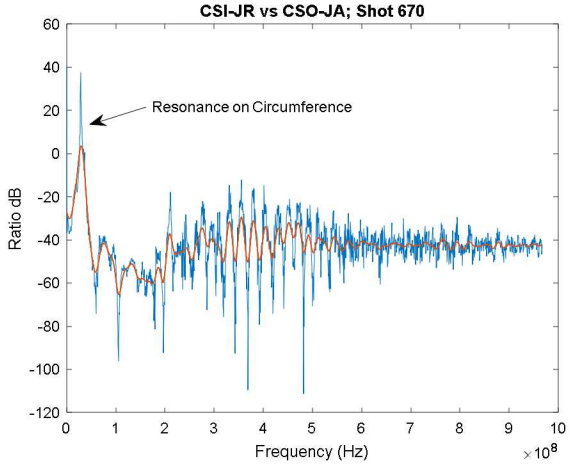

E-field SE AF (675, 670)

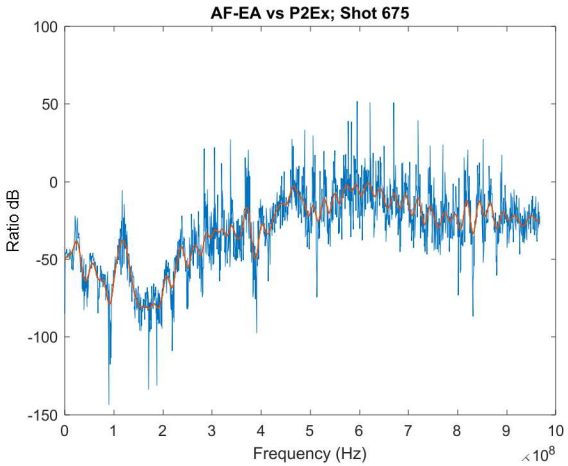

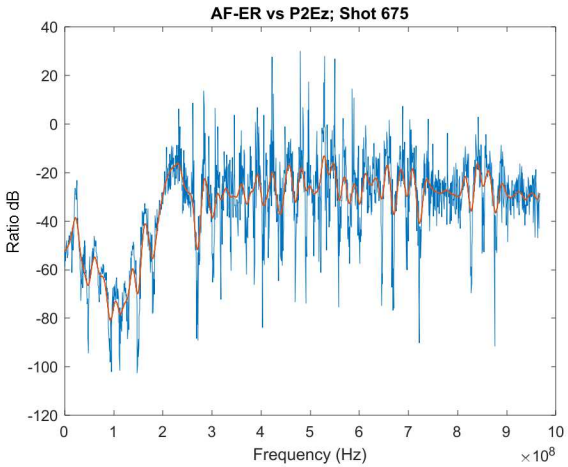

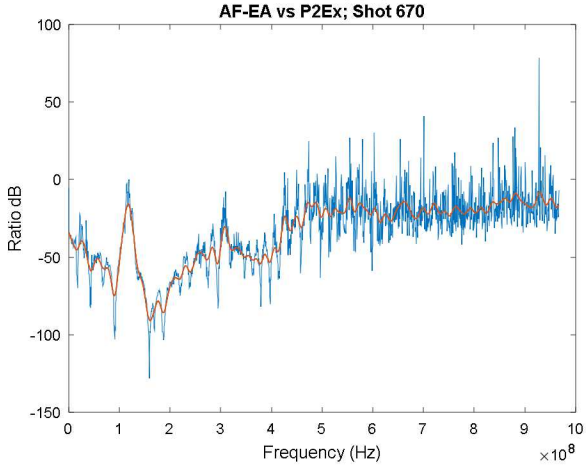

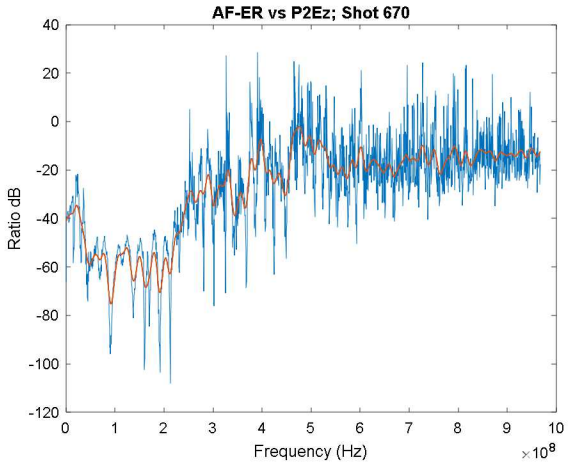

Shot 10690, 10670 Shielding Effectiveness Measurements

Intentional Degradations for this shot
- Removed forward nose section from CN
- Opened slit 6 on CS; CS/AF cone body parallel to beam
- Open slot Aperture on AF and aperture facing beam

Two electric field SEs were calculated using internal CN fields and externally measured electric fields
- CN-ER against P3-Ez
- CN-EA against P3-Ex

Two electric field and two surface current SEs were calculated on the Cylinder, CS, using associated inside and outside electric fields and surface currents
- CSI-EA against P4-Ex and CSI-ER against P4-Ez
- CSI-JA against CSO-JA and CSI-JR against CSO-JA

Two electric field SEs were calculated with internal AF fields and associated external fields
- AF-EA against P2-Ex and AF-ER against P2-Ez

E-Field SE for CN (690, 670)

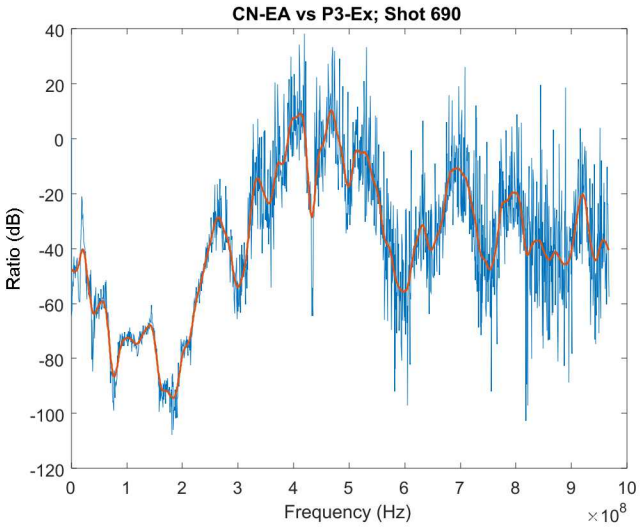

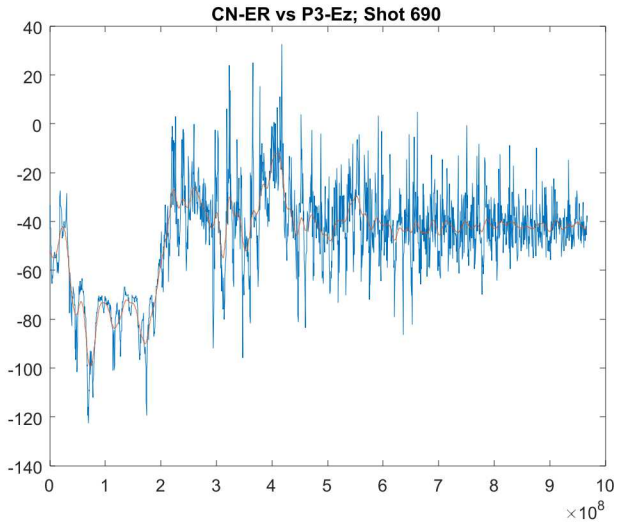

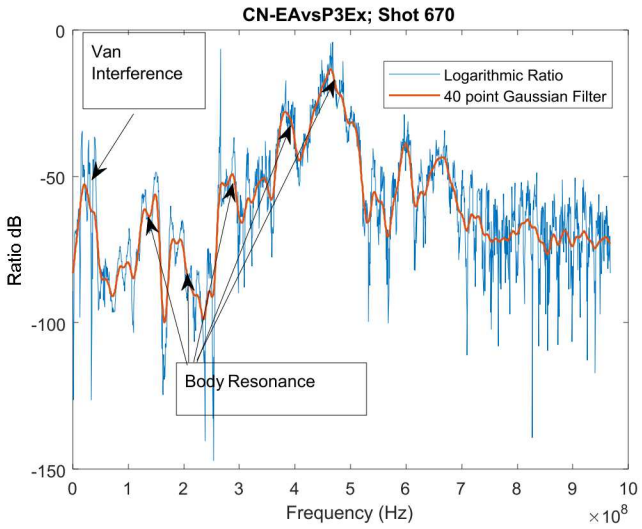

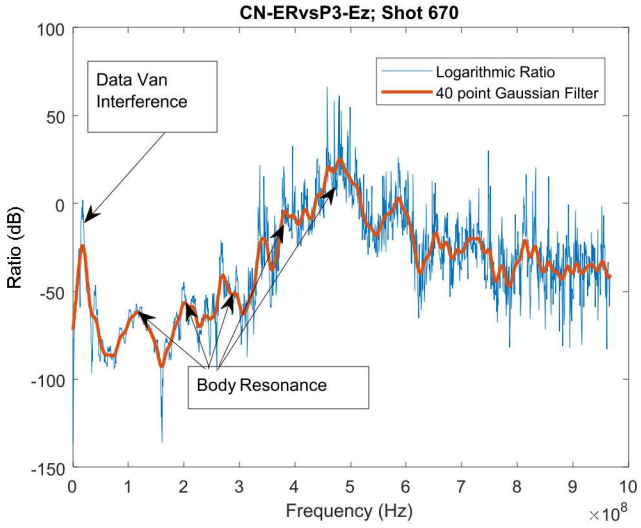

E-Field SE for CS (690, 670)

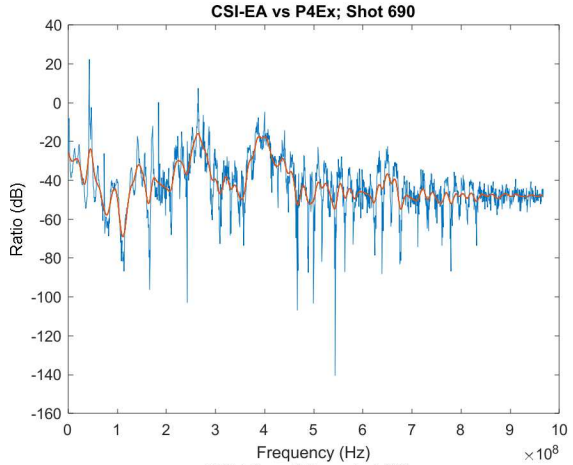

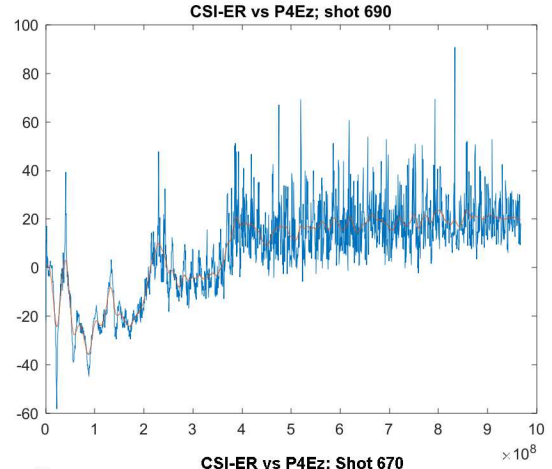

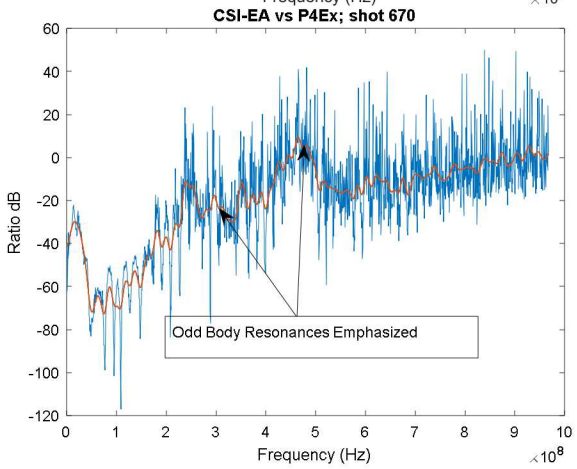

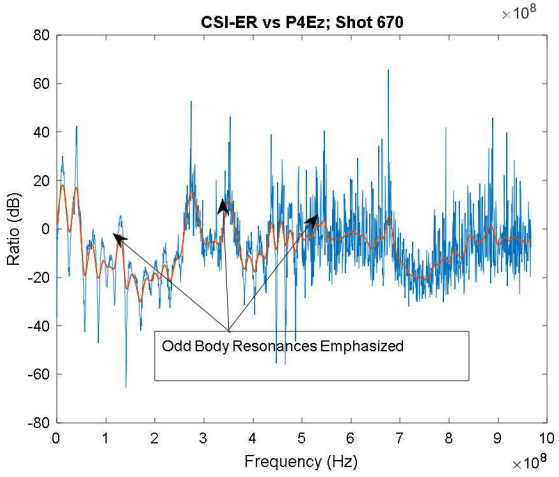

Current Density SE for CS (690, 670)

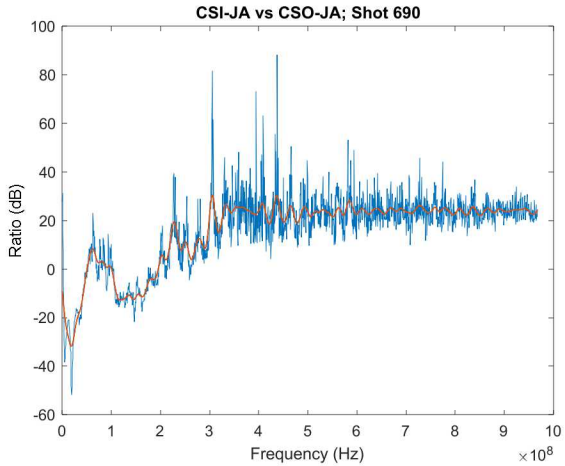

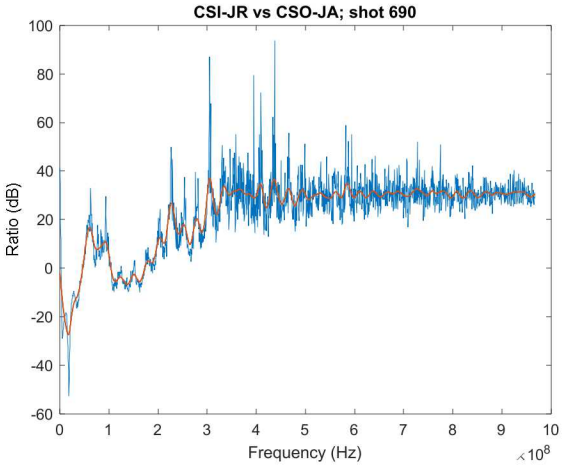

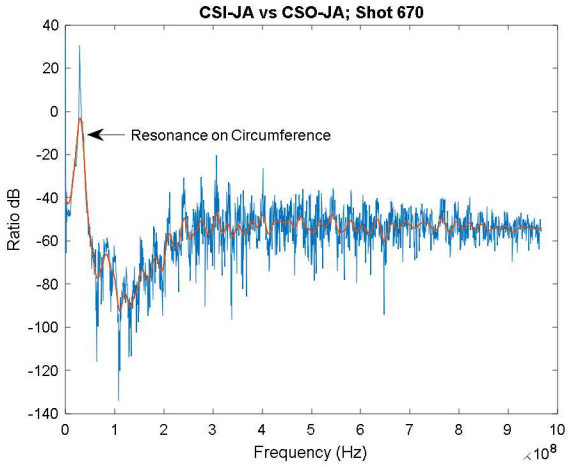

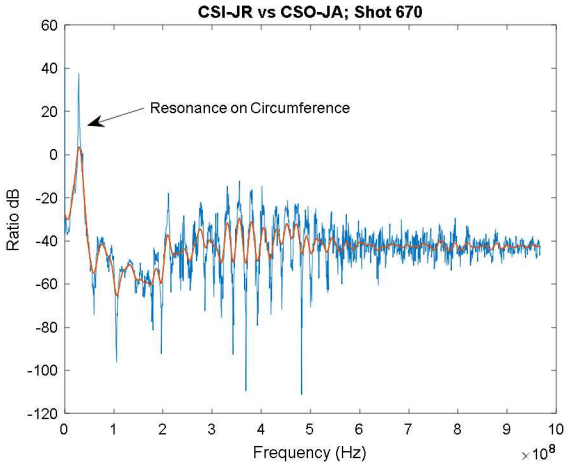

E-field SE AF (690, 670)

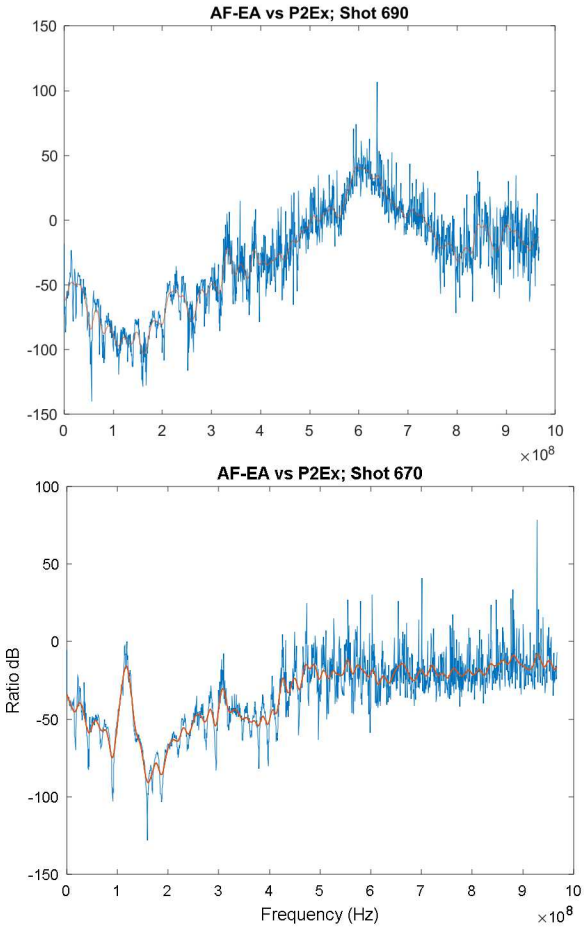

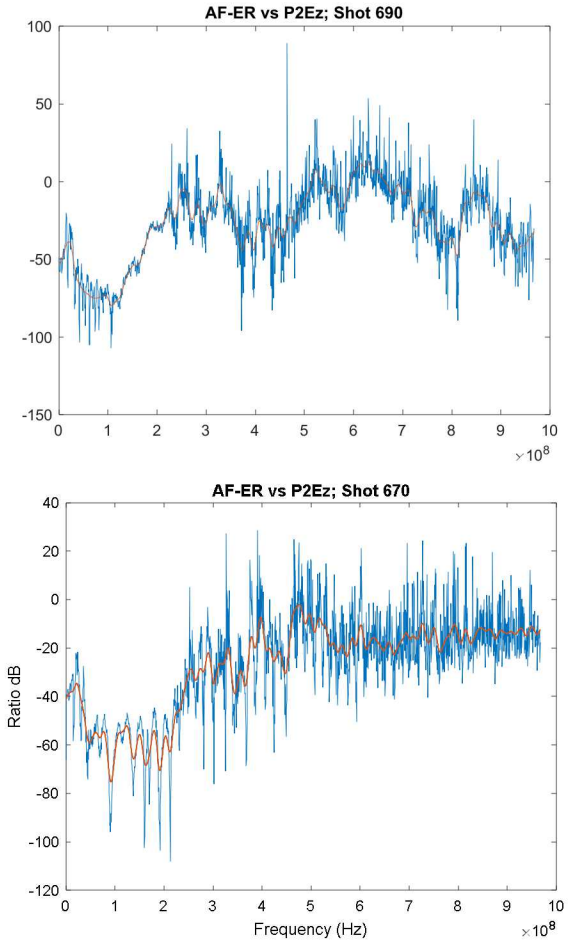

Shot 10705, 10670 Shielding Effectiveness Measurements

Intentional Degradations for this shot
- Removed forward nose section from CN
- Opened slit 6 on CS; CS/AF cone body parallel to beam
- Open slot Aperture on AF and aperture facing beam

Two electric field SEs were calculated using internal CN fields and externally measured electric fields
- CN-ER against P3-Ez
- CN-EA against P3-Ex

Two electric field and two surface current SEs were calculated on the Cylinder, CS, using associated inside and outside electric fields and surface currents
- CSI-EA against P4-Ex and CSI-ER against P4-Ez
- CSI-JA against CSO-JA and CSI-JR against CSO-JA

Two electric field SEs were calculated with internal AF fields and associated external fields
- AF-EA against P2-Ex and AF-ER against P2-Ez

E-Field SE for CN (705, 670)

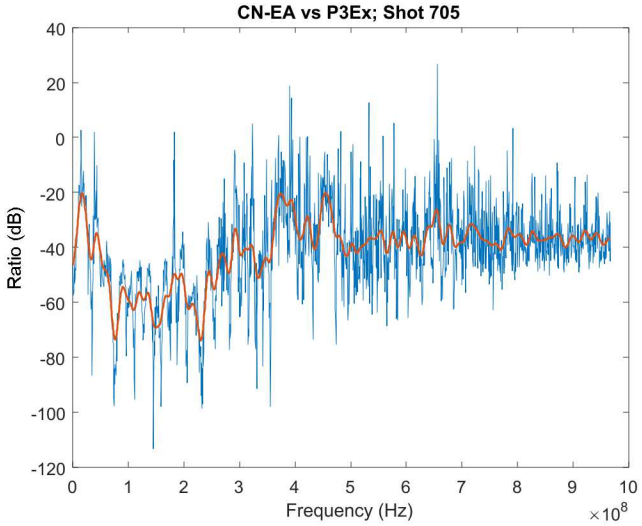

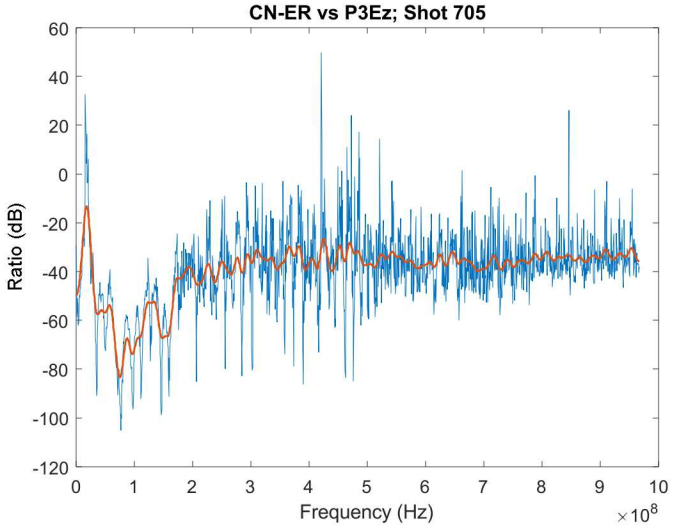

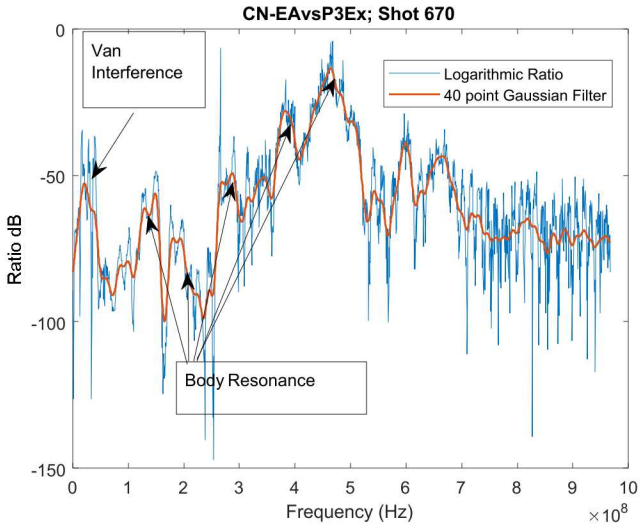

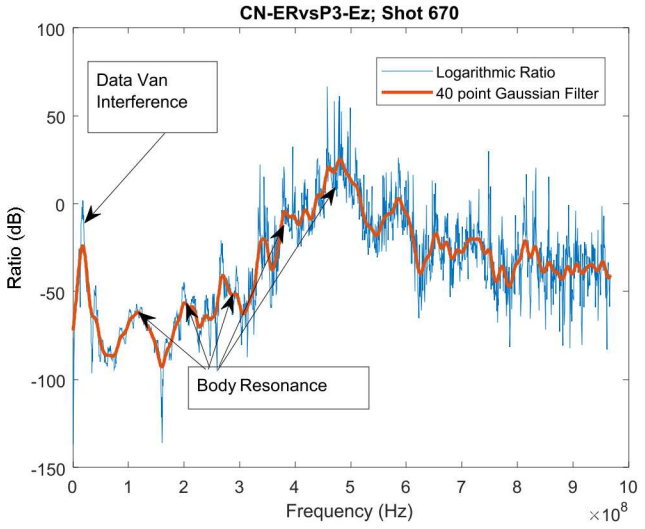

E-Field SE for CS (705, 670)

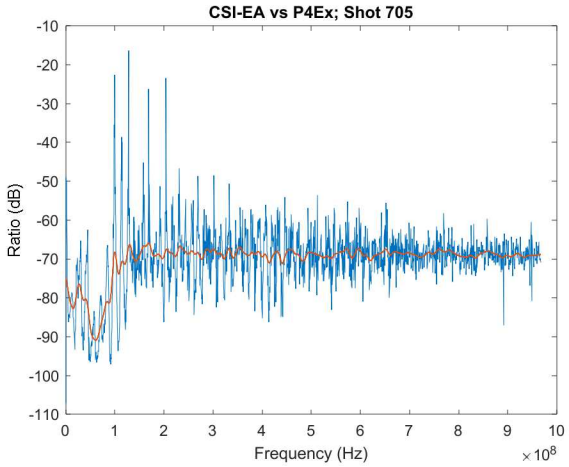

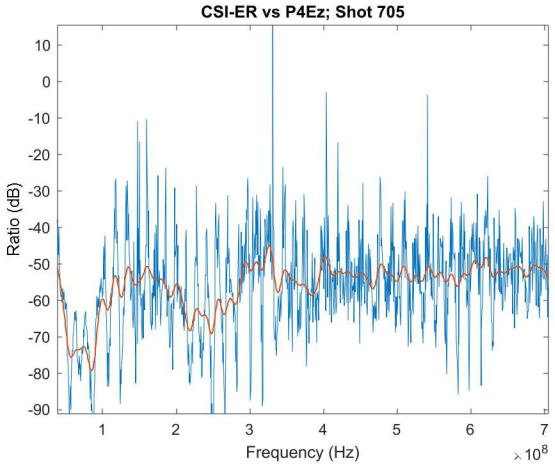

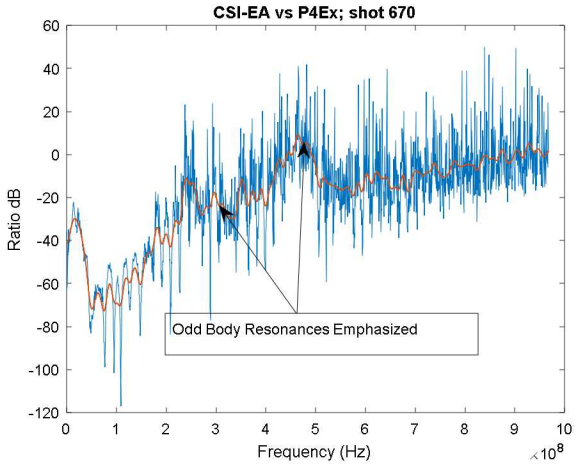

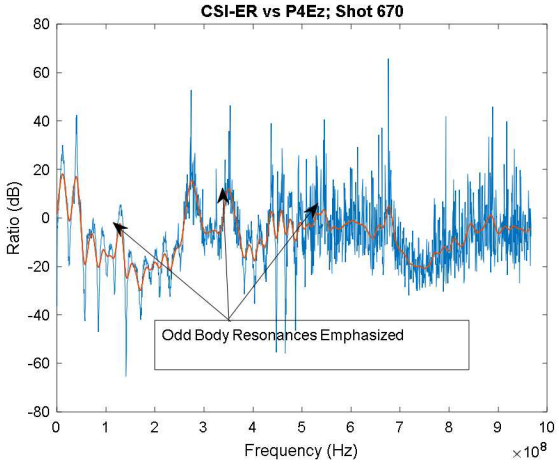

Current Density SE for CS (705,670)

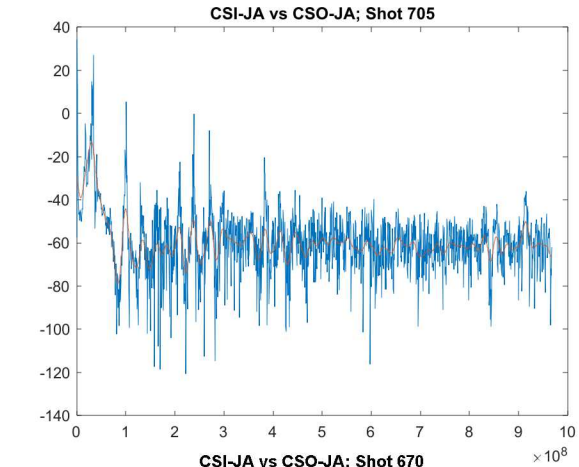

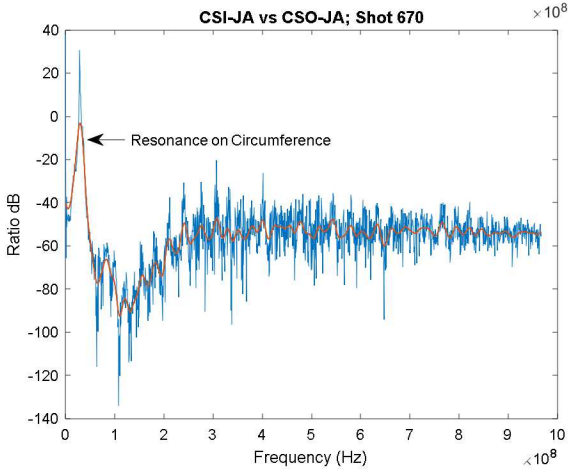

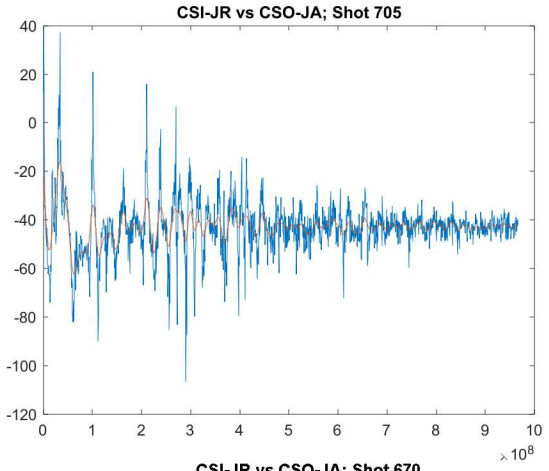

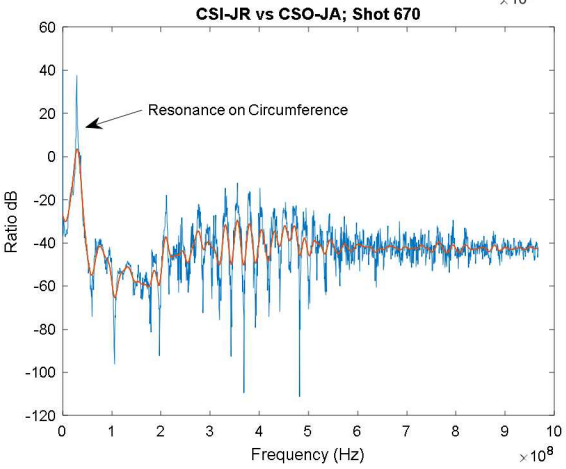

E-field SE AF (705, 670)

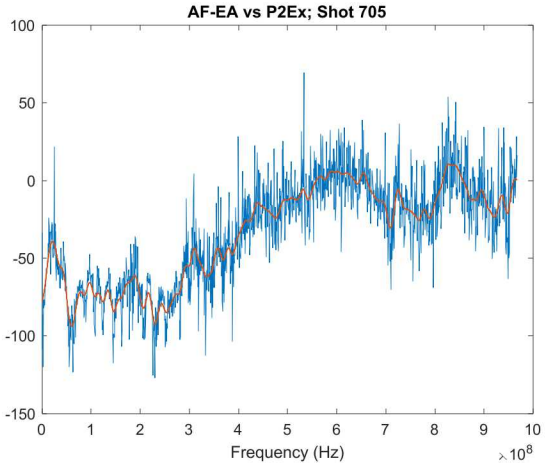

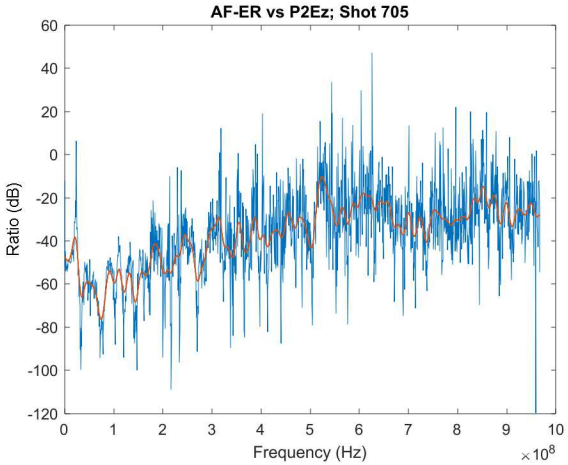

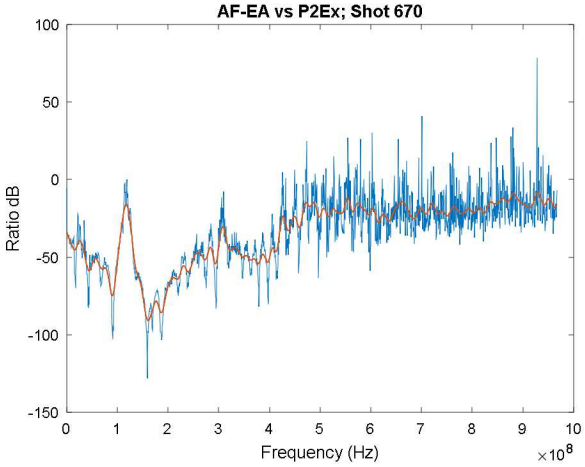

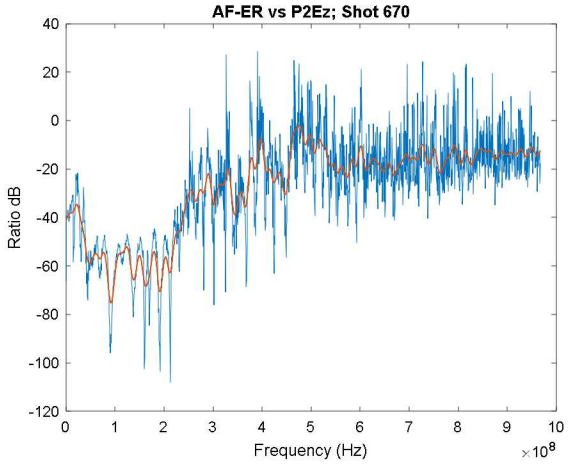

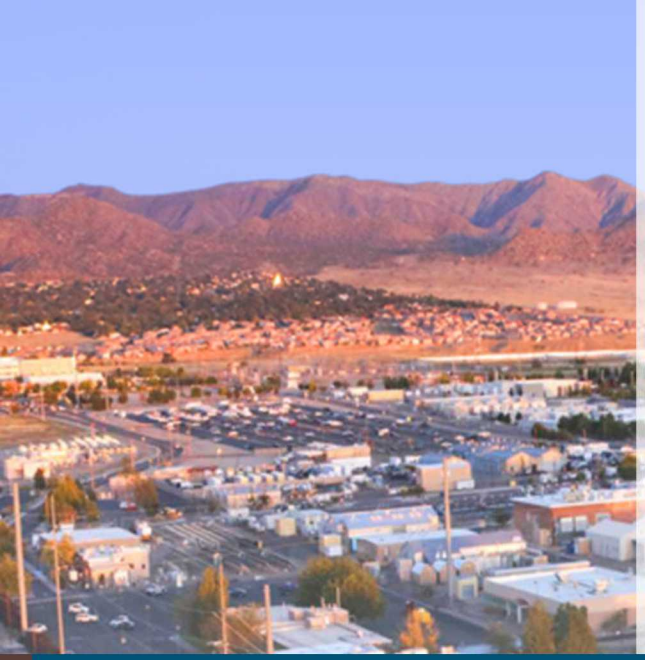

VIII. Courtyard Fields

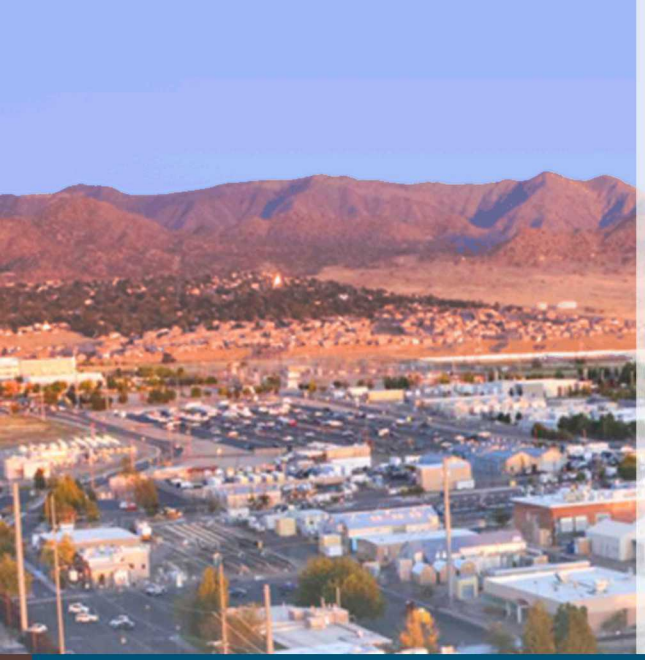

Courtyard Fields - Shot 10664

HERMES, Platform 4, Electric Fields

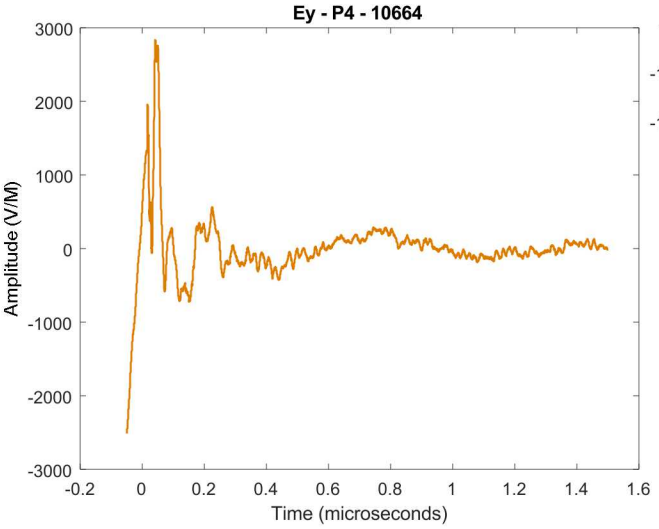

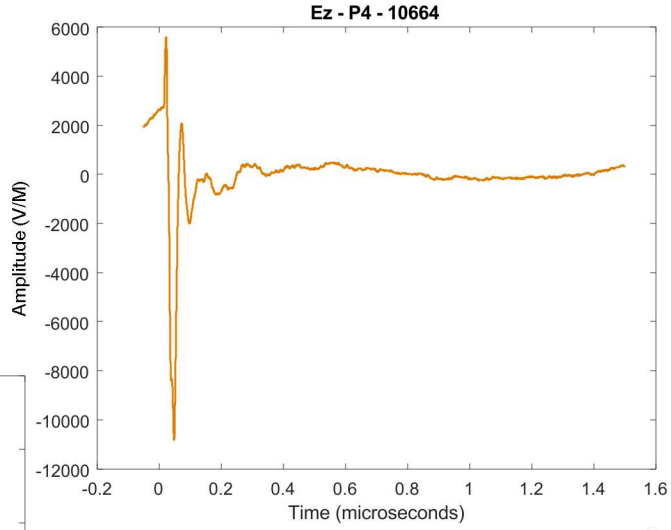

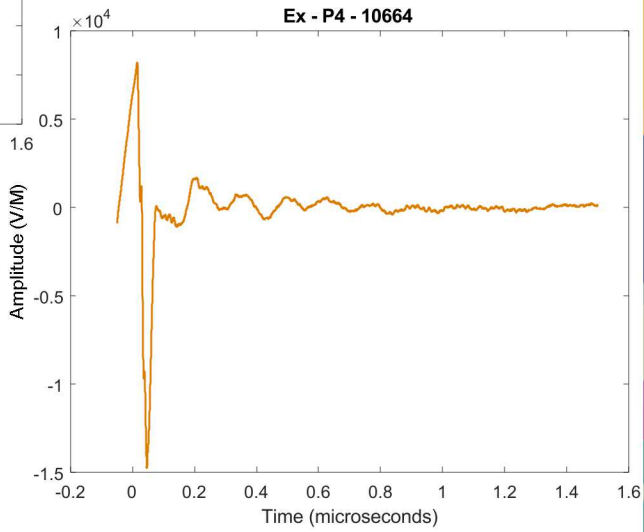

HERMES, Platform 4, Magnetic Fields

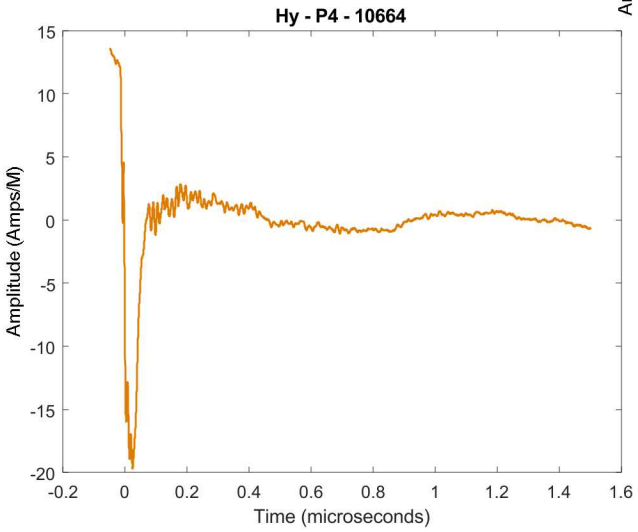

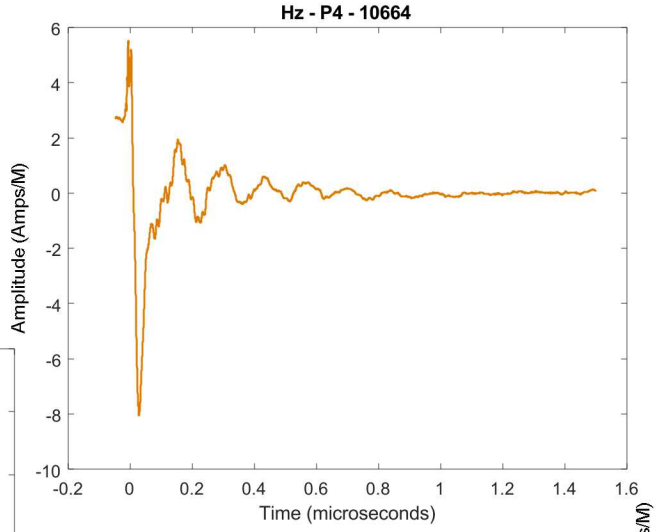

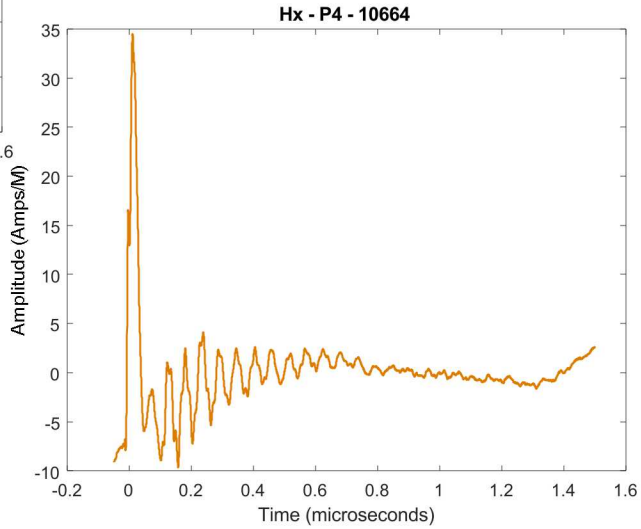

HERMES, Platform 3, Electric Fields

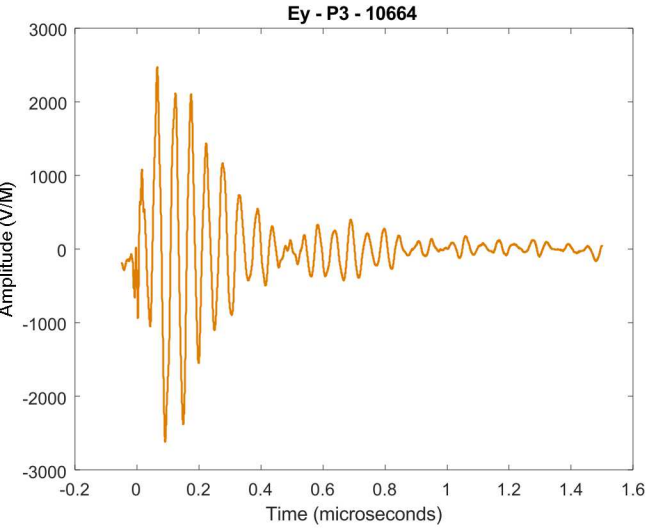

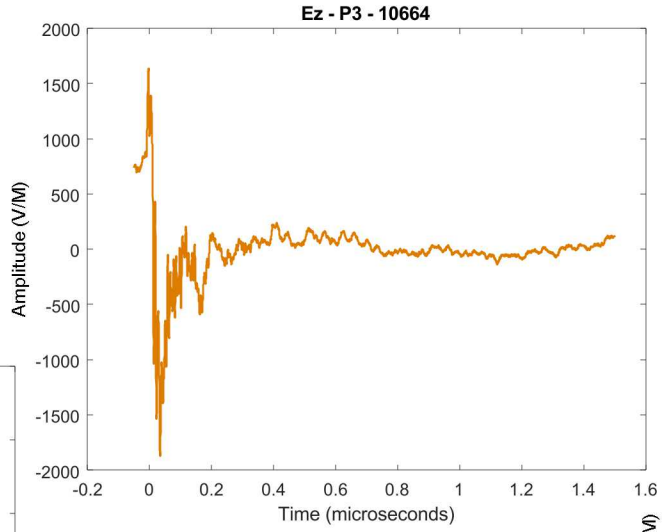

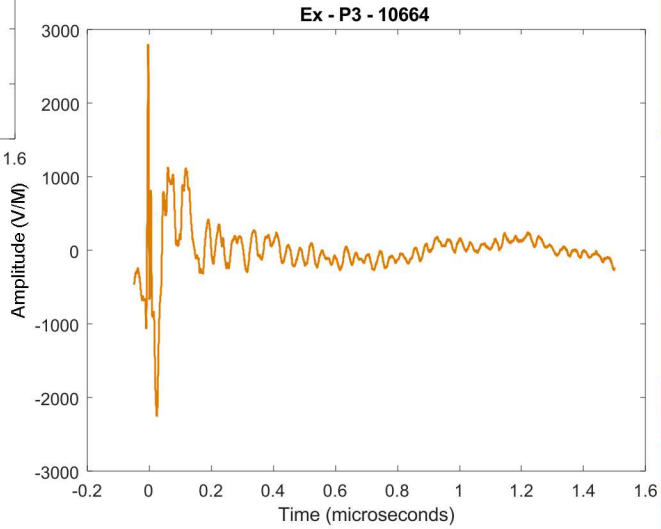

HERMES, Platform 3, Magnetic Fields

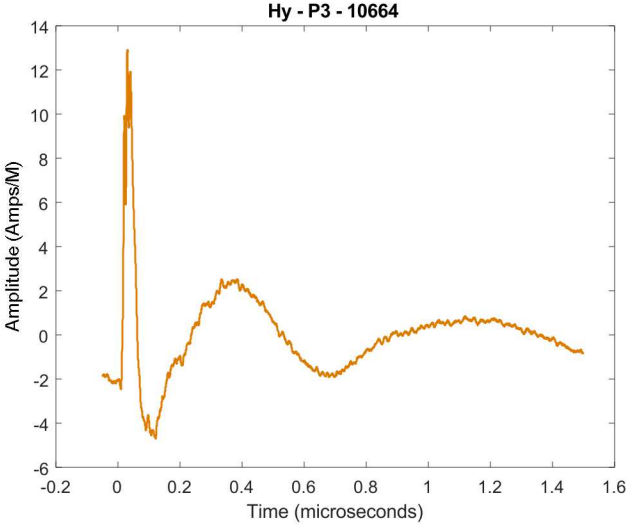

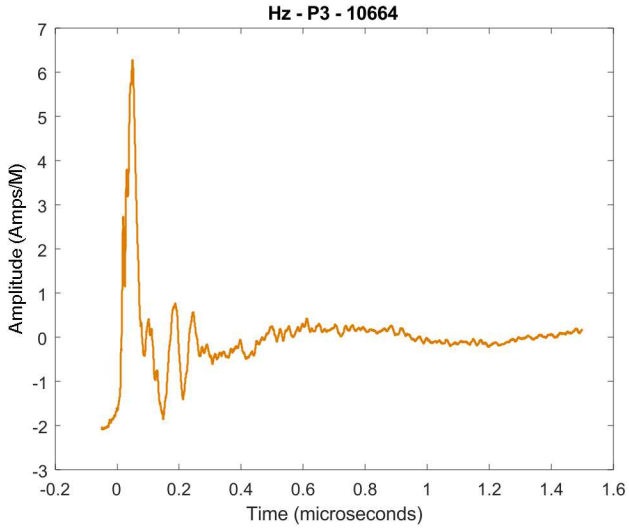

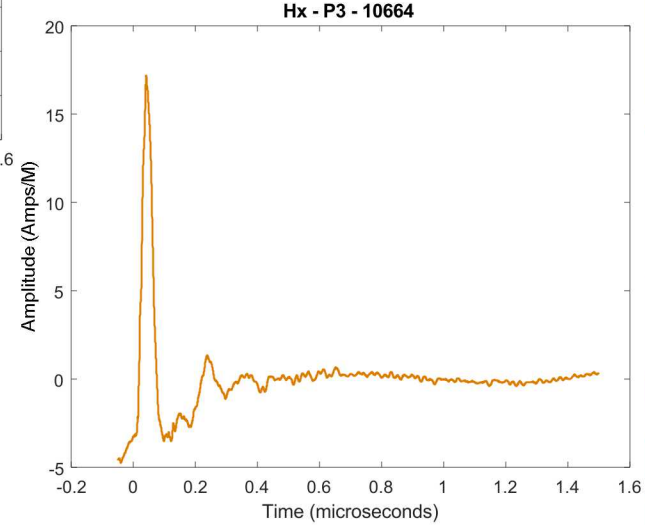

HERMES, Platform 2, Electric Fields

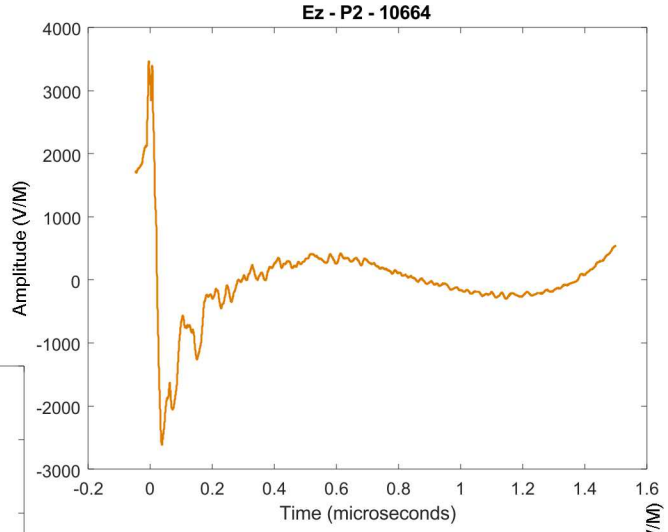

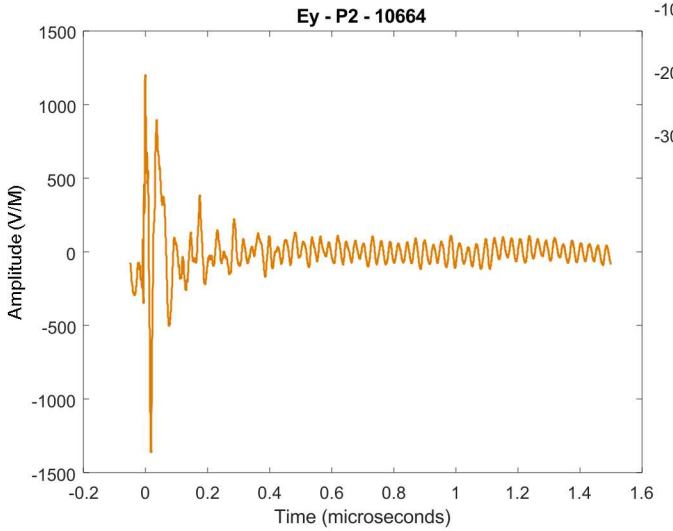

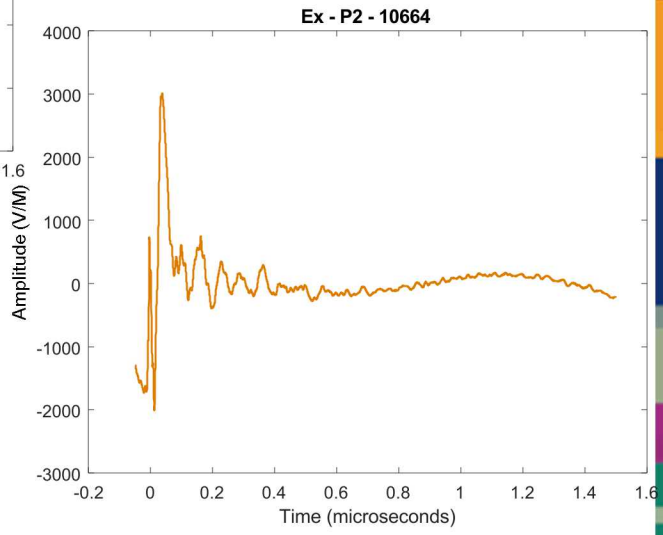

HERMES, Platform 2, Magnetic Fields

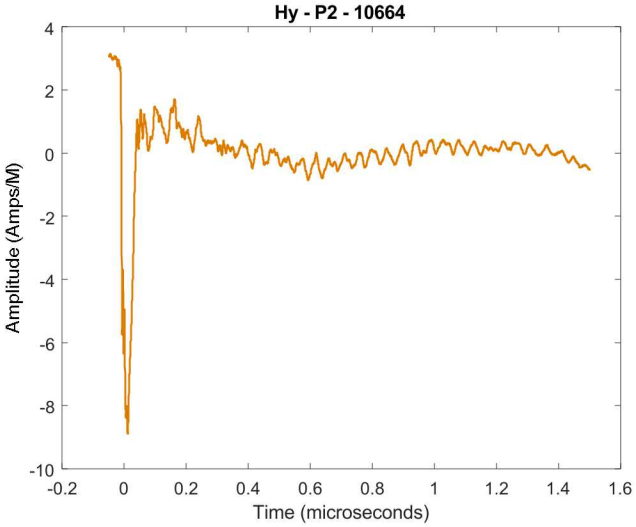

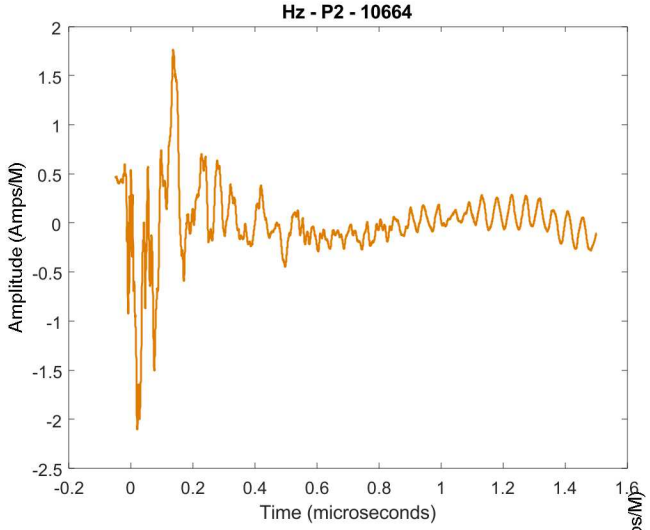

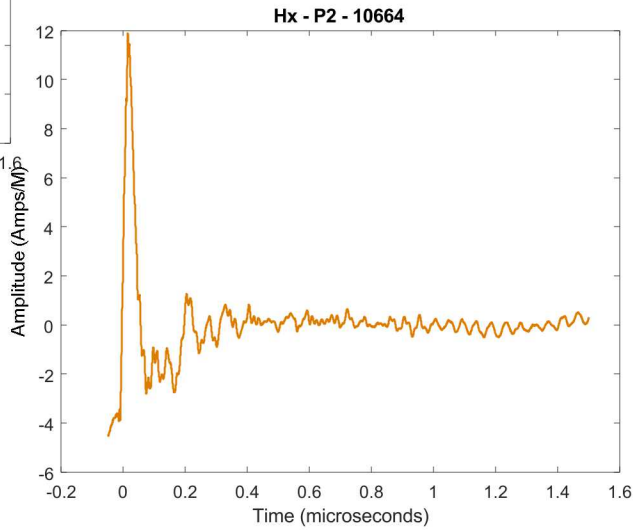

HERMES, Platform 1, Electric Fields

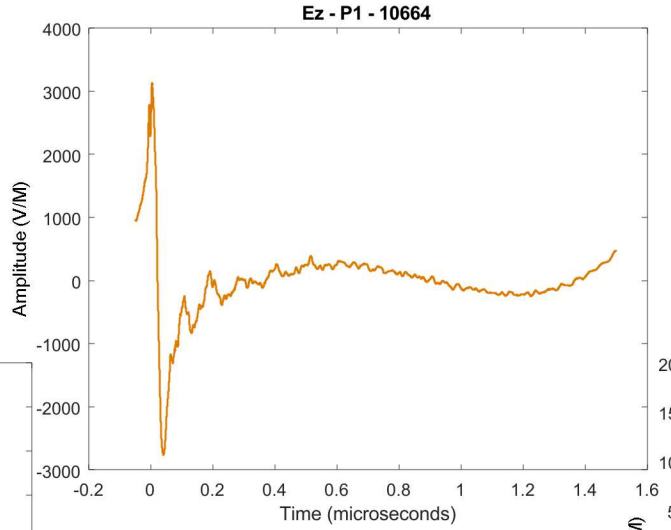

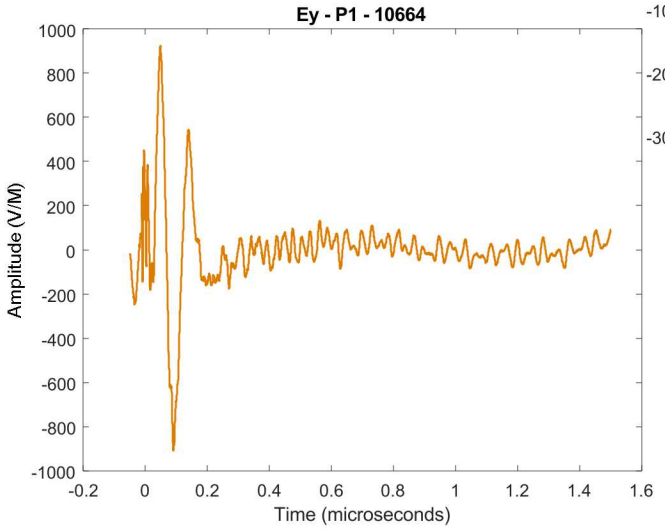

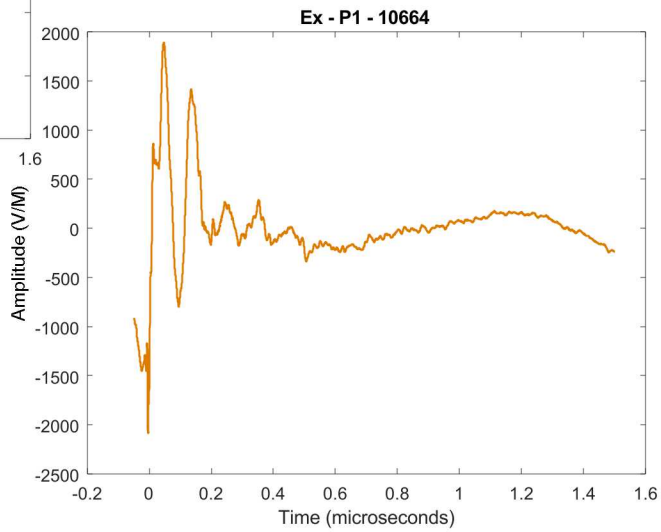

HERMES, Platform 1, Magnetic Fields

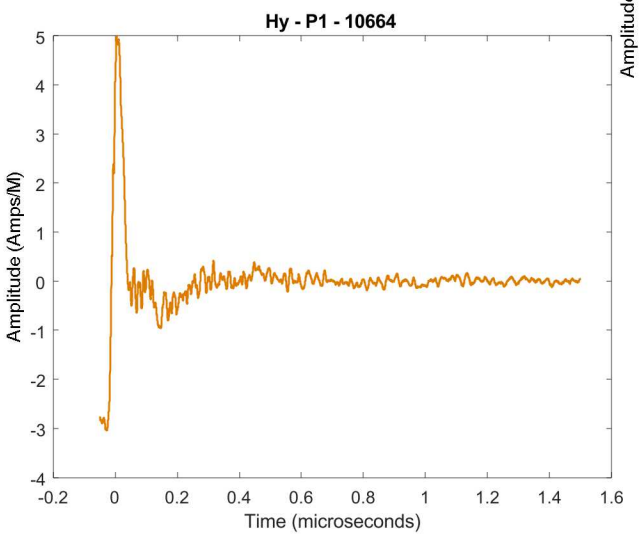

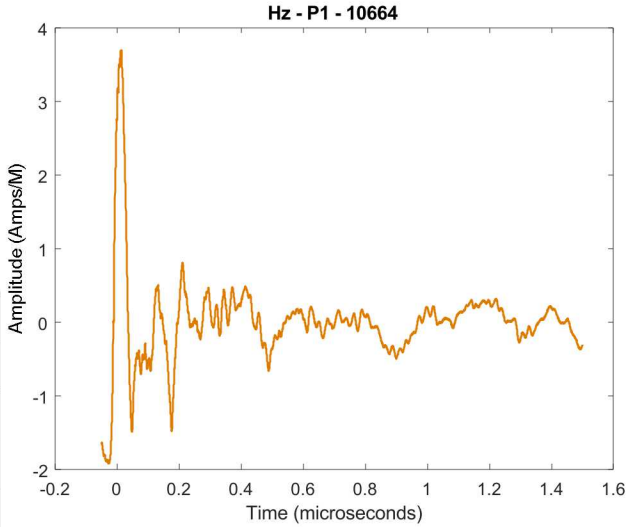

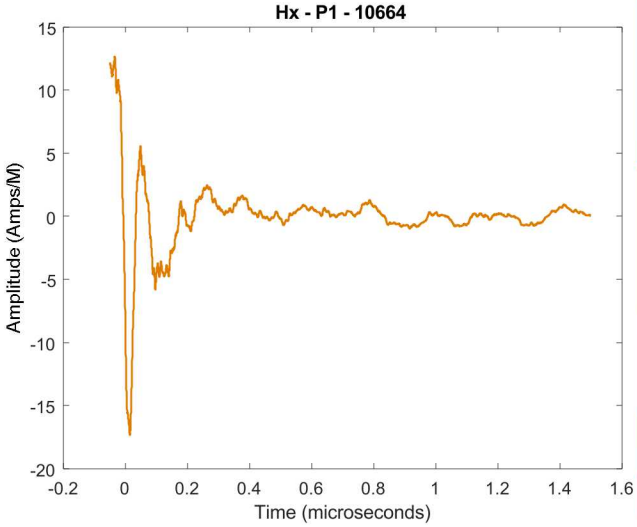

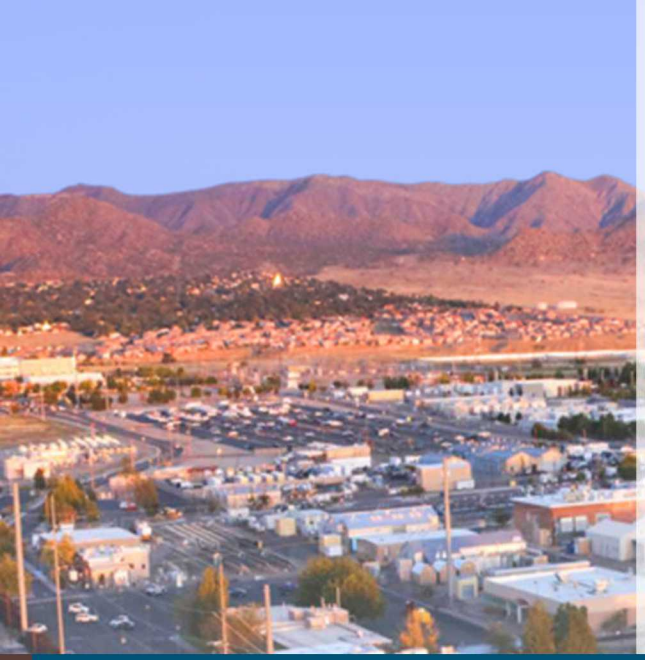

Courtyard Fields - Shot 10670

HERMES, Platform 4, Electric Fields

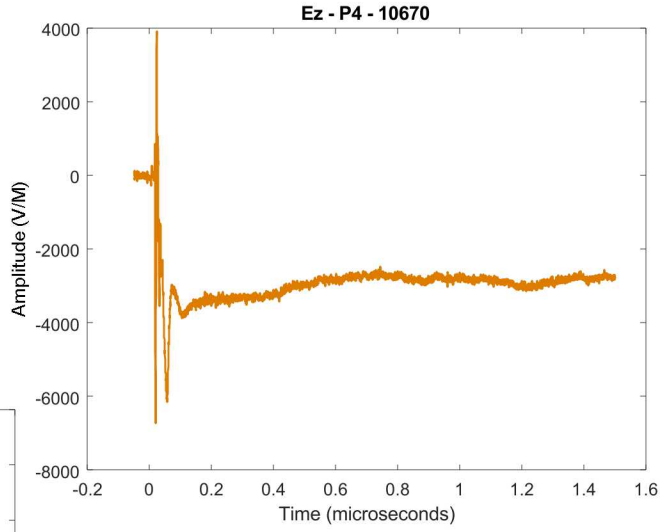

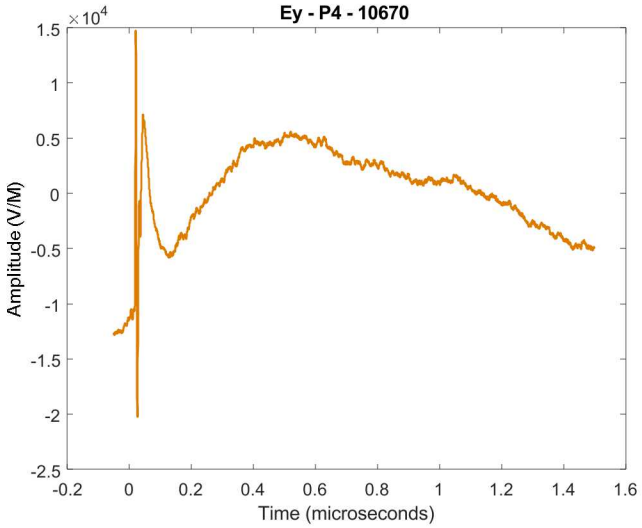

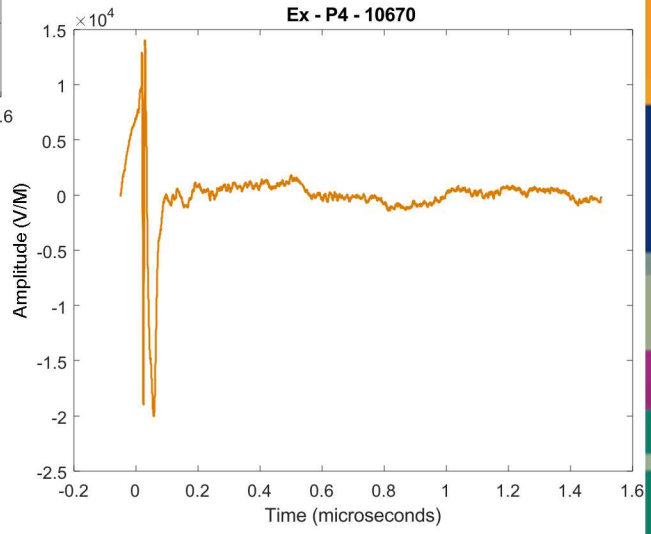

HERMES, Platform 4, Magnetic Fields

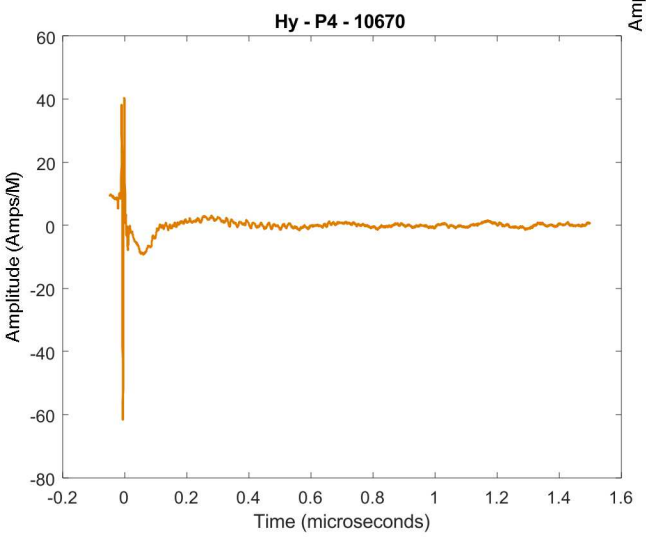

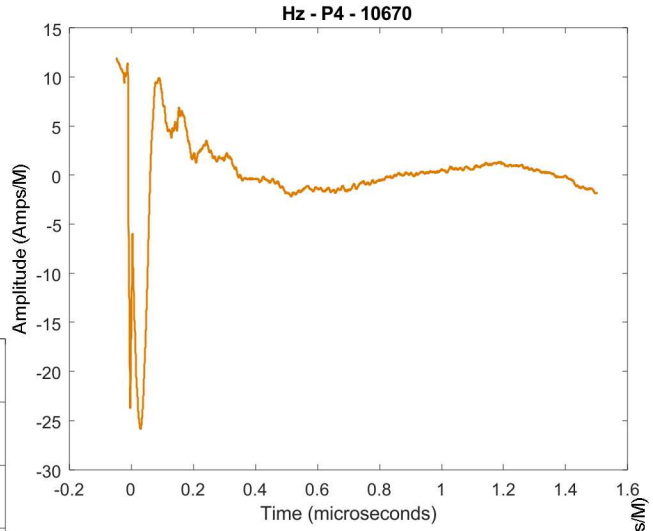

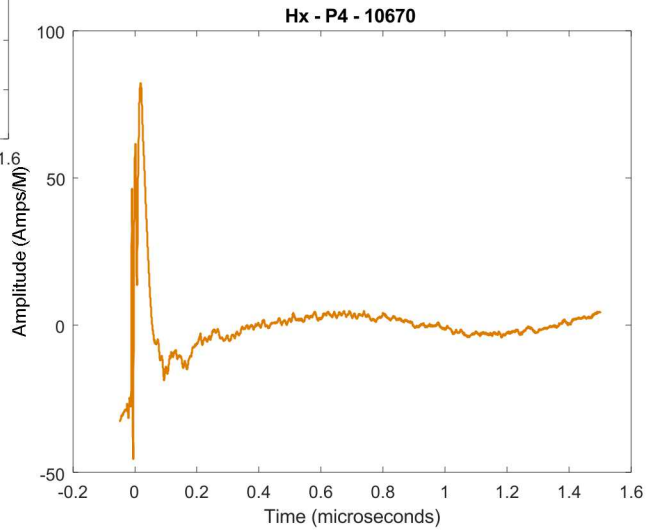

HERMES, Platform 3, Electric Fields

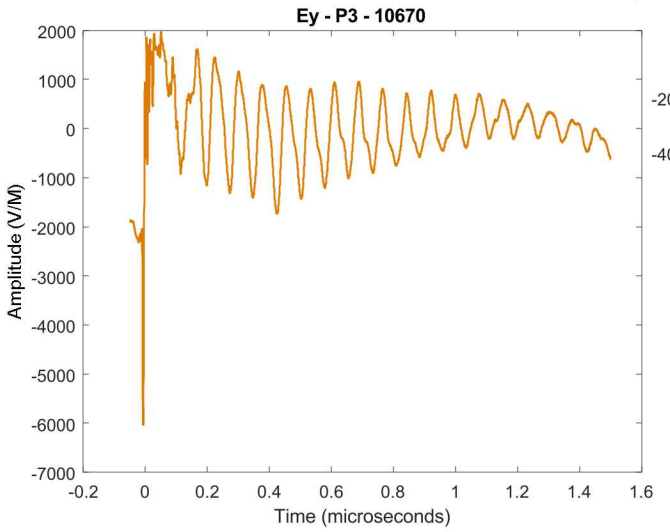

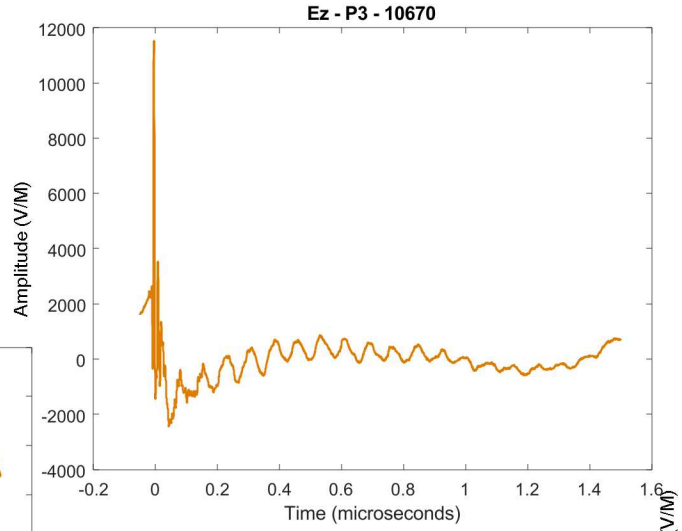

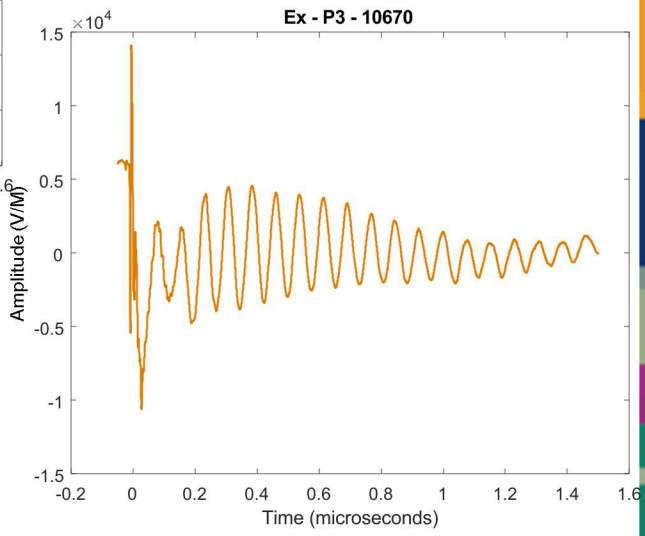

HERMES, Platform 3, Magnetic Fields

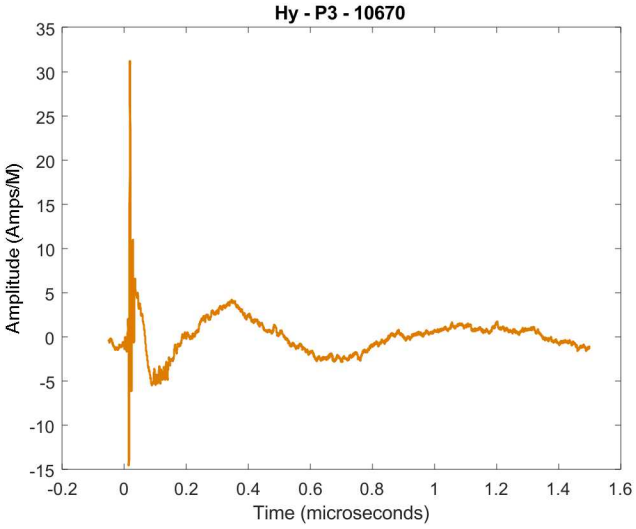

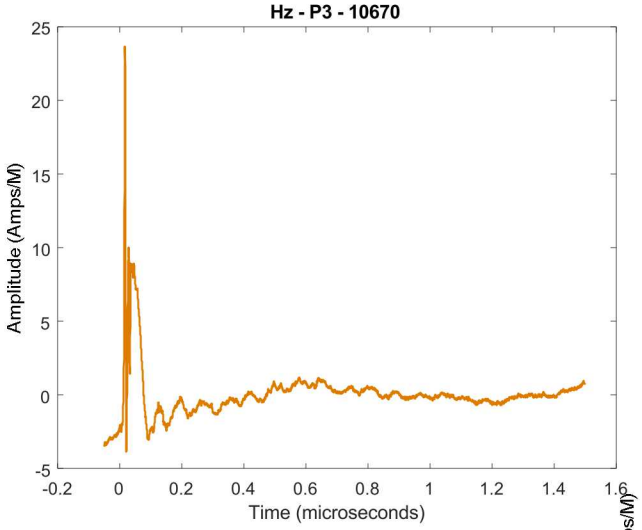

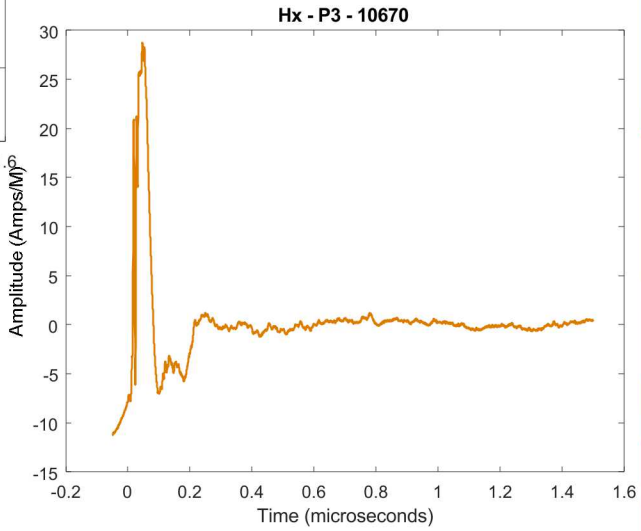

HERMES, Platform 2, Electric Fields

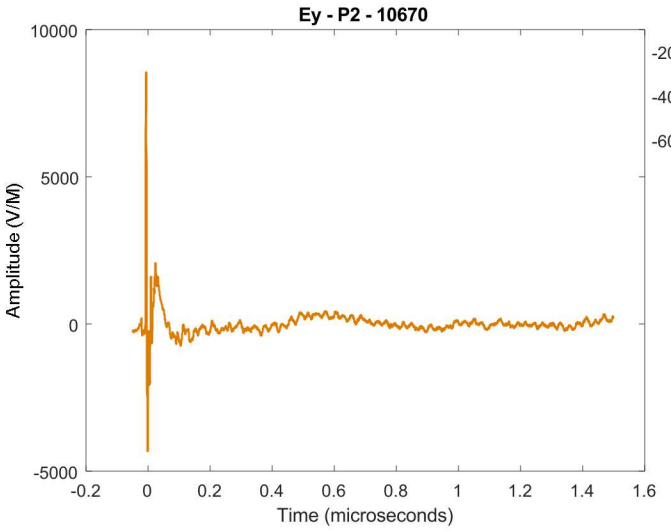

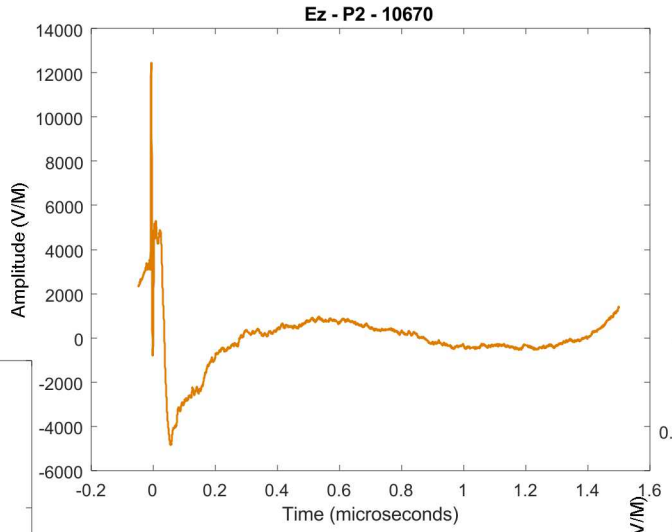

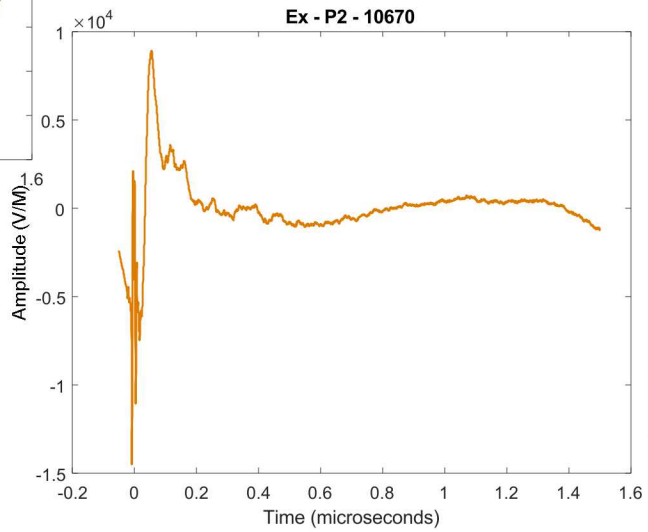

HERMES, Platform 2, Magnetic Fields

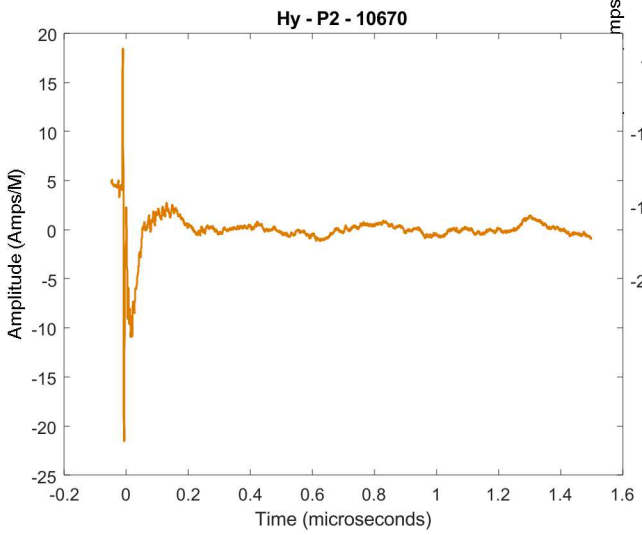

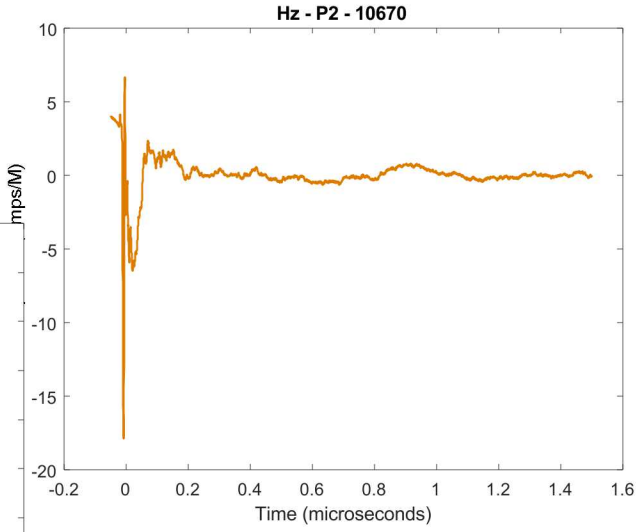

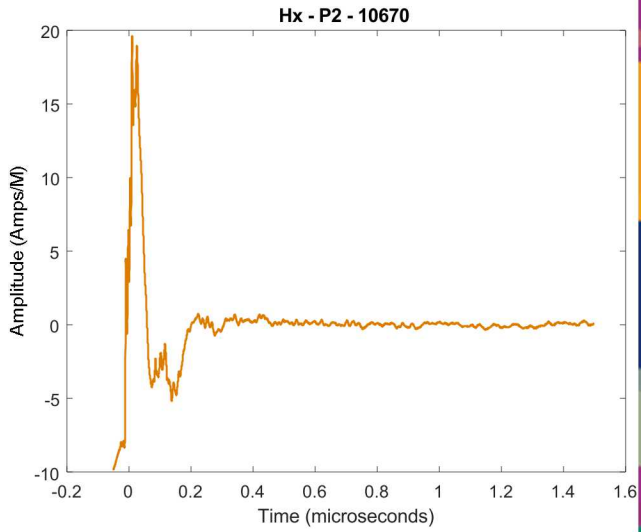

HERMES, Platform 1, Electric Fields

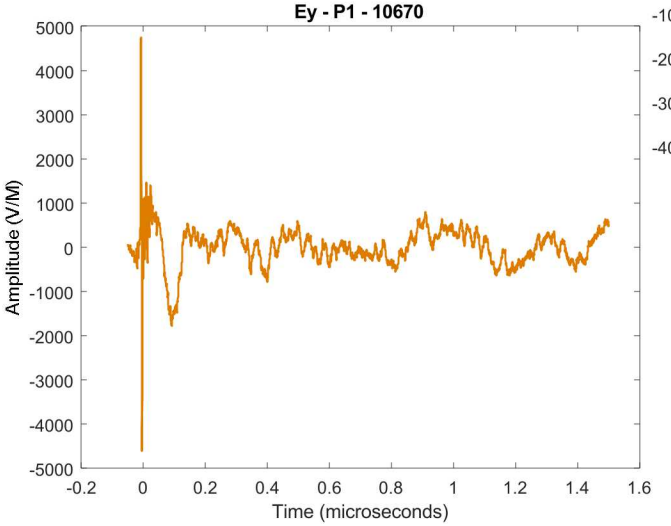

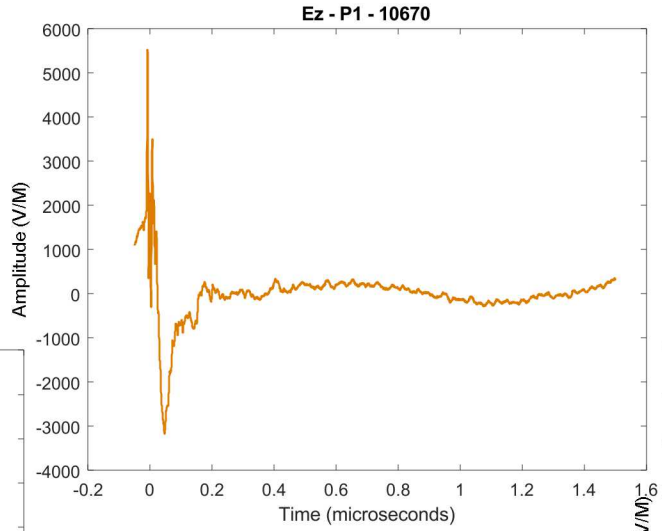

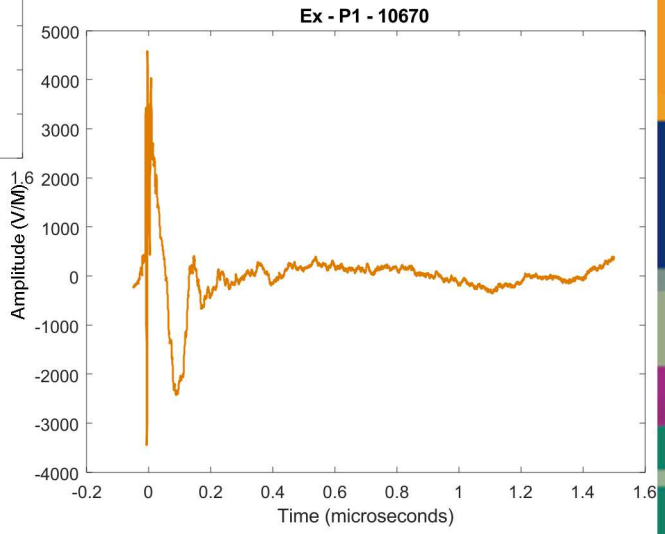

HERMES, Platform 1, Magnetic Fields

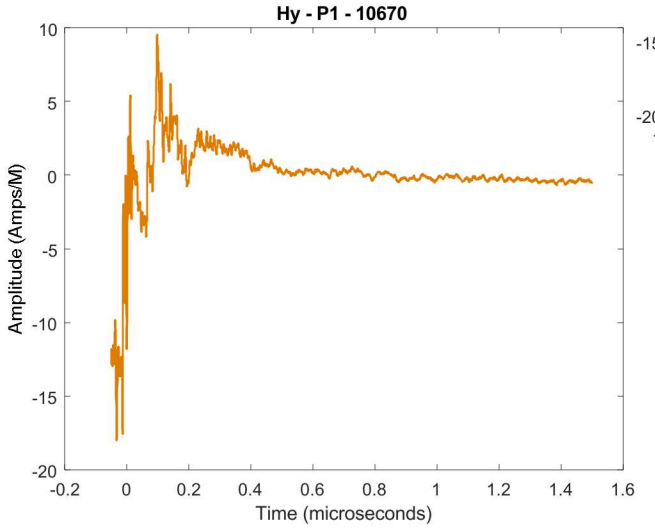

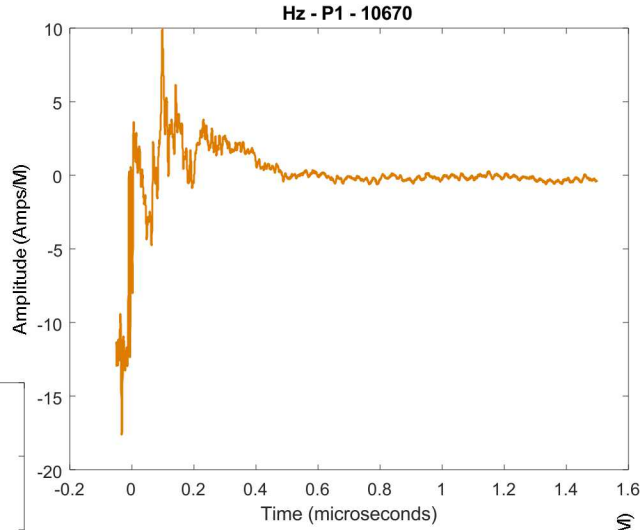

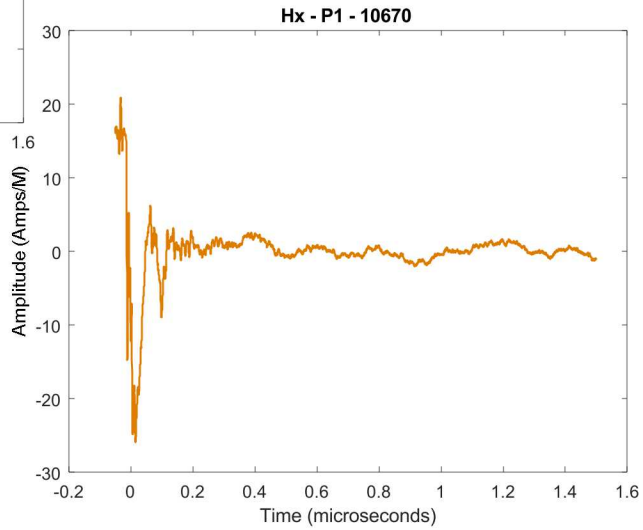

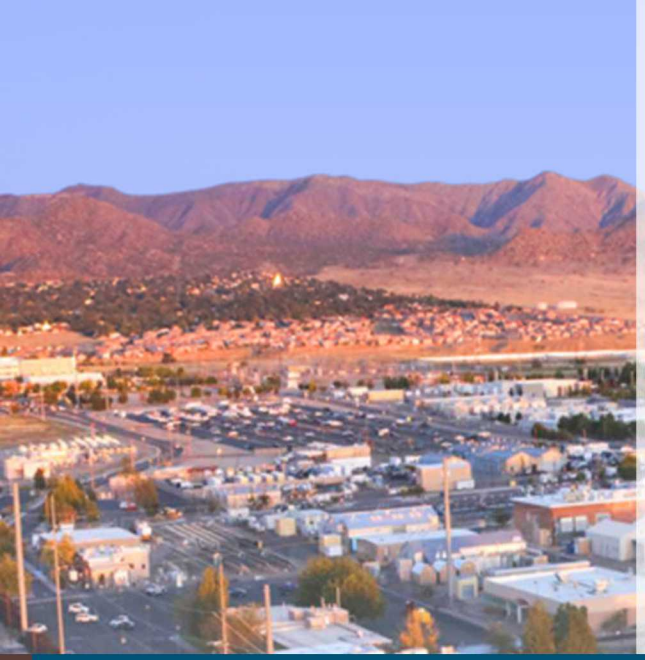

Courtyard Fields - Shot 10675

HERMES, Platform 4, Electric Fields

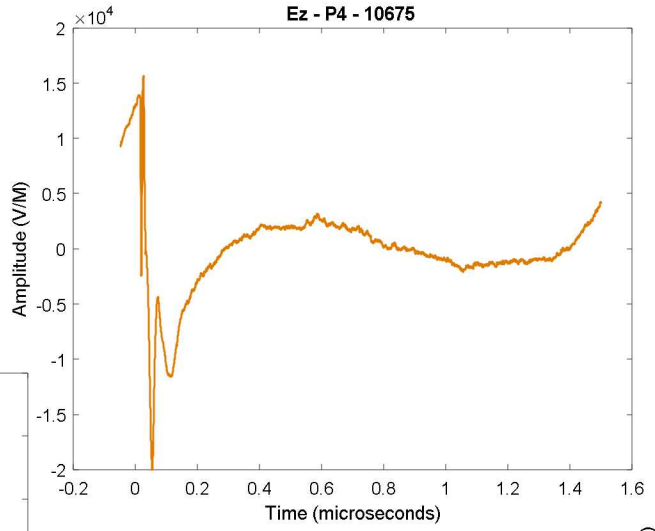

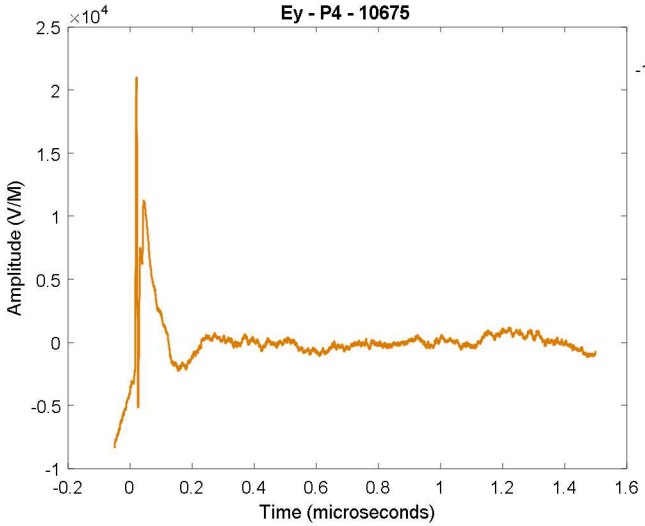

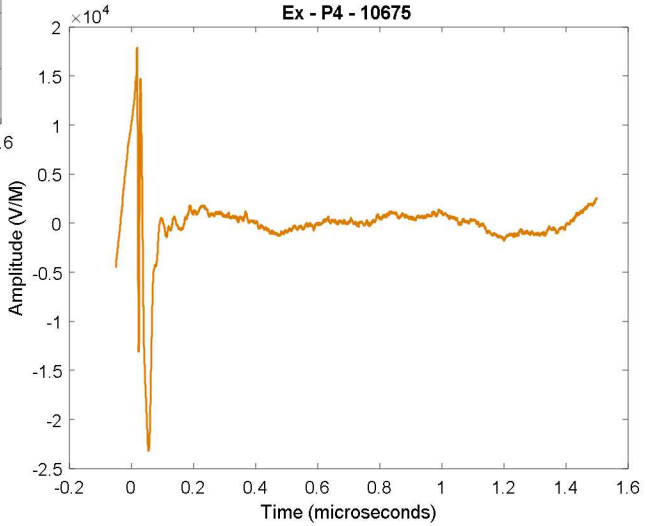

HERMES, Platform 4, Magnetic Fields

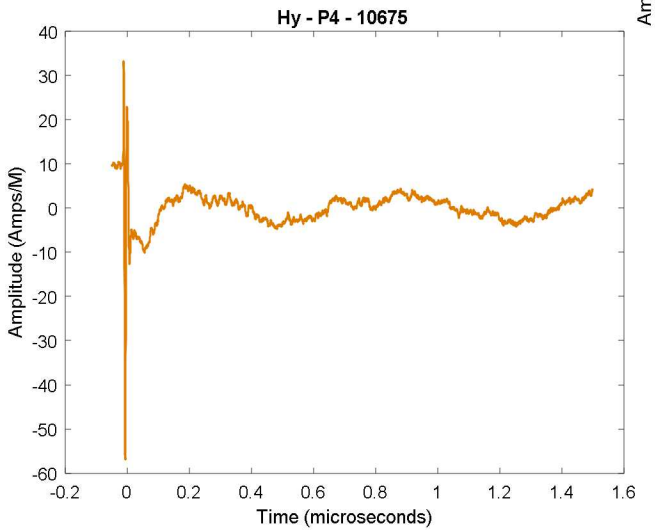

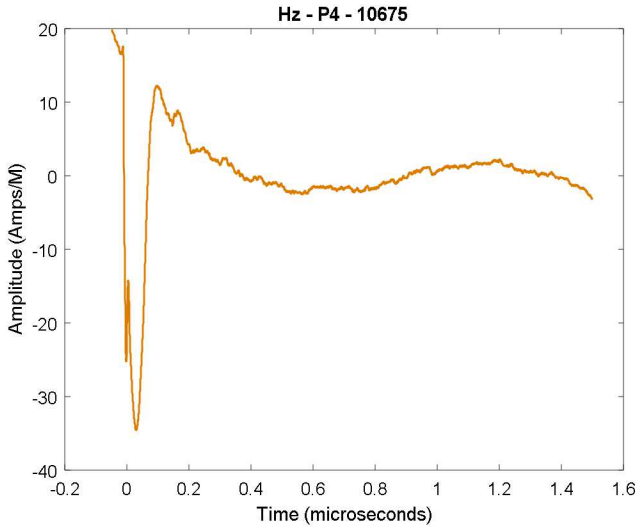

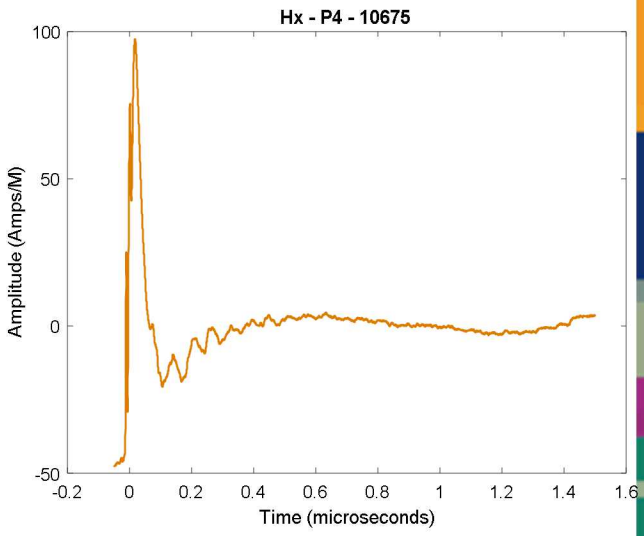

HERMES, Platform 3, Electric Fields

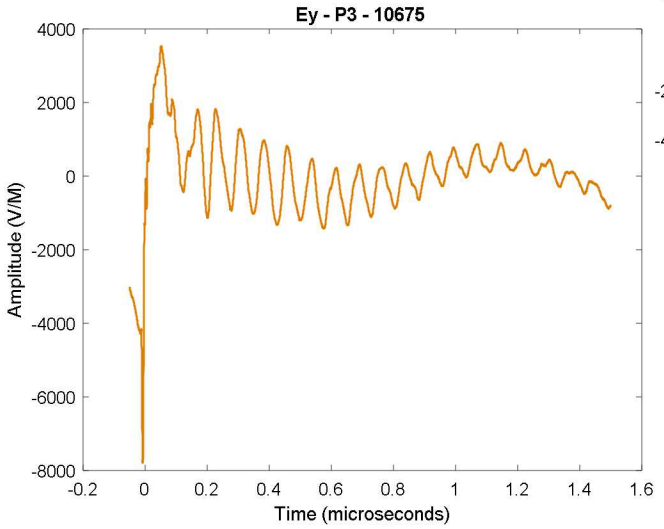

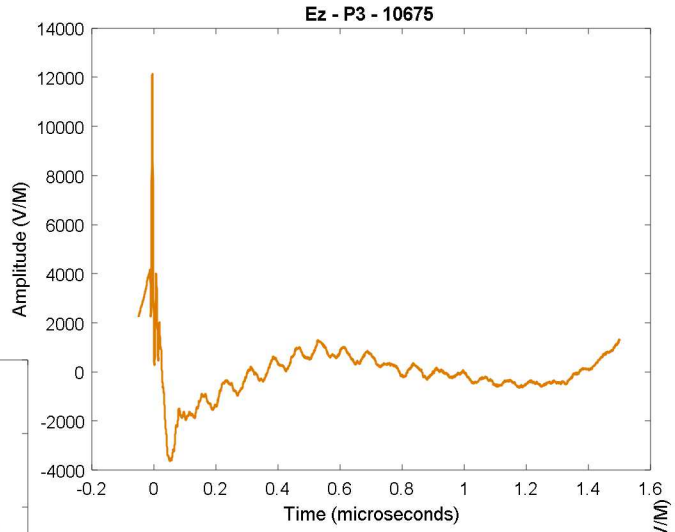

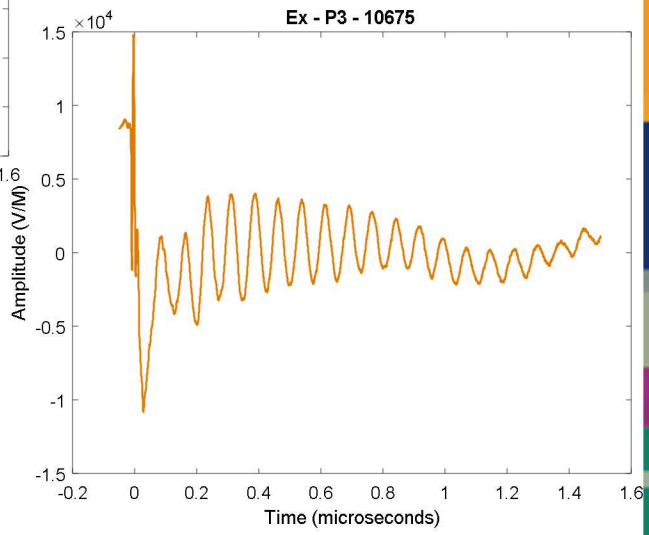

HERMES, Platform 3, Magnetic Fields

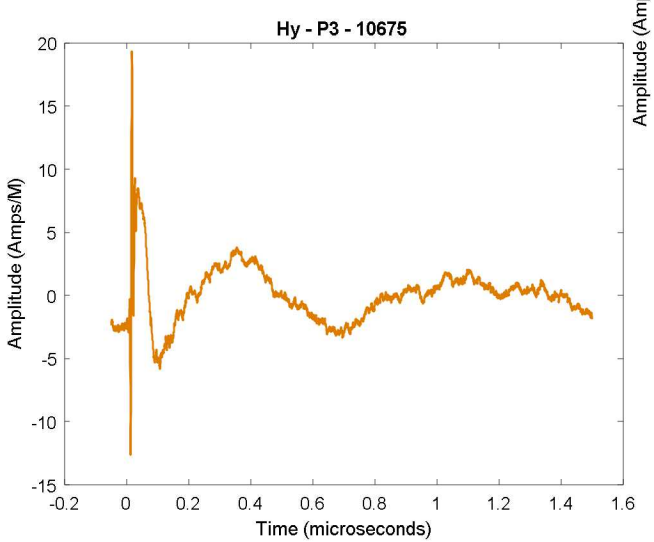

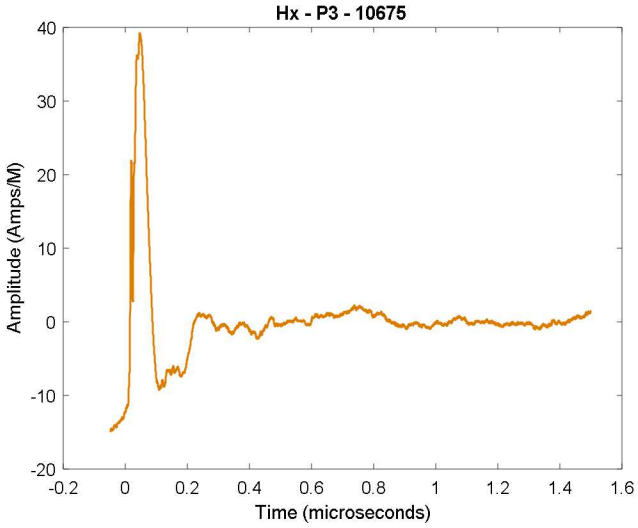

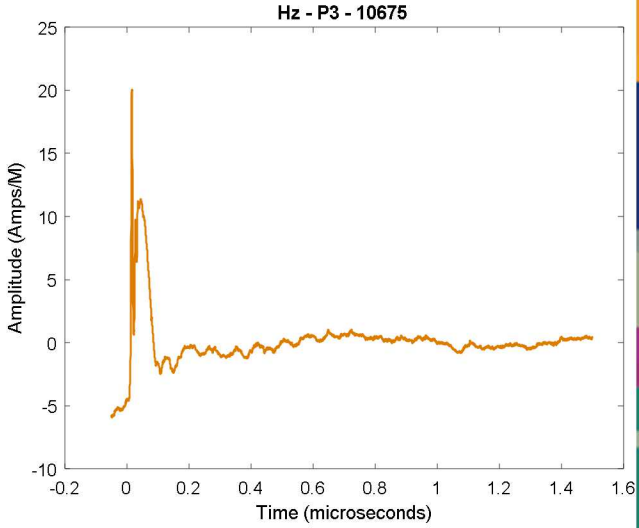

HERMES, Platform 2, Electric Fields

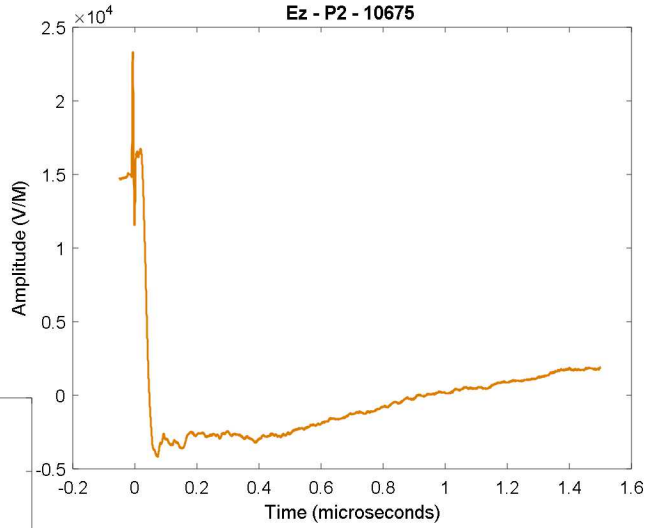

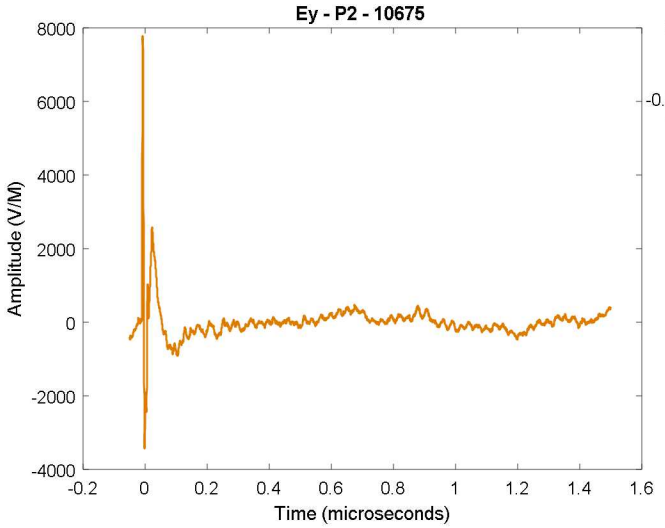

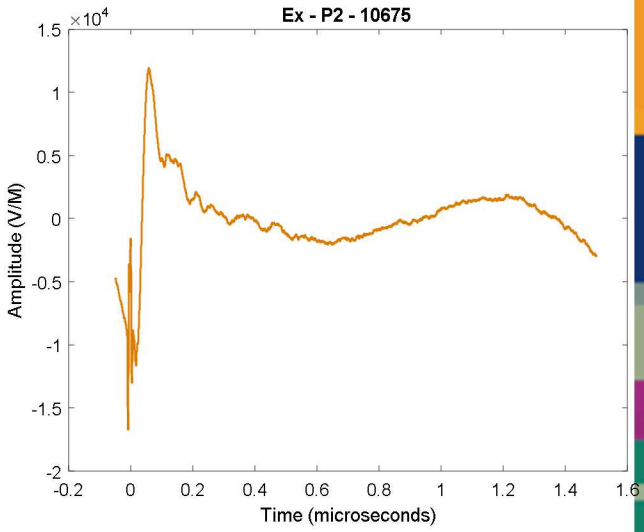

HERMES, Platform 2, Magnetic Fields

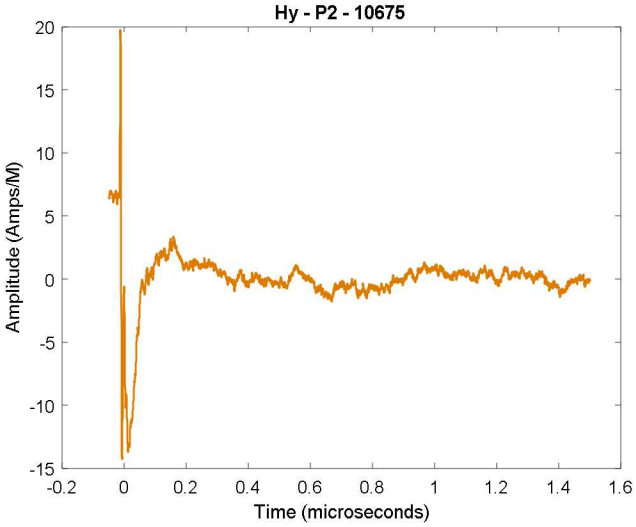

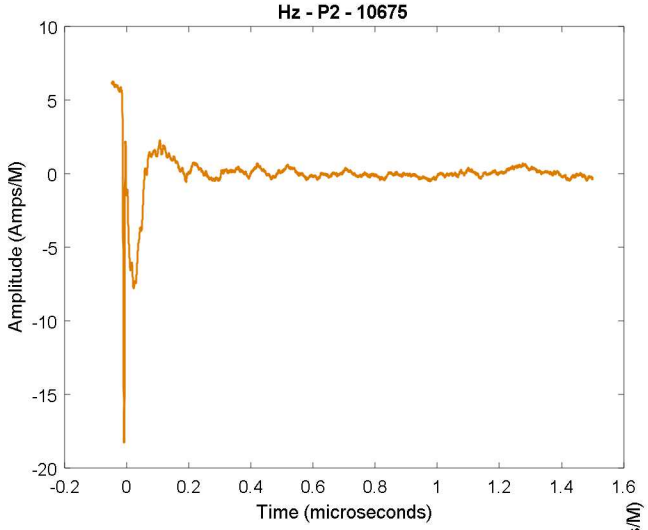

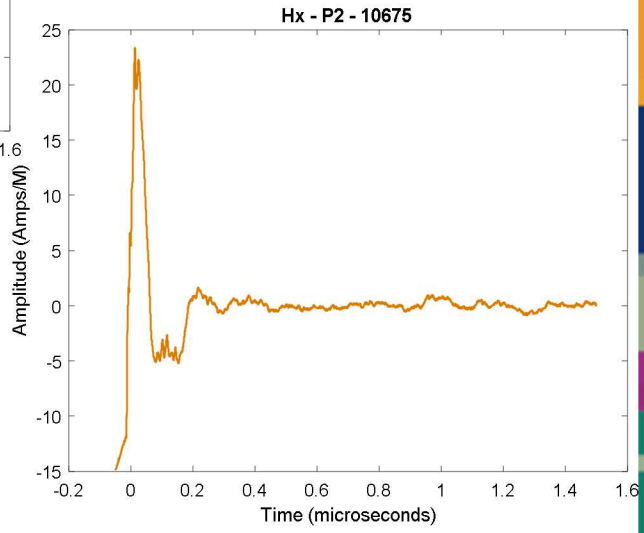

HERMES, Platform 1, Electric Fields

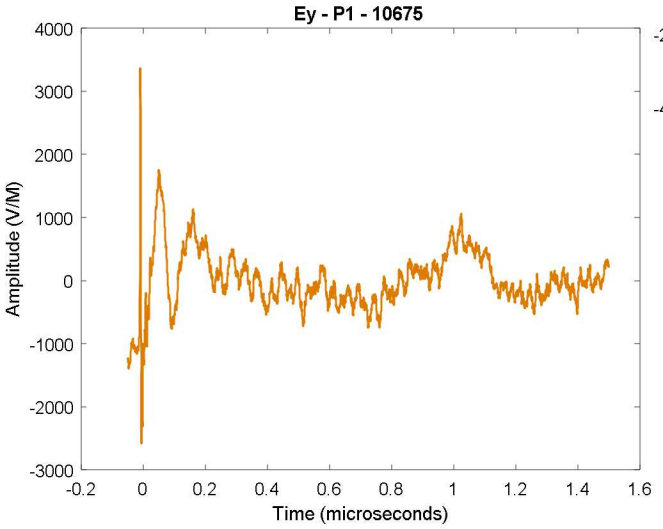

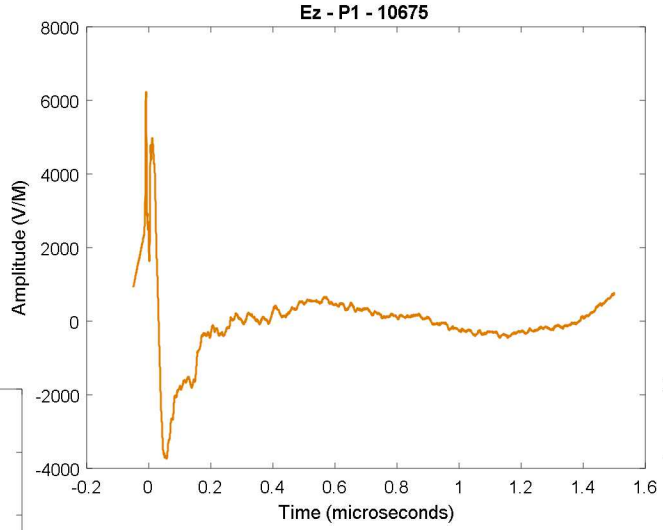

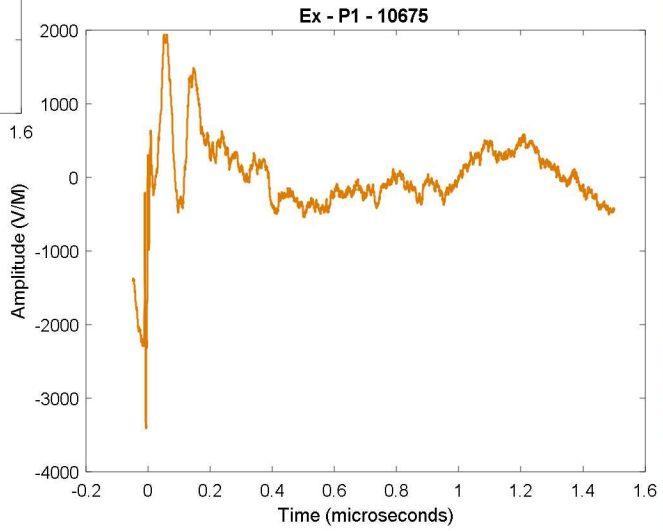

HERMES, Platform 1, Magnetic Fields

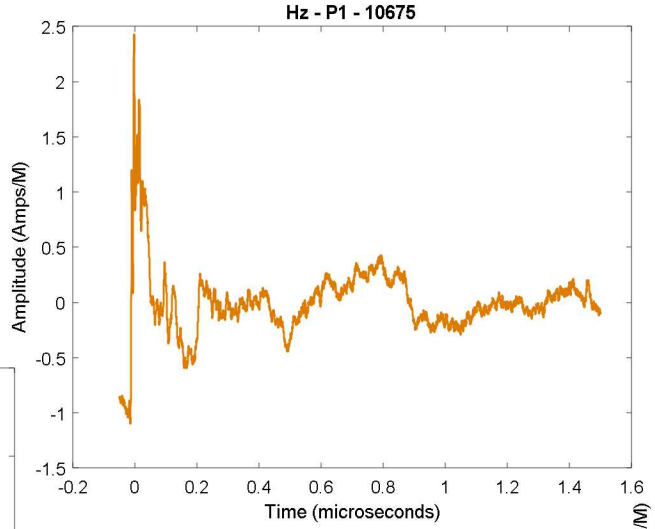

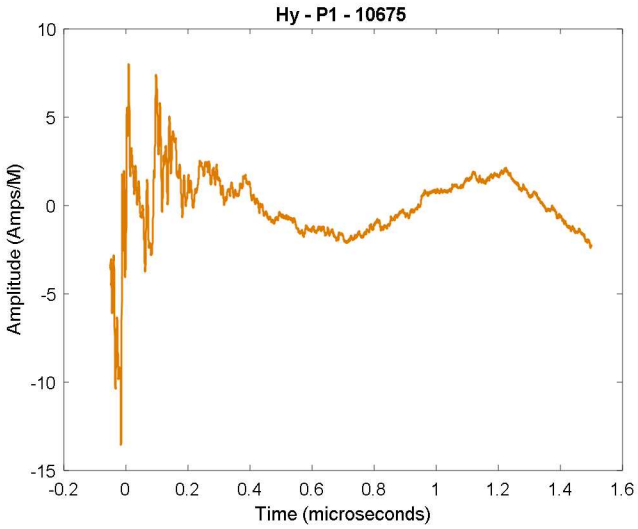

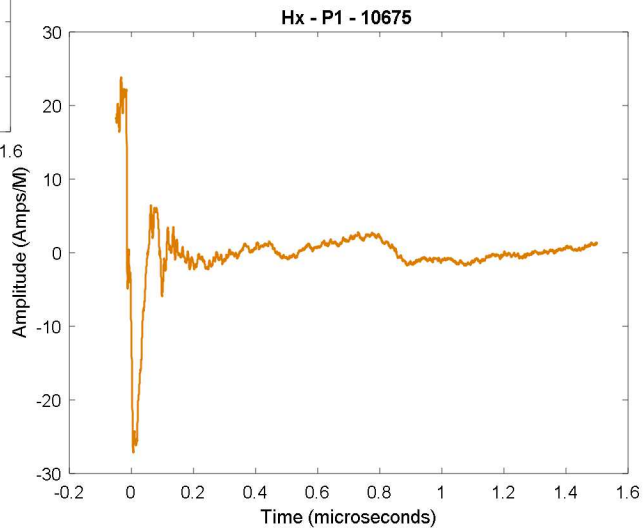

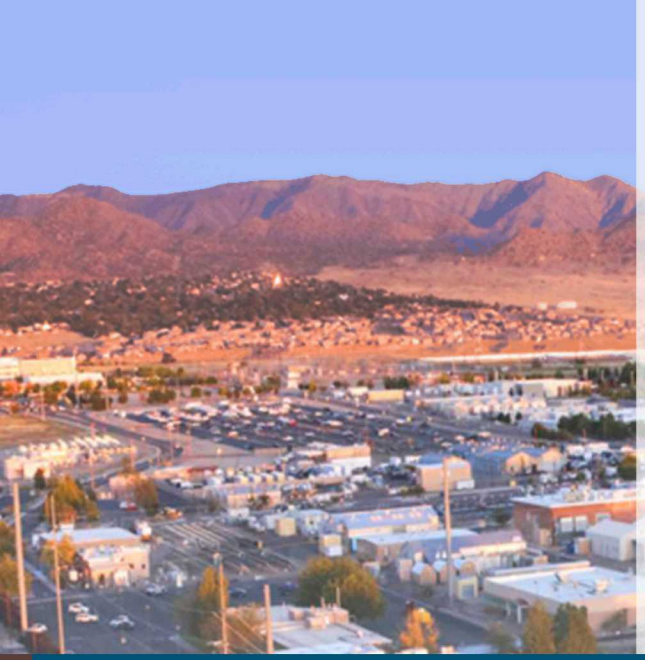

Courtyard Fields - Shot 10690

HERMES, Platform 4, Electric Fields

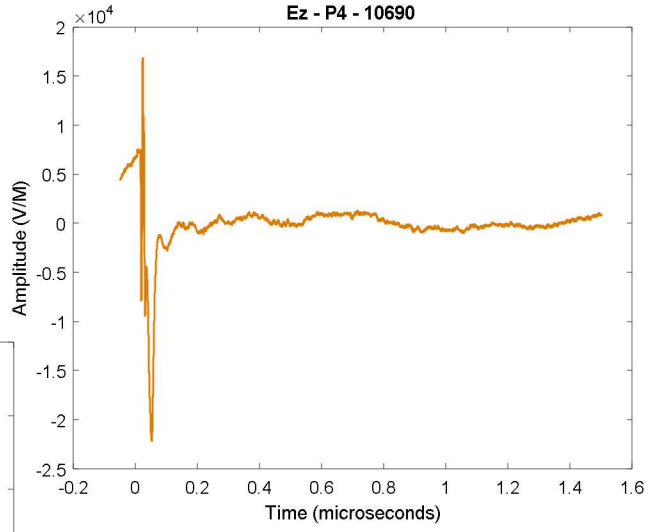

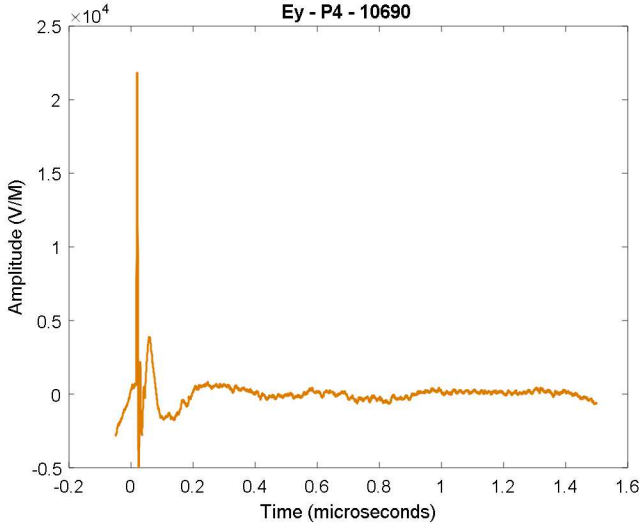

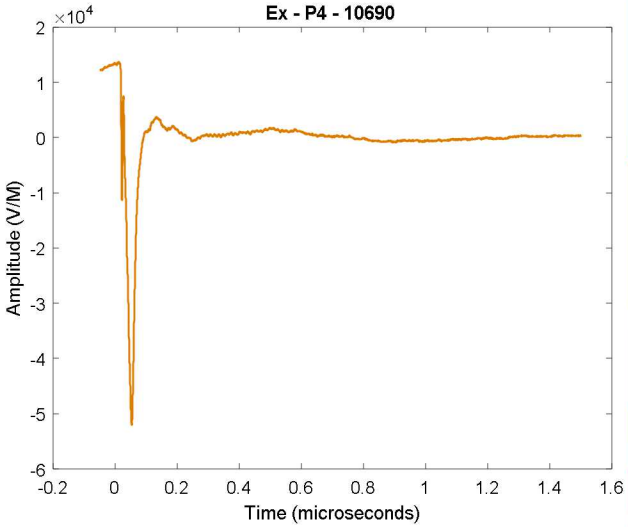

HERMES, Platform 4, Magnetic Fields

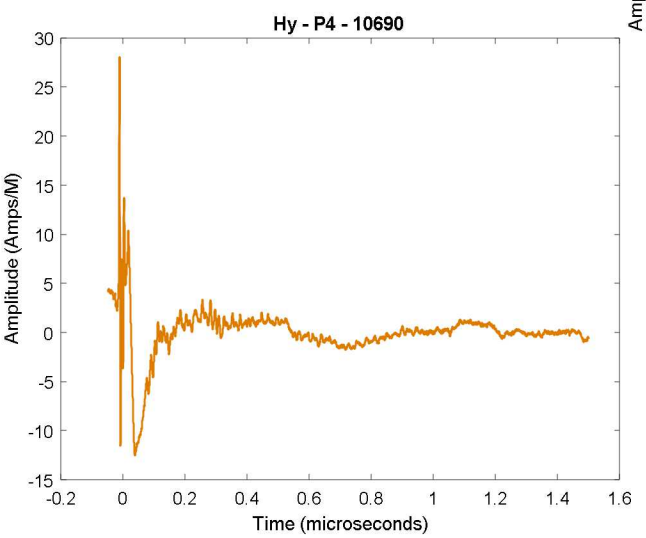

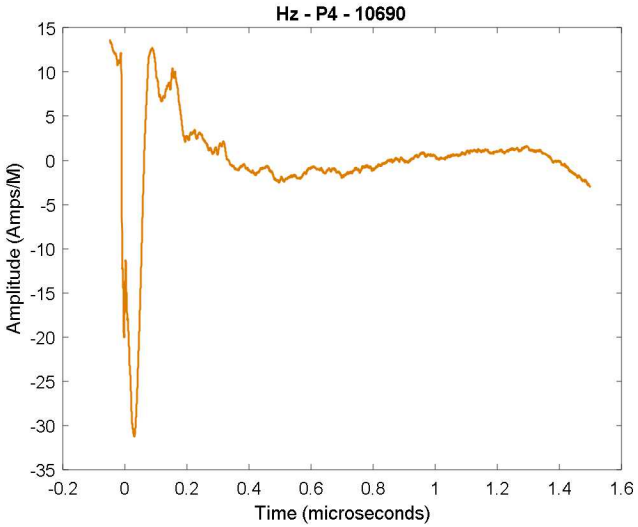

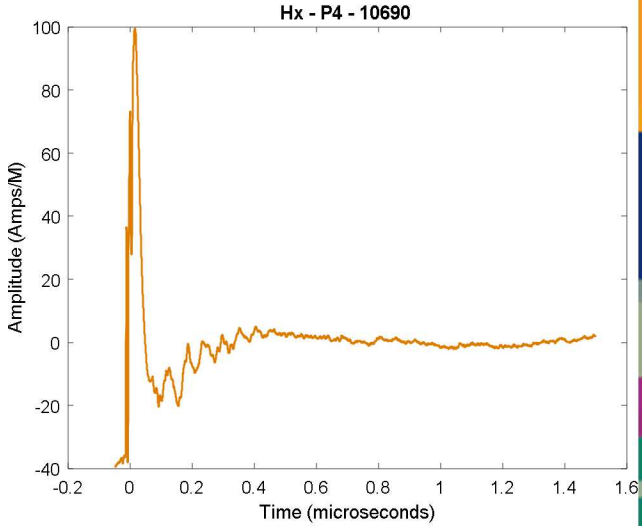

HERMES, Platform 3, Electric Fields

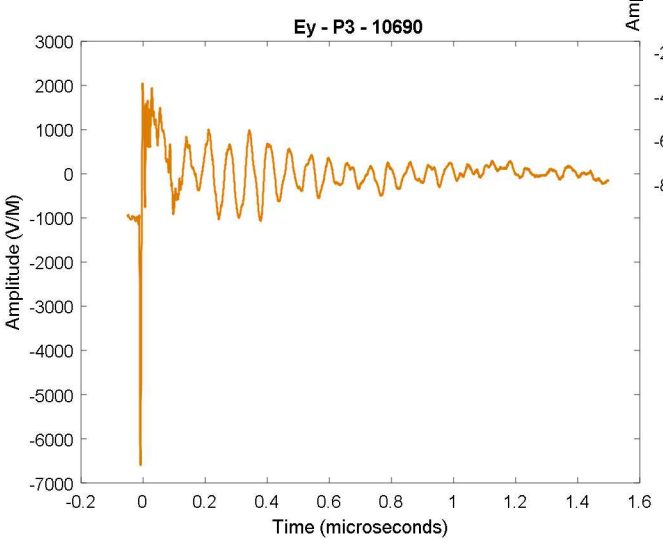

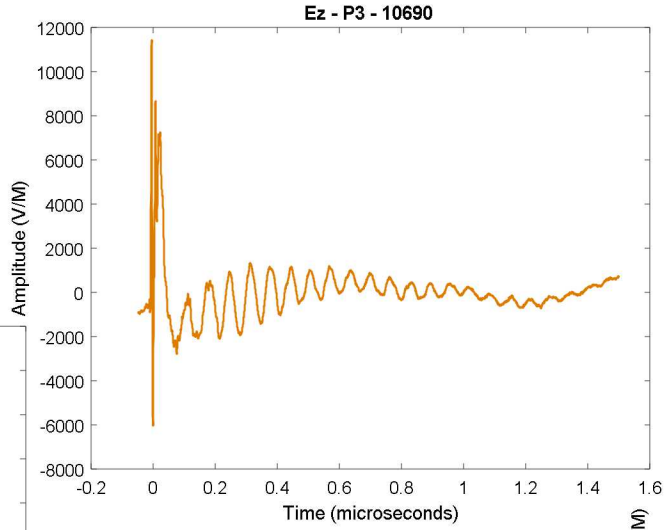

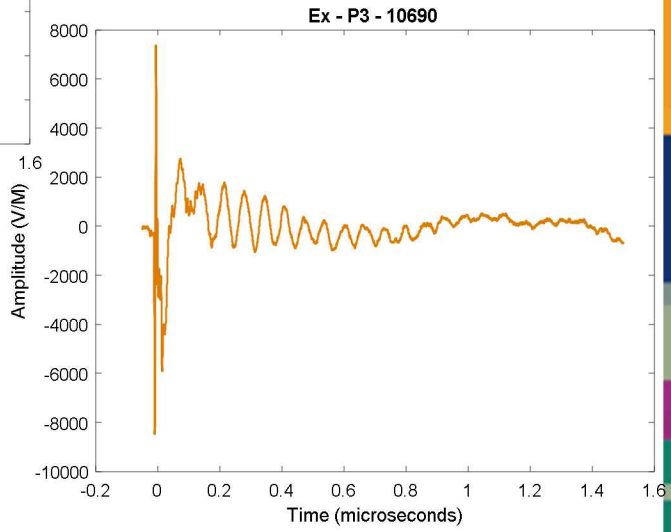

HERMES, Platform 3, Magnetic Fields

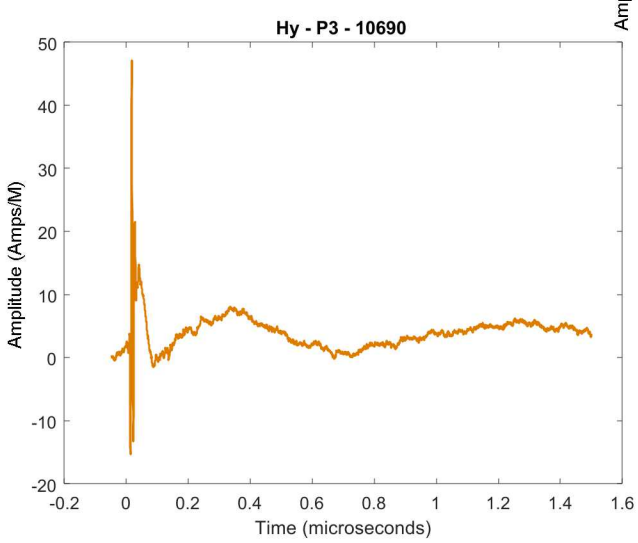

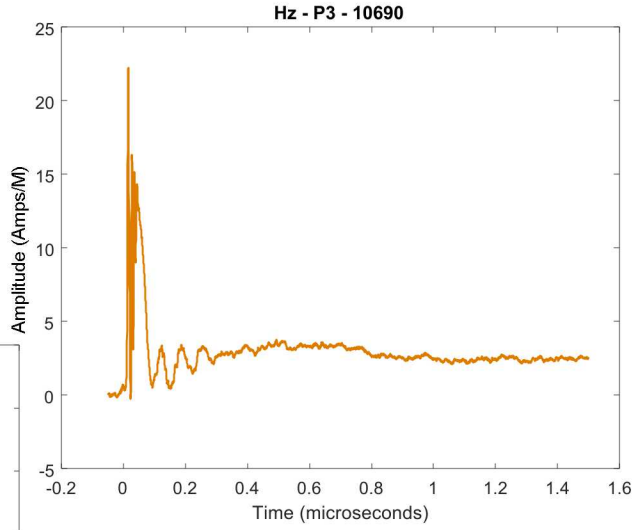

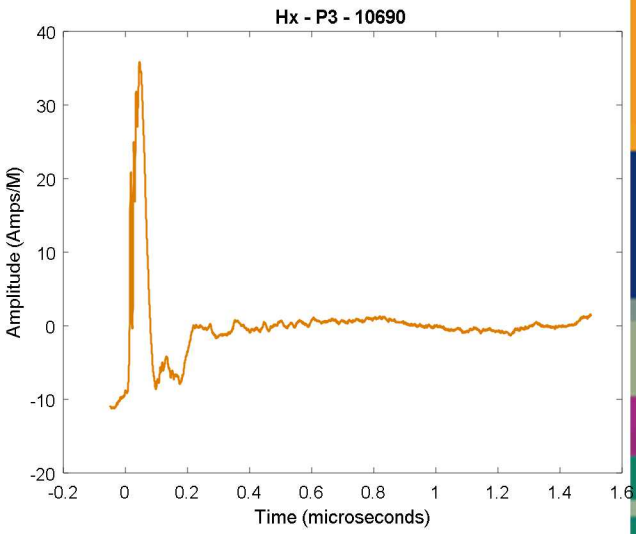

HERMES, Platform 2, Electric Fields

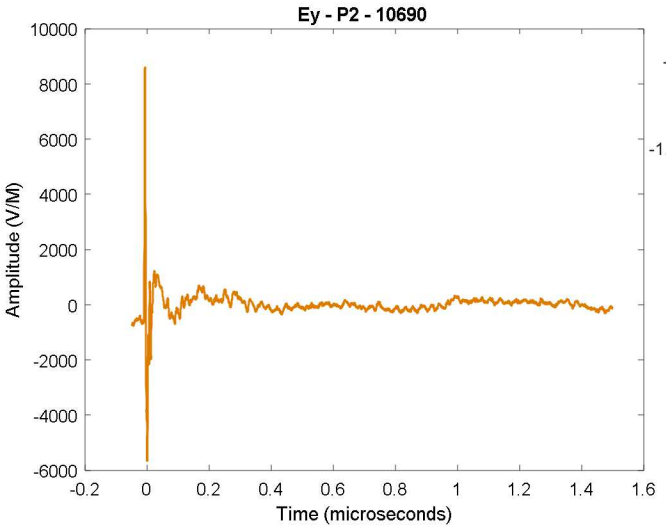

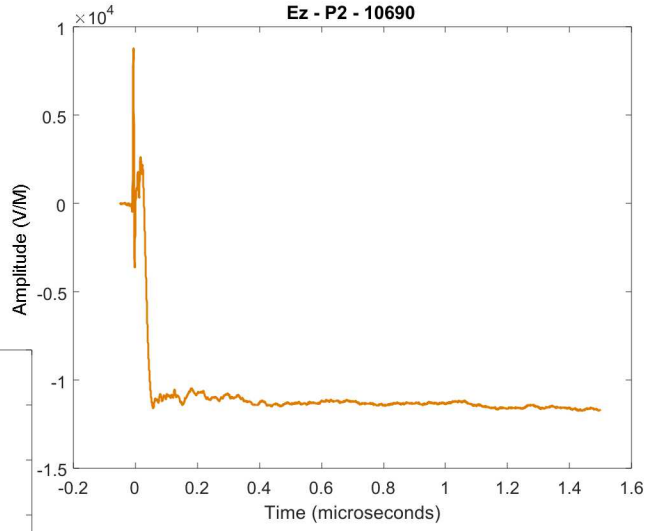

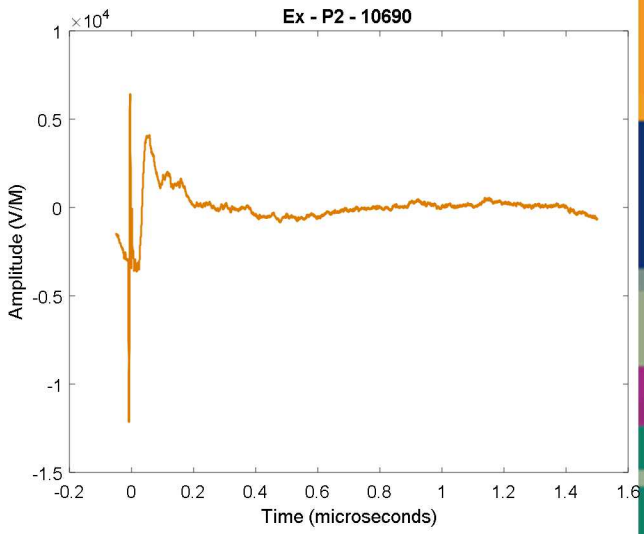

HERMES, Platform 2, Magnetic Fields

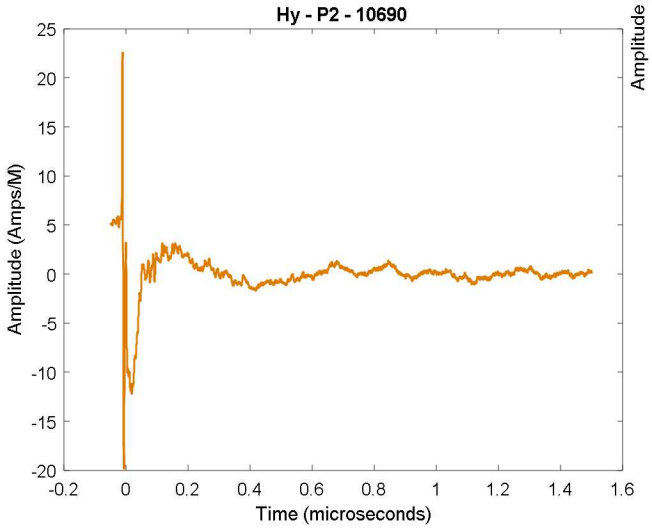

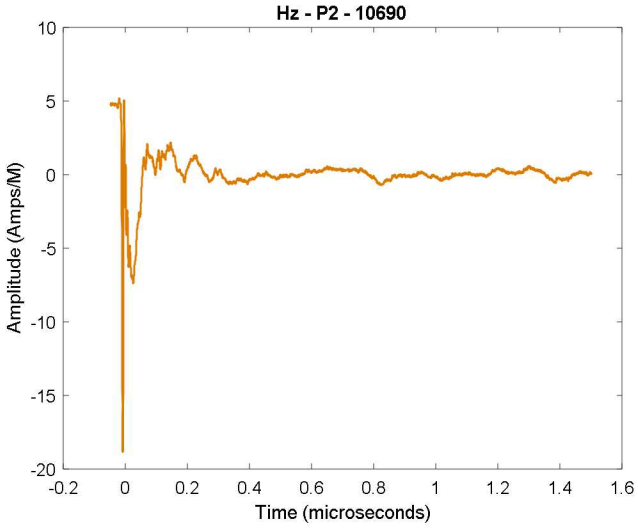

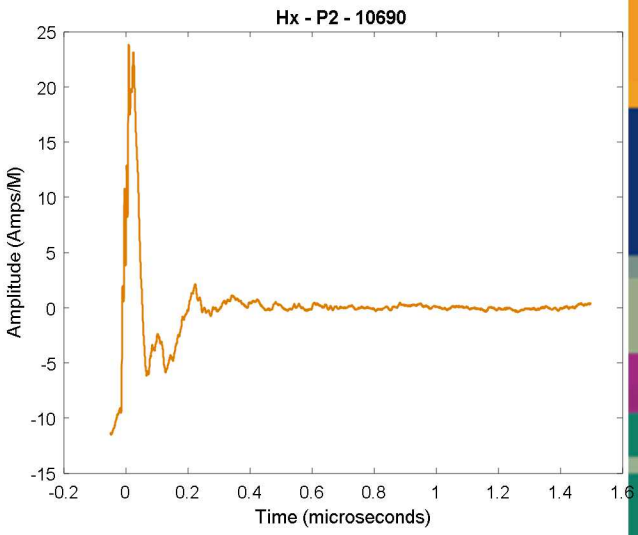

HERMES, Platform 1, Electric Fields

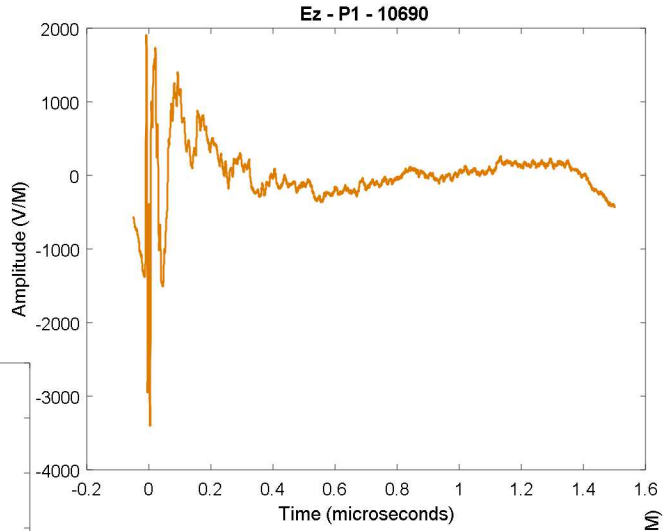

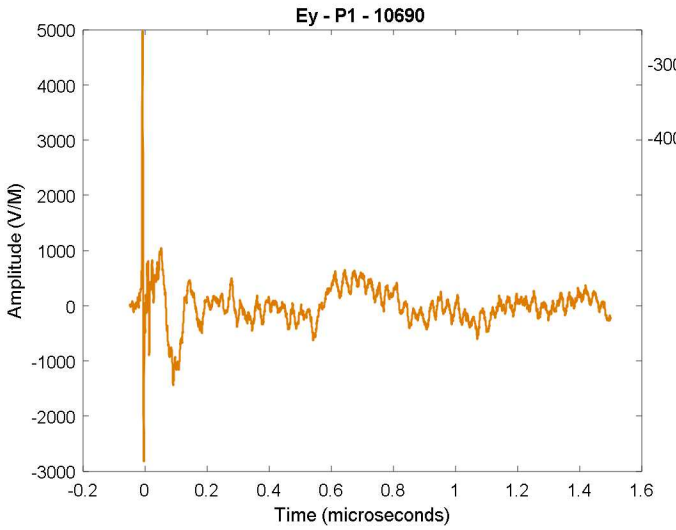

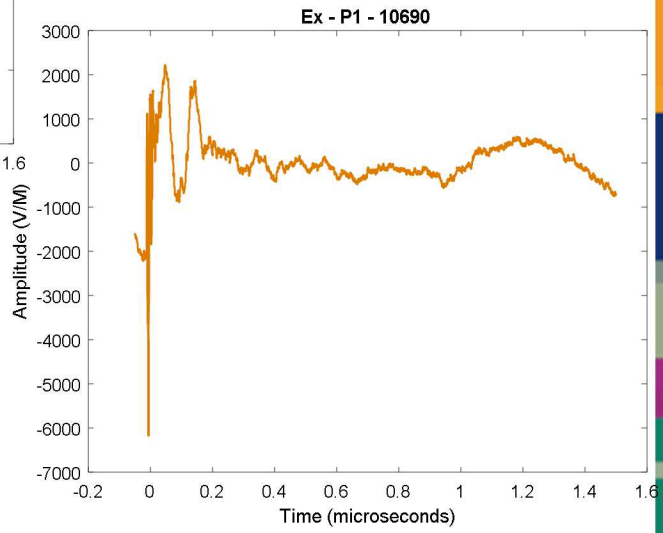

HERMES, Platform 1, Magnetic Fields

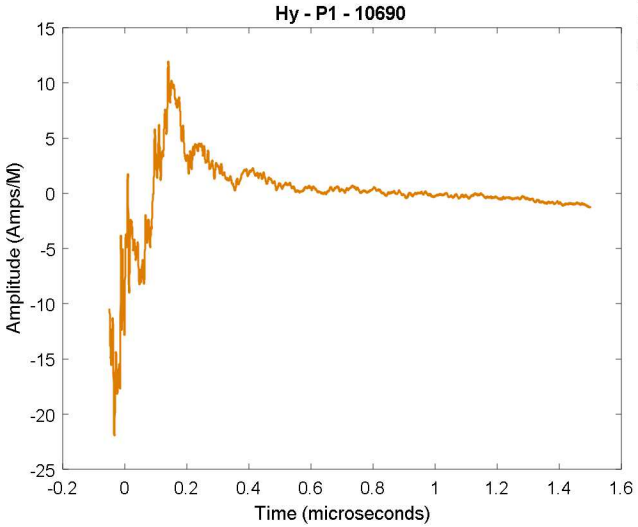

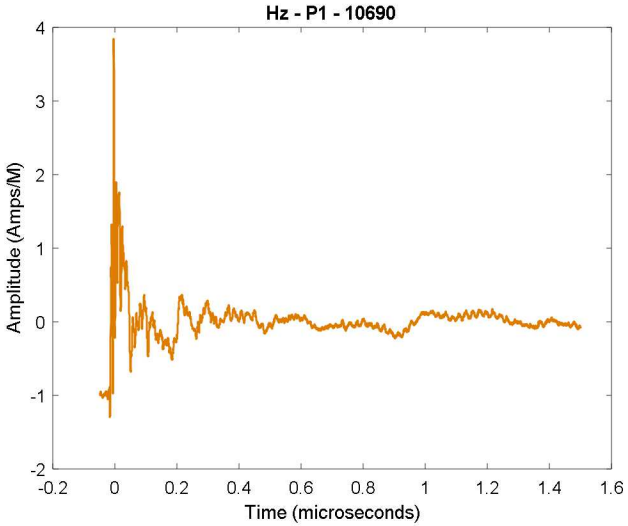

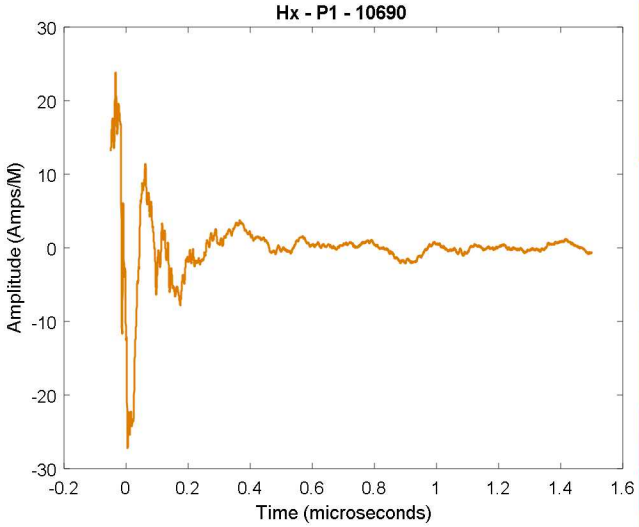

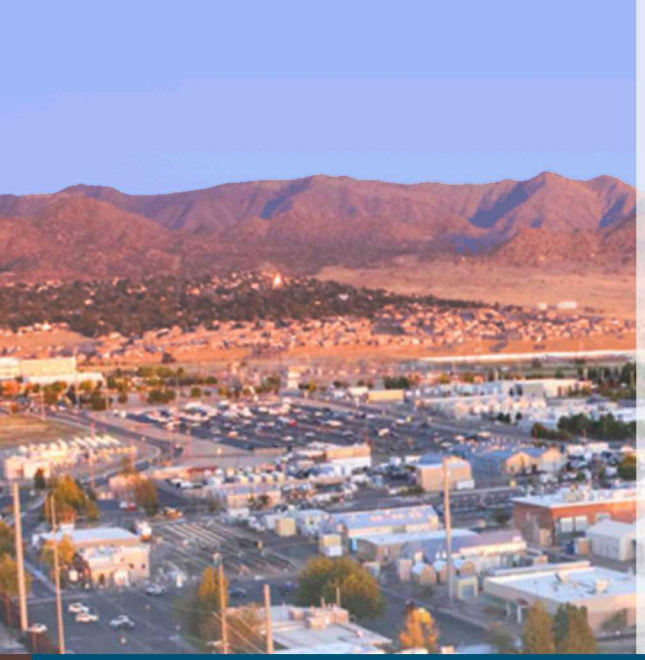

Courtyard Fields - Shot 10705

HERMES, Platform 4, Electric Fields

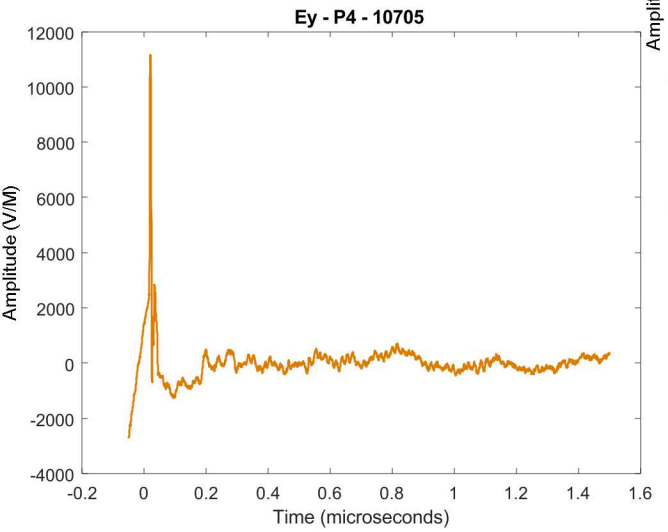

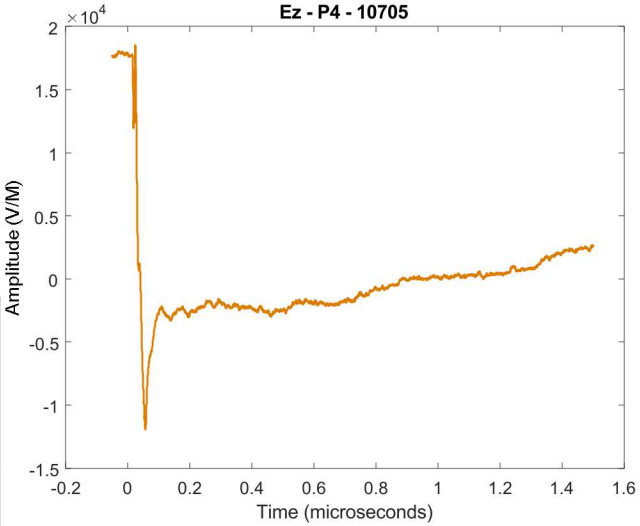

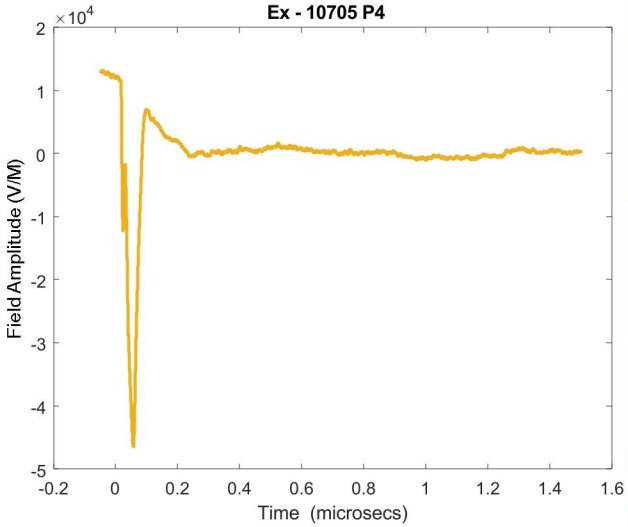

HERMES, Platform 4, Magnetic Fields

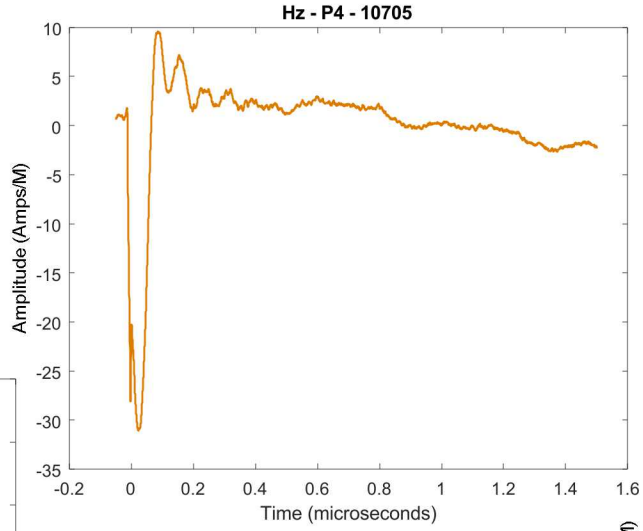

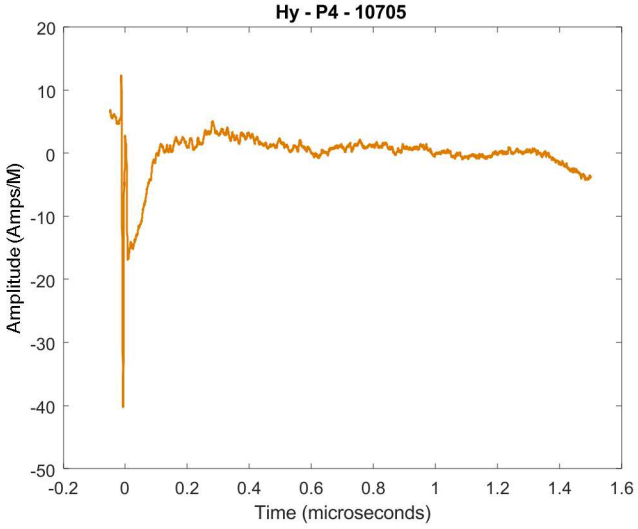

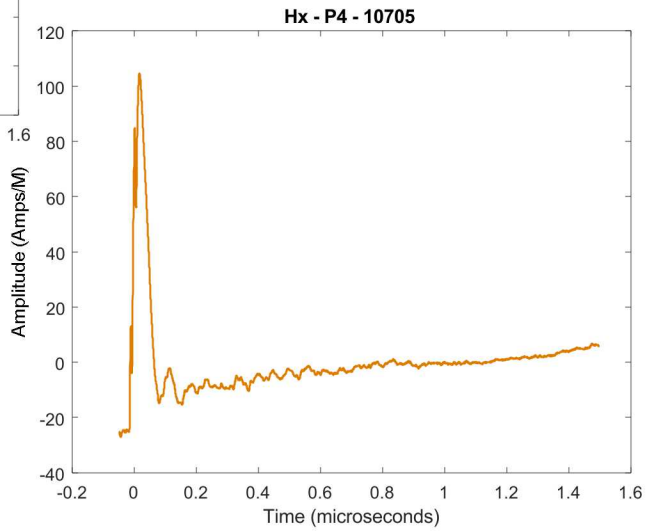

HERMES, Platform 3, Electric Fields

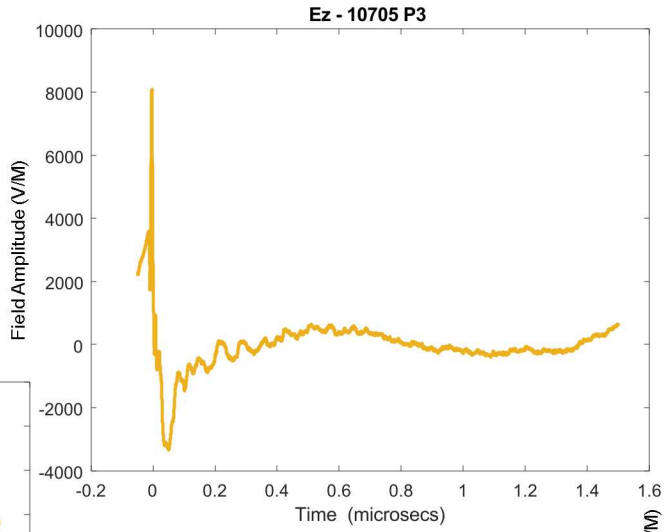

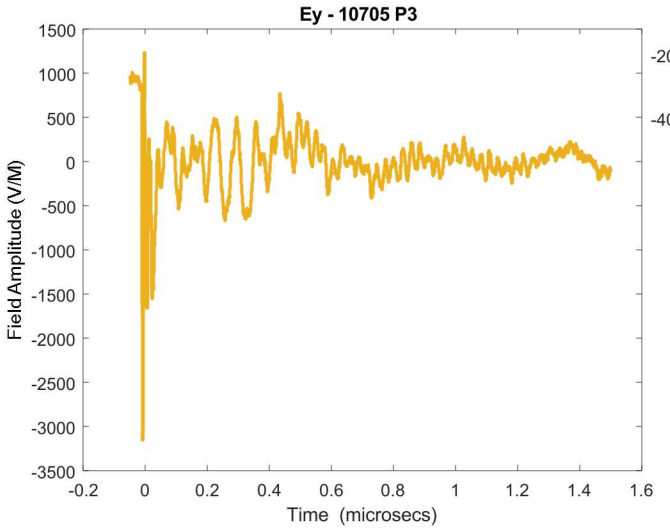

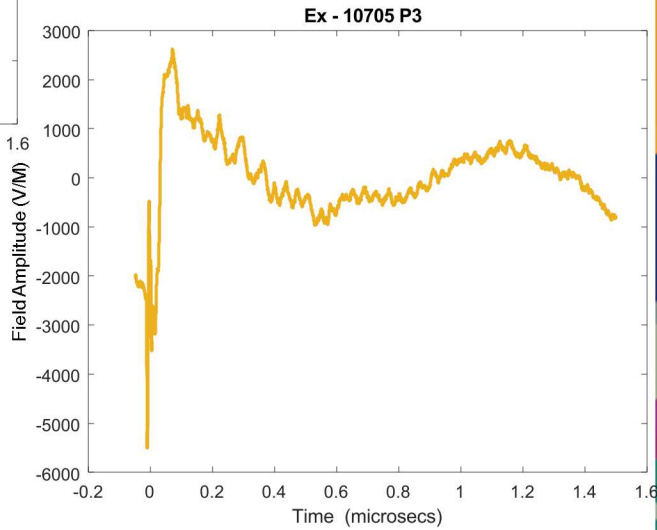

HERMES, Platform 3, Magnetic Fields

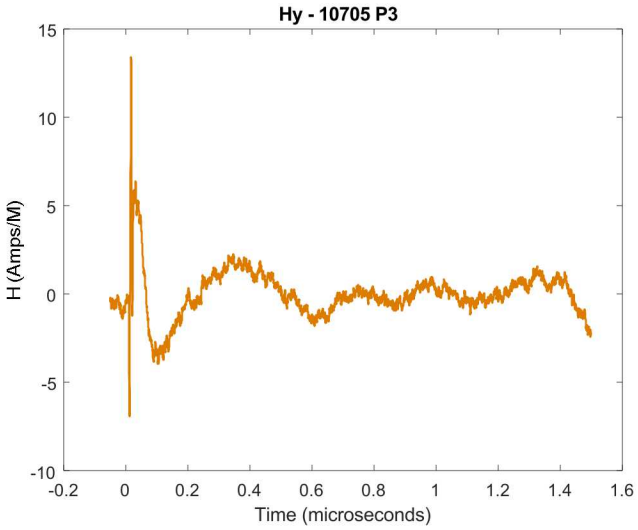

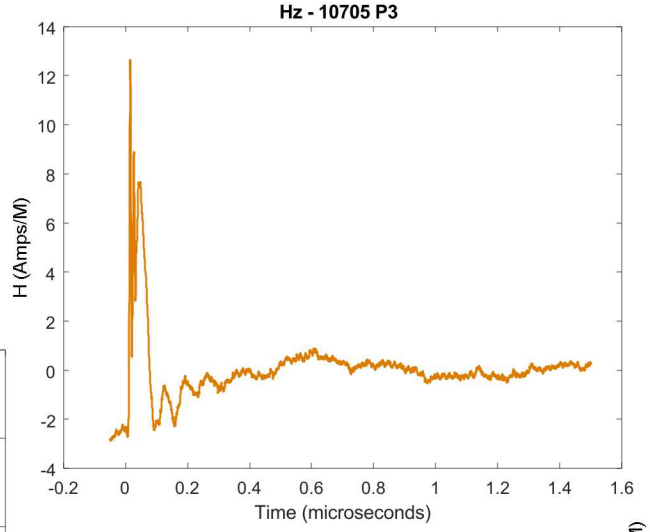

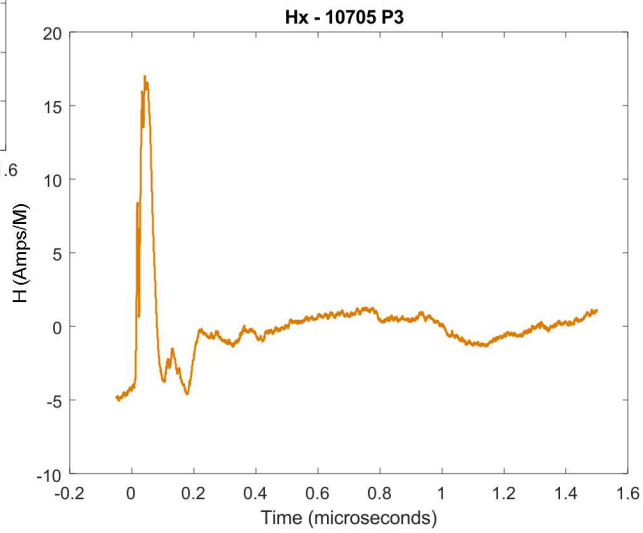

HERMES, Platform 2, Electric Fields

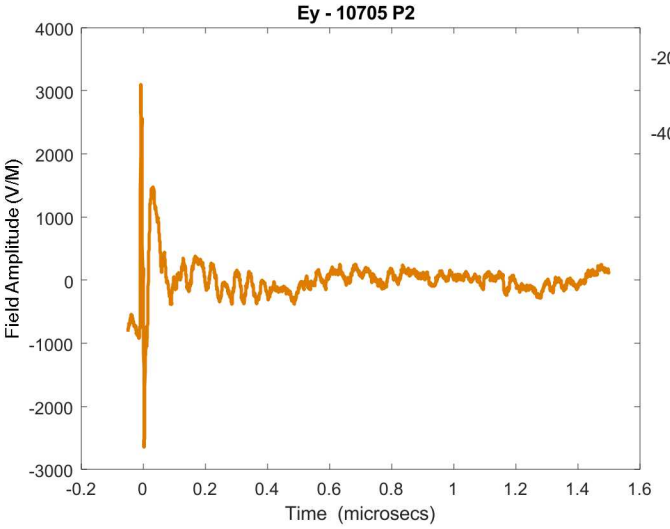

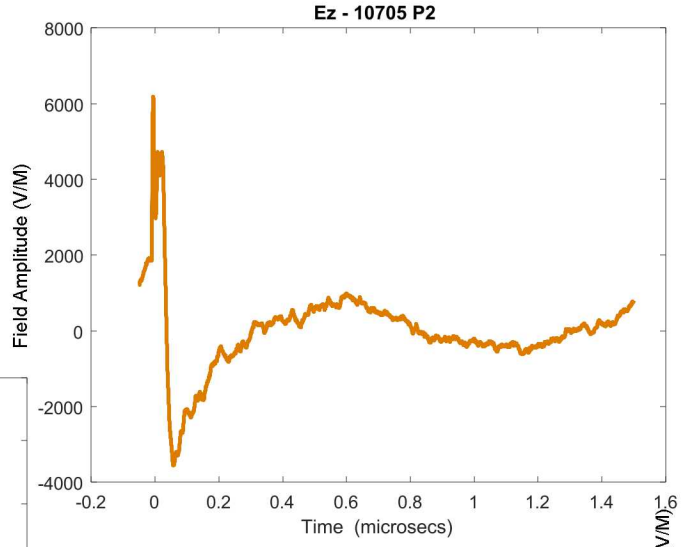

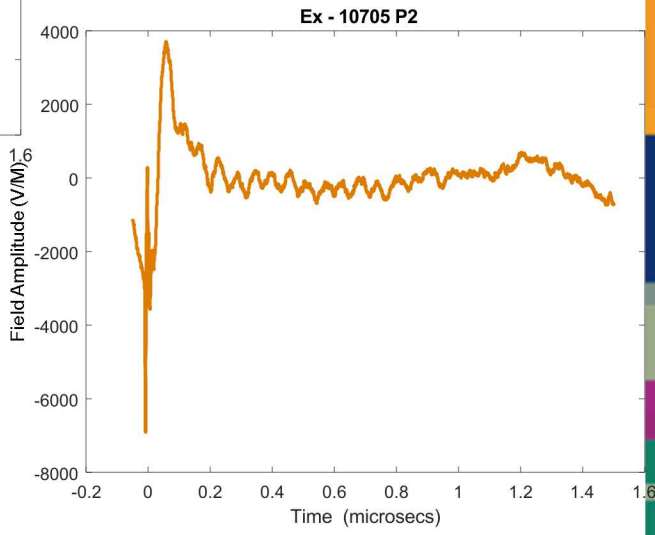

HERMES, Platform 2, Magnetic Fields

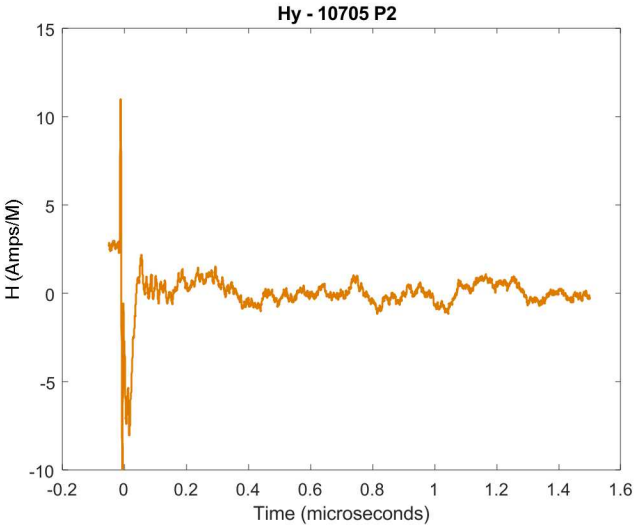

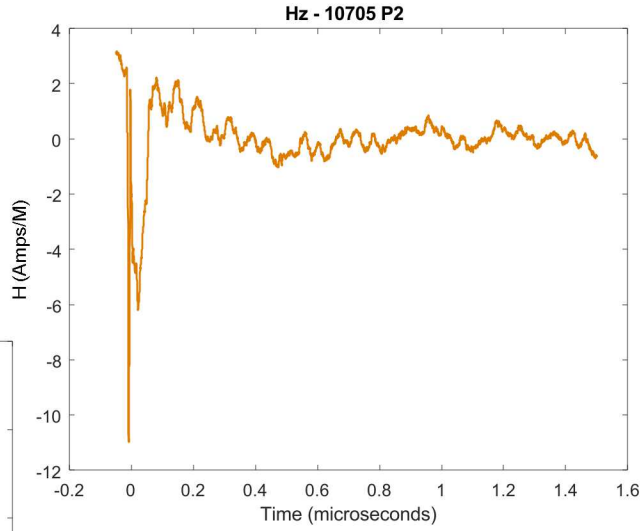

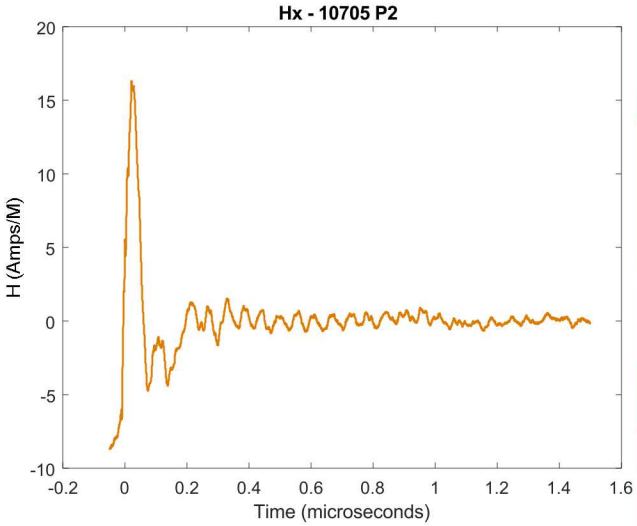

HERMES, Platform 1, Electric Fields

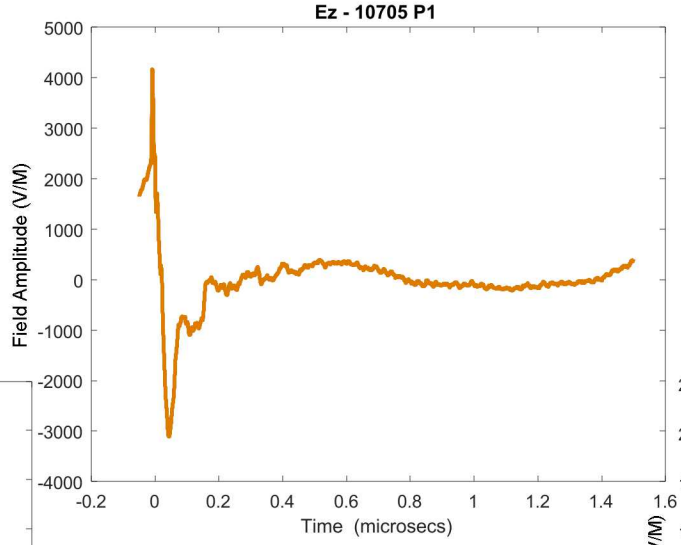

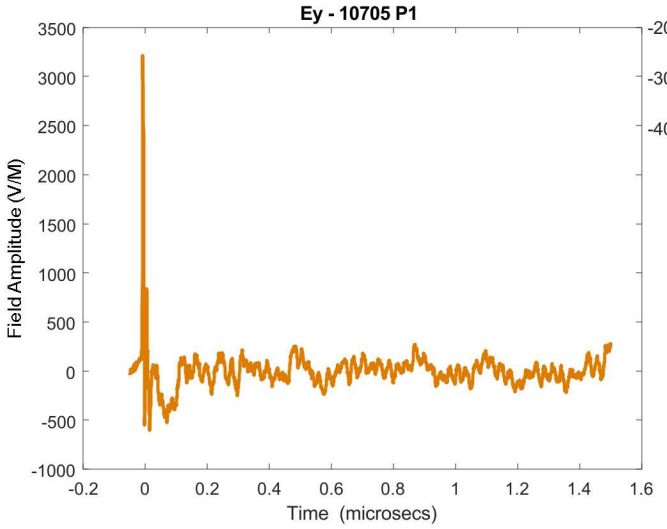

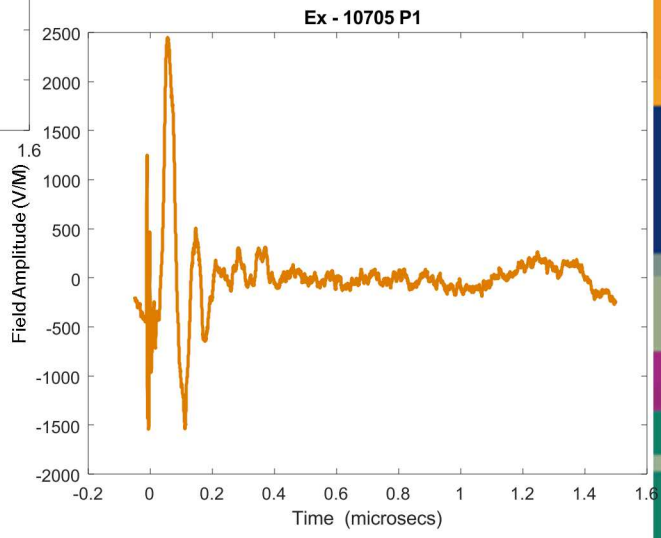

HERMES, Platform 1, Magnetic Fields

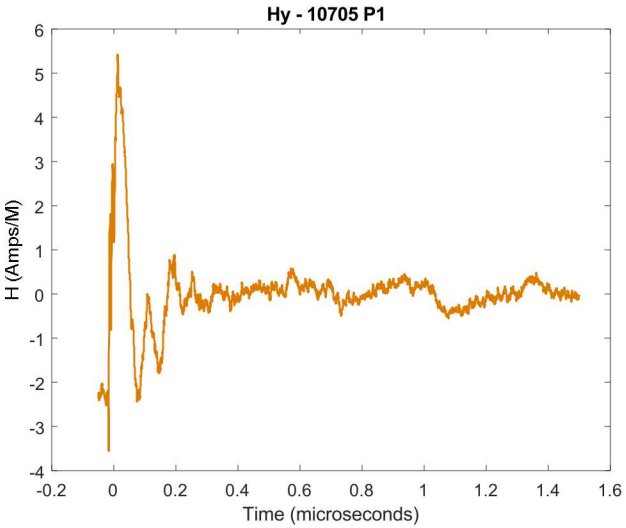

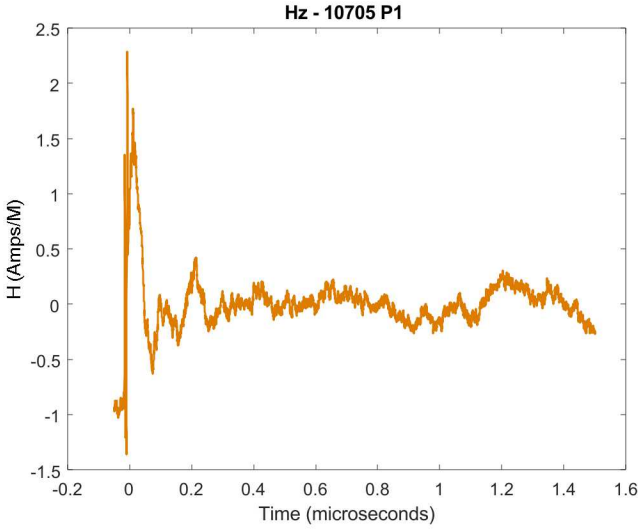

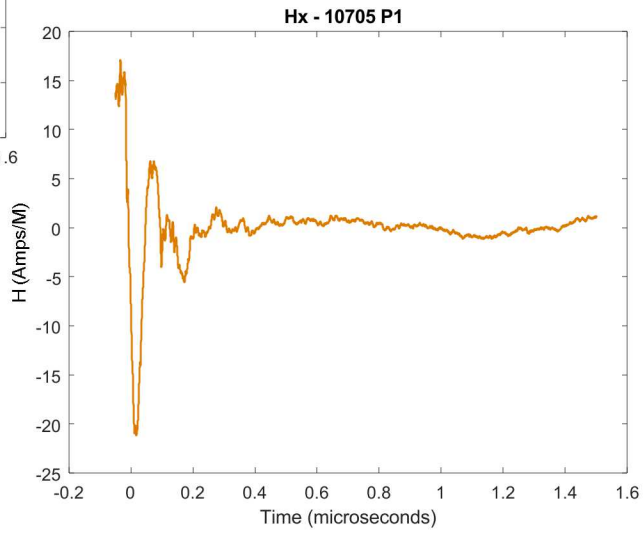

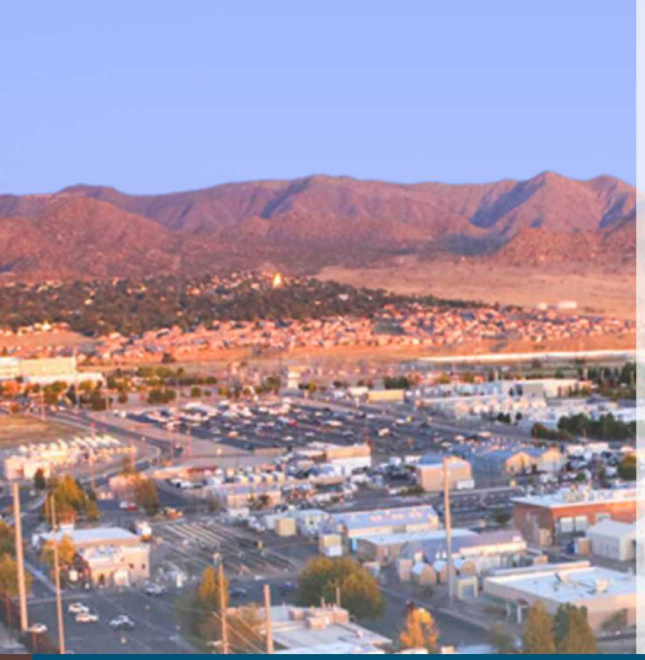

IX. Test Article Fields & Surface Currents

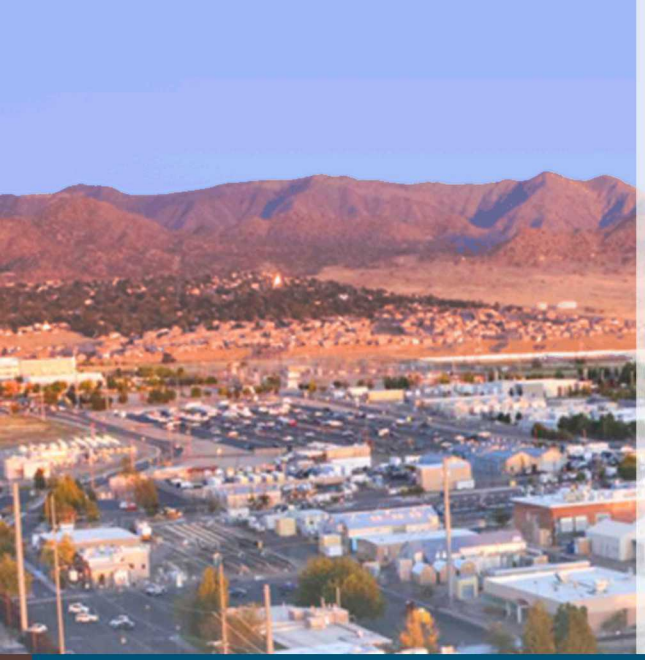

CN Fields & Surface Currents- Shot 10664

CN Fields

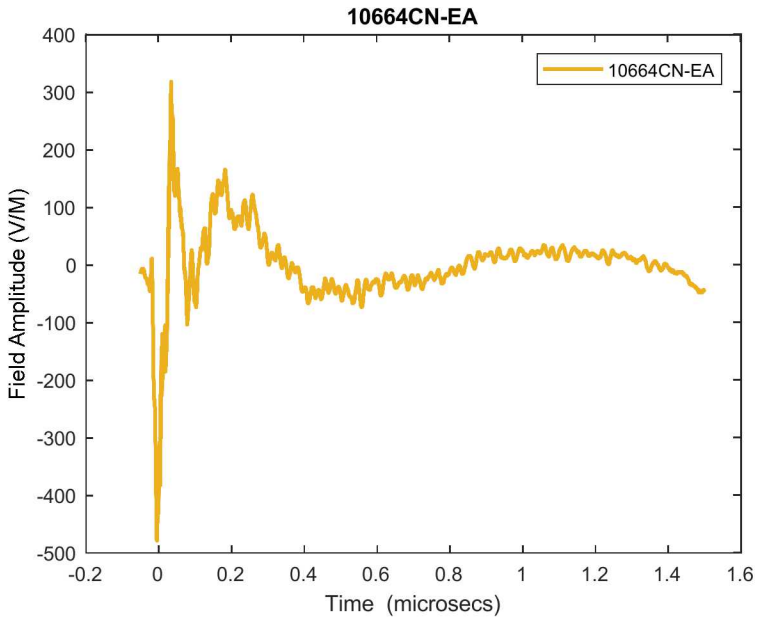
10664CN-EA
10664CN-EA
Field Amplitude (V/M)
Time (microsecs)
400
300
200
100
0
-100
-200
-300
-400
-500
-0.2
0
0.2
0.4
0.6
0.8
1
1.2
1.4
1.6

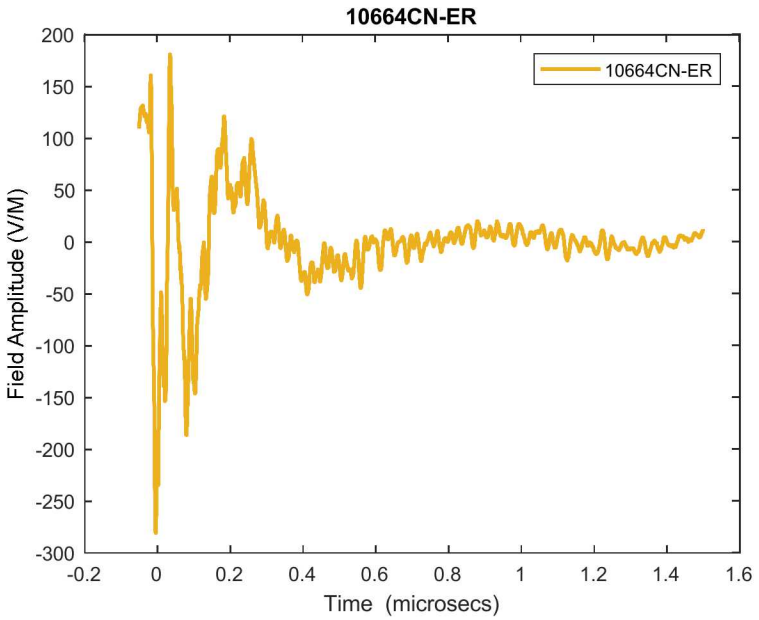
10664CN-ER
10664CN-ER
Field Amplitude (V/M)
Time (microsecs)
200
150
100
50
0
-50
-100
-150
-200
-250
-300
-0.2
0
0.2
0.4
0.6
0.8
1
1.2
1.4
1.6

CN Surface Currents

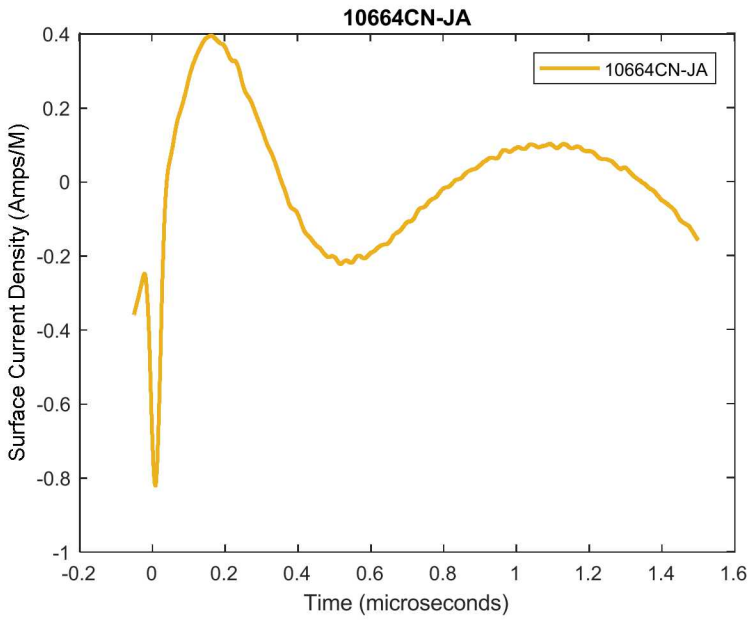

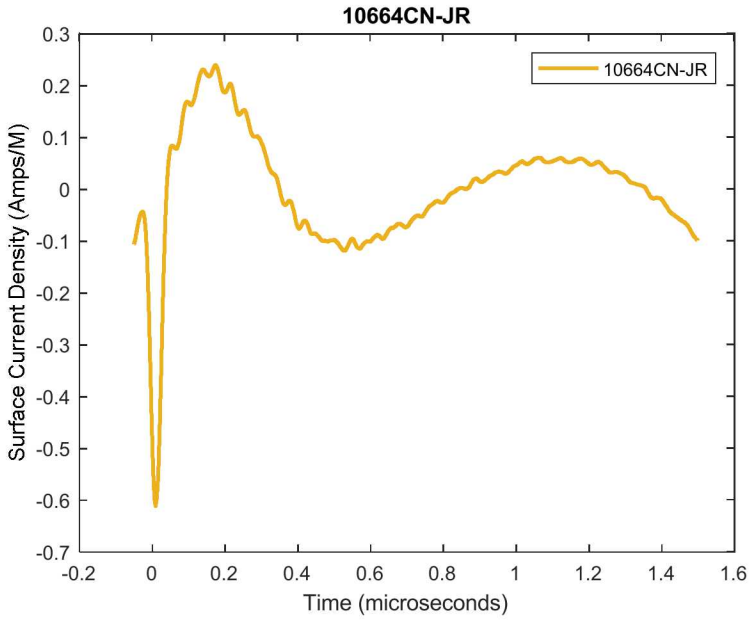

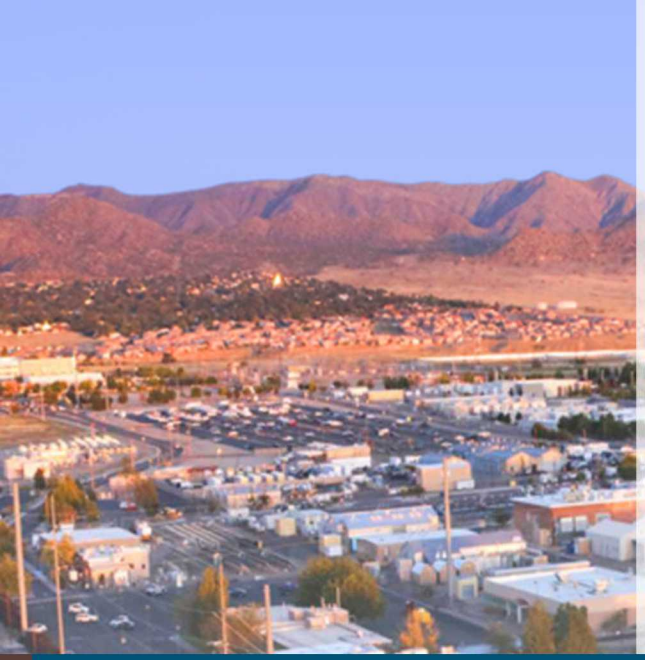

Cylinder, Fields & Surface Currents- Shot 10664

Cylinder, Inside Electric Fields

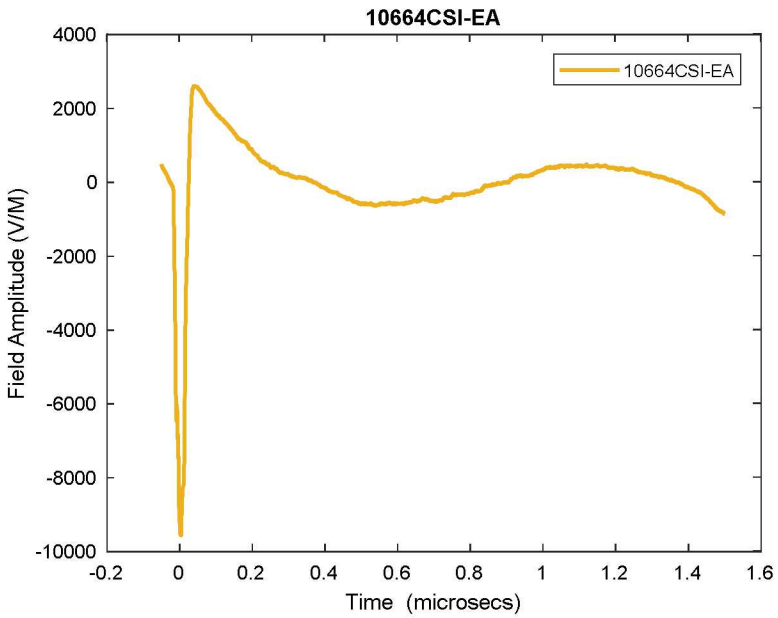

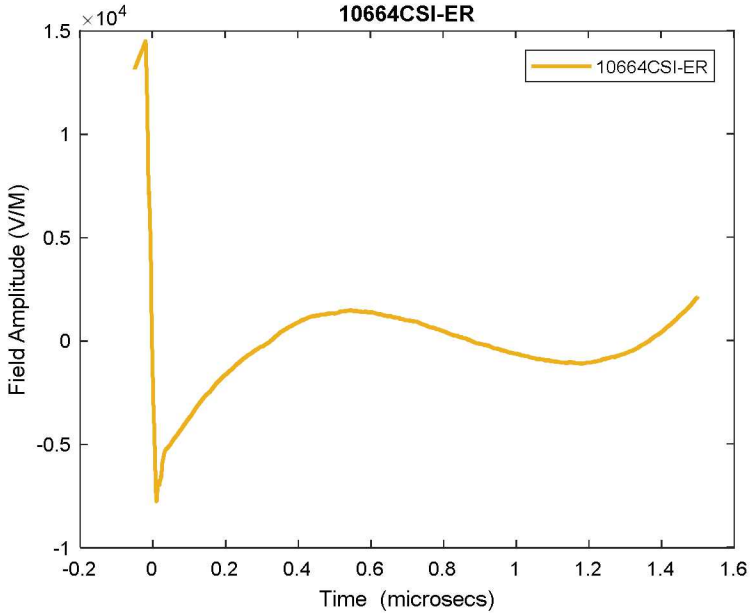

Cylinder, Inside Current Densities

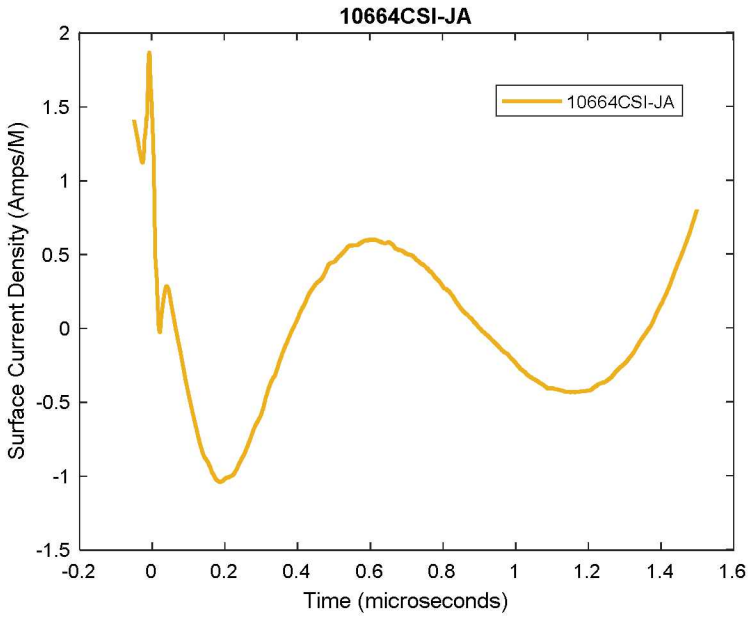

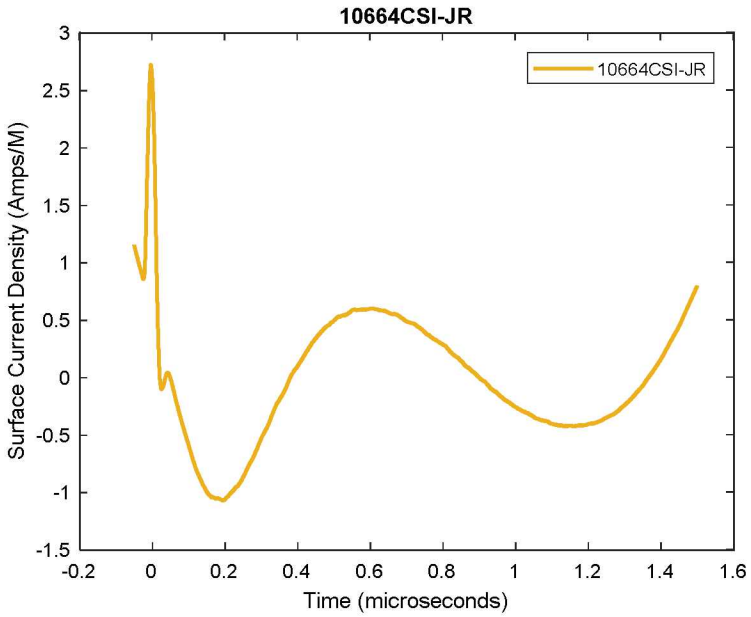

Cylinder, Outside Current Densities

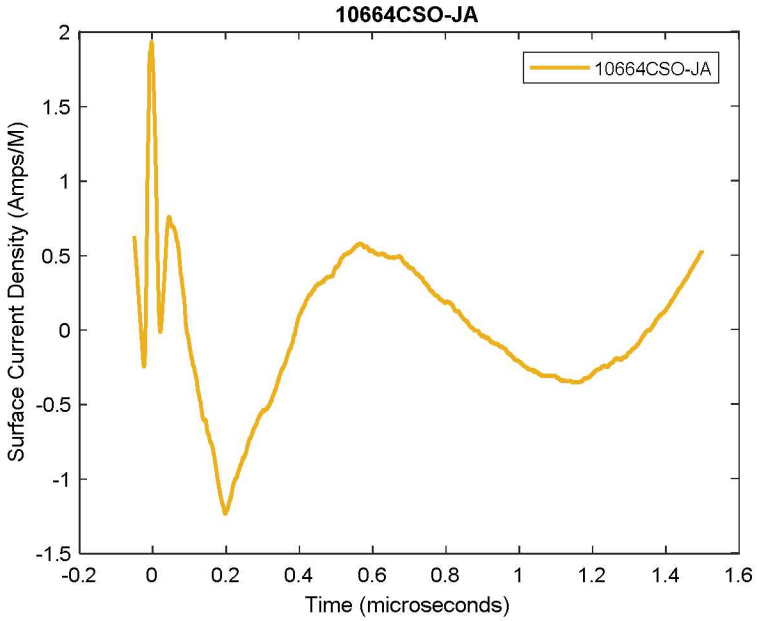

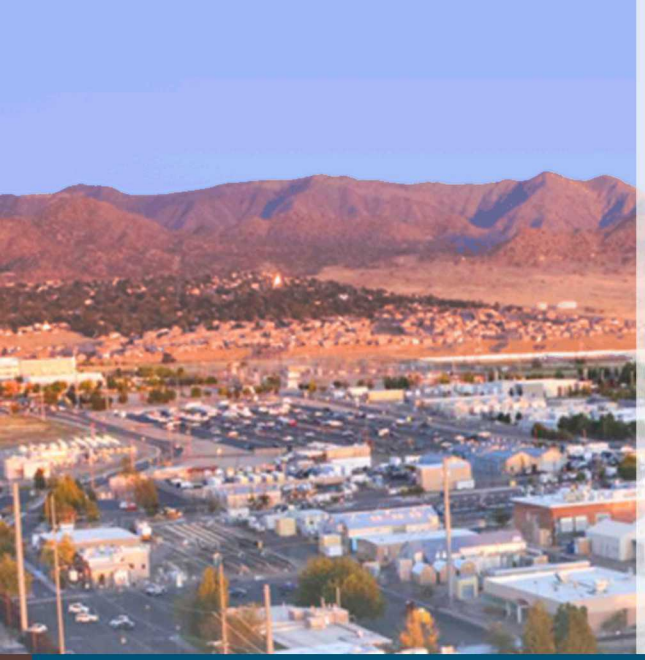

AF, Fields & Surface Currents- Shot 10664

AF – Witness Cable, Short

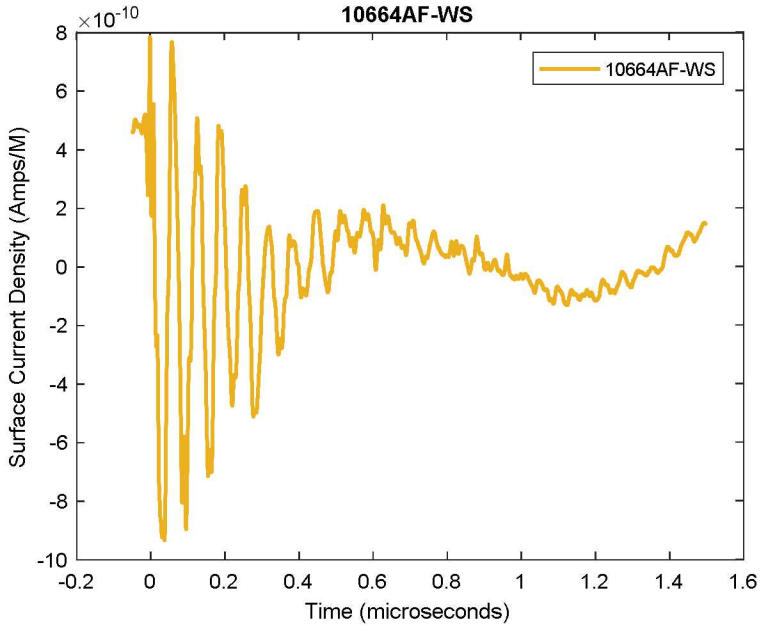

AF, Electric Fields

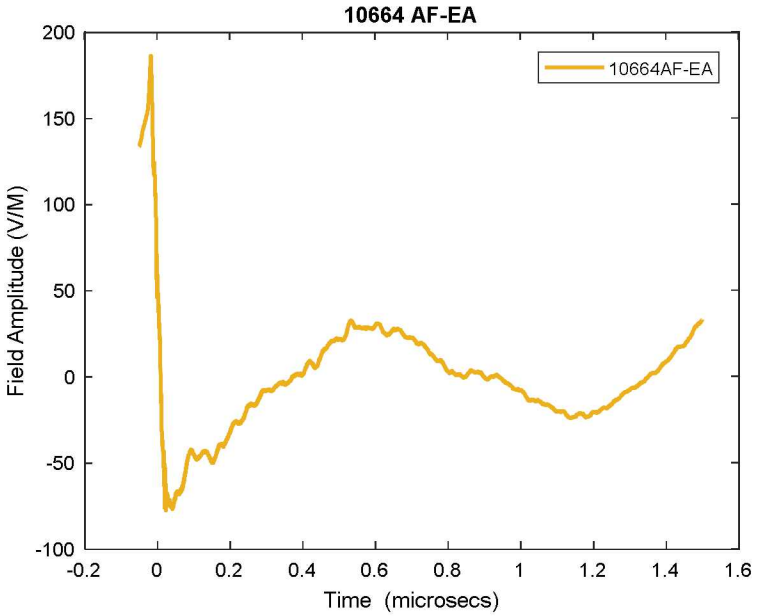

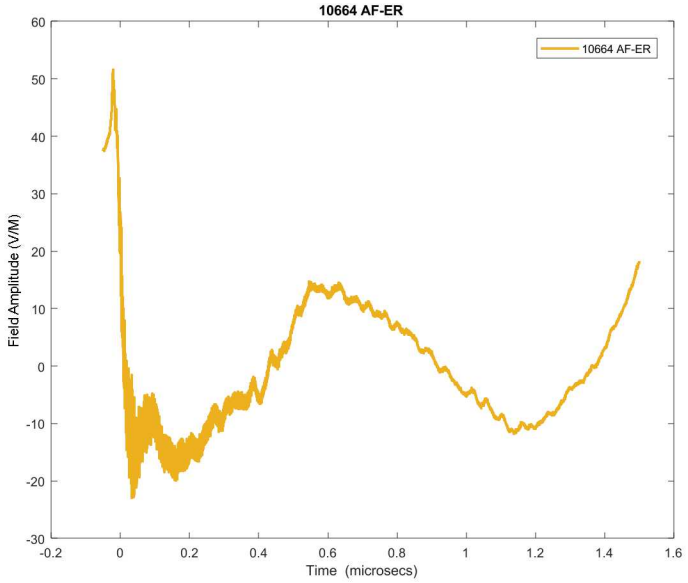

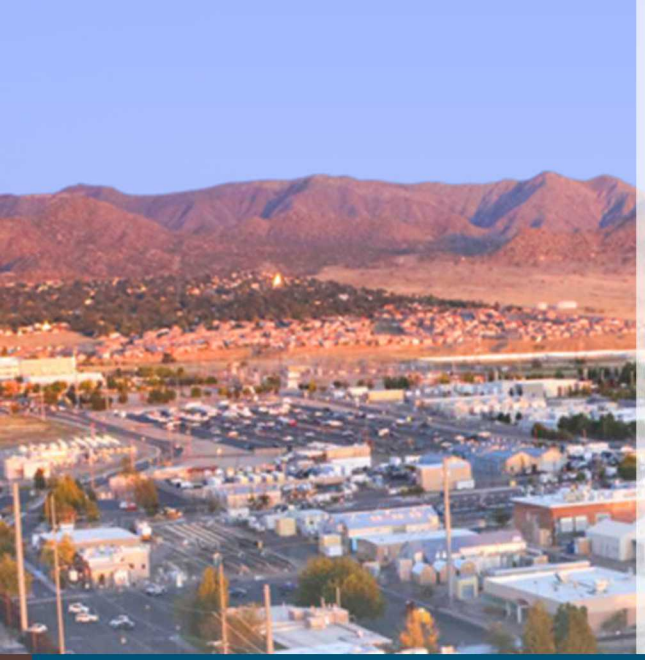

CN Fields & Surface Currents- Shot 10670

CN Fields

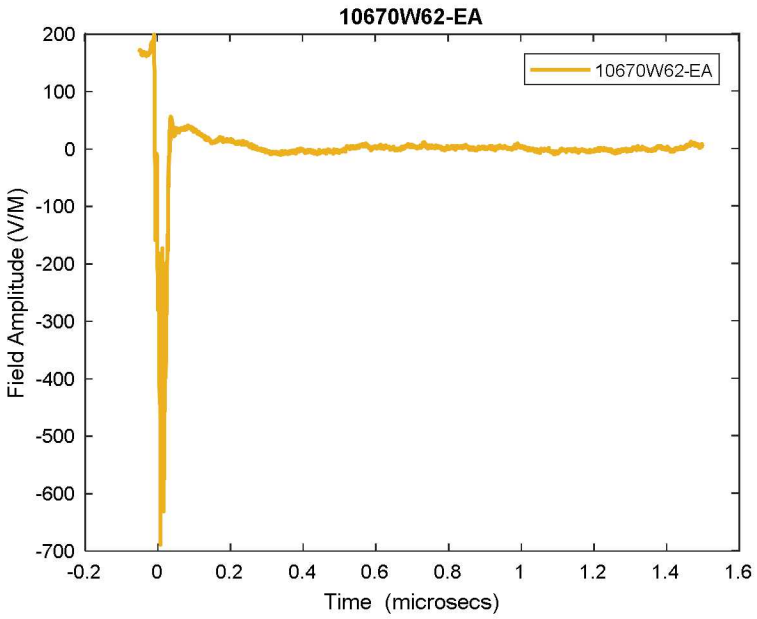
10670W62-EA
10670W62-EA
Field Amplitude (V/M)
Time (microsecs)
200
100
0
-100
-200
-300
-400
-500
-600
-700
-0.2
0
0.2
0.4
0.6
0.8
1
1.2
1.4
1.6

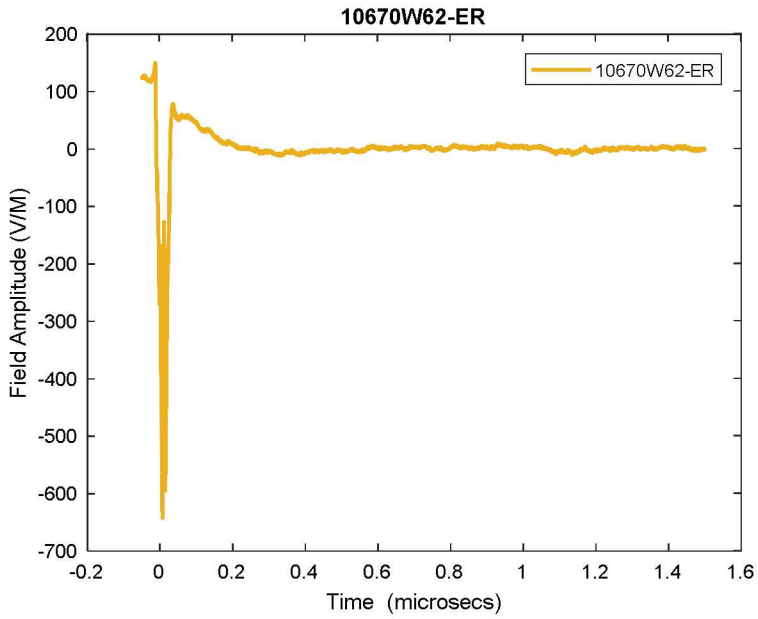
10670W62-ER
10670W62-ER
Field Amplitude (V/M)
Time (microsecs)
200
100
0
-100
-200
-300
-400
-500
-600
-700
-0.2
0
0.2
0.4
0.6
0.8
1
1.2
1.4
1.6

CN Surface Currents

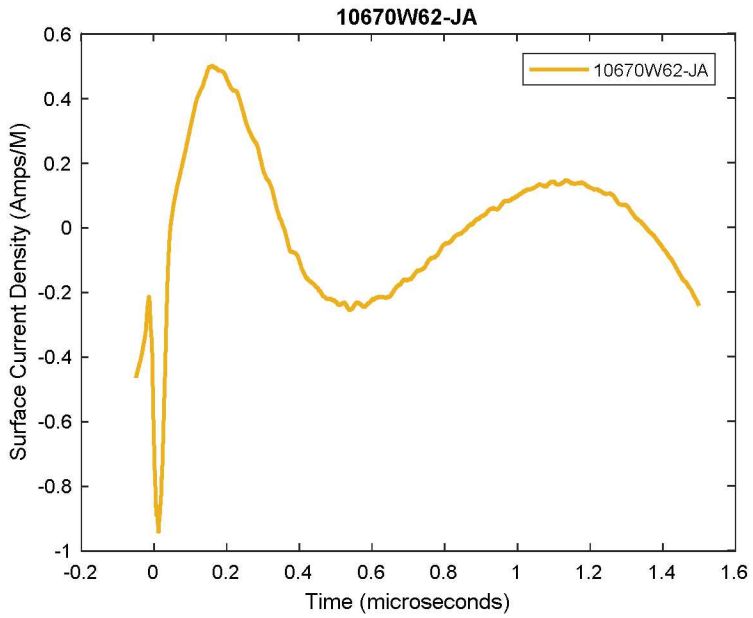

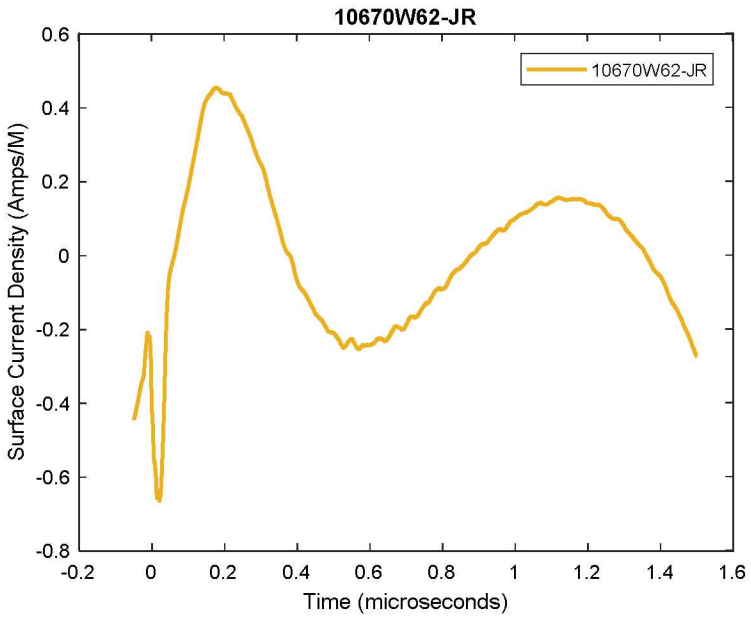

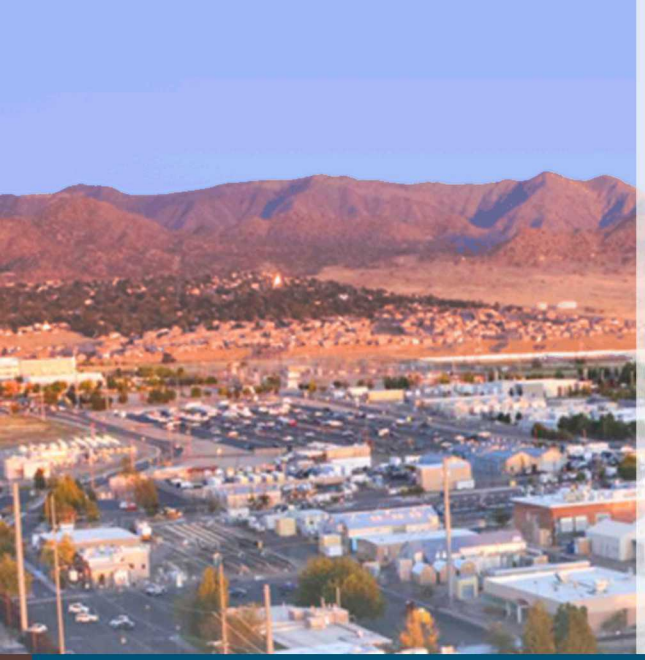

Cylinder, Fields & Surface Currents- Shot 10670

Cylinder, Inside Electric Fields

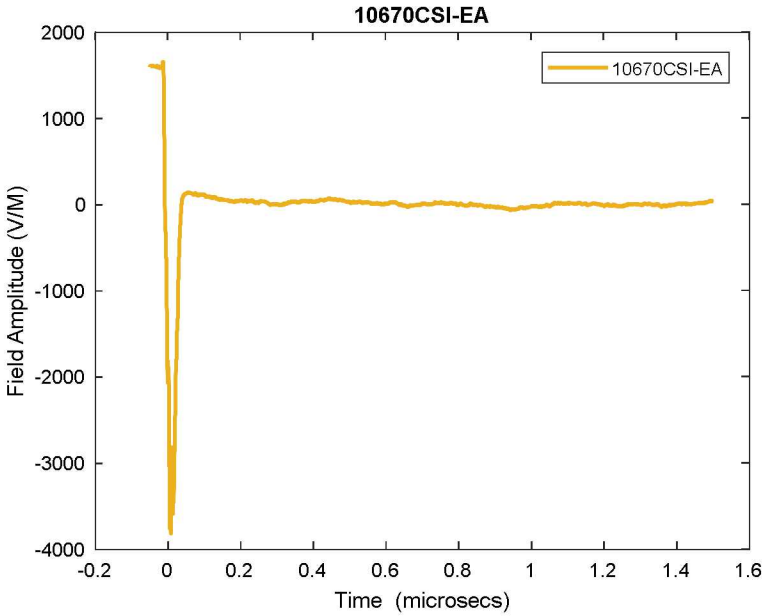

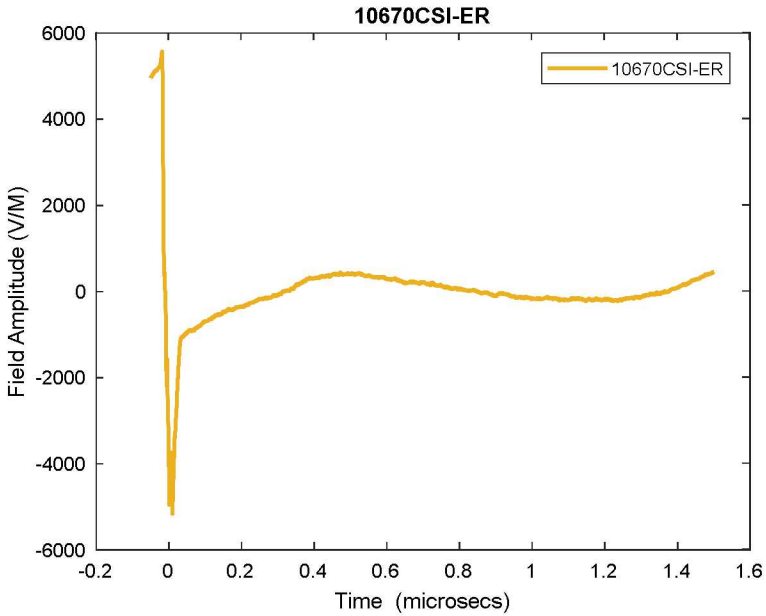

Cylinder, Inside Current Densities

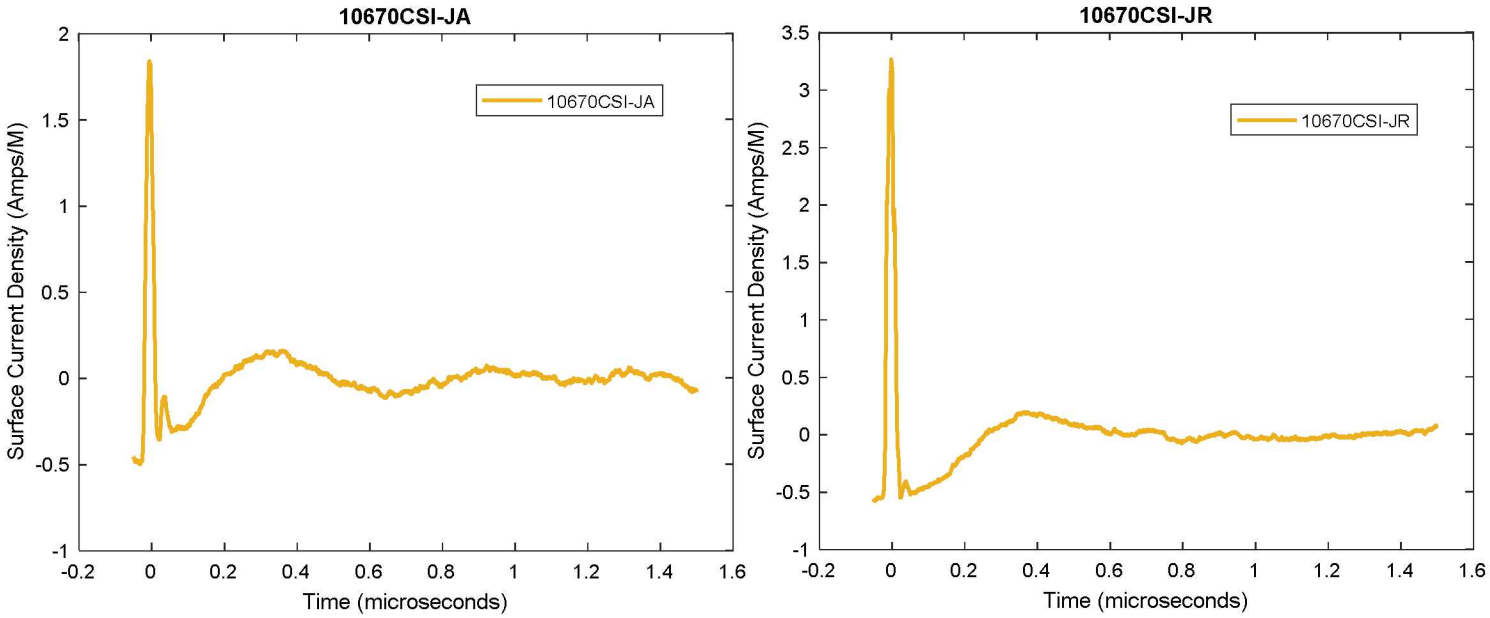

Cylinder, Outside Current Densities

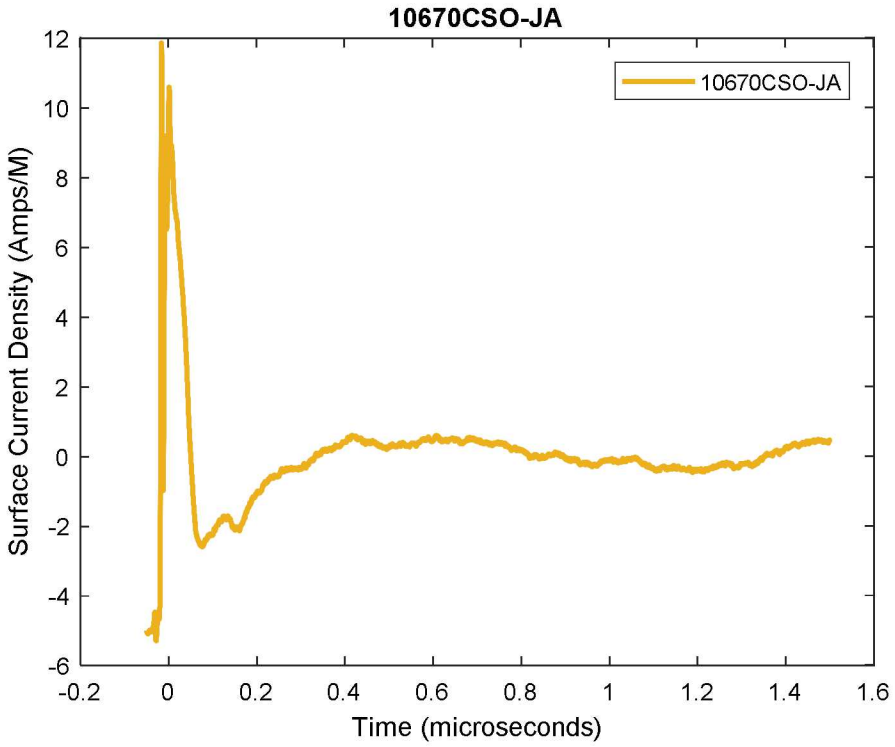

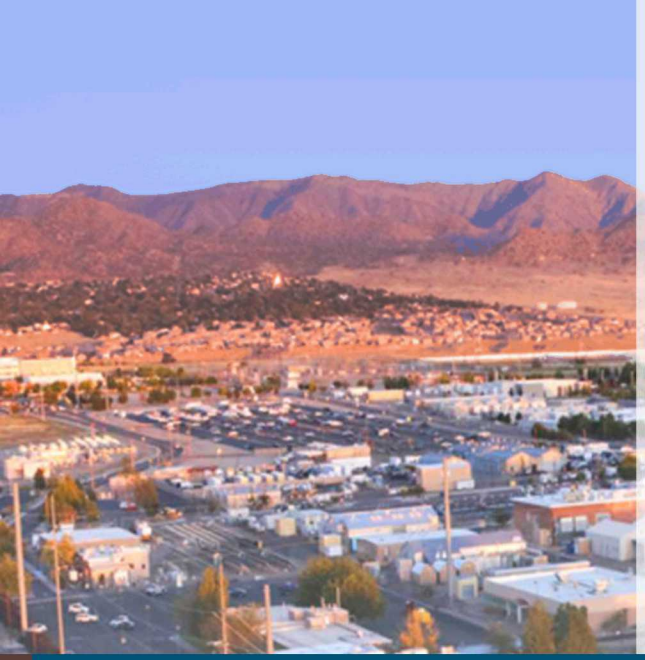

AF, Fields & Surface Currents- Shot 10670

AF – Witness Cable, Short

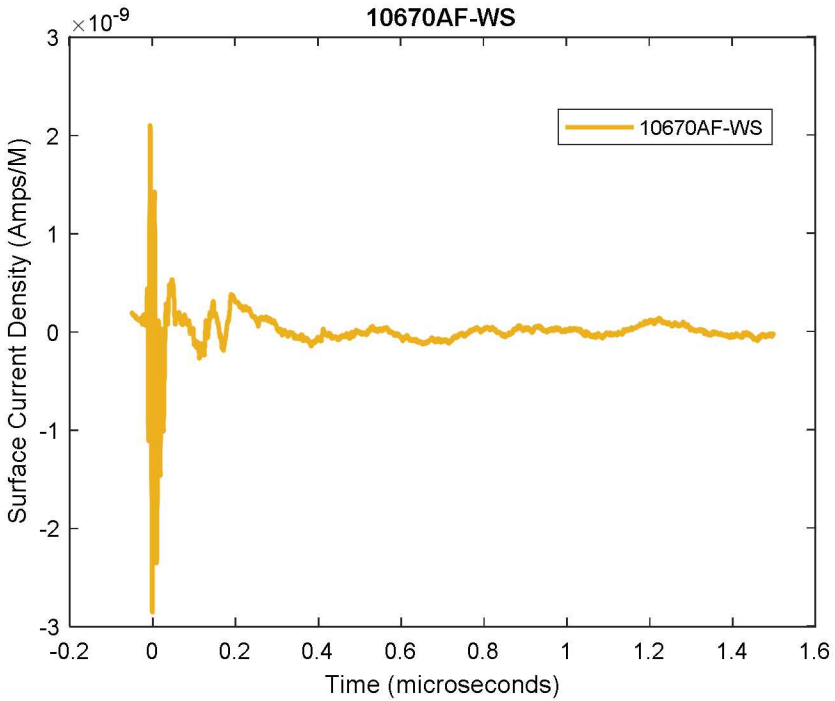

AF, Electric Fields

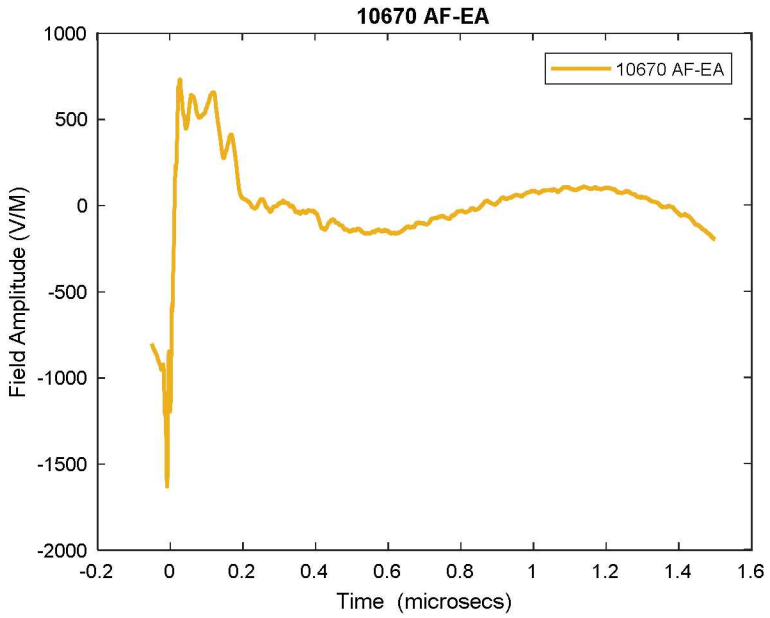

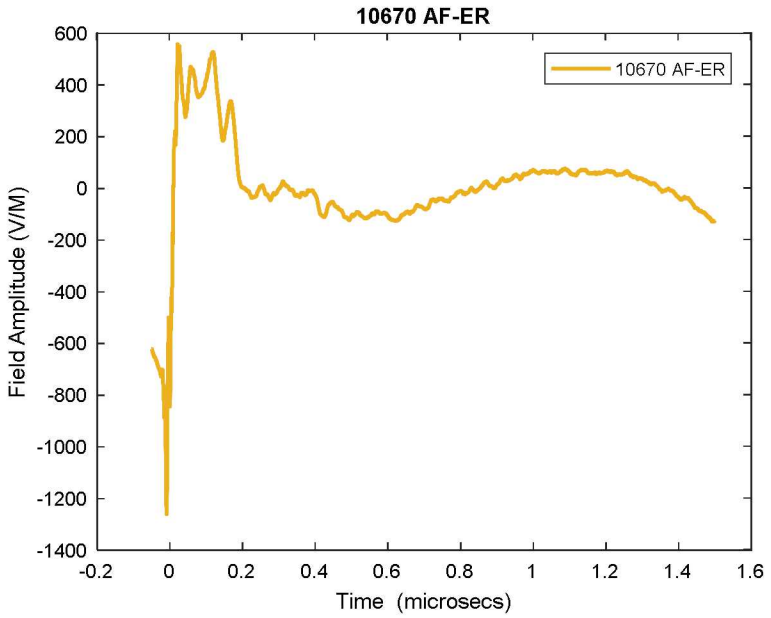

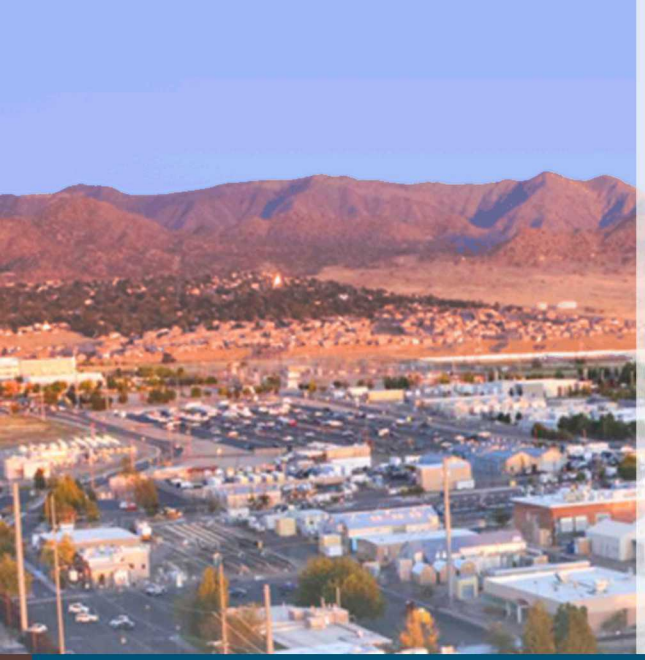

CN Fields & Surface Currents- Shot 10675

CN Fields

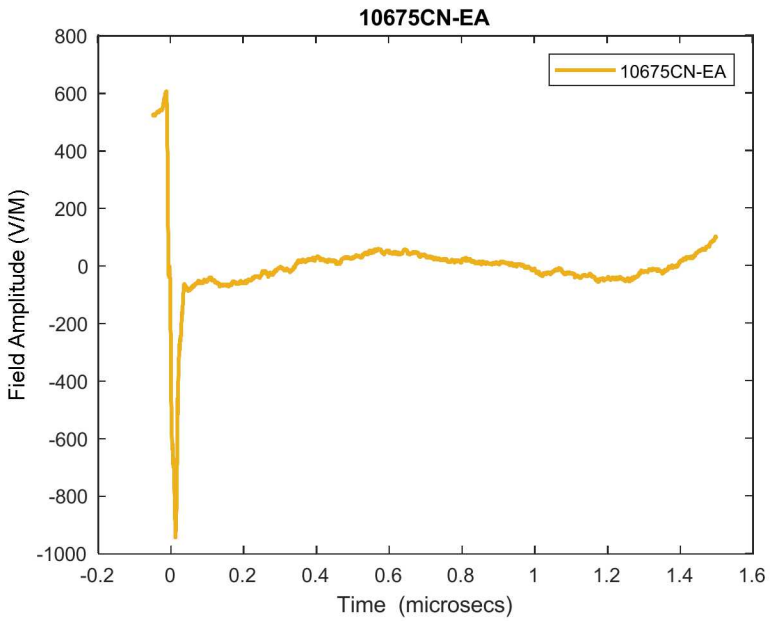
10675CN-EA
10675CN-EA
Field Amplitude (V/M)
Time (microsecs)
800
600
400
200
0
-200
-400
-600
-800
-1000
-0.2
0
0.2
0.4
0.6
0.8
1
1.2
1.4
1.6

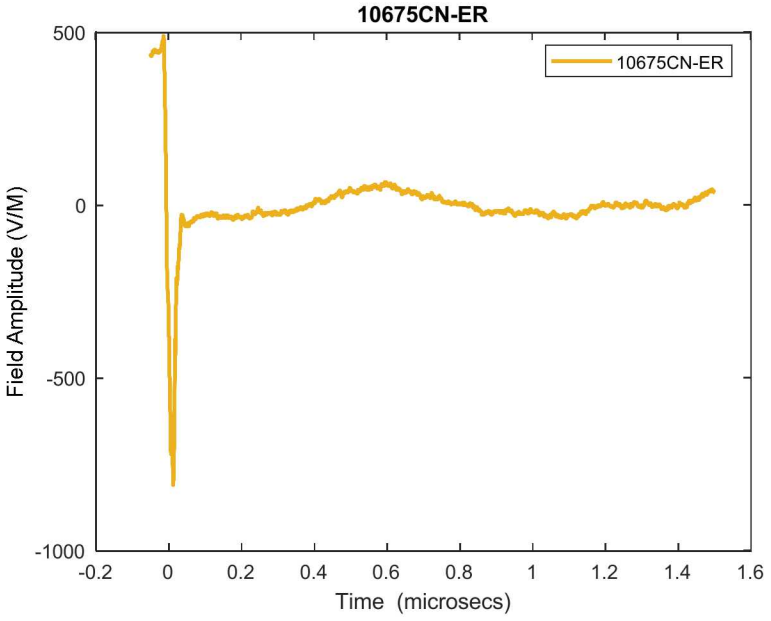
10675CN-ER
10675CN-ER
Field Amplitude (V/M)
Time (microsecs)
500
0
-500
-1000
-0.2
0
0.2
0.4
0.6
0.8
1
1.2
1.4
1.6

CN Surface Currents

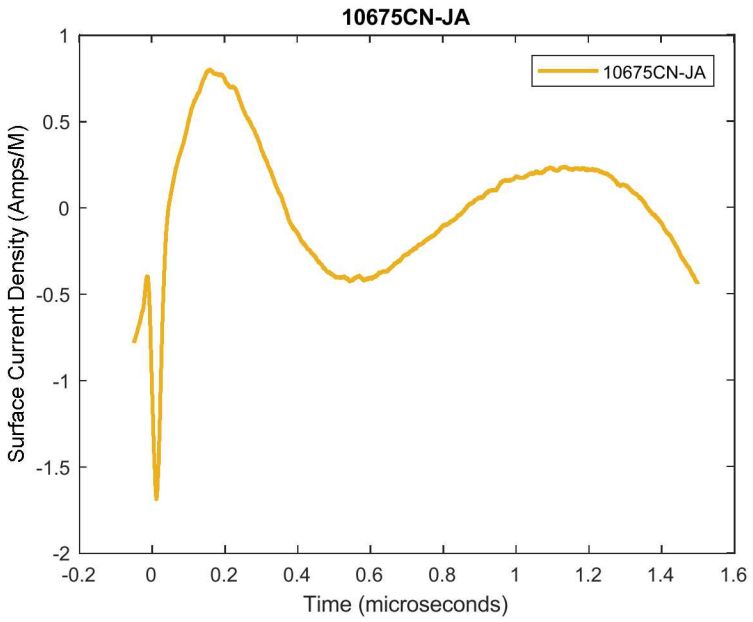

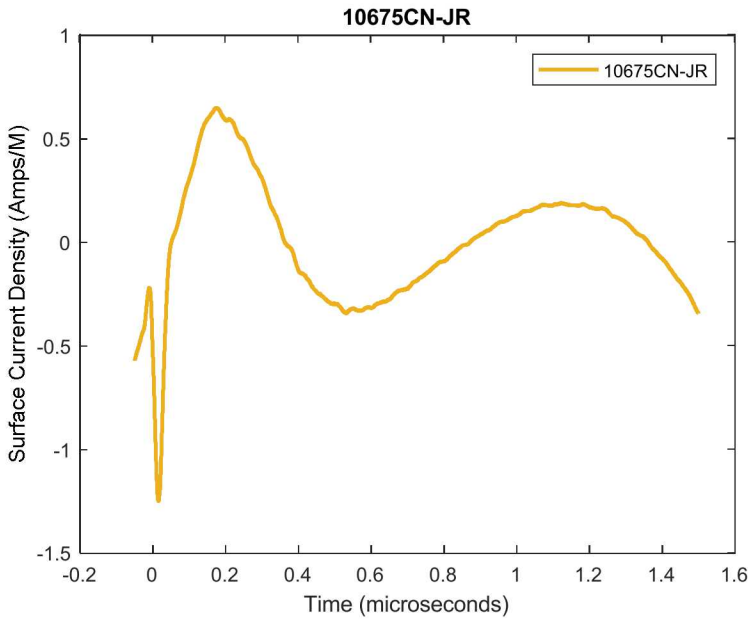

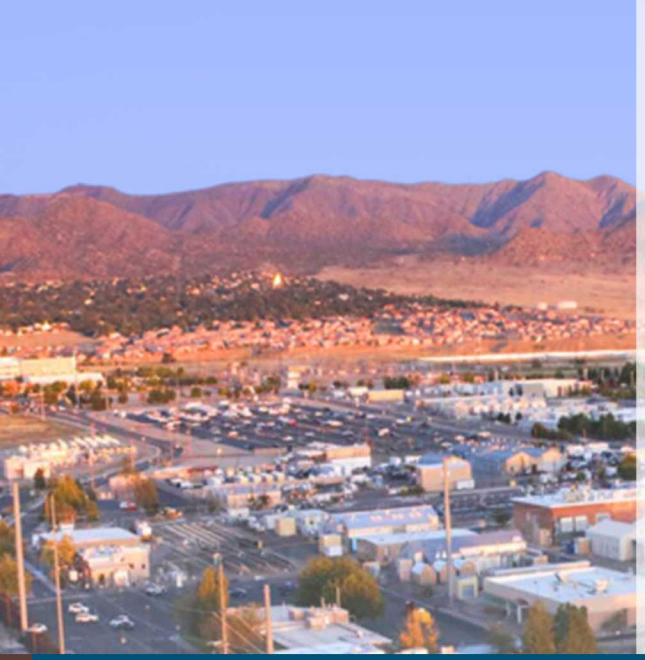

Cylinder, Fields & Surface Currents- Shot 10675

Cylinder, Inside Electric Fields

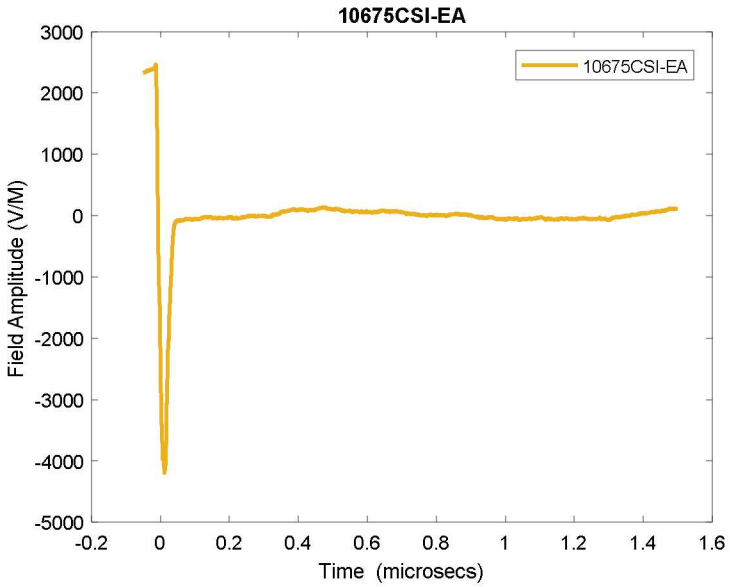

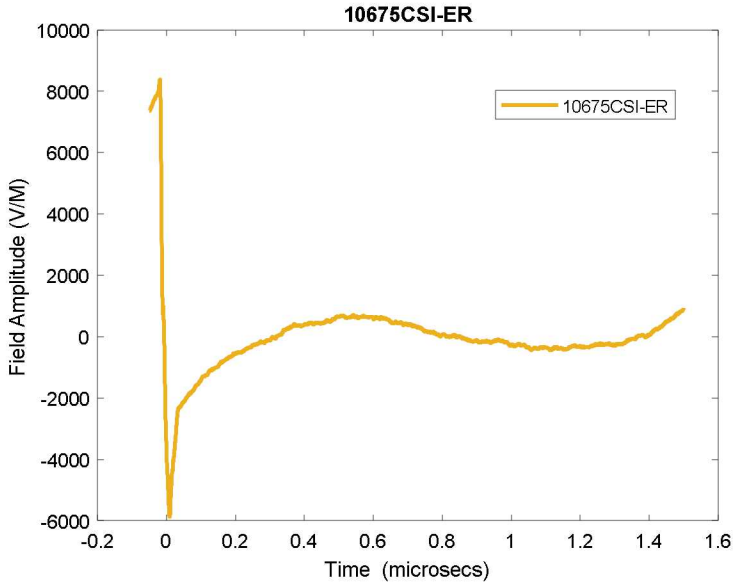

Cylinder, Inside Current Densities

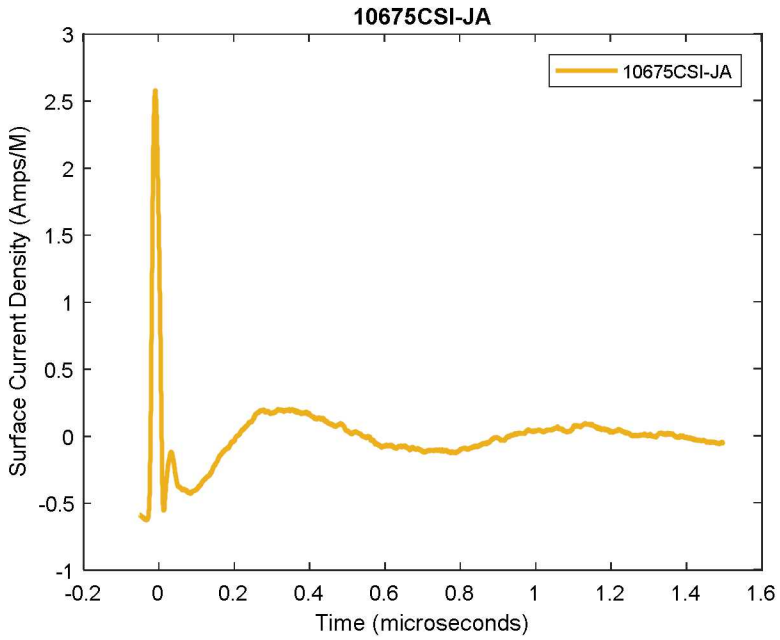

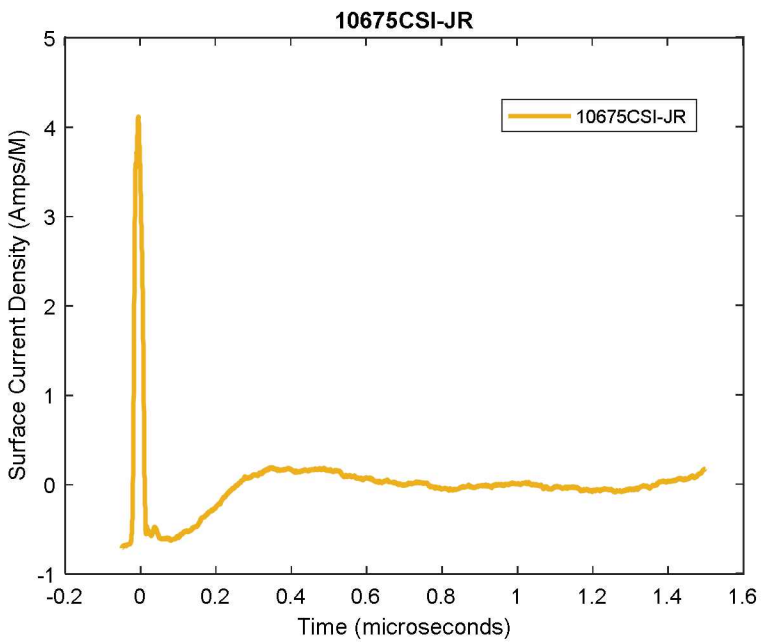

Cylinder, Outside Current Densities

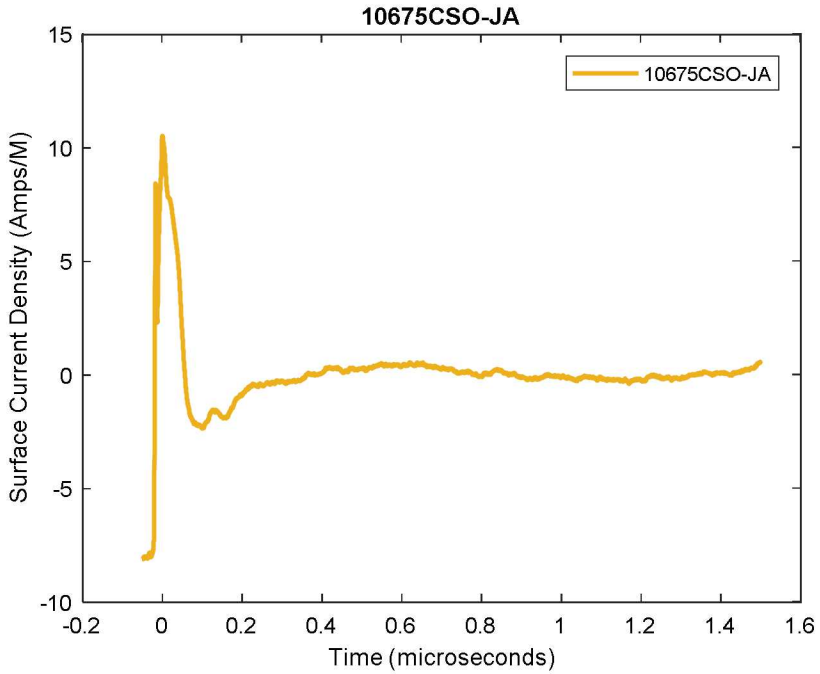

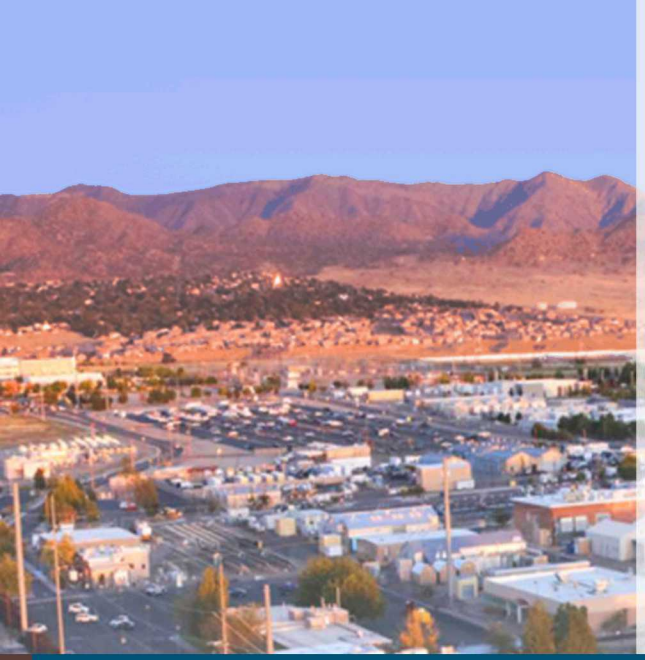

AF, Fields & Surface Currents- Shot 10675

AF – Witness Cable, Short

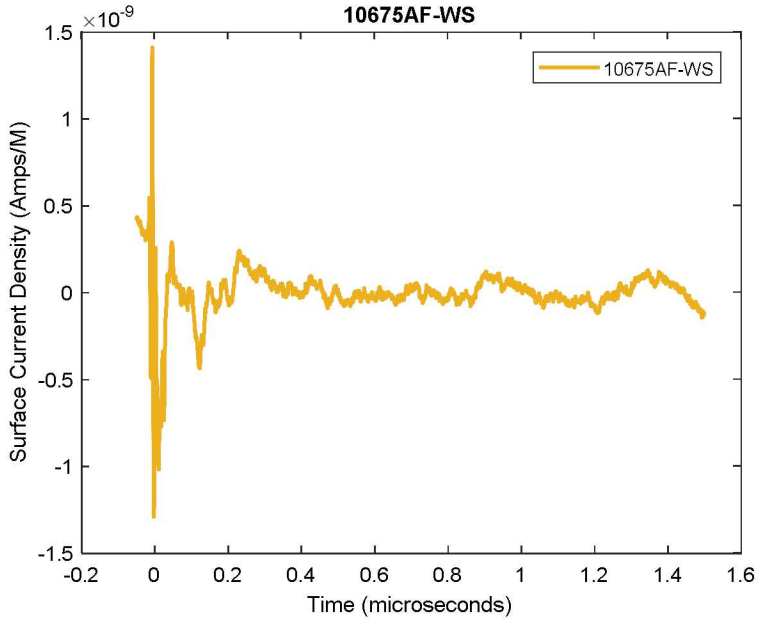

AF, Electric Fields

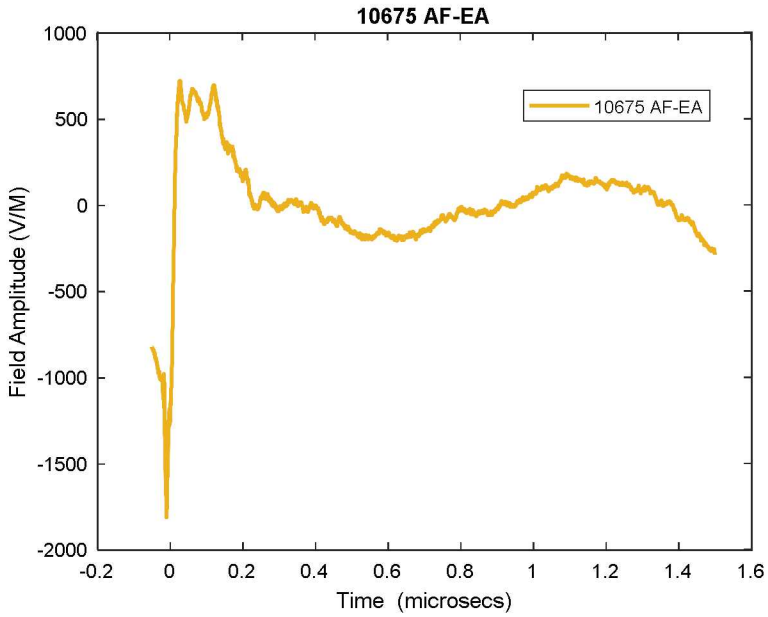

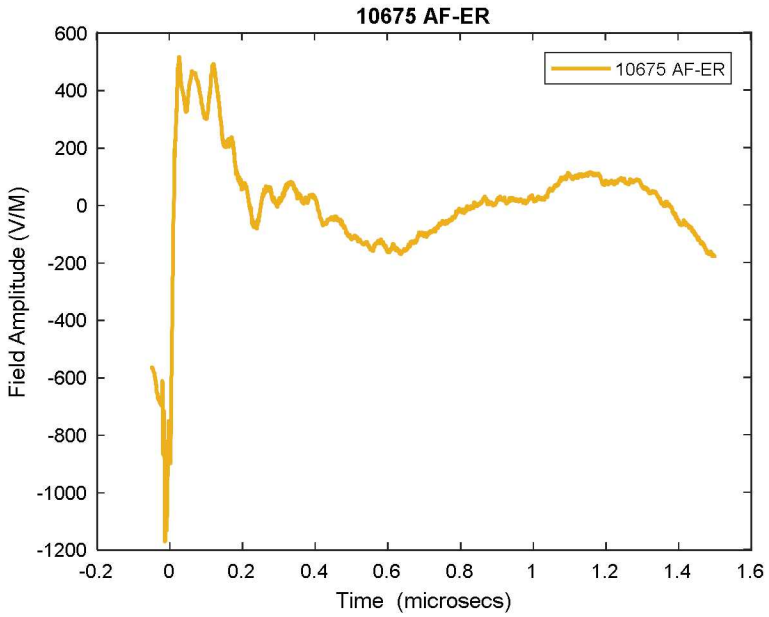

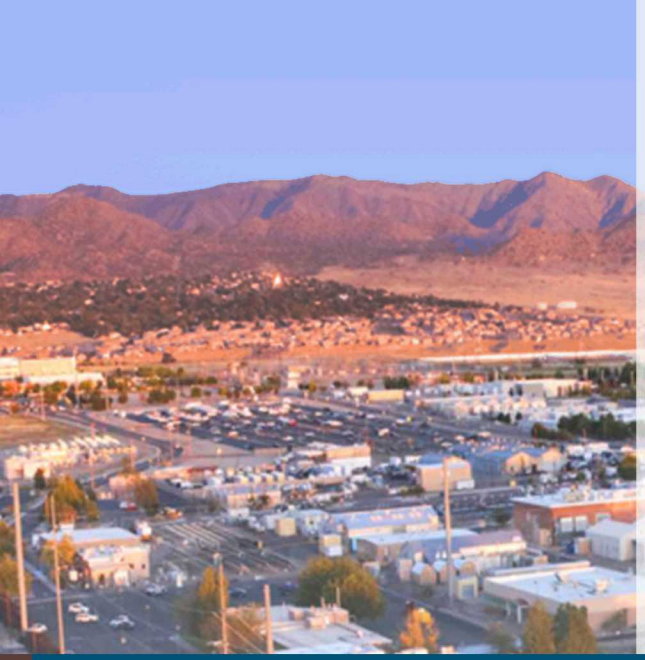

CN Fields & Surface Currents- Shot 10690

CN Fields

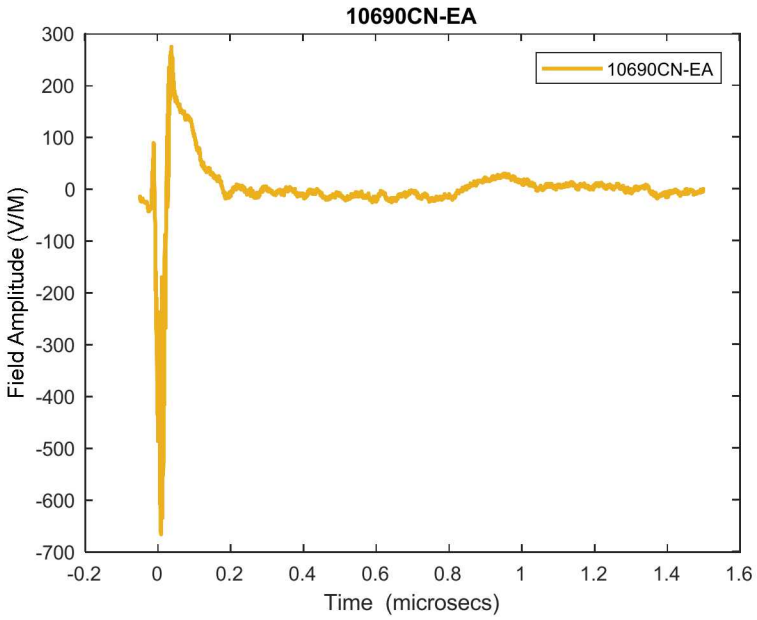
10690CN-EA
10690CN-EA
Field Amplitude (V/M)
Time (microsecs)
300
200
100
0
-100
-200
-300
-400
-500
-600
-700
-0.2
0
0.2
0.4
0.6
0.8
1
1.2
1.4
1.6

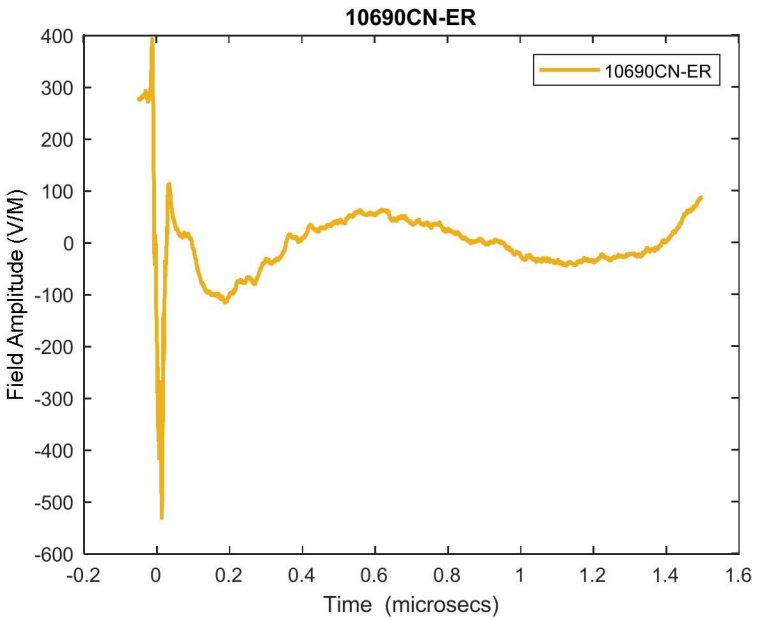
10690CN-ER
10690CN-ER
Field Amplitude (V/M)
Time (microsecs)
400
300
200
100
0
-100
-200
-300
-400
-500
-600
-0.2
0
0.2
0.4
0.6
0.8
1
1.2
1.4
1.6

CN Surface Currents

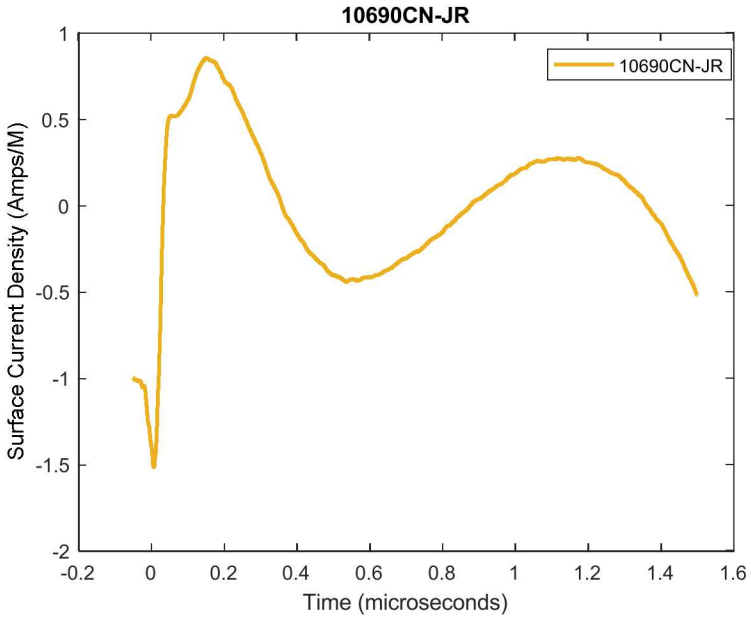

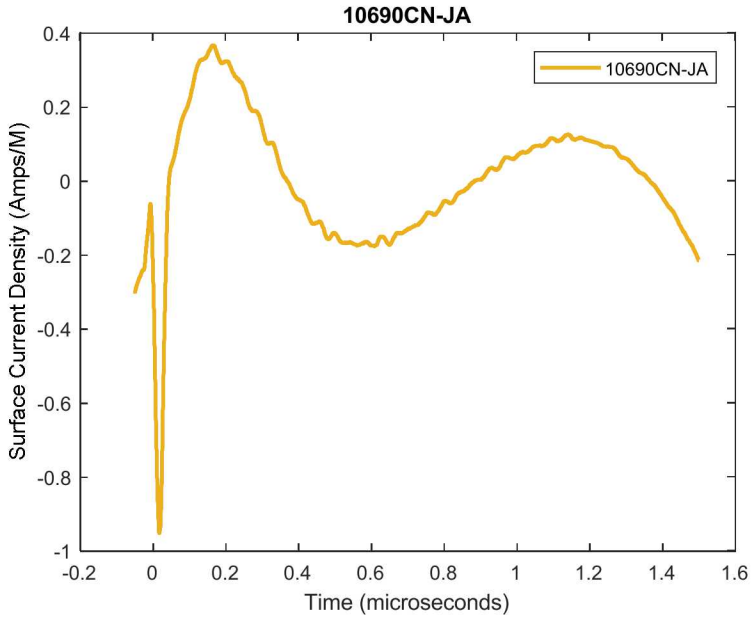

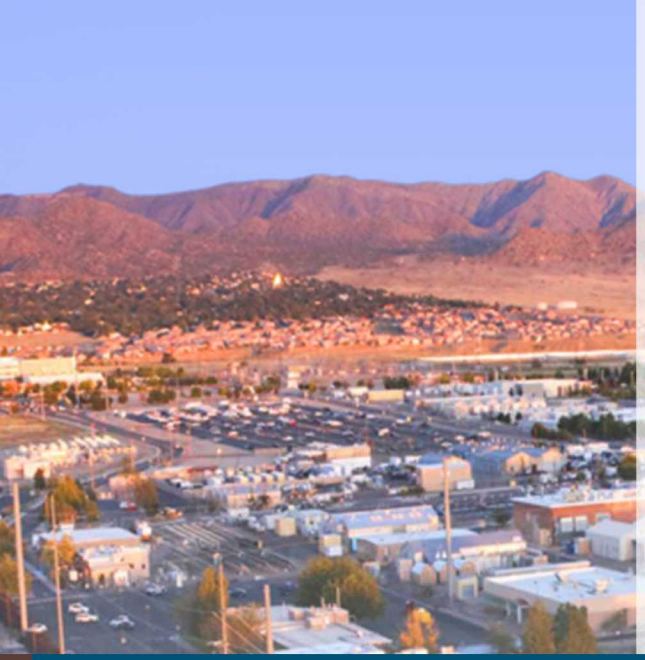

Cylinder, Fields & Surface Currents- Shot 10690

Cylinder, Inside Electric Fields

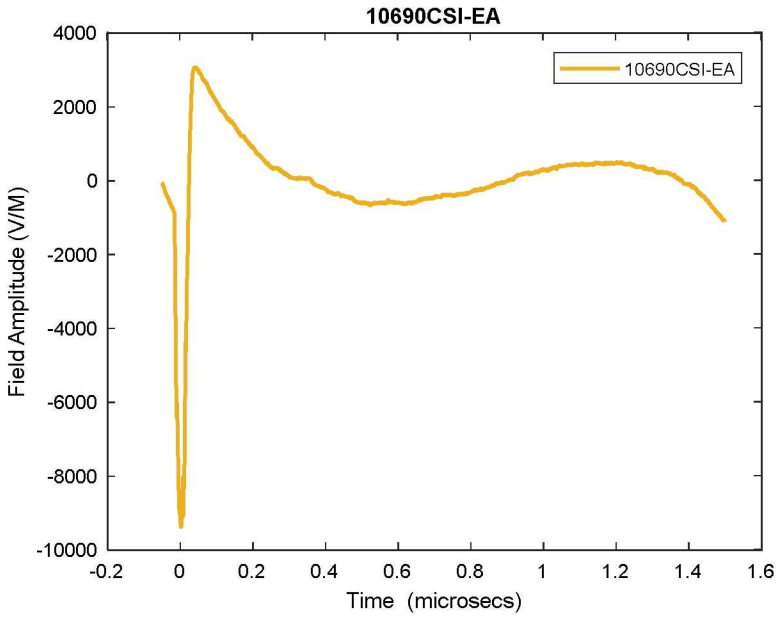

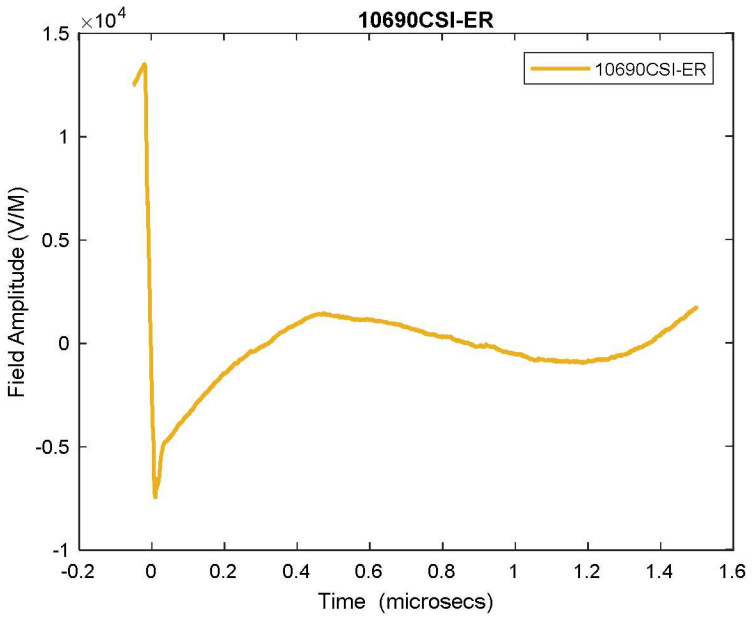

Cylinder, Inside Current Densities

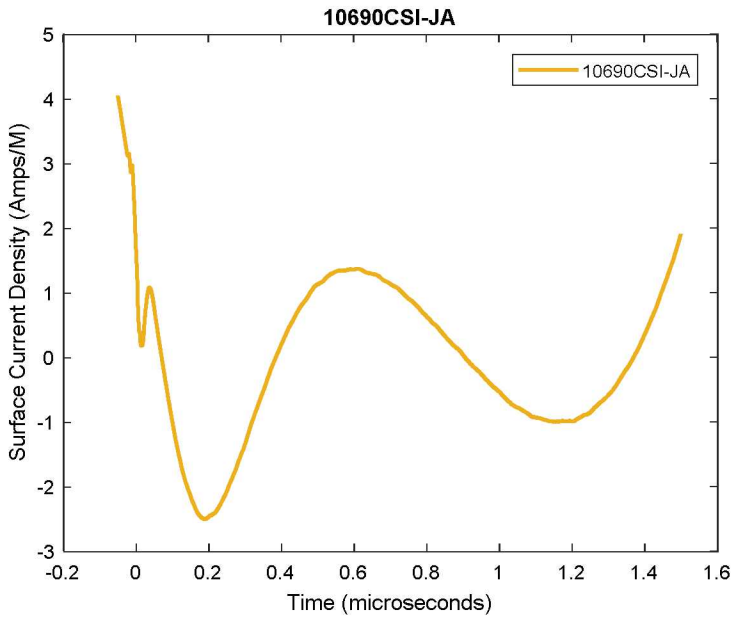

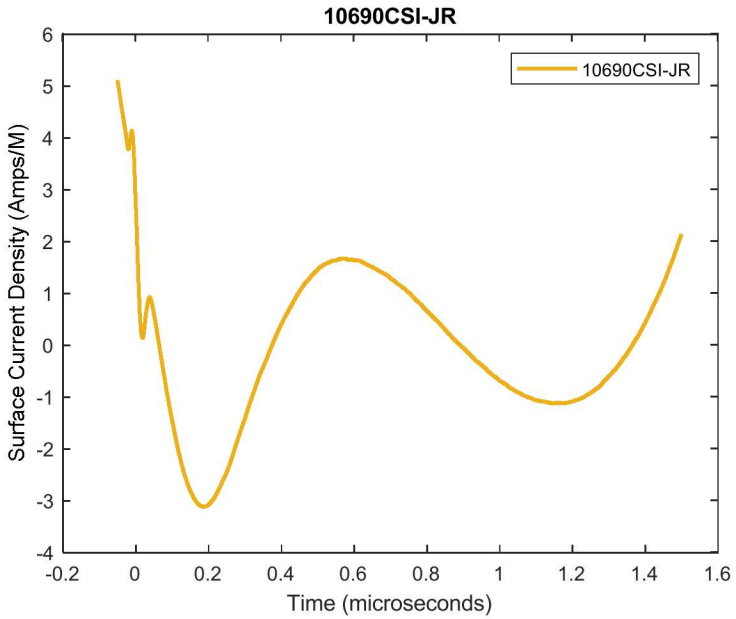

Cylinder, Outside Current Densities

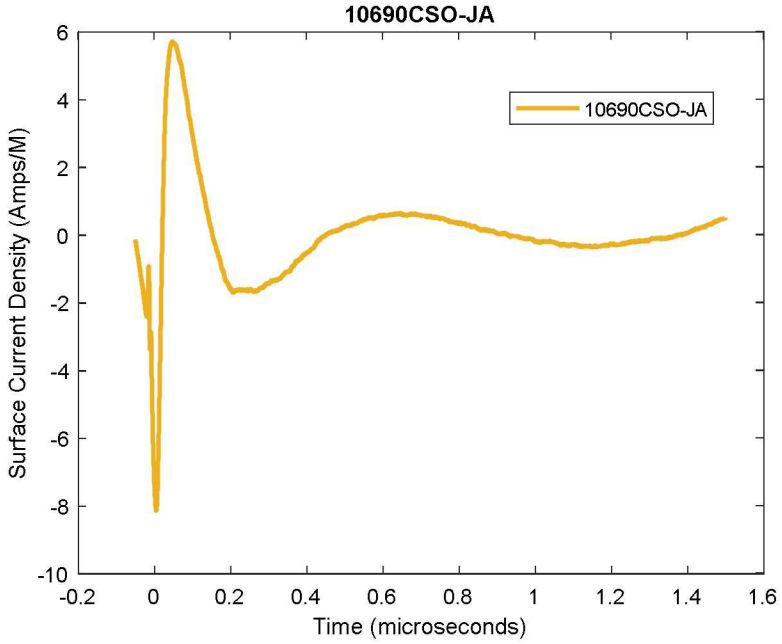

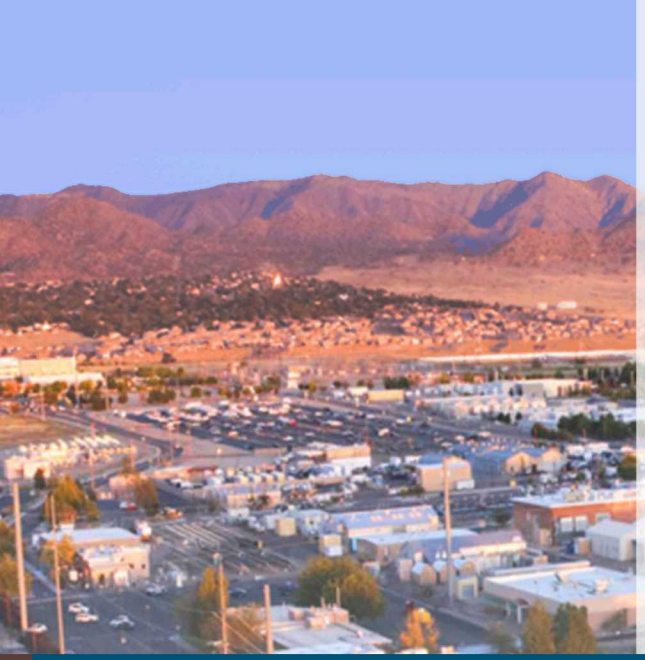

AF, Fields & Surface Currents- Shot 10690

AF – Witness Cable, Short

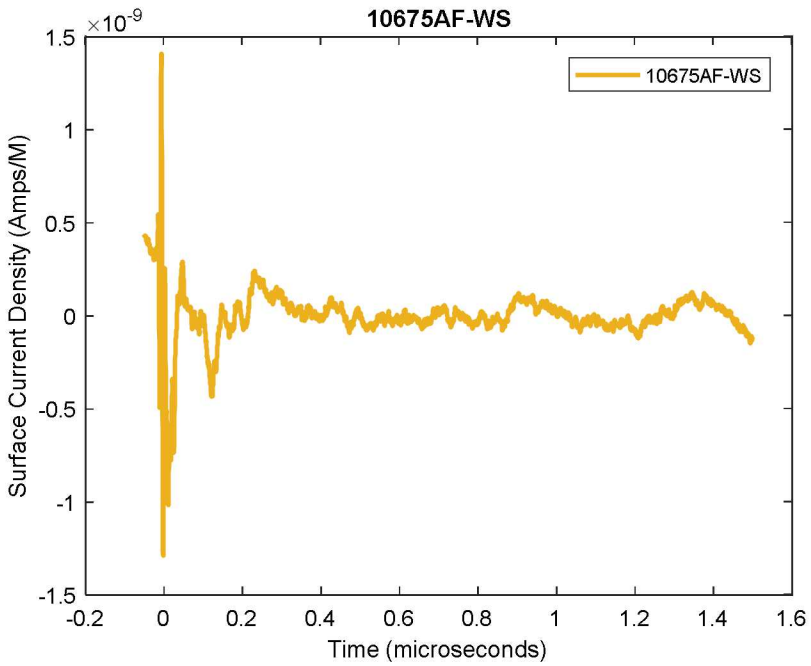

AF, Electric Fields

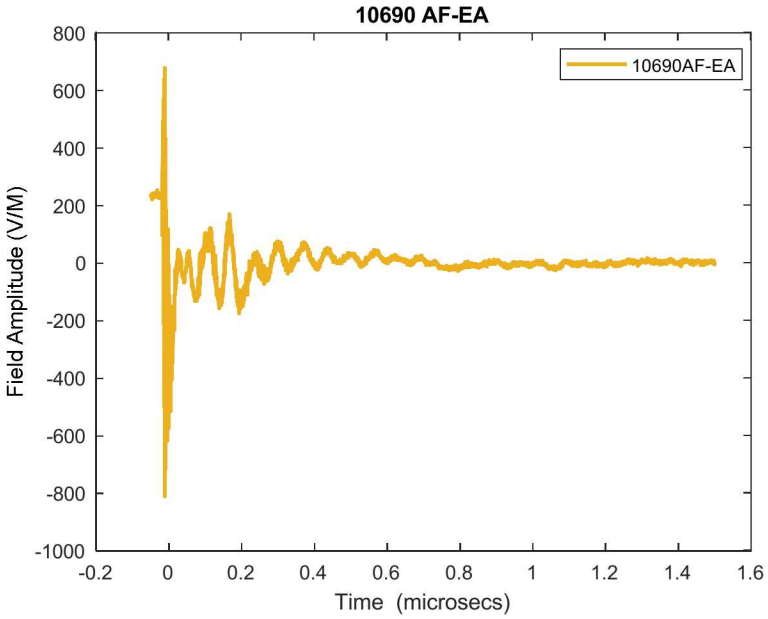

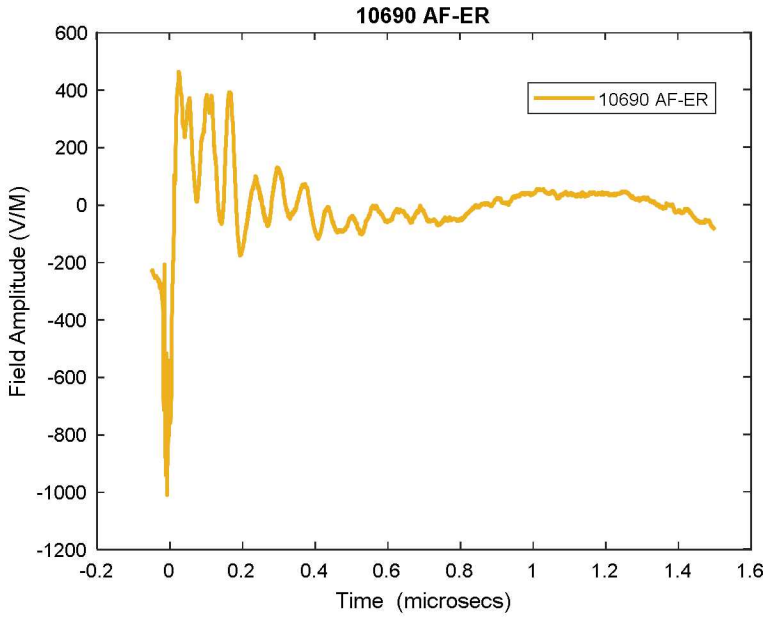

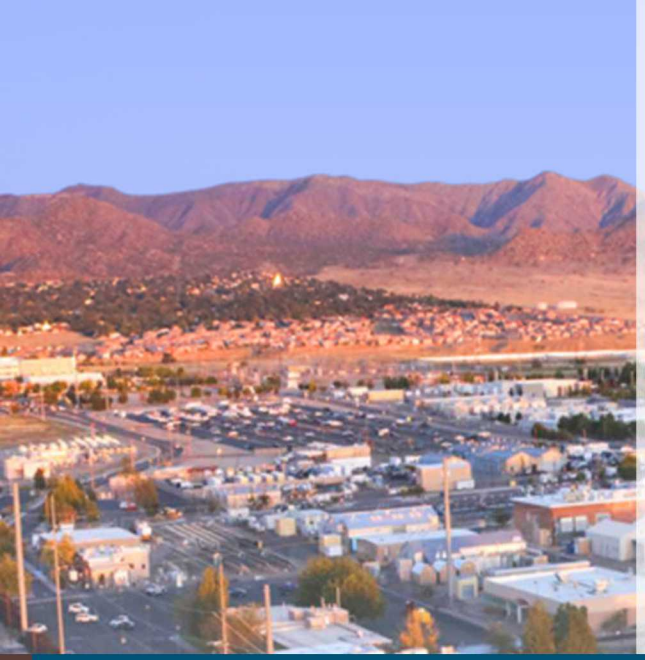

CN Fields & Surface Currents- Shot 10705

CN Fields

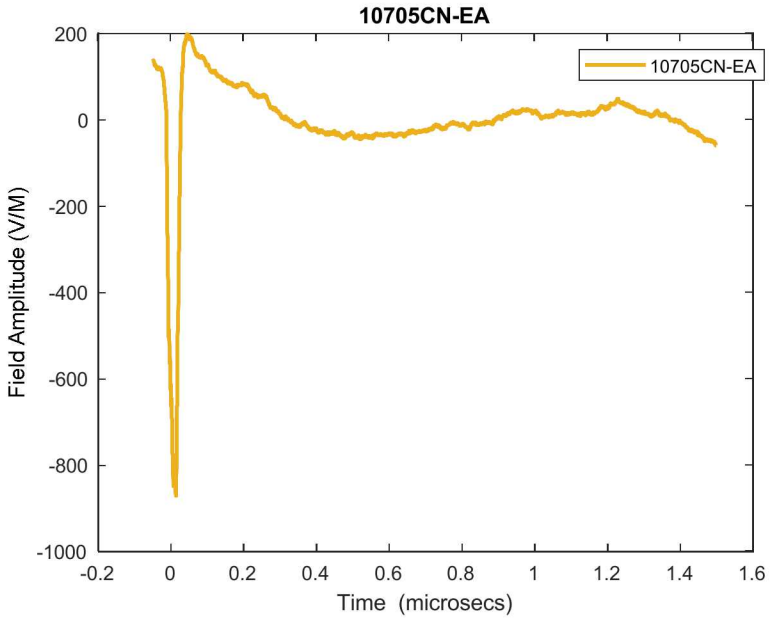
10705CN-EA
10705CN-EA
Field Amplitude (V/M)
Time (microsecs)
200
0
-200
-400
-600
-800
-1000
-0.2
0
0.2
0.4
0.6
0.8
1
1.2
1.4
1.6

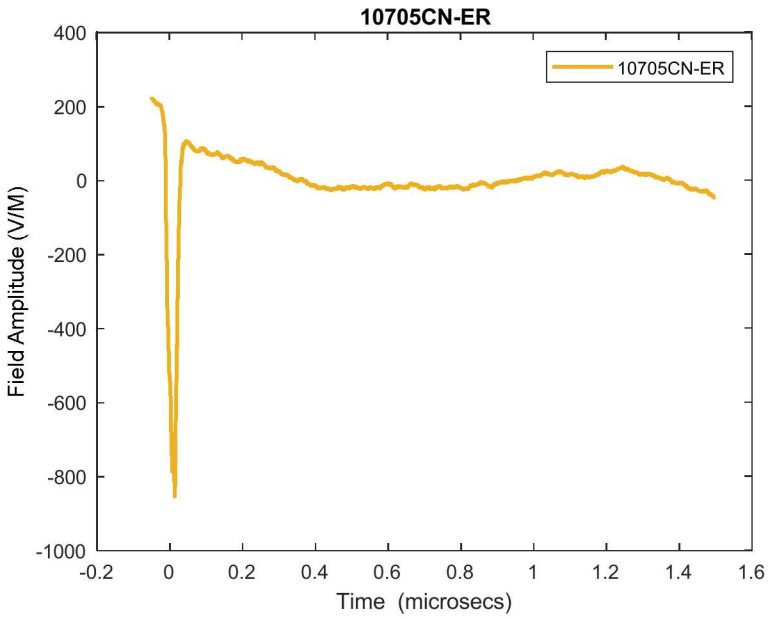
10705CN-ER
10705CN-ER
Field Amplitude (V/M)
Time (microsecs)
400
200
0
-200
-400
-600
-800
-1000
-0.2
0
0.2
0.4
0.6
0.8
1
1.2
1.4
1.6

CN Surface Currents

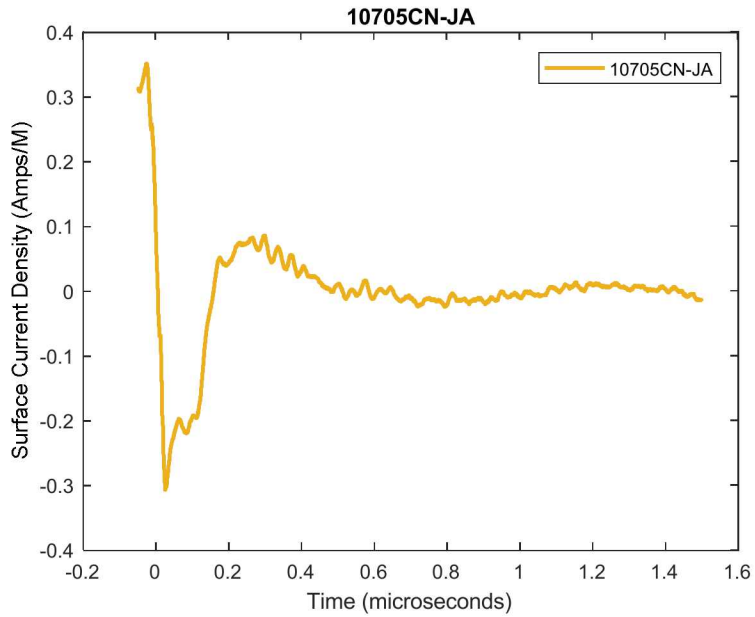

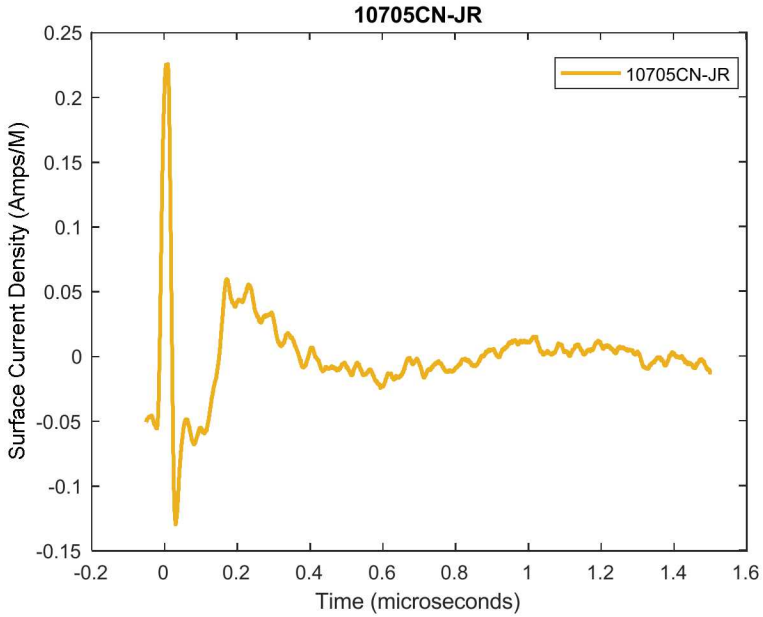

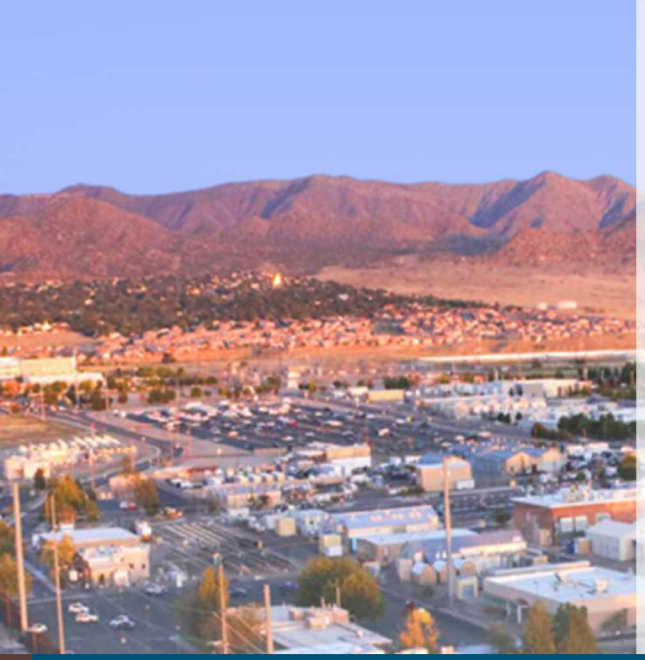

Cylinder, Fields & Surface Currents- Shot 10705

Cylinder, Inside Electric Fields

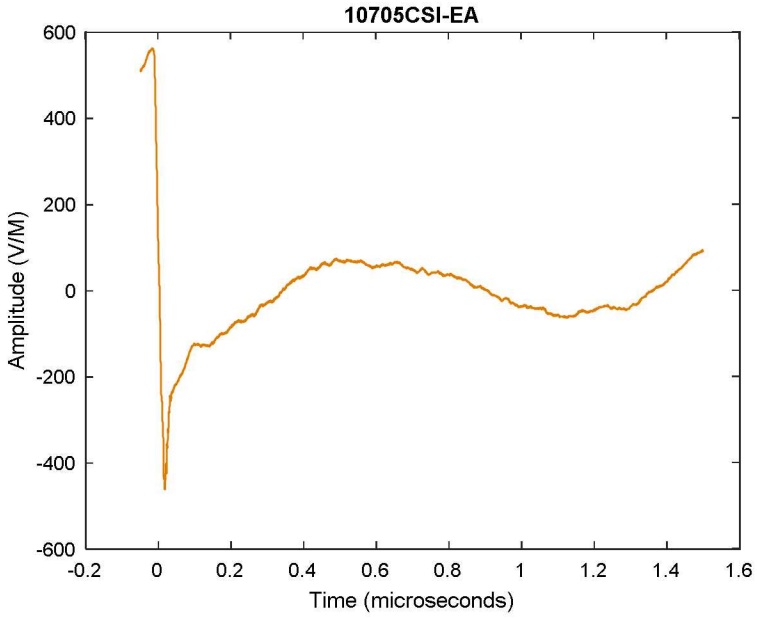

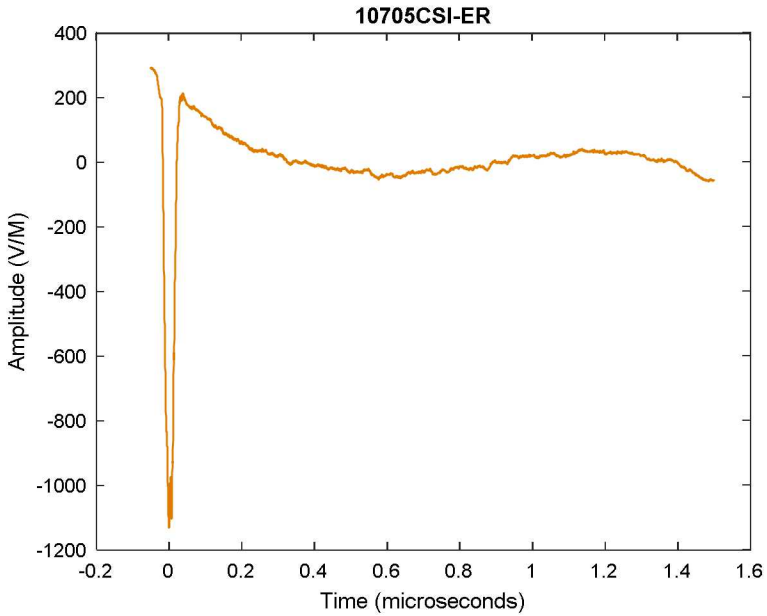

Cylinder, Inside Current Densities

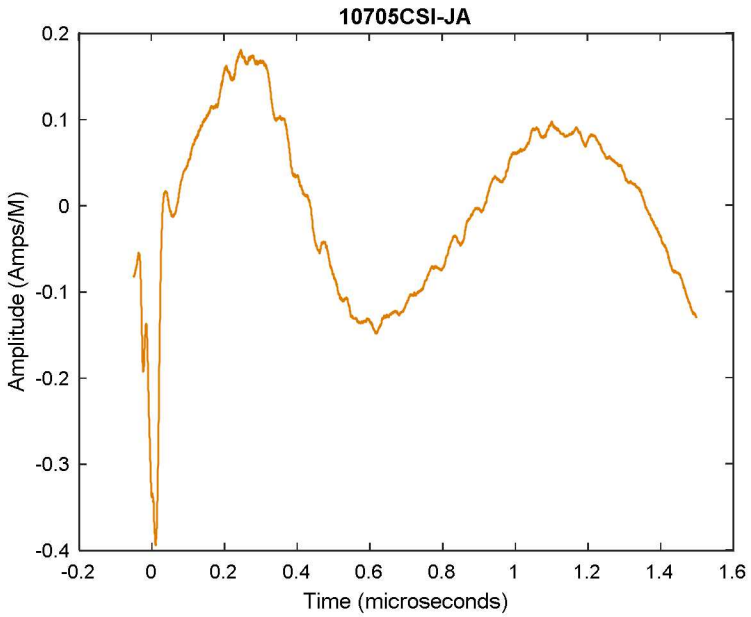

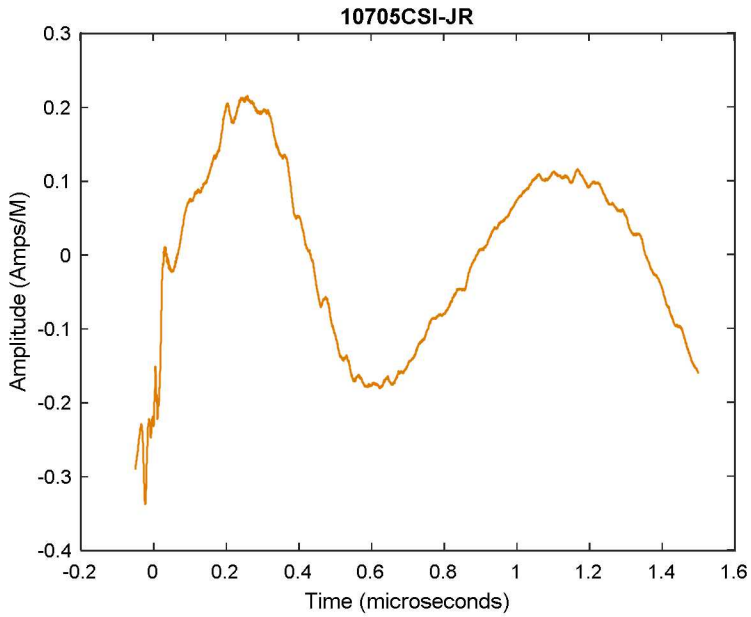

Cylinder, Outside Current Densities

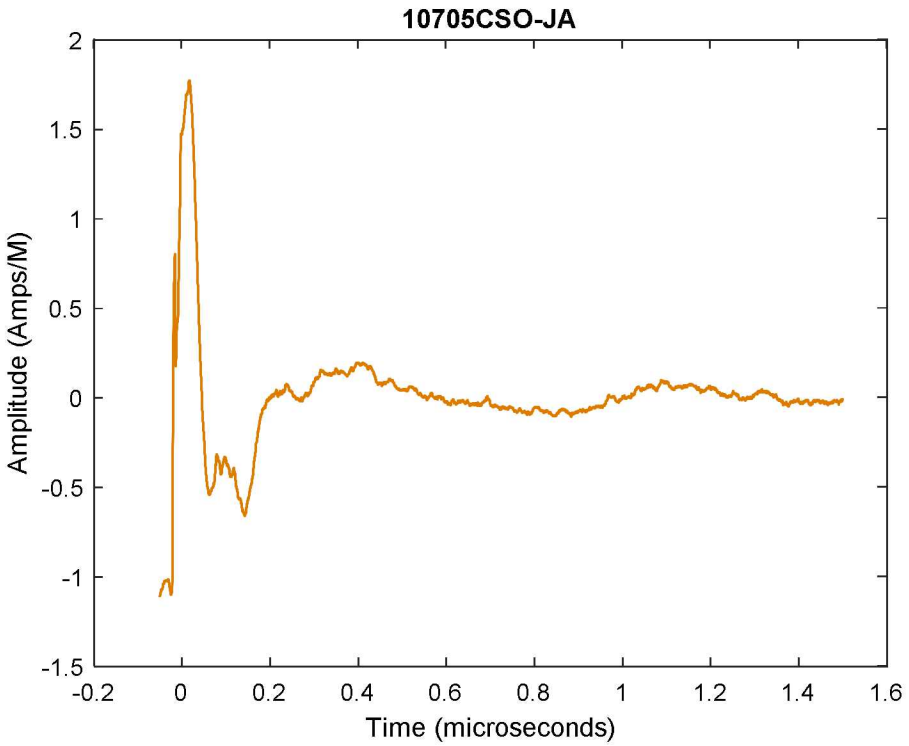

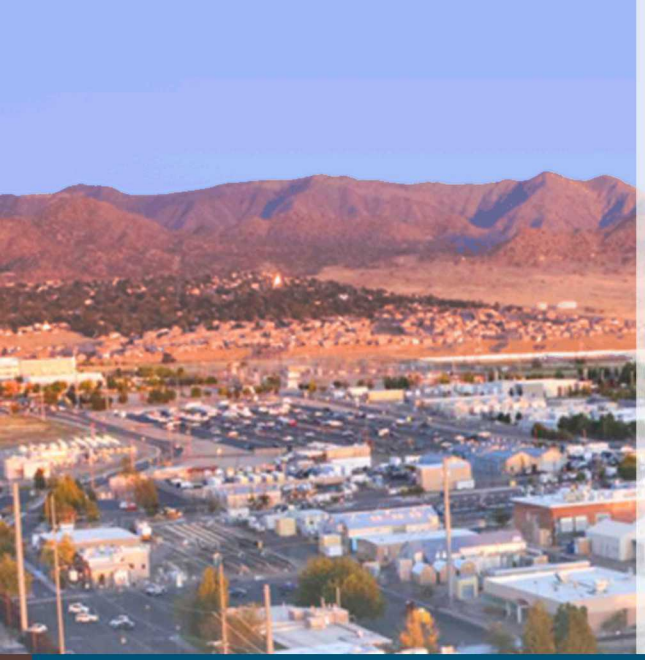

AF, Fields & Surface Currents- Shot 10705

AF – Witness Cable, Short

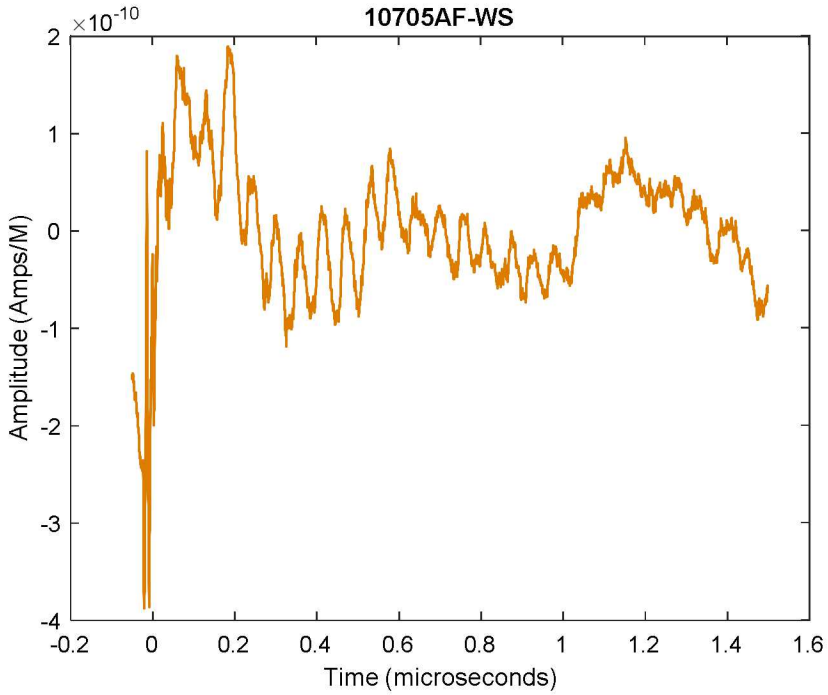

AF, Electric Fields

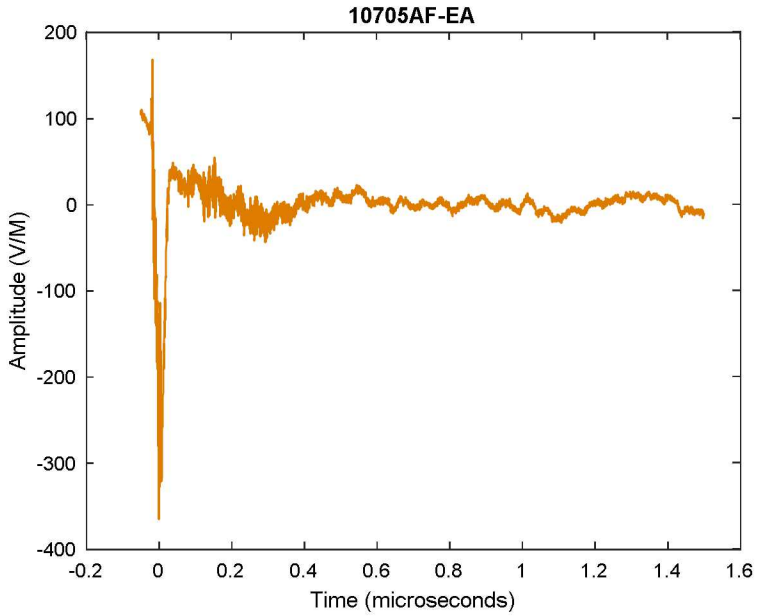

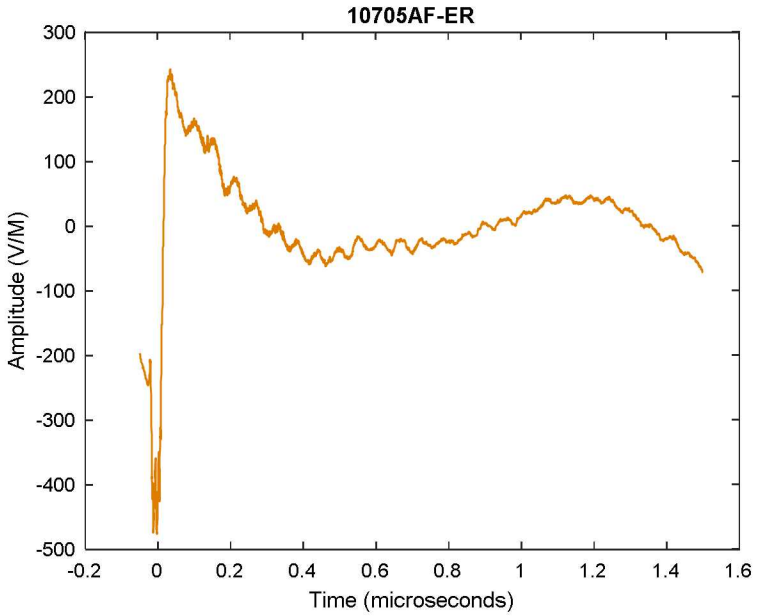

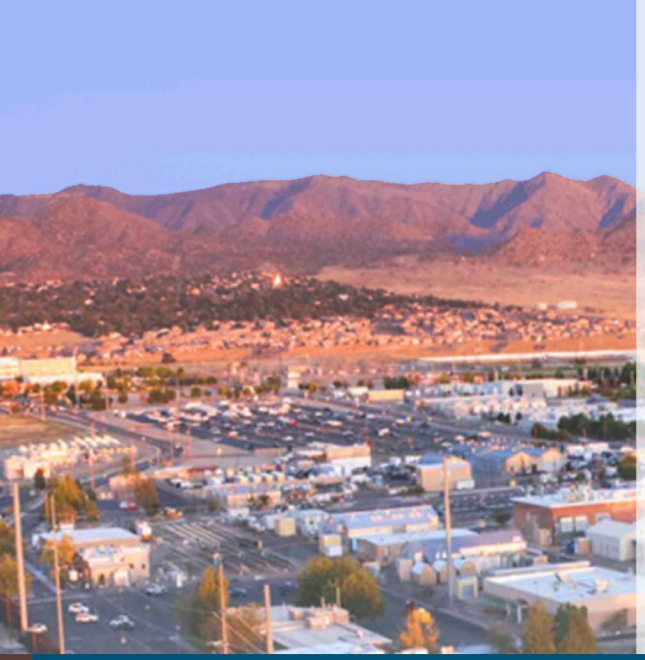

X. Signal Processing Advances

Signal Processing Advances

Removing external interferes

- Witness cable responses removed

Correcting for balun and cable distortions

- All cables and baluns swept before test

Removing extraneous noise, especially in high frequency, non-contributing bands

- Pulse extraction in time domain to limit noise
- A cosine-squared roll-off filter, peak centered at the maximum, is used to "window" salient time domain responses
- Finally, a low-pass, 3rd order Butterworth filter with a 3dB frequency at 1 GHz is used to further reduce noise

Starting with the Raw Scope Voltage…

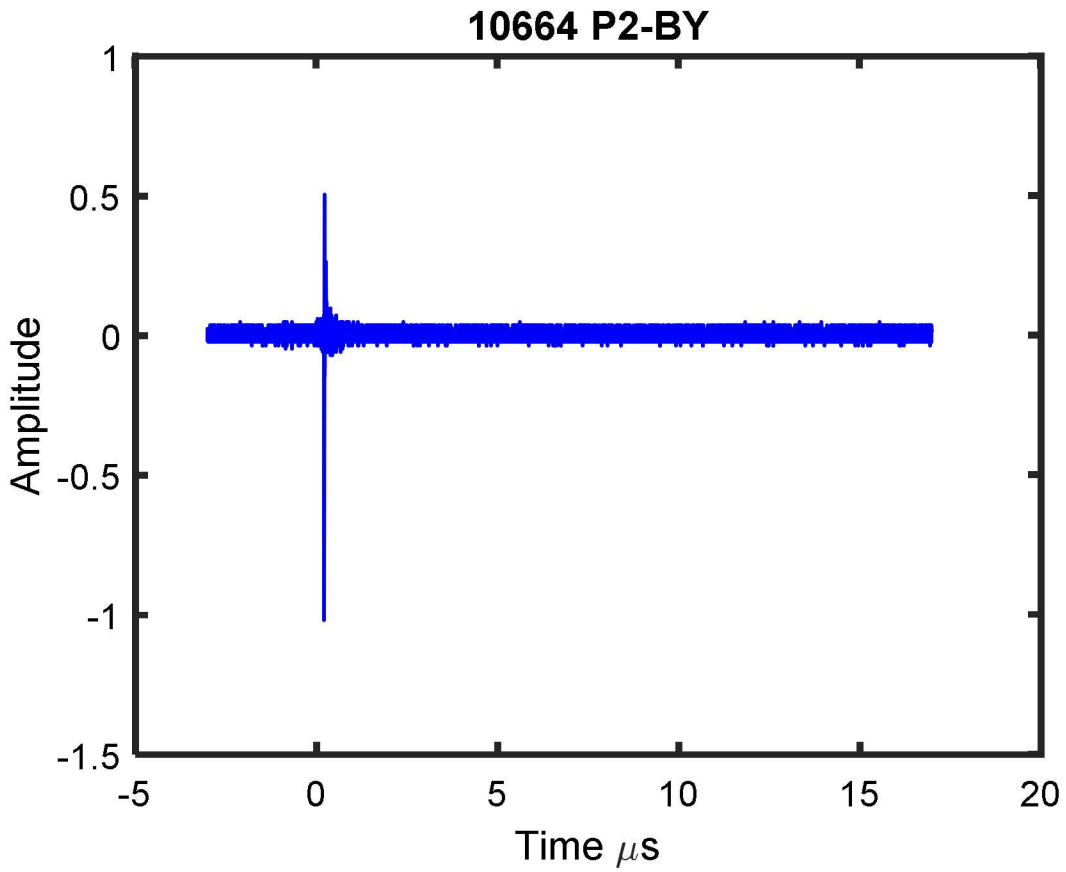

Removing Witness Cable Responses

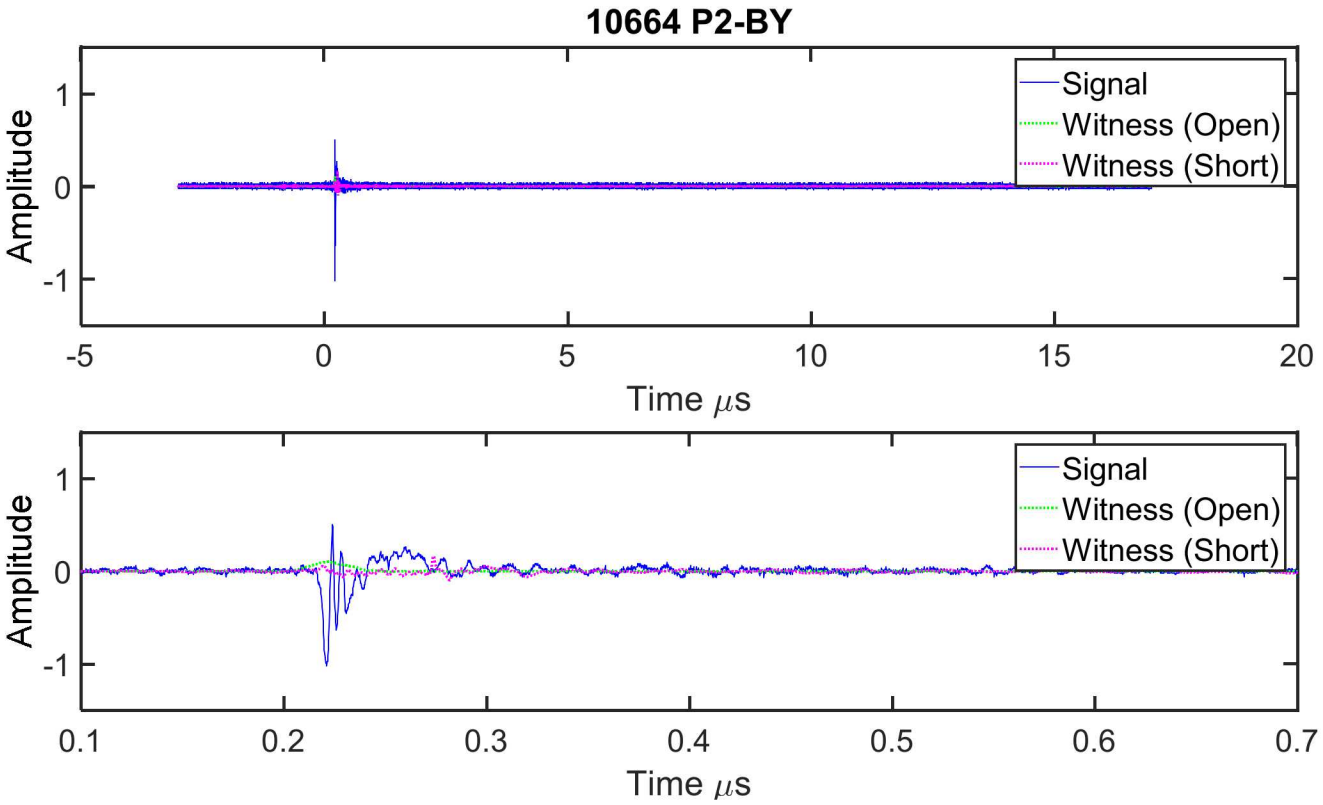

Correcting for Balun and Cable Distortions

The cable (between the scopes and sensors) sweeps with Network Analyzers and the balun sweeps (examples on right) are converted to complex numbers and multiplied to form the total response of the signal conditioner compensation (bottom, left). The Fourier Transform of the raw data is multiplied by th… response of the signal conditioner compensation to result in the total conditioner corre… the frequency domain (bottom, center). These compensated data are then inverse Fouri… the time data compensated for cable and balun responses (bottom, right).

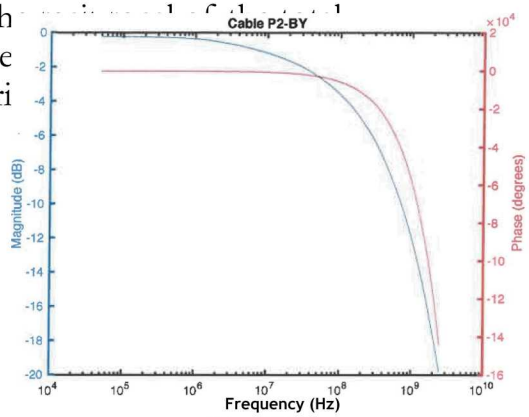

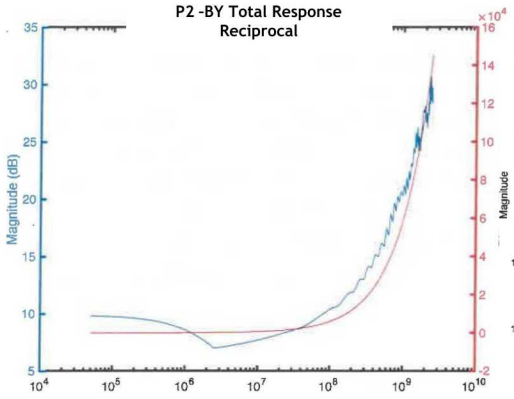

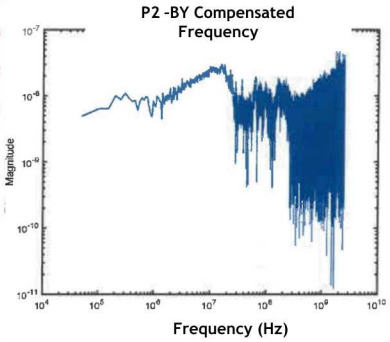

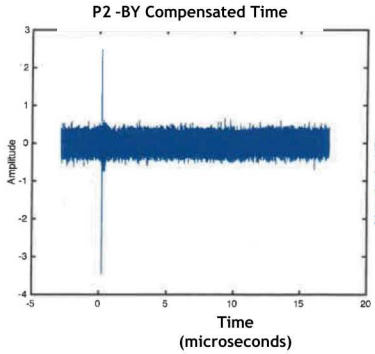

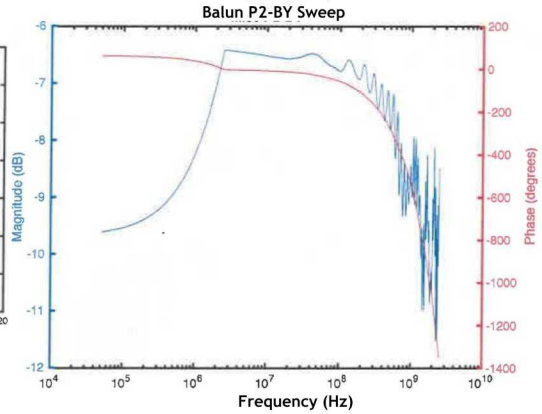

Pulse Extraction and filtering in Time Domain

To limit noise caused both by the originally acquired signals and the compounding of this noise by the balun and cable compensation process, the waveform is "extracted" and "windowed"

- The time-extracted waveform is obtained from the cable and balun compensated waveform is achieved by limiting the compensated waveform to 30 ns before the peak and 2 microseconds after the peak (bottom, left).
- Further a sine-squared window positioned between the peak value of the waveform and the end of the 2 microsecond duration, and the time-extracted waveform is multiplied by this window, forming the windowed waveform (bottom, center and right).

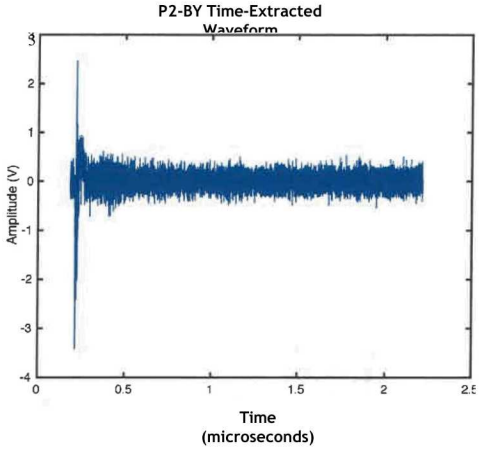

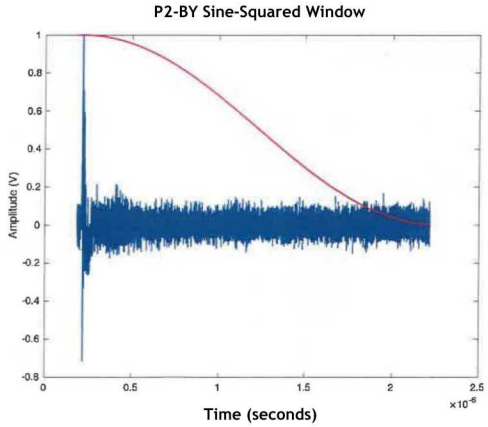

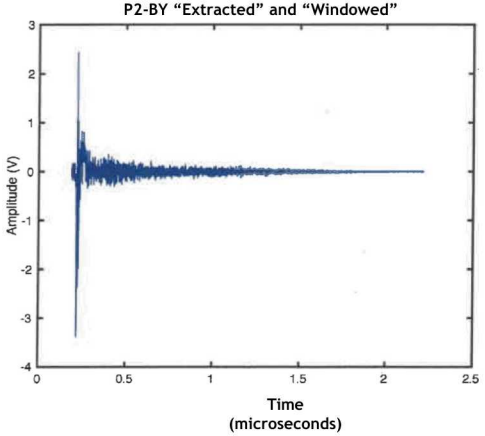

Butterworth Filter

In addition to the previously described signal processing steps, a low pass filter was also applied to the data as a last step.

- A 3 dB frequency of 1 GHz was chosen for the filter because the digitizers only had an analog bandwidth of 1 GHz and the signals being captured do not have much content above several hundred megahertz.

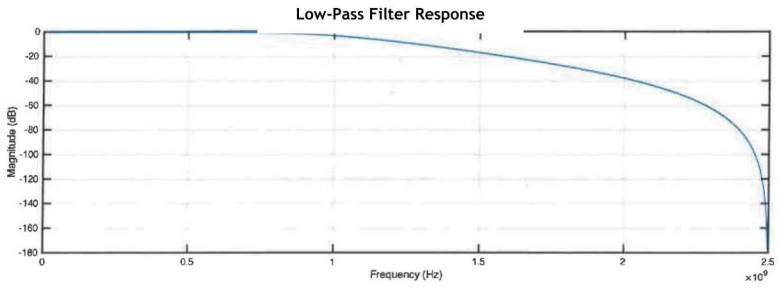

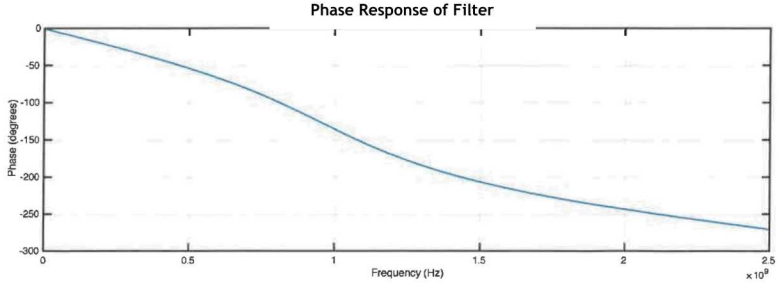

These Techniques Produced the "Corrected" Waveforms That Are the Starting Point for the "Final Corrections" Described in Section II